Targeting interference of CTLA-4 co-inhibition to tumour-specific T-cells to enhance activity and reduce toxicity

Dr Claire Roddie

Thesis submitted to the University College of London for the degree of Doctor of Philosophy

2015

Academic Department of Haematology

Supervised by Dr Karl S. Peggs, Dr Martin A. Pule, Dr Sergio A. Quezada

DECLARATION

I, Claire Roddie, confirm that the work presented in this thesis is my own. Where information has been derived from other sources, I confirm that this has been indicated in the thesis.

ABSTRACT

Blockade of Cytotoxic T lymphocyte antigen-4 (CTLA-4) can enhance anti-tumour responses in preclinical models. A monoclonal antibody targeting human CTLA-4 (αCTLA4 mAb), is FDA approved for clinical use against metastatic melanoma. Paradigms suggest that αCTLA4 mAb blocks CTLA-4 dually on CTLA-4^{hi} Tregs (restricting regulatory activity) and CTLA-4^{int-hi} CD4 Teff (enhanced expansion) resulting in intratumoural Teff dominance and a net gain in anti-tumour activity. More recently, antibody-dependent cellular cytotoxicity (ADCC)-mediated depletion of CTLA-4^{hi} Tregs in the tumour has been flagged as a critical factor driving anti-tumour immune responses.

We explored the ADCC hypothesis in an adoptive cell transfer model of murine melanoma. We compared intratumoural Treg numbers in groups receiving CTLA-4$^{+/+}$ or CTLA-4$^{-/-}$ tumour-specific T cells with/without exogenous αCTLA4 mAb. Exogenous αCTLA4 mAb resulted in diminished intratumoural tumour-specific Treg numbers in groups receiving CTLA-4$^{+/+}$ but not CTLA-4$^{-/-}$ T-cells. Endogenous CTLA-4$^{+/+}$ Tregs were depleted intratumourally with αCTLA4 mAb, irrespective of the CTLA-4 status of the adoptive cells. This data supports the proposed ADCC mechanism of αCTLA4 mAb and its dependence upon target cell CTLA-4 expression.

Furthermore, we engineered tumour-specific T-cells to secrete αCTLA-4 mAb on IgG2a isotype (high ADCC activity) or IgG1 isotype (low ADCC activity) for adoptive transfer into melanoma-bearing mice. We found that transduced primary murine T-cells could engraft, infiltrate tumours and secrete biologically active αCTLA4 mAb. Secreted IgG2a αCTLA-4 mAb was strongly associated with intratumoural depletion of CTLA-4^{hi} Tregs, but unexpectedly CTLA-4-replete transduced Teff were also vulnerable to depletion, and this significantly compromised the anti-tumour potential of this therapy. Intratumoural depletion of CTLA-4^{hi} T-cells was not associated with (secreted) IgG1 αCTLA-4 mAb or (secreted) isotype control mAb.

We believe that depletion of intratumoural Tregs is an important area for cancer immunotherapy, but our experience of αCTLA-4 mAb underlines the importance of careful immunomodulatory target selection to avoid toxicitiy.

ACKNOWLEDGEMENTS

TABLE OF CONTENTS

LIST OF FIGURES

LIST OF TABLES

CHAPTER 2

ABBREVIATIONS

ACT	adoptive cellular therapy
ADCC	antibody dependent cell mediated cytotoxicity
ANA	anti-nuclear antibody
α-CTLA-4 mAb	anti-CTLA-4 monoclonal antibody
APCs	antigen presenting cells
BM	bone marrow
BSA	bovine serum albumin
CARs	chimeric antigen receptors
CFSE	carboxyfluorescein succinimidyl ester
ConA	concanavalin A
CTLA-4	cytotoxic T lymphocyte antigen 4
CTLA-4-Ig	cytotoxic T lymphocyte antigen 4 immunoglobulin
DC	dendritic cell
DLI	donor lymphocyte infusion
DMSO	dimethyl sulfoxide
DNA	deoxyribonucleic acid
dNTPs	deoxyribose nucleoside triphosphates
dsDNA	double stranded DNA
eBFP	blue emission variant of eGFP
EDTA	ethylenediaminetetraacetic acid
eGFP	emerald green fluorescent protein
ELISA	enzyme-linked immunosorbent assay
ER	endoplasmic reticulum
FACS	fluorescence-activated cell sorting
FCS	foetal calf serum
FcγR	Fc gamma receptor
GM-CSF	granulocyte macrophage colony stimulating factor
GMP	good manufacturing practice
Gvax	GM-CSF secreting tumour cell based vaccine
HBSS	Hank's buffered salt solution
HEK 293 T cells	human embryonic kidney cells
Hu152Tg	human CTLA-4 transgenic (murine strain)
IRAE	immune related adverse event
IFNγ	interferon gamma
IL-	interleukin-
i.d.	intradermal (injection)
i.v.	intravenous (injection)
KDEL	endoplasmic reticulum protein retention receptor 1
LB	Luria Bertani
LN	lymph node
M-CSF	macrophage colony stimulating factor
LTR	long terminal repeat
MHC	major histocompatibility complex
MLV	Moloney murine leukaemia virus
mRNA	messenger ribonucleic acid
PB	peripheral blood
PBS	phosphate buffered saline
PCR	polymerase chain reaction
RD114	amphotropic simian type D envelope plasmid
rHuIL-2	recombinant human interleukin 2
RNA	ribonucleic acid
RPM	revolutions per minute

RPMI	Roswell Park Memorial Institute medium
RT	radiotherapy (5 Gray of total body irradiation-murine dose)
shRNA	short hairpin RNA
scFv	single chain variable fragment
siRNA	small interfering RNA
SNP	single nucleotide polymorphisms
s.c.	subcutaneous
SD	standard deviation
TBI	total body irradiation
T_{CM}	central memory T cells
TCR	T cell receptor
Teff	CD4 T effector cells
T_{EM}	effector memory T cells
T_{SC}	stem cell memory T cells
TIL	tumour infiltrating lymphocyte
TNF	tumour necrosis factor
Tregs	CD4 T regulatory cells
tRNA	transfer RNA
TRP1	tyrosinase related protein 1
VSV-G	vesicular stomatitis virus glycoprotein
WT	wild type

CHAPTER 1

1. INTRODUCTION

1.1 Context of the project

Despite significant advances, existing adoptive immune cellular therapies (ACT) have limited clinical effectiveness in patients with cancer. Genetic redirection of T cell specificity through transduction with T cell receptors (TCRs) or major histocompatibility complex (MHC) unrestricted chimeric antigen receptors (CARs) can overcome some of the limitations of naturally occurring tumour infiltrating lymphocytes (TILs), namely low precursor frequency and low TCR avidity for tumour associated self-targets (1-4). Despite this, mechanisms of immune tolerance such as expression of the co-inhibitory T-cell transmembrane receptor Cytotoxic T-Lymphocyte Associated Antigen-4 (CTLA-4) consistently blunt the induction, magnitude and maintenance of anti-tumour immunity (5, 6). This project undertakes to investigate strategies to dissociate the beneficial anti-tumour effects of CTLA-4 inhibition from the unwanted autoimmune toxicities reported widely in the literature (7).

1.2 CTLA-4 structure and function

1.2.1 CTLA-4 as an antagonist to CD28

Regulation of T cell responses is modulated by opposing signals transmitted through two related cell-surface receptors of the immunoglobulin superfamily, CD28 and CTLA-4 (figure 1.1).
CD28 is constitutively expressed on resting and activated T cells and provides costimulatory signals upon T cell receptor engagement by antigen-bound-MHC. Its ligands are B7.1 (CD80) and B7.2 (CD86), expressed predominantly on antigen presenting cells (APC), and binding leads to TCR-mediated T cell proliferation through up-regulation of IL-2 and anti-apoptotic pathways and improved survival (8). CD28 is thought to lower the TCR signalling threshold for activation (reducing the required APC contact time for proliferation) and CD28 knockout mice have significantly impaired T cell responses to antigenic encounter and defective B cell responses(9).

Figure 1.1: CTLA-4 is a vital negative regulator of T cell responses, promoting immune tolerance. It is constitutively expressed on CD4 Tregs and is transiently expressed on CD4 T effector (Teff) and CD8 T cells on activation.
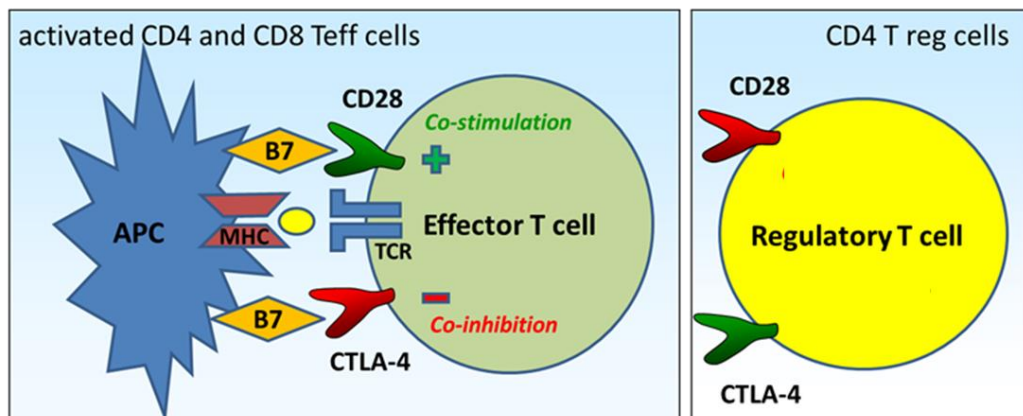
CTLA-4 is a vital negative regulator of T cell responses, preventing autoimmunity and maintaining immune tolerance. It is co-localised to chromosome 2 with CD28, with which it shares a homologous amino acid sequence. There is high conservation within the transmembrane domain and MYPPPY sequence shared by CD28 and CTLA-4, where binding to B7-1 and B7-2 is controlled (8, 10).

CTLA-4 is responsible for the regulation of CD28 signalling and the prevention of uncontrolled polyclonal T cell activation. In dimerised form, CTLA-4 has a 10- to 20- fold higher affinity and avidity for B7.1 and B7.2 than CD28, the strongest interaction being CTLA-4-CD80 and the weakest being CD28-CD86. CTLA-4 can outcompete CD28 at the immunological synapse, converting T cell activation into anergy. Blockade of CD28 is sufficient to induce T cell anergy, and in the absence of interleukin-2 (IL-2), anergised T cells undergo apoptosis (11).

The degree of CTLA-4 localisation to the immunological synapse is directly proportional to the TCR signal strength, such that high affinity TCR-peptide-MHC interactions are more strongly regulated by CTLA-4 than weak interactions. Stronger TCR signalling is driven by high TCR avidity (slow off rates) or higher TCR occupancy at elevated antigen concentration (12).

1.2.2   CTLA-4 expression

CTLA-4 is constitutively, ubiquitously expressed on CD4 regulatory T cells but only transiently expressed on activated CD8 and CD4 effector T cells. Molecular studies reveal CTLA-4 mRNA transcripts in effector T cells at one hour post-TCR engagement with antigen in the presence of appropriate CD28 co-stimulation. CTLA-4 protein is detected later, at 24 hours post-TCR engagement, reaches a peak concentration at 48 hours, and expression is lost after 96 hours (13, 14).

CTLA-4 is predominantly concentrated in intracellular vesicles within T cells. In the event of T cell stimulation, CTLA-4 is transported from the golgi to the site of T cell-antigen-APC contact on the cell membrane in phospholipase D[40]-containing vesicles. CTLA-4 is expressed only transiently on the cell surface due to negative regulation by a process of rapid, continuous CTLA-4 endocytosis (9, 15) into clathrin coated pits mediated via CTLA-4 interaction with the clathrin adaptor protein complex AP2 (16). These dynamic and directionally regulated continuous processes of export and internalisation are demonstrated in a series of experiments showing endocytosis of labelled anti-CTLA-4 monoclonal antibody (mAb) by activated T-cells. In these experiments the rate of uptake was slow and continuous and the intracellular concentration of mAb increased over time suggesting intracellular CTLA-4 accumulation with no saturation of the mechanism (12). Endocytosed CTLA-4 can be recycled to the cell surface or degraded in lysosomes (9, 17).

The preferential intracellular localisation of CTLA-4 reflects the physiological necessity to limit cell surface expression of this potent, high avidity co-inhibitory receptor, and also as a mechanism to direct the localisation of its expression on TCR engagement (12).

Mechanisms governing CTLA-4 gene expression are complex, but we know that CTLA-4 is upregulated upon T cell activation in T effectors, and constitutively expressed in Tregs, a subset of T cells that promote self-tolerance. The X-linked forkhead/winged helix transcription factor Foxp3 is characteristically associated with Tregs, and is thought to promote the expression of CTLA-4 and CD25, and to downregulate the expression of IL-2 and Interferon Gamma (IFNγ) (149). FoxP3 is known to bind to the upstream promoter of CTLA-4, enhancing its transcription in Tregs. Other groups have shown that the proximal promoter of CTLA-4 contains a binding site for the transcription factor Nuclear Factor of Activated T cells (NFAT1) and that unlike for IL-2, CTLA-4 transcription requires NFAT1 binding without AP-1(Fos/Jun). Upon T cell activation, NFAT1 is dephosphorylated in the cytosol and translocates to the nucleus of T cells for DNA binding. It is also reported using chromatin immunoprecipitation

studies that histones in activated T cells are increasingly acetylated and undergo conformational change around the CTLA-4 promoter and can facilitate NFAT1 access and binding, leading to enhanced CTLA-4 gene expression (150).

1.2.3   CTLA-4 mechanism of action

CTLA-4 is thought to limit effector T-cell activation and proliferation via autonomous (cell-intrinsic) and non-autonomous (cell-extrinsic) pathways.

CTLA-4 and CD28 are expressed in parallel on TCR-engaged activated effector T cells. CTLA-4 preferentially binds B7.1 and B7.2 on adjacent APCs which prevents CD28/B7 costimulation on TCR-stimulated T cells with a consequent reduction in IL-2 and cyclin/cyclin dependent kinase transcription, and inhibition of other TCR-driven pro-proliferative signal-transduction pathways such as ERK and JNK (18, 19). CTLA-4 may direct negative signalling within the immune synapse. It is known that T-cell-APC engagement induces clustering of TCR and MHC-peptide complexes within the immunological synapse via TCRδ phosphorylation and cytoskeletal rearrangement. CTLA-4 is recognised to co-immunoprecipitate with TCRδ and SHP-2 phosphatase, and CTLA-4-B7 binding in this context can promote SHP-2 mediated de-phosphorylation of TCRδ and prevent TCR signalling (20).

The immunological synapse, the interface between T-cells and APCs, consists of a central supramolecular activation cluster (cSMAC) containing TCR/CD3, peptide and MHC, and a peripheral SMAC (pSMAC) containing adhesion molecules (leukocyte function-associated antigen 1 (LFA-1) and intercellular adhesion molecule-1 (ICAM-1). CTLA-4, CD28 and other costimulatory receptors also accumulate in the immune synapse to create an aggregate of TCR-based signalosomes with the potential to generate T cell activation/anergy. Of note, there is little current direct evidence to support the hypothesis that CTLA-4 delivers a cell intrinsic negative signal into T cells.

There is a body of evidence to support the theory that CTLA-4 exerts its biological effect by directly competing for ligand binding with CD28. Lipid-bilayer modelling demonstrates that CTLA-4 recruitment to the cSMAC results in CD28 exclusion, particularly at low levels of B7 expression (21). Further evidence for a cell extrinsic role for CTLA-4 that is independent of intracellular signalling derives from studies of transgenic mice that lack the cytoplasmic domain of CTLA-4. These animals have been shown to upregulate surface expression of CTLA-4

in response to T cell stimulation, to survive to adulthood and to reproduce normally. With age, they accumulate activated T cells (levels 10 times higher than age-matched controls) with a skew towards T-helper 2 (Th2) phenotype. Most animals ultimately succumb to lymphoproliferation (22).

Many groups support the hypothesis of a non-cell autonomous 'effector extrinsic' CTLA-4 effect as being the dominant immunosuppressive mechanism governed by CTLA-4. It is proposed that CTLA-4-replete T cells can regulate co-existing populations of CTLA-4-depleted T cells, and evidence for this comes from bone marrow (BM) chimera and co-transfer studies (23, 24). The effector-extrinsic effect is mediated mainly through CTLA-4^{hi} Tregs (25-27), but some groups argue that activated CTLA-4^{hi} Teff cells can also effect extrinsic control of T cell function. Corse and Allison show that in co-transfer experiments, CTLA-4-replete antigen specific T cells can prevent accumulation of CTLA-4-deficient antigen specific T cells, and that this is optimal at ratios of 1:1 or 1:2, (CTLA-4$^{-/-}$:CTLA-4$^{+/+}$) but is significantly diminished at higher ratios (26, 27).

CTLA-4 has many additional proposed modes of coinhibitory activity. Some groups support a pro-motility function for CTLA-4, where the TCR-mediated STOP signal is interrupted by CTLA-4 resulting in a short dwell time of T cell on APCs(24). Recent work also points towards a CTLA-4-mediated modification of APC phenotype which is described in Chapter 1.2.4 (15).

1.2.4   CD4 T-regulatory lymphocytes (Tregs) and CTLA-4

CD4+CD25+FoxP3+ CD4 Tregs can suppress inflammation and autoimmunity in mice and humans (28). Sakaguchi redefined CD4 Tregs mechanistically through an observation that depletion of a minor population of CD25+ CD4+ T cells from a CD4+T cell suspension induced a spectrum of autoimmune disease upon transfer into immunocompromised hosts (29).

CD4 Tregs fall broadly into two categories. 'Naturally occurring' Tregs are produced in the thymus and express CD4, CD25, GITR (glucocorticoid-induced TNFR-related protein), OX40 and CTLA-4. They are developmentally dependent upon the X-linked forkhead/winged helix transcription factor Foxp3. 'Inducible' Tregs arise from naïve CD4 T cells as a result of tolerogenic encounters in the periphery (30). Peripheral conversion of conventional non-regulatory CD4 T cells to regulatory phenotype following antigen exposure under certain conditions is recognised as being important to T cell homeostasis and control of inflammation.

Conditions which drive peripheral conversion include suboptimal antigen stimulation, transforming growth factor β (TGFβ), indoleamine2,3 dioxygenase (IDO) and retinoic acid (31, 36). Tregs often predominate in the tumour microenvironment supporting tumour outgrowth (4, 31), and in human cancers have been reported to correlate with poor outcome (32, 33).

The basic biology of Tregs indicates that they require TCR triggering to become functional/suppressive, but thereafter do not proliferate upon TCR engagement with or without co-stimulation and suppress other cells in a non-MHC restricted manner and mediate bystander suppression. Unlike Teff, they do not produce effector cytokines such as IL-2, IL-4 or IFNγ, but express receptors for gamma chain cytokines and are dependent on an exogenous supply to prevent cytokine-deprivation apoptosis in vitro (28, 34, 35).

Tregs are proposed to exert immunosuppressive effects through multiple mechanisms. They can secrete lymphoid and myeloid cell suppressive cytokines such as IL-10 and TGFβ; they can function directly as cytotoxic cells killing other immune cells in a similar manner to CD8 T cells; they can express cell surface (and/or secreted) molecules that interact with receptors on effector T cells leading to cell cycle arrest, and by virtue of their high level of CD25 expression, they can outcompete other T cell populations for IL-2 leading to Bim-mediated apoptosis of non Treg populations (35).

The second broad target for Treg-mediated immunosuppression is antigen presenting cells (APC). CTLA-4^{hi} Tregs can downregulate expression of the costimulatory molecules B7.1 and B7.2 on mouse and human dendritic cells (DCs) in vitro (36, 37). One proposed mechanism is CTLA-4 mediated trogocytosis whereby CTLA-4^{hi} T cells extract cell surface B7.1 and B7.2 through the immunological synapse from the APC to which they are conjugated (15, 38). Some investigators suggest that Treg mediated suppression of DC proliferation in vitro can be reversed by anti-CTLA-4 mAb (39), but this is not evident in all studies.

CTLA-4 expression is thought to be important to Treg function and is controlled by the transcription factor FoxP3 (40). The consequences of organism-wide failure to express CTLA-4, demonstrated in a transgenic murine model, are polyclonal T cell expansion, overwhelming autoimmunity and premature death (41, 42). Milder phenotypes have been described in mice lacking CTLA-4 exclusively on CD4 Tregs (26, 43). CTLA-4 deficient Tregs have been described as anergic and less suppressive in vitro than their wild type (WT) counterparts. Adoptive transfer of CTLA-4 deficient Tregs into murine recipients has been associated with systemic autoimmunity and premature death, effects not completely reversed by preservation of CTLA-

4 expression on Teff (43, 44). In murine models of cancer, adoptive transfer of purified CTLA-4 deficient Tregs is associated with enhanced antitumour immunity(45).

Figure 1.2: Major Mechanisms by Which Tregs Can Directly Suppress Responder Foxp3⁻ T Cells. (35)
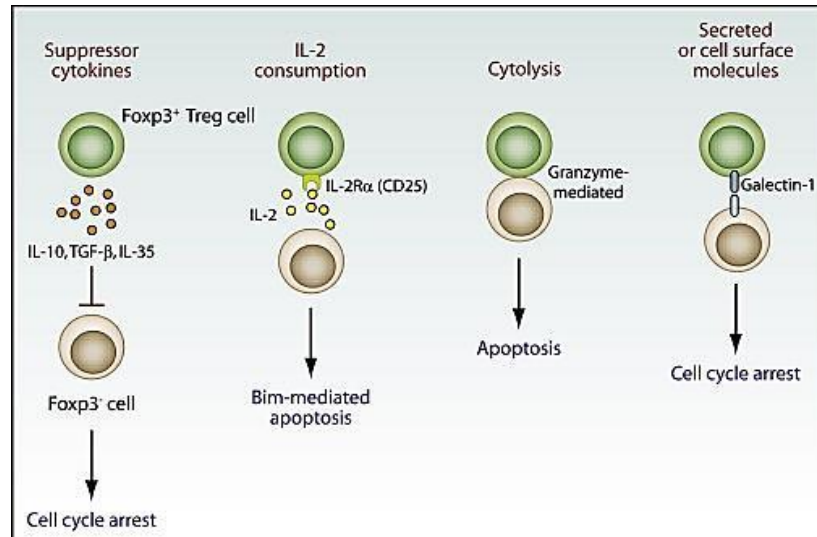
1.2.5   Immunotherapeutic potential of CTLA-4 blockade

There is broad consensus that CTLA-4 is a good target for immunotherapeutic manipulation, as blockade of this receptor through mAb technology has been shown to 'release the brakes' on immune responses in pre-clinical models of cancer and in human subjects with cancer in the context of clinical trials (46, 47). In the murine melanoma setting, CTLA-4 blockade with mAb is associated with a favourable shift in intratumoural lymphocyte predominance from regulator to effector T cells and tumour rejection (46). Mechanistically, Quezada and Peggs showed that maximal anti-tumour activity is achieved when αCTLA-4 mAb binds both Teff and Treg compartments in vivo (48). Specifically targeting Tregs afforded no tumour protection and specifically targeting Teff cells mediated partial protection in these experiments.

Ipilimumab, an IgG1k anti-human CTLA-4 is now licensed for use in humans by the Food and Drug Administration (FDA, USA) and the National Institute for Clinical Excellence (NICE) for treatment of metastatic melanoma (49). The utility of this treatment is limited by the fact that only a subset of patients will respond and that many will develop autoimmune complications, sufficiently severe in up to 25% of patients (Grade 3-4 toxicity) as to preclude further treatment with Ipilimumab (50). A recent review of Ipilimumab toxicity reported that 29 of 110 treated patients experienced grade 3/4 immune-related adverse events (IRAEs) and that

these patients had higher than expected 1-, 2- and 3-year survival rates of 79, 59 and 46% compared with 24, 17 and 15% in the group that did not experience significant toxicity (P<0.0005) (51). Pooled analysis of long-term survival data from Phase II and Phase III trials of Ipilimumab in unresectable metastatic melanoma defines overall survival as 20%-26% at 3 years, with a plateau in the survival curve at 3 years demonstrating durability of response with this agent (52). Many groups are investigating biomarkers to generate a predictive tool to identify patients likely to respond and/or likely to suffer IRAEs from CTLA-4-mAb-mediated blockade.

There is lack of consensus on whether the specificity of CD4 T cells that proliferate in response to CTLA-4 blockade is broadly reactive to self MHC/ubiquitous antigens and capable of significant toxicity, or whether a tissue antigen specific skew in CD4 T cell expansion promotes improved anti-tumour responses (53). TCR spectratyping of peripheral T cells from spleens of CTLA-4$^{-/-}$ mice revealed conflicting results: in one study a diverse and unbiased TCR repertoire was identified, suggesting a universal, antigen-independent mechanism of activation and expansion (54), and in another study a restricted repertoire was observed (55). Ise et al show that adoptive transfer of antigen-specific CTLA-4$^{-/-}$ T cells results in TCR-dependent accumulation in tissues expressing the tissue-specific antigen, supporting the hypothesis that absence of CTLA-4 on antigen restricted T cells could generate a tissue-specific effective immune response (53).

Snyder et al explored this further in a clinical study of patients treated with CTLA-4 blockade. They performed whole-exome sequencing on tumours and matched blood samples and revealed a neoantigenic profile in tumours, the presence of which correlated with strong responses to CTLA-4 blockade. Neoantigens were shown to activate Ipilimumab-treated patient T cells in vitro (56). This is encouraging data as it may in future allow tailoring of treatment to likely responders based on a genetic signature. What we do not ascertain from this study is whether the incidence of IRAEs was higher in responders, and/or whether this risk can be defined on a genetic level. If there is a correlation, then it becomes even more critical to develop tumour- specific targeting strategies.

It is widely reported that CTLA-4 polymorphisms are associated with autoimmunity in humans, but there is limited published data on the impact of these polymorphisms on tumour immunology. In one study, patients with metastatic melanoma treated with CTLA-4 blockade were demonstrated to possess seven different common single nucleotide polymorphisms (SNPs) of CTLA-4, three of which were associated with clinical responses to treatment but no

clear correlation with (severe) autoimmune sequelae. It is possible that the variable clinical response/toxicity profiles observed in clinical studies of αCTLA-4 could relate to common genetic variations in the CTLA-4 gene (57, 58).

Given that a significant number of patients receiving therapeutic αCTLA-4 mAbs do not get an anti-tumour response or develop autoimmune toxicity that necessitates cessation of treatment, it is appropriate to endeavour to target CTLA-4 blockade to the tumour microenvironment more specifically than is currently achieved with systemic administration of antibody. In an attempt to uncouple the beneficial anti-tumour effect of αCTLA-4 mAb therapy from IRAEs, Simmons et al generated a GM-CSF secreting tumour cell vaccine (Gvax) to secrete αCTLA-4 mAb for use in vivo in murine models of B16F10 melanoma and CT26 adenocarcinoma. They showed that mice treated with αCTLA-4 mAb secreting tumour cell vaccine had similar overall survival to those treated with unmodified tumour cell vaccine and systemically administered αCTLA-4 mAb, but with lower serum αCTLA-4 levels and lower serum concentrations of autoimmunity-associated antibodies. They conclude that durable, local secretion of αCTLA-4 mAb from modified Gvax improves the anti-tumour efficacy of tumour cell vaccination with lower systemic antibody exposure, and has the potential to reduce the incidence of IRAEs (59).

We believe that one of the potential problems with tumour-cell vaccination strategies is a reliance on the presence of functional, endogenous non-exhausted T cells of sufficient avidity for target antigen to induce anti-tumour responses. Even if a vaccine can induce or enhance a response to one or more tumour-associated antigens (TAAs), most studies have failed to document a clinical benefit, including gp100 in melanoma (49, 60). Adoptive cellular therapy using endogenous tumour-derived, tumour-reactive T cells expanded in vitro or genetically modified T cells redirected through CAR or TCR towards tumour-associated antigen, hold significant promise as immunotherapeutics and could conceivably be used as vehicles for payload secretion of αCTLA-4 mAb to the tumour, minimising antibody exposure in the periphery, or modified to lose intrinsic CTLA-4 expression to potentially render transferred T cells resistant to tumour-mediated co-inhibition.

1.2.6   α-CTLA-4 antibody engineering

Antibody-mediated blockade of CTLA-4/B7 interactions in preclinical models of cancer is thought to be efficacious through a dual effect on Tregs and activated Teff (48). CTLA-4 blockade in vivo has been shown to mediate expansion of Teff and Treg populations in secondary lymphoid organs (LN) and peripheral blood (PB) of mice and humans (61-63). In the tumour, αCTLA-4 mAb promotes an increase in the ratio of Teff to Treg cells, which is not seen in the periphery and has previously been ascribed to preferential expansion of Teff over Treg cells in this niche. It is unclear why this ratio reversal should be restricted to tumour and why targeting a receptor on two diametrically functionally opposed populations promotes tumour rejection rather than equilibrium or escape (61, 63-66).

Simpson et al showed that the mode of action of αCTLA-4 mAb is microenvironment-dependent. In LN, αCTLA-4 mAb is associated with an expansion of absolute numbers of Teff and Tregs, but in the tumour αCTLA-4 mAb results in Teff expansion, with a dramatic parallel diminution of Tregs (67). Simpson demonstrates that αCTLA-4 mAb mediates depletion of Tregs in the tumour by antibody dependent cellular cytotoxicity (ADCC), dependent upon tumour-infiltrating FC γ receptor IV (FcγRIV) expressing macrophages which act as effectors. Depletion of intratumoural Treg rather than Teff is due to their higher surface expression of CTLA-4. Interestingly, a small population of CTLA-4^{hi} Teff was also eliminated, highlighting the importance of receptor density for ADCC using mAbs (67, 68).

Given the ADCC hypothesis described above, attention has turned towards the potential impact of mAb isotype on effector function. Selby et al showed complete rejection of murine CT26 adenocarcinoma with murine IgG2a αCTLA-4 mAb (isotype classically associated with ADCC), but not with murine IgG1 αCTLA-4 isotype (associated with blocking function) (69). Recent evidence reports a critical role for activating FcγRs in the activity of antibodies targeting CTLA-4, as different FcγRs can alter the biological impact of mAb therapy (67-69).

The final activity of a given immunomodulatory mAb may therefore vary in PB, LN and tumour depending on the relative target molecule density on individual T cell subsets, the presence of innate effector cells and FcγR expression. This raises the possibility of differential biological responses to treatment between the primary tumour, the periphery and metastatic sites within an individual patient and between patients (70) and informs the scope of our project.

1.3   Aims of the project

CTLA-4 is recognised to compromise anti-tumour immune responses and its mechanism of action is purported to be multifactorial. Blockade of endogenous CTLA-4 through systemic mAb therapy promotes rejection of some human tumours, but is often complicated by severe autoimmune toxicity. We aim to explore different methods for targeting CTLA-4 inhibition to the tumour microenvironment with the objective of improving anti-tumour responses and minimising the incidence of IRAEs.

Ablation of CTLA-4 from tumour-reactive T cells

One possible approach is genetic ablation of CTLA-4 from tumour-reactive T cells. This could in theory generate a therapeutic agent with resistance to inhibitory signalling within the tumour microenvironment to permit engraftment and persistence and an augmented anti-tumour activity profile. Provided the cells are tumour-antigen specific, the risk of toxicity to non-tumour tissues is minimal. The possible disadvantages of this approach mainly relate to new paradigms in the field which support a predominantly cell extrinsic suppressive mode of action for CTLA-4, largely mediated through B7 sequestration by Tregs (9, 15) and other CTLA-4^{hi} populations (26). This could potentially compromise the efficacy of a CTLA-4 ablated adoptively transferred tumour reactive population, through endogenous T cells providing a CTLA-4 reservoir to sequester B7.1 and 2 on APCs. Corse and Allison describe the effector extrinsic effect of CTLA-4-replete T cells (WT) acting in trans to inhibit the accumulation of CTLA-4 depleted T cells (ko) and note that it is dependent upon the ko:WT ratio, such that beyond ratios of 1:1 or 1:2, hyperaccumulation of CTLA-4$^{-/-}$ T cells was no longer restored to WT T cell frequencies at the peak of expansion (26). We believe that adoptive transfer of CTLA-4-deficient T cells into the right (e.g. lymphodepleted) environment with a high ko:WT CTLA-4 ratio, would support the expansion and activation of CTLA-4-deficient cells.

Mab-mediated blockade of CTLA-4 on tumour-reactive T cells

An alternative strategy is the generation of tumour-reactive T cells to secrete CTLA-4 blocking antibody/single chain Fv. Payload secretion of αCTLA-4 mAb in response to tumour-specific TCR engagement with antigen could potentially restrict antibody exposure to the tumour

microenvironment and minimise systemic autoimmune toxicity. This has the potential to overcome the possible limitations of CTLA-4 ablation described above.

We accept that αCTLA-4 mAb secretion from tumour-cell-vaccines has been reported previously to good effect in a preclinical model (59). At the current time we believe that insufficient evidence supports the further investigation of tumour vaccines in melanoma and would rather concentrate the potential gains of tumour-targeted blockade of co-inhibitory receptors to adoptive cellular therapies, and in particular, to CAR T cell therapies. There is currently a strong clinical research emphasis in our institution and others to exploit the potential of CAR-based and other adoptive cell transfer models to treat cancer. Genetic modification of CAR T cells to ablate CTLA-4 or to secrete αCTLA-4 mAb could offer a potential advantage in terms of engraftment and persistence, two frequently observed limitations of this new technology.

Summary

Assimilating these hypotheses, we plan to investigate the relative value of cell intrinsic CTLA-4 ablation versus cell extrinsic CTLA-4 blockade in a well-characterised murine melanoma model, examining genetic ablation of CTLA-4 from tumour-reactive T cells for adoptive transfer with localized secretion of αCTLA-4 mAb from tumour reactive T cells.

The murine melanoma model system in question centres upon the transgenic TRP1 mouse. This mouse possesses an MHC Class ll restricted TCR targeting the endogenous melanocyte differentiation antigen tyrosinase-related-protein (TRP1) found on melanoma tumours and normal melanocytes (71, 72). The TRP1 model is well described and utilised in the literature in models of adoptive transfer due to the potent, reproducible anti-melanoma activity of the transgenic T cells. It is recognised that exposure to TRP1 expressing tumours such as B16/BL6 allows transgenic CD4+ TRP1 T cells to expand and differentiate into Interferon Gamma (IFNγ) secreting cytotoxic T cells (47). T-cell secretion of IFNγ into the tumour microenvironment leads to upregulation of MHC Class II on the tumour promoting further T cell activation and immune lysis of tumour (46,72).

Our aim is to genetically modify and adoptively transfer TRP1 CD4 T cells into melanoma-bearing C57/BL6 mice to help answer our experimental hypotheses. Our primary outcome measures are tumour growth and infiltration and our secondary outcomes are an assessment

of lymphocyte activation and function and the effect of CTLA-4 manipulation on these parameters. There are no robust models available to us to assess self-reactivity other than serum antibodies as markers of autoimmunity.

We recognise from clinical studies that targeting CTLA-4 blockade to the tumour microenvironment has the possible advantages of enhancing anti-tumour efficacy by concentrating the antibody amongst TILs whilst minimising systemic autoimmune toxicity from indiscriminate endogenous polyclonal CD4 T cell activation in the periphery.

CHAPTER 2

2. MATERIALS AND METHODS

2.1 Molecular biology techniques

2.1.1 Molecular buffers and bacterial media

Plasmid DNA was stocked at 1µg/µL in nuclease free water (Gibco) and stored at -20∘C. The bacterial media and buffers are listed in Table 2.1.

Table 2.1   Buffers and media for molecular biology

Buffers/media	Composition
1 X phosphate-buffered saline	137mM NaCl, 2mM KCl, 10mM sodium hydrogen phosphate (dibasic), 2mM potassium hydrogen phosphate (dibasic) (pH 7.4)
1 X tris-acetate EDTA buffer (TAE) EDTA	40mM Tris (pH 7.8), 20mM sodium acetate, 1mM
Luria Bertani agar	LB broth plus bacto-agar 15g/L
Luria Bertani broth	1% bacto-tryptone, 0.5% bacto-yeast extract, 10% NaCl (pH 7.0)
6 X gel loading buffer	0.25% bromophenol blue, 0.25% xylene cyanol FF, 30% glycerol in water
Hyperladder I and II	

2.1.2 Restriction digestions and ligations

New England Biolabs (NEB) (Ipswich, MA) supplied all restriction enzymes. Diagnostic plasmid DNA digestions were incubated for 2-3 hours at 37∘C according to manufacturers' instructions (0.5µL each enzyme, 3µL 10X buffer, 1µg DNA, made up to a final volume of 30µL in nuclease free water (Gibco).

Plasmid DNA digestions prior to ligation were incubated at 37◦C for 3 hours (5µg plasmid DNA, 5µL each enzyme, 10µL 10X buffer, made up to a final volume of 100µL in nuclease free water), and then run on and extracted from a 1.5% agarose gel.

DNA fragment ligations were performed using the NEB Quick Ligase kit (Ipswich, MA). Ligations used 1.5µL quick ligase, 1-1.5µL digested plasmid(s), 10µL buffer, made up to a final volume of 20µ with nuclease free water, and were incubated at room temperature (RT) for 5 minutes, transferred directly onto ice, and then used for bacterial transformation.

2.1.3   Agarose gel electrophoresis

Electrophoreses were run in 1% agarose gels, (Invitrogen, Carlsbad, CA) with 5µg/mL ethidium bromide (Dutscher Scientific, Essex, UK). Hyperladder I and/or II (Bioline, UK) were run concurrently to accurately size DNA bands obtained.

DNA band sizes were assessed on the non-UV transilluminator 'The Dark Reader/ DR-195M' (MoBiTec Molecular Biotechnology). Relevant bands were cut out and DNA purification was performed according to the QIAquick Gel Extraction kit (Qiagen, Hilden, Germany) manufacturers' instructions.

2.1.4   Transformation of competent bacteria

Competent bacteria were purchased from NEB (Ipswich, MA) and stored at -80◦C in aliquots of 50µL. High efficiency NEB5α C2987H E-Coli were used for ligation reactions. Sub-cloning efficiency NEB5α C2988J E-Coli were used for sub-cloning and retransformation.

For transformation, competent bacteria were thawed on ice, transferred into 0.5µL heat-shock-optimised eppendorf tubes, and inoculated with 1-2µg of plasmid DNA or 3-5µL of ligation mix. Following incubation on ice for 30 minutes, bacteria were heat-shocked for 35 seconds at 42◦C and then returned onto ice for 2 minutes. Transformed bacteria were then incubated in 250µL of super optimal broth (NEB, Ipswich, MA) in a bacterial shaker at 37◦C, at 200 revolutions per minute (rpm) for 40 minutes, prior to being spread on warmed, antibiotic-laden LB agar plates. Plates were incubated overnight at 37◦C and all clones were selected based on appropriate display of antibiotic resistance, most commonly ampicillin (50µg/mL).

2.1.5   DNA purification and quantitation

Single colonies were picked from LB agar plates and grown as minipreps overnight at 37◦C in 3mL of LB broth with ampicillin (50µg/mL). Midipreps (150mL) were seeded from successful minipreps. The QiaPrep Spin Miniprep kit and the Macherey-Nagel Nucleobond Xtra kits were used to extract and purify plasmid DNA from mini- and midipreps respectively, according to manufacturers' instructions.

DNA concentration was defined by the Thermo Scientific NanoDrop 1000 spectrophotometer using the formula: Concentration (ng/µL) = $Absorbance_{260nm}$ x Dilution factor x 50.

2.1.6   Polymerase chain reaction (PCR) and Oligonucleotide Extension PCR

PCR reactions were performed with the very High-Fidelity Phusion Polymerase kit (NEB, Ipswich, MA). It possesses a pyrococcus-like polymerase enzyme fused to a double strand DNA binding domain which facilitates simultaneous fusions of many different fragments with sequences not typically tolerated by polymerases and with almost no introduced PCR error. Table 2.2 summarises the reagents required for one 50µL PCR reaction. The reactions were run in a Bio-Rad (UK) thermal cycler, looped to 35 cycles (parameters listed in table 2.3).

Gene synthesis by oligonucleotide extension/overlap PCR is a technique used in the generation of several constructs in this project and the High-Fidelity Phusion Polymerase kit is key to this technique in our hands. It is possible to synthesise short pieces of DNA by assembling overlapping oligonucleotides using PCR-mediated ligation. The initial sequence design comprises a series of separate hybridisation units which constitute the complete sequence required. Forward and reverse oligonucleotides are designed to overlap each hybridisation unit such that when the oligonucleotides are mixed, PCR-ligated and undergo PCR amplification, a full-length product is generated (see Figure 2.1). The next step is to sub-clone the gene synthesised product into an expression vector. Due to the risk of single base mutations using this technique, we mandate that multiple clones be screened by restriction digest prior to sequencing and downstream testing.

Figure 2.1: gene assembly by oligonucleotide extension PCR
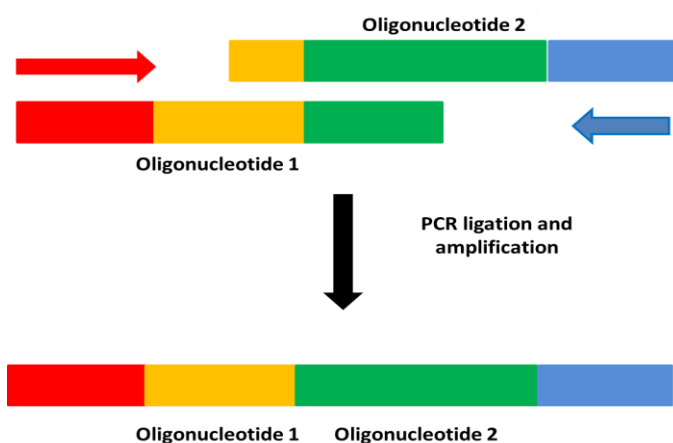
Table 2.2   Polymerase chain reactions (for one reaction – total volume 50µL)

Component	Stock concentration	Volume added	Final concentration
HiFiD buffer	5x	10µL	1x
dNTPs	2.5mM	1.5µL	200µM each dNTP
Forward primer	1µg/µL	1µL	0.5µM
Reverse primer	1µg/µL	1µL	0.5µM
Phusion polymerase		0.5µL	
Template	1µg/µL	1µL	0.5µM
Nuclease free water		to final volume 50µL	

Table 2.3   Thermocycler parameters for PCR (35 cycles)

Phase	Time	Temperature
Denature and activate Phusion	2 minutes	98◦C
Denature amplicons	40 seconds	98◦C
Anneal oligos to template	40 seconds	65◦C
Extension	1 minute/kb of amplification	72◦C
Recursion	Loop to denaturation step x35 times	
Clean up any unfinished amplifications	10 minutes	72◦C

2.1.7 Sequencing

Verification of DNA sequences was performed by the UCL WIBR Scientific Support service using standard or customised primers.

2.2 Tissue culture

2.2.1 HEK 293T cells

HEK 293T cells are derived from human embryonic kidney cells and are characterised by their ease of transfection and high transgene expression (73). 293T cells fulfilled two main functions in this project: expression testing of constructs by transfection, and as a retrovirus producing cell line. Optimal culture conditions involved 1:4 passage every 2-3 days in Isocove's Modified Dulbecco's Medium (IMDM) (Sigma Aldrich), supplemented with 10% heat-inactivated fetal calf serum (FCS) (Invitrogen/Gibco), 2mM L-glutamine (Gibco), 100U/mL penicillin and 100µg/mL streptomycin (Gibco).

2.2.2 SupT1 cells

In this project, SupT1 cells underwent retroviral transduction to create human and murine CTLA-4 expressing target cell lines. They are a human T-lymphoblast suspension cell line expressing CD4, CD8, CD3,but not surface immunoglobulin (Ig), CD2 or CD25 (74). Optimal culture conditions include 1:4 passage every 2-3 days in (complete) Roswell Park Memorial Institution medium (RPMI-1640) supplemented with 10% heat-inactivated FCS (Invitrogen/Gibco), 2mM L-glutamine (Gibco), 100U/mL penicillin and 100µg/mL streptomycin (Gibco).

2.2.3 B16/BL6 murine melanoma

The highly tumorigenic and poorly immunogenic B16/BL6 melanoma cell line has been described previously (75). A fresh aliquot was thawed for each new experiment, passaged 1:4 every 2-3 days for optimal cell health, and maintained in complete RPMI. In tumour challenge

experiments, cells were injected intradermally to the right murine flank in 100μL of sterile phosphate buffered saline.

2.2.4 GM-CSF secreting cellular vaccine (Gvax)

B16/BL6-expressing granulocyte-macrophage colony stimulating factor (GM-CSF) has been described previously (75). Irradiated at 150Gray, each dose is 1×10^6 cells which is injected in sterile PBS intradermally into murine recipients on the contralateral flank to the B16/BL6 tumour site.

2.2.5 Transfection of cell lines

Transfection is the process by which DNA is introduced into a cell for short-term transcription, translation and gene expression and is essential for checking new plasmid constructs.

The protocol stipulates a 72 hours timeframe: 293T cells are plated on day 1 at a density of 1.5×10^6/100mm plate in 10mL of complete IMDM. After 24 hours, cells are 50-60% confluent and ready for transfection with 470μL of plain RPMI, 30μL Genejuice (Merck Millipore) and a maximum of 12.5μg of plasmid DNA. The mixture is incubated at room temperature for 15 minutes and then added drop-wise to the plated 293T cells before cells are returned to the incubator at 37∘C and 5% CO_2. Transfection can be checked at 48-72 hours. Genejuice (Merck Millipore) is a transfection reagent that comprises a nontoxic cellular protein and a small amount of a novel polyamine that together form lipid miscelles which can hold small amounts of DNA. Fusion of these miscelles with the cellular envelope injects DNA directly into the cell.

2.2.6 Antibody binding experiments

Secretory antibody constructs were checked by transiently transfecting 293T cells followed by harvesting of the (antibody-rich) culture supernatant at 72 hours through a 0.22μm filter. Incubation of supernatant with CTLA-4 expressing cell targets for 30 minutes followed by secondary anti-murine Fc antibody staining identified successful transfectants.

2.3   Retroviral vectors

2.3.1   Vector and retrovirus production

Modified wild type (WT) retroviruses are vehicles for the delivery, stable integration and expression of cloned genes into (dividing) cells. The vector must behave as a retroviral genome to allow it to pass as a virus from the producer cell line, and so contains regions of wild type retroviral genome 'in cis' for incorporation into a retroviral particle. This includes the packaging sequence (to ensure capsidation of vector RNA into virions), the tRNA binding site (to allow reverse transcription of vector RNA into DNA in the target cell), long terminal repeat (LTR) sequences that permit 'jumping' of reverse transcriptase between RNA strands during DNA synthesis, and other sequences necessary for integration of vector DNA into the host cell chromosome. Vector genomes do not require that the viral structural proteins gag, pol and env be retained, with the result that non-viral genes can be cloned into the remaining space. The overall length of the construct cannot exceed 10 kilobase-pairs (kbp), since packaging efficiency declines with increasing length of RNA (76).

All retroviral vectors used in this project are based on the Moloney murine leukemia virus plasmid, and virus was produced by transient triple transfection of HEK 293T cells with envelope, gag-pol and vector plasmid DNA (77).

Selection of viral envelope is dependent upon the target cell. The amphotropic RD114 simian type D envelope plasmid can deliver genes to dividing cells of most mammalian species, including human cell lines and primary lymphocytes (78). For primary murine lymphocytes, typing of retroviral particles with ecotropic receptor results in high transduction efficiency. These and Peqpam-env gag-pol plasmid were kindly supplied by Martin Pule from GMP grade stock.

To generate virus, 293T cells are plated at a density of 1.5×10^6/100mm plate in 10mL of cIMDM on day 1. On day 2, cells that are 50-60% confluent can undergo triple transfection with 470uL of plain RPMI, 30uL of Genejuice (discussed in Chapter 2.2.6), 3.125µg/plate of envelope plasmid, 4.6875µg/plate gag-pol and 4.6875µg/plate of vector (12.5µg represents the maximum DNA load for 30uL of this reagent). Following incubation at room temperature for 15 minutes, the mixture is added dropwise to plated 293T cells. Virus is harvested at 48 and 72 hours post-transfection and is mixed, aliquotted and frozen directly at -80∘C.

2.3.2 Transfer constructs

All retroviral vectors used in this project were based on the Moloney murine leukemia virus plasmid (77), and the SFG.IRES2.eBFP and SFG.IRES2.eGFP backbones for subcloning were kindly provided by Martin Pule. Use of the internal ribosome entry site (IRES) element has been previously described (79). The retroviral LTR promoter has been shown to be associated with long term expression of inserted genes (77). Emerald green fluorescent protein (eGFP) (accession no. U55761) and blue fluorescent protein (eBFP) (accession no. AX_766758) were two of the marker proteins expressed in the original constructs. All recombinant DNA manipulations were verified by DNA sequencing (see section 2.1.7).

Plasmids encoding human and murine CTLA-4 for cell surface expression

The sequences for human and murine CTLA-4 were located on www.ensembl.org. DNA was generated by Phusion PCR using High-Fidelity Phusion Polymerase (NEB, Ipswich, MA) and human (blood-derived) and murine (splenocyte) genome as template. Fragments were cloned into SFG.I2.eBFP2 to create *SFG.huCTLA4.I.dCD34ngg* and *SFG.muCTLA4.I.dCD34ngg.* Truncated human CD34 (dCD34) was used as a marker gene as eBFP is limited by dim fluorescence and fast photo-bleaching. CD34 expression enables selection of transduced cells with a commercially available kit (Miltenyi Biotech, Auburn, CA)(see figure 3.1 for plasmid maps).

Plasmids encoding 10D1 anti-human CTLA-4 mAb

The sequence for 10D1 therapeutic anti-human CTLA-4 antibody was extracted from a patent filed by Medarax (US2010047244 (A1) and was originally derived by vaccinating a human Immunoglobulin transgenic mouse (80). It has been adapted by Martin Pule into a single chain Fv and constructed by oligonucleotide assembly (see Chapter 2.1.6).

Plasmids permitting 10D1 cell surface expression, KDEL-restriction (i.e. retention within the endoplasmic reticulum) and secretion of scFv were generated in the first instance. This was followed by a second phase of recloning 10D1 scFv as a full length antibody in different isotypic forms for secretion by cells, with a novel, truncated, non-immunogenic, non-signalling cell-surface marker (dmuCD19). Tricistronic vectors comprised 10D1 heavy and light chains linked by TAV-2A (ref) with dmuCD19 located behind IRES (see Chapter 5, figure 5.3 for

plasmid maps: *SFG.mAb_10D1_mIgG1-LC-2A-HC.I2.d_muCD19* and *SFG.mAb_10D1_mIgG2a-LC-2A-HC.I2.d_muCD19)*. The murine IgG1 backbone, pFUSEss-CH1g-mG1, was sourced from Invivogen, and was grown in low salt Zeocin broth.

Plasmids encoding UC10-4F10 anti-murine CTLA-4 mAb

The sequence for the UC10-4F10 anti-murine CTLA-4 antibody was kindly shared by Jeffrey Bluestone (81). As with 10D1, UC10-4F10 scFv was initially generated by oligonucleotide assembly. Testing of secreted scFv revealed that it did not effectively bind murine CTLA-4 despite correct sequence. It was recloned as a full length antibody in IgG2a and IgG1 isotypic forms in tricistronic format with a dmuCD19 marker (*SFG.mAb_4F10bluestone_mIgG1-LC-2A-HC.I2.d_muCD19* and *SFG.mAb_4F10bluestone _mIgG2a-LC-2A-HC.I2.d_muCD19*).

Plasmids encoding 9D9 anti-murine CTLA-4 mAb

9D9 anti-murine CTLA-4 in IgG1 and IgG2a isotype were generated through processes outlined above. Once species-specific binding was established, full length sequences were subcloned into tricistronic vectors to generate *SFG.mAb_9D9anti-CTLA4_mIgG1-LC-2A-HC.I2.d_muCD19* and *SFG.mAb_9D9anti-CTLA4 _mIgG2a-LC-2A-HC.I2.d_muCD19* (see figure 6.1 for plasmid maps).

Plasmids encoding human and murine CTLA-4 targeting siRNA

pSuper.retro.puro is a mammalian expression vector that directs intracellular synthesis of siRNA transcripts. We modified it to replace the puromycin resistance sequence with truncated murine CD19 as a marker gene (82). We ligated a single pair of annealed oligonucleotides (performed at 95∘C) into modified pSuperRetro.d_muCD19 between two unique restriction sites to create *pSuperRetro.d_muCD19.siRNA_**hu**CTLA4* and *pSuperRetro.d_muCD19.siRNA_**mu**CTLA4* (see figure 3.2a for plasmid maps).

2.3.3   Retroviral transduction of suspension cell lines

Retroviral transduction requires target cells to be in exponential phase to effectively incorporate transgene, and suspension cell lines were split (1:10) 24 hours prior to retrovirus exposure. Retronectin is a chimeric peptide of human fibronectin produced in E-Coli and has been shown to improve retrovirus-mediated gene transfer into mammalian cells due to co-localisation of virus and target cells. A retronectin-coated, non-tissue culture (TC) treated 6-well plate should be prepared and refrigerated in advance.

At 24 hours, retronectin is aspirated from wells prior to a 30 minute incubation of 250µL/well of correctly pseudotyped viral supernatant at room temperature. Cells are plated at a concentration of $3x10^5$/well with an extra 1.5mL of retroviral supernatant per well. Spin transduction occurs at 1000g for 40 minutes at room temperature (83) and transduction efficiency is assessed 48-72 hours later.

2.3.4   Retroviral transduction of adherent cell lines

Adherent cells will tolerate multiple transductions over successive days and it is possible to achieve high expression of a single transgene and/or to express multiple transgenes. On day 1, cells are trypsinised, washed and plated at $3x10^5$cells/well of a 6-well plate in complete medium. The first transduction step is at 24 hours when complete medium is replaced by (2mL) viral supernatant plus   1µL of 10mg/mL Polybrene. Second and subsequent transductions are performed daily from day 3 onwards provided cells are not over-confluent. Polybrene (hexadimethrine bromide) is a cationic polymer used to increase the efficiency of retroviral infection of cells in culture by neutralizing the charge repulsion between virions and sialic acid expressed on the cell surface (84).

2.4   In vivo and ex vivo experiments

2.4.1   Mice

One of the goals of the project is to generate a method for selectively expanding and transducing tumour reactive lymphocytes with a view to blocking or knocking down CTLA-4. We elected to test our constructs in the well described B16/BL6 transplantable murine

melanoma model using transgenic T cells for adoptive transfer into C57BL/6 recipients. All animals were handled in accordance with institutional guidelines and home office regulation.

2.4.1.1 C57BL/6 mice

Males were supplied by the Charles Rivers Facility (Margate, Kent) at 6-8 weeks of age to act as B16/BL6 recipients.

2.4.1.2 Human CTLA-4 transgenic mice (Hu152Tg)

Transgenic animals were bred and colonies maintained at the Charles Rivers Facility (Margate, Kent).

Human and mouse CTLA-4 genes are composed of four exons, with overall protein sequence homology of 76%. Human CTLA-4 is capable of interacting with mouse B7-1 and B7-2 to biological effect. At Memorial Sloan Kettering Cancer Centre, a 17-kb DNA construct coding for a chimeric CTLA-4 molecule comprising human extracellular and mouse transmembrane and intra-cytoplasmic domains was used to create a human CTLA-4 transgenic mouse (Hu152Tg). The complex chimeric CTLA-4 DNA construct was generated using bacterial artificial chromosome cloning vector (BAC) technology to include upstream regulatory sequences that govern gene expression. BACs accommodate large inserts (150-250 kb or more) and do not pose a strong risk of genetic rearrangement. They can be introduced into chromosomal DNA by electroporation or transfection or by microinjection into the oocyte pronucleus where they integrate at random in the genome.

Backcrossing of the Hu152Tg mouse into murine CTLA-4 $^{-/-}$ animals produced human CTLA-4 homozygous progeny which were remarkable in their normal lifespans, normal lymphoid and myeloid development, and lack of features to suggest autoimmunity. Cross species CTLA-4-B7 ligation protects Hu152Tg from the lymphoproliferative disease seen in CTLA-4$^{-/-}$ mice (41, 42, 48). The CTLA-4 transgenic strain is further discussed in Chapter 5.1.5.

2.4.1.3 TRP1 transgenic mice

This Class II restricted TRP1 transgenic CD4+ T cell mouse strain recognises a peptide derived from the melanoma differentiation antigen, tyrosinase-related-protein 1 (TRP1) presented on I-Ab.

The TRP1 TCR was generated from white-based brown B^w (cappuccino) mutant mice. The B^w mutation is an irradiation-related inversion of exon 1 of the tyrp1 gene resulting in total absence of TRP1 protein in melanocytes and other tissues.

B^w mice were backcrossed for 8 generations onto the C57BL/6 background using a speed congenic-based technique and immunised once with 10^7 plaque forming units (pfu) of recombinant TRP1 vaccinia virus (TRP-1 rVV) followed by 100μg of murine TRP1 protein three weeks later. Ultimately, hybridomas were generated and screened for reactivity against TRP1 protein/truncated TRP1 peptides. The most reactive clone was defined as having Vα3.2 and Vβ14 TCR chains which were cloned, validated by sequencing, subcloned into TCR cassette vectors, and co-injected into fertilized C57BL/6 embryos that yielded 13 founders. Founder number 9, in which the transgene insertion site was found on the Y chromosome, was successfully bred and crossed into RAG1$^{-/-}$ (black) mice and subsequently into RAG1$^{-/-}$ B^w (cappuccino) mice to create TRP1 transgenic mice[72]. The monoclonal TCR directed against TRP1 is avid, as it has not undergone central or peripheral deletion [85].

2.4.1.4 TRP1 CTLA4$^{-/-}$ transgenic mice

TRP1 mice were crossed with CTLA-4$^{-/-}$ mice to create congenically marked CD45.1$^{+/+}$ B^W RAG$^{-/-}$ TRP1CTLA-4$^{-/-}$ transgenic animals [67]. These CTLA-4 deficient mice will act as a comparator against which to assess the impact of proposed strategies for CTLA-4 silencing.

2.4.2   Harvesting spleens and lymph nodes

Organs were collected in cRPMI and dispersed through a 70μm nylon mesh (BD Falcon). Cells were washed in Phosphate Buffered Saline (PBS) prior to incubation in red cell lysis buffer (Sigma-Aldrich) for 5 minutes at room temperature, followed by a double wash step in sterile PBS prior to downstream processing/applications.

2.4.3   Generation of bone marrow-derived macrophages

Bone marrow (BM)-derived macrophages were produced according to the protocol referenced here, with some minor modifications (86). Bone marrow of C57BL/6 mice was flushed aseptically from femora tibiae and fibulae in cRPMI using a syringe and needle technique. The resulting cellular effluent was washed in cRPMI and resuspended at a concentration of 4×10^5 cells per 100mm non-TC-treated plate in conditioned medium (RPMI + 20% FCS + 30% L929 supernatant. L929 is a fibroblast cell line that secretes M-CSF (87). L929 cells are cultured in cIMDM (with 10% FCS) and after 72 hours in vitro, their supernatant is collected, centrifuged at 3000rpm for 5 minutes and filtered with a bottle top filter prior to making aliquots for downstream applications.

BM-derived macrophages are differentiated in vitro over 5-7 days in conditioned medium. Lipopolysaccharide (LPS) is added at a concentration of 10ng/mL (Sigma Aldrich) to cultures on day 4 to promote an inflammatory M1 phenotype. Harvesting requires the use of 0.25% trypsin (Invitrogen), and each 10cm dish yields approximately 7×10^6 macrophages. Quantitation and flow cytometric assessment of macrophage purity and differentiation status precedes downstream applications. A typical antibody panel would comprise MHC class II (Ia/b), murine FC gamma receptor 4 (FcγRIV), CD11b and iNOS/NOS2 (nitric oxide synthase 2). Plating for ADCC assays is described in Section 2.4.11.

2.4.4   Purification of T cells from spleen and lymph node

Magnetic microbead purification of T cells was achieved by negative selection for CD3 or by positive or negative selection for CD4. The kits and columns were used according to manufacturers' instructions (Miltenyi Biotech, CliniMACS® cell sorting, Auburn, CA).

2.4.5   Retroviral transduction of murine lymphocytes

2.4.5.1 Polyclonal lymphocyte transduction

Retrovirus was prepared and frozen at -80∘C in advance as described in Chapter 2.3.1. Harvesting of spleen and lymph node was performed according to Chapter 2.4.2, and purification of T cells as described in Chapter 2.4.4.

The resulting lymphocyte pellet was analysed by flow cytometry and counted using the MUSE cell analyser (Merck Millipore) to enable T cell quantitation (see Chapter 2.4.7). T cells were then stimulated in vitro at 37∘C for 24 hours at a concentration of $1x10^6$ T cells/well of a TC-treated 24-well plate in 2µg/mL Concanavalin A (ConA) and 1ng/mL of Interleukin 7 (IL-7)[88]. Anti-CD3 (1µg/mL) and anti-CD28 (1µg/mL) coated non-TC-treated plates were also used as an alternative to ConA/IL-7 for T cell stimulation [135].

After 24 hours at 37∘C in 5% CO_2 T cells were harvested, counted and $1x10^6$/well added to retronectin-coated (12-24µg/mL) non-TC-treated 24-well plates for transduction. T cells were resuspended in 700µL retroviral supernatant and 700µL cRPMI supplemented with 100IU/mL of recombinant human interleukin 2 (rHuIL-2). Spin transduction settings were as follows: 90 minutes at 2000 revolutions per minute (rpm) at 32∘C with no brake, followed by an overnight incubation at 37∘C. At 16 hours post transduction, 1mL of fresh cRPMI + 20IU/mL rHuIL-2 replaced viral supernatant. Purity, viability and transduction efficiency were assessed by flow cytometry 48-72 hours later and transduced cells were selected using murine CD19 microbeads (Miltenyi Biotech, Auburn, CA). Cell count was ascertained on the MUSE cell analyser (Merck Millipore) using the Count and Viability reagent provided.

2.4.5.2 WT TRP1 transduction

Total CD4 T cell numbers obtained post spleen/extended lymph node harvest from WT TRP1 transgenic donors were low compared with C57BL/6 donors, comprising approximately 7-10% of total live cells, with absolute CD4 T cell numbers of 400-500 $x10^3$ CD4 T cells per mouse. Multiple permutations of cell culture, stimulation and spin transduction protocols were tested.

CD4 positive magnetic bead/column selection at the point of organ harvest was not routinely used as we observed a low yield of CD4 T cells and an adverse effect on cell viability with

excessive cell handling (data not shown). Our approach was to disperse LN and spleen through a 70µm nylon mesh followed by a red cell lysis step (Sigma-Aldrich) and a wash step in cRPMI. Cells were counted on the MUSE cell analyser (Merck Millipore) and stained for FACS analysis to elucidate total CD4 T cell numbers obtained. TRP1 T cells were then activated at a concentration of $1x10^6$ TRP1 T cells/well of a 24-well plate with 2µM TRP1 peptide (10mM stock) and rHuIL-2 (10IU/mL) in 1.5mL of cRPMI at 37◦C in 5% CO_2. The culture was unselected and we showed the presence of TRP1-derived (non-CD4+) CD11b+, CD11c+, MHC Class II+ expressing cells which we believe fulfilled a role in antigen presentation in these cultures.

Retroviral transduction was performed after 24 hours of in vitro stimulation. TRP1 T cells were harvested, counted and added to retronectin-coated plates at $1x10^6$ CD4 T cells per well in 750µL of retroviral supernatant and 750µL of cRPMI supplemented with 100IU/mL of rHuIL-2. Spin-transduction settings were as follows: 90 minutes at 32◦C and 2000rpm with no brake. As in the polyclonal setting, cells were incubated at 37◦C with fresh cRPMI+ 20IU rHuIL-2 added at 16 hours post-transduction. Transduction efficiency was measured 48-72 hours later. These techniques were also used in the retroviral transduction of TRP1 CTLA-4$^{-/-}$ CD4 T cells.

For in-vivo experiments, cells underwent positive selection for murine CD19 using a commercially available kit according to manufacturers' instructions (Miltenyi Biotech, Auburn, CA). Cells were then injected intravenously in sterile PBS into recipient mice in volumes of 200µL/mouse.

We discovered that vaccination of WT TRP1 donors with two standard doses of Gvax resulted in a 3-4-fold increase in CD4 T cell numbers obtained, and an improved viability in vitro over cells derived from non-vaccinated animals (figure 6.8a) (75). The higher CD4 yields with donor vaccination hold promise regarding the generation of sufficient numbers of transduced cells for in vivo experiments, but vaccination may alter the biology of the model (see Chapter 6.2.6).

2.4.7   Exogenous therapeutic antibodies

9H10 α-murine-CTLA-4 (sourced from BioXCell, USA) and 10D1 α-human-CTLA-4 (kindly provided by Alan Korman)(80) were administered intraperitoneally (i.p.) at doses of 100-200µg/mouse in a final volume of 200µL/mouse of sterile PBS.

2.4.8   Staining for fluorescence activated cell sorting (FACS) analysis

Fluorescence Activated Flow Cytometry (FACS) was performed on the BD LSR Fortessa (BD, San Jose, CA) and analysis was done with FloJo 10 software (Tree Star Inc., Ashland OR). Electronic cell sorting was performed on the MoFlo^{TM} XDP (Beckman Coulter).

Cell surface staining was performed for 30 minutes in the dark on ice using cold buffers and reagents, followed by a double wash in staining buffer. Each sample comprised 1-3 x 10^6cells/well of a 96-well round-bottomed plate, stained in 40μL of staining buffer (PBS, 2% FCS, 0.1% sodium azide) supplemented with 10% superblock (500μL rat serum; 500μL mouse serum; 500μL anti-FcR (rat-anti-mouse CD16/32); 0.1% sodium azide; 200μL FCS; 8.10mL PBS).

Diagnostic α-murine mAbs used and their dilutions in staining buffer/superblock are listed in Table 2.4. Diagnostic α-human mAbs are listed in Table 2.5.

Fixable dead cell dyes (eBioscience) were routinely used in staining. They cannot enter live cells, but covalently label amines throughout the cytoplasm of dead cells, giving dead cells a 50-fold greater fluorescence than live cells. Covalent labelling means that cells can be aldehyde-fixed and permeabilised without losing viability discrimination.

For intracytoplasmic staining, cells were fixed with Cytoperm/Cytofix solution (BD Biosciences) according to manufacturer's instructions, and stained for a further 30 minutes at 4∘C in the dark with antibodies diluted in 40μL of cytoperm solution enriched with 10% superblock. The murine Foxp3 Buffer Set (BD Pharminogen) was used for intranuclear staining and cells were incubated for 30 minutes at 4∘C in the dark in 40μL of antibody/ Fox-Perm solution/10% superblock.

Intracellular anti-murine-Fc staining was crucial to confirm the presence of intracellular antibody-Fc within transduced T cells (see Chapters 5 and 6). T cells were restimulated with TRP1 peptide and exogenous DCs in vitro over 4 hours. Brefeldin A was added one hour into the culture to permit accumulation of antibody intracellularly. Brefeldin A is a lactone antibiotic which inhibits protein transport from the endoplasmic reticulum to the Golgi apparatus indirectly by preventing formation of transport vesicles (145).   Following restimulation, diagnostic antibody labelling proceeded as described above apart from the need in this case for an antibody panel exclusively comprising rat-derived mAbs, and the use of rat serum instead of superblock to minimise the risk of non-specific anti-murine Fc staining.

Table 2.4   Murine antibodies for FACS

Antibody	Clone	Supplier	Dilution
FoxP3-AF700	FJK-16s	eBioscience	1:100
FoxP3-PE	FJK-16s	eBioscience	1:100
CTLA-4-APC	UC10-4B9	eBioscience	1:100
CTLA-4-PE	UC10-4B9	eBioscience	1:100
Ki67-FITC	SolA15	eBioscience	1:400
Ki67-PERCP	SolA15	eBioscience	1:300
Granzyme-APC	GB11	Invitrogen	1:100
Granzyme-PE	GB12	Invitrogen	1:100
Eomes-PE	Dan11mag	eBioscience	1:100
CD44-APC	IM7	eBioscience	1:200
CD62L-v450	MEL-14	eBioscience	1:200
PD-1-v450	RPM1-30	eBioscience	1:200
CD19-AF700	eBio1D3	eBioscience	1:100
CD19-PE	1D3	eBioscience	1:200-1:300
Anti-murine IgG2a-APC	N/A	Jackson Immuno	1:50-1:100
Anti-murine IgG1- APC	N/A	Jackson Immuno	1:50-1:100
IFNg-FITC	XMG1.2	eBioscience	1:100
TNFα-APC	MP6-XT22	eBioscience	1:100
IL-2-PE Cy7	JES6-5H4	eBioscience	1:100
NK1.1-NC655	PK136	BioLegend	1:200
Vb14-FITC	14-2	BD Pharmingen	1:200
FcγRIV-FITC	Unknown	labelled in house	1:100
Viability-APC EFluor780	N/A	eBioscience	1:1000
Ia/b-v450	AF6-210.1	eBioscience	1:200

Table 2.4   Murine antibodies for FACS (continued)

Antibody	Clone	Supplier	Dilution
Viability-v450	N/A	eBioscience	1:1000
CD3-PerCP-Cy5.5	17A2	BioLegend	1:200
CD4-v500	RM4-5	BD Pharmingen	1:300
CD4-PE	RM4-5	BD Pharmingen	1:300
CD8-BV650	53-6.7	BioLegend	1:300
CD8-v450	53-6.7	eBioscience	1:300
CD45.1- APC Efluor780	A20	eBioscience	1:200
CD45.1-PE Cy7	A20	eBioscience	1:200
CD25-PE	PC61.5	eBioscience	1:200
CD25-FITC	PC61.5	eBioscience	1:200
CD11b-APC	M1/70	eBioscience	1:200
NOS2-PE	SXNFT	eBioscience	1:100

Table 2.5 Human antibodies for FACS

Antibody	Clone	Supplier	Dilution
CD34-PE Cy7	581	BD Pharmingen	5µL/test
Anti-human (pan) Fc-APC	N/A	Jackson Immuno	1:50-1:100
CTLA-4-APC	BNI3	BD Pharmingen	5µL/test
CTLA-4-APC	L3D10	Biolegend	5µL/test

2.4.9   Antibody dependent cytotoxicity assays (ADCC)

Experimental design to demonstrate ADCC in vitro is well published (89). In this project, the aim was to demonstrate that exogenous α-CTLA-4 mAb added to cultures of CFSE-labelled CTLA-4^{hi} target cells and activated effector macrophages would result in target cell lysis in vitro.

SupT1 cells expressing human or murine CTLA-4 were washed in PBS and resuspended at 1×10^6/mL prior to staining with 5 µmol/L CFSE (Invitrogen, Carlsbad, CA) for 10 minutes at 37°C (described in Chapter 2.4.9). Cells were resuspended at 1×10^5/mL and added to round bottomed 96-well plates at 1×10^4 cells per well. Stimulated effector cells (BM-derived macrophages described in Chapter 2.4.3) were then applied at different concentrations to generate 10:1, 5:1 and 0.5:1 effector to target (e:t) ratios. Antibodies for testing were added at 50µg/mL, comparing isotype control and experimental antibody in triplicate wells. It was expected that the therapeutic impact of ADCC-capable mAb would be quenched at lower e:t ratios.

Plates were incubated for 16 hours at 37°C and 5% CO_2 prior to cell harvesting. 5×10^3 Pacific Blue microbeads (Life Technologies) were added to each sample and data acquisition was stopped after 2.5×10^3 events. The fraction of antibody-mediated cell kill was calculated as follows:

%αCTLA-4 antibody survival= [WITH αCTLA-4 absolute number viable CFSE labelled/WITHOUT αCTLA-4 absolute number viable CFSE labelled] x100.

2.4.10   Carboxyfluorescein succinimidyl ester (CFSE) labelling

CFSE can be used to monitor lymphocyte proliferation, both in vitro and in vivo, due to the progressive halving of CFSE fluorescence within daughter cells following each cell division. This permits observation of 7-8 cell divisions before CFSE fluorescence is too low to be distinguished above background autofluorescence. In order to quantify cytotoxicity displayed in the ADCC assay described in Chapter 2.4.8, target SupT1 cells were CFSE-labelled.

Cells were resuspended at 5×10^6/mL in PBS/0.1% bovine serum albumin (BSA) and labelled with 5µM CFSE (Invitrogen, Carlsbad, CA). To obtain a 5µM solution of CFSE (one vial should be diluted in 20µL DMSO from the kit and left at RT), 2µL CFSE is resuspended in 1mL of warm PBS/BSA 0.1%. It is imperative to then move quickly to add 1mL of diluted CFSE to 1mL of cells,

to mix thoroughly to obtain homogeneous staining, prior to incubation at 37◦C for 10 minutes. After this, the reaction must be promptly quenched (add 5x volumes of cold RPMI medium and incubate for 5 minutes on ice), and in order to minimise cell toxicity and to obtain clean labelling, 4 wash steps must be performed. To accommodate this it is important to start with approximately double the number of cells needed for the experiment, as many will be lost in the washing steps.

2.4.11 Enzyme linked immunosorbent assays (ELISA)

Mouse IgG2a and IgG1 Ready-SET-Go ELISA kits were used (affymetrix, eBioscience) according to manufacturer's instructions to quantitate the antibody production capacity of transduced cell lines and primary lymphocytes in this project.

Corning Costar 9018 ELISA plates were coated with 100µL/well of capture antibody and incubated overnight at 4◦C. The following day, wells were washed twice in wash buffer (1x PBS, 0.05% Tween-20) and blocked for 2 hours at RT in blocking buffer followed by two further washes in wash buffer.

Generation of the standard curve required 2-fold serial dilutions of the reconstituted standard with assay buffer A. Blank wells contained only buffer A. The sample wells were loaded with 100µL/well of Assay Buffer A followed by the addition of 100µL/well of the samples to be tested, followed by 2-fold serial dilutions as per the standard wells. 50µL of detection antibody was added to all wells (except one row of the blank wells), and the plate was sealed and incubated at RT for 3 hours. Following this, the plate was washed 4 times in wash buffer and then 100µL of substrate solution (teramethylbenzidine (TMB) was added to each well followed by further incubation at RT for 15 minutes. 100µL of stop solution (1M H_2SO_4) was then added to each well. Plates were read on the Varioskan Flash multimode reader (Thermo Scientific) at 450nm, and concentrations read from the standard curve multiplied by the dilution factor.

2.4.12 Isolation of lymph nodes (LNs) and tumour infiltrating lymphocytes (TILs)

Mice were humanely sacrificed with CO_2. Lymph nodes (inguinal/axillary/brachial) and tumours were dissected into cRPMI. Lymph nodes were dispersed through a 70-µm filter, washed in cRPMI and counted on the MUSE cell analyser (Merck Millipore) prior to staining for FACS analysis. Tumours were mechanically disrupted using scalpels and digested in 0.33mg/mL

DNase (Sigma-Aldrich) plus 0.27mg/mL Liberase TL (Roche) in serum-free RPMI for 30 minutes at 37°C, followed by dispersal through 70µm filters. Samples were washed in cRPMI and subsequently stained for FACS analysis.

Pacific Blue microbeads (Life Technologies) were added to tumour samples to enable quantitation of absolute cell numbers per tumour sample (microbeads normalised to known sample volume, which is then normalised to tumour wet weight). The following formula is used for this calculation: absolute cell number =number of cells acquired/(tumour wet weight/[number of beads acquired/number of beads added to sample]).

Experimental outcome measures included tumour weight, and analysis of T cell numbers, surface phenotype and function within lymph nodes and tumours, with specific evaluation of transferred and endogenous populations. Attempts are being made within the lab to assess serum levels of murine antinuclear antibody (ANA) and double-stranded DNA antibody (dsDNA) (Signosis, USA) by ELISA, as surrogate markers of systemic toxicity associated with CTLA-4 blockade.

Restimulation assays were set up to detect intracellular cytokines. TIL and LN homogenates were incubated at 37°C for 4 hours with 50×10^3 murine dendritic cells (DCs) pulsed with B16 tumour cell lysate and 2µM TRP1 peptide in cRPMI. 1:1000 Brefeldin A (BD Pharmingen) was added after 1 hour in vitro. Cells were then washed and stained for flow cytometry as described in section 2.4.7.

2.4.13 Irradiation of murine recipients

Mice were batched into groups of 5 into transfer boxes to receive a dose of 5Gy of total body irradiation. They then had a 4-6 hour recovery period prior to any further procedure/intervention. A registered current dosimeter was worn at all times. The irradiator used was an AGO HS320/250 X-ray cabinet.

2.4.14 Statistical analysis

Statistical analysis was performed using GraphPad Prism 5.0. (GraphPad Softward. Inc.) Experiments were repeated two or three times as indicated. Statistical significance was elicited by a Student's t test (between two groups or conditions) or analysis of variance with a post-

hoc test (three or more groups or conditions). P-values <0.05 were considered statistically significant.

CHAPTER 3

3. CELL INTRINSIC SILENCING OF CTLA-4

3.1 Introduction

3.1.1 CTLA-4 expression and function

CTLA-4 is a vital negative regulator of T cell responses. Its physiological function is in the maintenance of immune tolerance which prevents self-reactivity and autoimmunity, but is thought to compromise the generation of anti-tumour immune responses. Blockade of this receptor through mAb technology has been shown to 'release the brakes' on immune responses in pre-clinical models of cancer (46, 47). One of the limitations of tumour immunotherapy is the lack of persistence and anergy of tumour reactive immune cells in immunologically hostile tumour microenvironments. We hypothesise that absence of CTLA-4 on tumour-specific effector T cells may enhance their immune function within the tumour and reduce the incidence of immune toxicity compared with systemic administration of αCTLA-4 mAb.

One concern about a strategy to ablate CTLA-4 on cells for adoptive transfer is that the predicted CTLA-4$^{-/-}$ benefits of proliferation and activation may be compromised by the non-cell autonomous 'effector extrinsic' CTLA-4 effect (90). Co-transfer experiments have suggested that CTLA-4-replete T cells can regulate co-existing populations of CTLA-4-depleted T cells. At CTLA-4$^{-/-}$:CTLA-4$^{+/+}$ ratios of 1:1 or 1:2, CTLA-4-replete antigen specific T cells can prevent accumulation of CTLA-4-deficient antigen specific T cells. This effect is diminished at higher ratios (26, 27).

An additional concern regarding the validity CTLA-4 ablation on T cells in this context is that the vast majority of published data on the anti-tumour properties of CTLA-4 blockade is generated using mAb-mediated receptor blockade rather than genetic ablation of the receptor. We know that certain CTLA-4 polymorphisms are associated with better response rates to αCTLA-4 mAb therapy for cancer so it is possible that ablation of the receptor holds promise as a therapeutic strategy (58).

3.1.2 Strategies to 'knock down' expression of CTLA-4

There are several methods by which silencing of CTLA-4 in tumour-specific effector T cells can be achieved. Proteins can be eradicated from cells by several methods: at the genomic level by zinc finger nucleases (ZFNs) (91, 92) or by TALENs (93) and the CRISPR/Cas system (94); at the messenger ribonucleic acid (mRNA) level by small interfering RNA (siRNA) or microRNA (miRNA) (95-97); and at the protein level by blocking/depleting antibodies or by endoplasmic reticulum (ER) retention sequences (98, 99).

TALENs are nucleases derived from the bacterium Xanthomonas that cleave specific genomic sequences in vivo when linked to the catalytic domain of the restriction enzyme Fok1, and can be used for gene editing and mutagenesis. They do this by means of 2 major eukaryotic DNA repair pathways: the error-prone break repair method NHEJ (non-homologous end joining) and the precise gene method HDR (homology directed repair) (93).

Munro and Pelham originally described the KDEL amino acid sequence in the endoplasmic reticulum (ER) and its function in intracellular protein retention in 1987 (98, 99) . In this project, the KDEL strategy offers a method for reduction of CTLA-4 cell surface expression through ER- anchored αCTLA-4 scFv binding of freshly transduced CTLA-4 protein. This theoretically enables testing of intrinsic ('in cis') CTLA-4 knockdown. Potential problems with this technique include cellular toxicity from ER stress generated by high volume protein retention which can lead to apoptosis (100).

3.1.3 Small interfering RNA (siRNA)

RNA interference (RNAi) was first described in 1998 (101). The presence of intracellular double-stranded RNA (dsRNA) in eukaryotes can silence gene expression and scientific exploitation of this observation has generated an important research tool. Mechanistically, RNAi machinery is triggered by intracellular strands of dsRNA which the endogenous enzyme (Dicer) cleaves into siRNA fragments. These fragments are used to generate an RNA-induced silencing complex (RISC) which unwinds to seek out and degrade complementary mRNA, leading to gene silencing. The effect can last for 3-7 days in rapidly dividing cells, and for several weeks in non-dividing cells. (95). Synthetic siRNA has been shown to induce sequence-specific knockdown in mammalian cell lines (102).

Circumventing the transient nature of the siRNA effect is the retroviral vector system pSUPER which directs the synthesis of siRNAs in eukaryotes and leads to stable expression of siRNA and stable suppression of gene expression with no requirement for repeated dosing. The polymerase-III H1-RNA gene promoter produces a small RNA transcript lacking a poly-adenosine tail, but with a termination signal consisting of 5 thymidines. The gene specific insert must be a 19-nucleotide (nt) sequence derived from the target transcript, separated by a 9-nt spacer, from the reverse complement of the same 19-nt sequence. The transcript folds back on itself to form a 19-base pair stem-loop structure (82).

An advantage of siRNA is that it can target specific sequences of mRNA due to its small size. Disadvantages include off-target interactions and toxicity, immunogenicity, eradication by the host immune system and a limitation of its capacity to achieve knockdown due to saturation of the mechanism (95-97). RNAi can provoke a strong cytotoxic response in mammalian cells (103).

Silencing of CTLA-4 by siRNA has been investigated in vitro in the context of chronic Hepatitis B. Transient transfection by electroporation of human CTLA-4 siRNA into T lymphocytes from patients with chronic Hepatitis B mediated a reduction in CTLA-4 mRNA transcripts detectable by real time polymerase chain reaction (RT-PCR) compared with siRNA control, and was associated with increased Interleukin -2 (IL-2) and Interferon Gamma (IFNγ) secretion following stimulation with phytohaemagluttinin (PHA) (104). To my knowledge there is no published work to date in tumour biology using CTLA-4 siRNA. Of note, a group in Japan have shown that siRNA mediated silencing of another T cell co-inhibitory receptor (programmed cell death 1 (PD-1) in vitro enhances tumour-specific human T cell effector functions (IFNγ production and antigen-specific cytotoxicity) (105).

3.1.4 Aims/hypotheses

We elected to generate human and murine CTLA-4 specific siRNA constructs using the pSuper system, aiming to downregulate the expression of CTLA-4 in tumour-reactive T cells for adoptive transfer into murine models of melanoma.

3.2   Results

3.2.1   Generating CTLA-4 high cell lines as 'targets' to test constructs

Figure 3.1a shows SFG plasmids coding for human and murine CTLA-4 with an IRES-linked truncated human CD34 (dCD34) marker gene. CTLA-4 was generated by Phusion PCR (described Chapter 2.1.6) and subcloned into SFG.I2.eBFP2 to permit surface expression of the receptor. Transient transfection of 293T cells with these constructs and flow cytometric analysis at 72 hours confirmed dCD34/CTLA-4 dual positivity for both constructs, with no cross-species effect. Capillary sequencing confirmed correct sequences.

Figure 3.1a: plasmid maps for human and murine CTLA-4. This shows human and murine CTLA-4 linked by an IRES to a truncated human CD34 marker gene. **Key:** LTR=long terminal repeats; HuCTLA4=human CTLA4; MuCTLA4=murine CTLA4; IRES=internal ribosomal entry site; dHuCD34=truncated human CD34;SD=splice donor;SA=splice acceptor. CTLA-4 sequences flanked by BglII and MluI restriction sites.
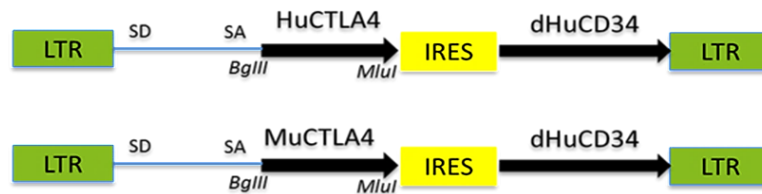
Figure 3.1b: 293T cells are transduced to stably express Human or Murine CTLA-4. Transduction with RD114 retroviral supernatant and positive selection for the human CD34 marker protein yielded a purity of 78% human CTLA-4/huCD34 and a purity of 97% murine CTLA-4/huCD34 co-expressing cells. **Key:** HuCD34=human CD34.
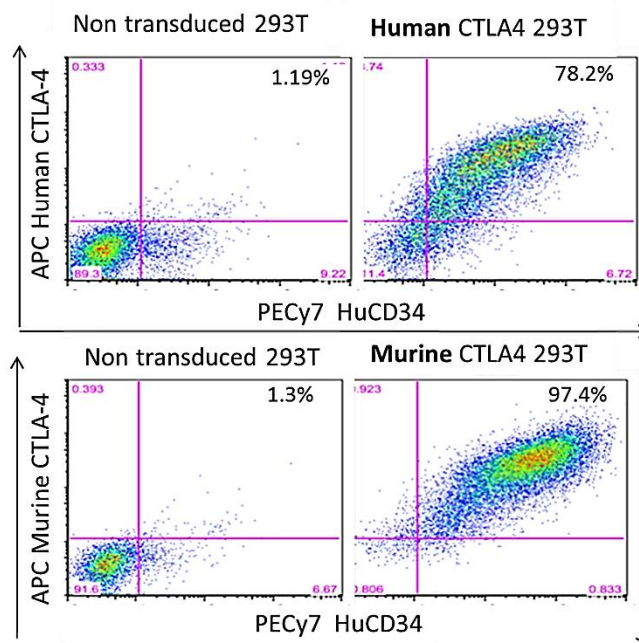
Figure 3.1c: SupT1 cells are stably transduced with human or murine CTLA-4. The human CTLA-4 cell purity is 92% and the murine CTLA-4 purity is 97%. **Key:** NT=non-transduced; CTLA4= cytotoxic T lymphocyte antigen 4; αCTLA4 mAb=anti-CTLA-4 monoclonal antibody; FSC=forward scatter.
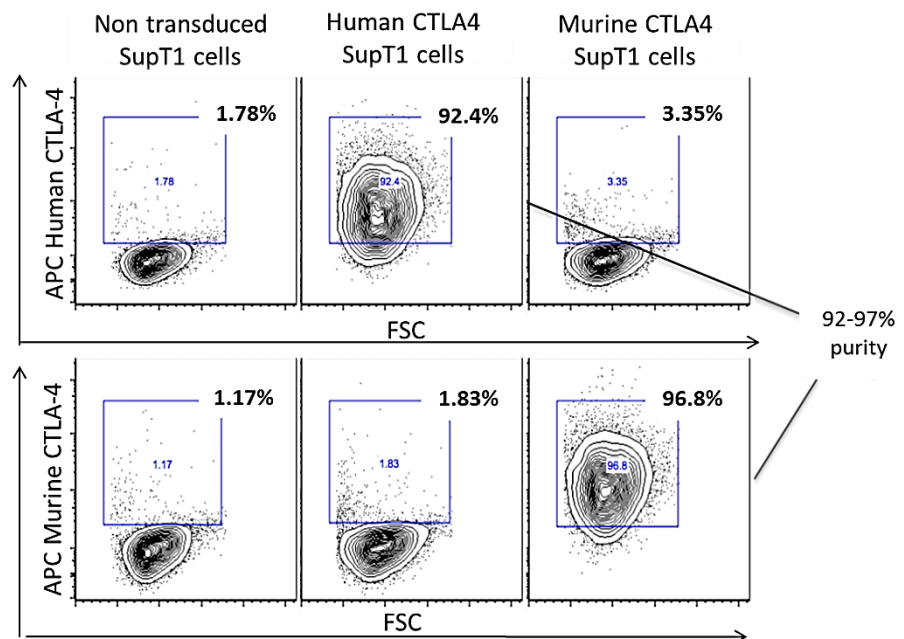
In order to generate stable, surface-restricted CTLA-4 expressing cell lines, RD114 retroviral supernatant was produced by triple transfection of 293T cells according to the method outlined in Chapter 2.3.1. Single transduction of 293T cells (Figure 3.1b) and double transduction of SupT1 cells (Figure 3.1c) was followed by positive selection for human CD34 to enrich CTLA-4^{hi} populations using magnetic columns/beads (Miltenyi Biotech, CliniMACS® cell sorting, Auburn, CA).

3.2.2   Generating siRNAs to target CTLA-4

Twelve separate siRNAs to target human or murine CTLA-4 were generated from oligonucleotide pairs, designed by Martin Pule, annealed for ligation into pSuperRetro.d_muCD19, a mammalian expression vector that directs intracellular synthesis of siRNA transcripts, and uses a truncated version of murine CD19 as a marker/selection protein (25). Further details can be found in Materials and Methods section 2.3.2. Correct sequences were verified prior to testing in cell lines. Diagrammatic representation of these constructs is seen in Figure 3.2a.

Figure 3.2a: vector maps of siRNA hairpins targeting human and murine CTLA-4. 19-nt sequences (complementary) are linked by 9-nt spacer. **Key:** 5' PCMV=specially designed long terminal repeat (LTR) from the murine stem cell PCMV virus that permits work with hard-to-transduce cell lines; Hi-RNA promoter= H1 RNA polymerase –lll gene promoter (produces small RNA transcript); PGK promoter= mouse phosphoglycerate kinase 1 promoter; siRNA=small interfering RNA; Hu CTLA-4= human CTLA-4; Mu CTLA-4= murine CTLA-4; dmuCD19= truncated murine CD19.
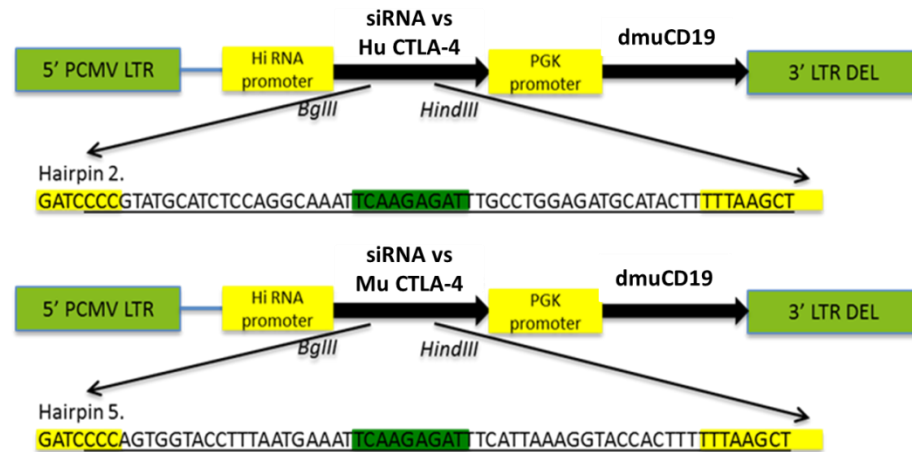
3.2.3   Testing siRNAs in cell lines by transfection

Transient co- transfection of CTLA-4 and siRNA plasmids into 293T cells demonstrated that two of six human CTLA-4 siRNA constructs and two of six murine CTLA-4 siRNA constructs showed species-specific CTLA-4 knockdown capability in transfected 293T cells, and the best human and murine clones were selected for downstream applications.

Figure3.2b shows transfection of CTLA-4 siRNA into 293T cells transduced to express high levels of human or murine CTLA-4. Analysis of CD19+/transduced cells reveals an almost 50% reduction in human CTLA-4 (by flow cytometry) in human CTLA-4 siRNA transfected cells, and an almost 85% reduction in murine CTLA-4 expression in cells transfected with murine CTLA-4 siRNA, with no obvious cross-species effect.

CD19 positive cell viability was assessed by flow cytometry (see Chapter 2.4.7 for method and details) and human and murine CTLA-4 siRNA transfected 293T cells with low CTLA-4 expression had equivalent viability to control siRNA at 72 hours post-transfection, suggesting no additional toxicity from CTLA-4 siRNA in excess of that of control siRNA (data not shown).

Figure 3.2b: human and murine CTLA-4 specific siRNA down-regulate CTLA-4 in a species specific manner compared with control siRNA in a 293T cell in vitro model. Human CTLA-4/murine CD19 double positivity drops from 20.4% to 11% with human CTLA-4 siRNA, and murine CTLA-4/murine CD19 double positivity drops from 27.9% to 3.66% with murine CTLA-4 siRNA compared with control siRNA. Gated on live singlets.
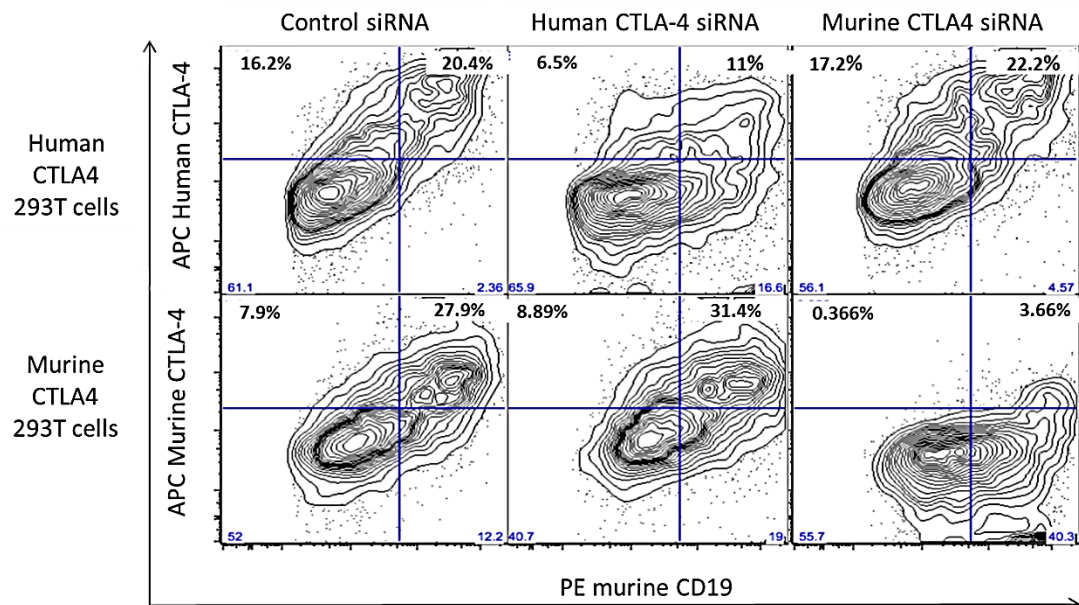
3.2.4 Extracellular versus intracellular expression of CTLA-4 in primary lymphocytes

Moving away from cell lines into primary lymphocytes introduces a new challenge in flow cytometric assessment of CTLA-4. Surface staining for primary lymphocytes reveals very low expression levels, even in the context of optimal stimulation (13). In contrast, intracellular CTLA-4 staining in primary T cells reveals high concentrations of the receptor, reflecting its high concentration in intracellular vesicles. For this reason, we decided to use intracellular staining for CTLA-4 to determine a clear CTLA-4 positive population to use as a reference point for any down-regulation achieved with siRNA or other gene/mRNA/protein silencing strategies.

3.2.5 In vitro testing of murine CTLA-4 siRNA in C57BL/6 lymphocytes by transduction

Using methods detailed in section 2.4.5.1, C57BL/6 T cell retroviral transduction efficiencies of 40-50% were obtained for siRNA constructs (see figure 3.3a), but with no clear reduction in CTLA-4 protein at 72h post-stimulation (data not shown).

Figure 3.3a: retroviral transduction of murine CTLA-4 siRNA versus control siRNA in C57BL/6 lymphocytes. Transduction efficiency is measured by dmuCD19 expression at 72 hours post stimulation with ConA+IL-7. Murine CTLA-4 siRNA is not associated with a reduction in intracellular CTLA-4 at 72 hours post stimulation. **Key:** t/d=transduced; dMuCD19=truncated murine CD19.
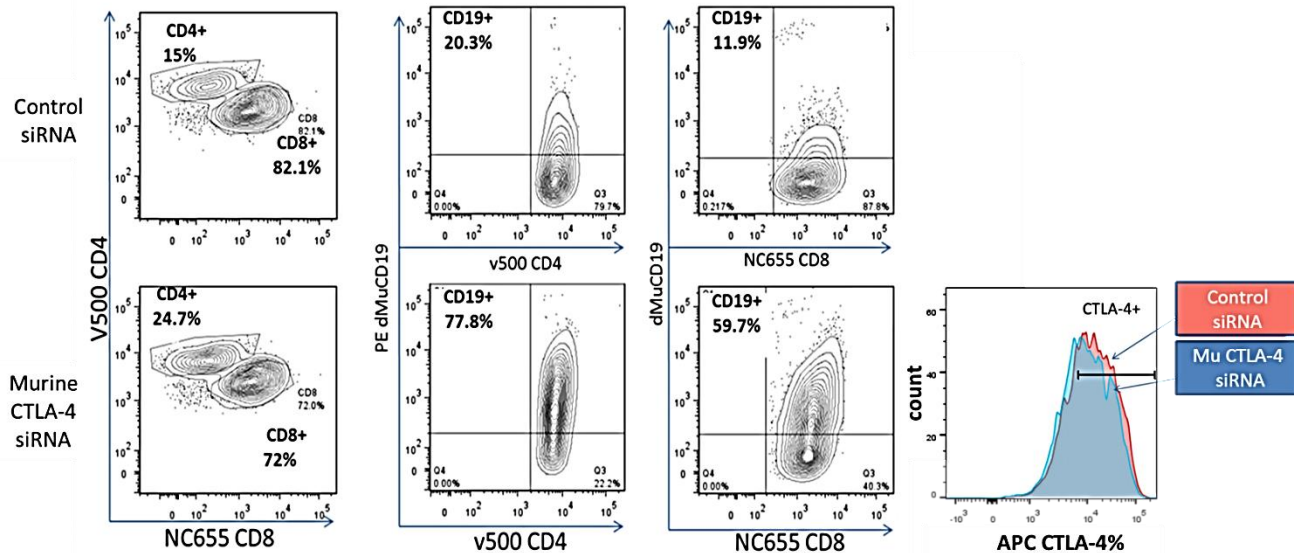
Given that CTLA-4 recirculates from cell surface to intracytoplasmic stores and accumulates intracellularly with no obvious saturation of the mechanism (12), we concluded that an in vitro time course experiment over 10 days may permit the emergence of a siRNA effect once existing intracellular CTLA-4 stores could be diminished/depleted, or fail to be replenished.

Figure 3.3b shows that there was a modest reduction in intracellular CTLA-4 protein in murine CTLA-4 siRNA transduced CD4 effector and CD4 regulatory populations at day 8 and day 10 post-transduction compared with control siRNA. Restimulation with rHuIL-2 at day 7 of in vitro culture suggests attenuated CTLA-4 upregulation in the murine CTLA-4 siRNA transduced CD4eff population (and to a lesser extent in the CD4reg compartment) compared with the control condition. At day 10, CD4 Teff transduced with control siRNA responded with a rise in CTLA-4 expression from 19% to 32%, compared with a corresponding 9% to 10% rise in the murine CTLA-4 siRNA transduced cells.

Figure 3.3b: transduction of C57BL/6 lymphocytes with murine CTLA-4 siRNA is associated with a modest reduction in intracellular CTLA-4 expression at days 8 and 10 of in vitro culture in the CD19+ population compared with control siRNA. Re-stimulation with rHuIL-2 at day 7 shows an attenuated CTLA-4 response in the murine CTLA-4 siRNA condition in both CD4eff and CD4reg. Gated on live, CD3+, dMuCD19+ singlets.   **Key:** MurineCTLA-4=α-murine-CTLA-4 mAb; CD4reg=CD4 regulatory T-cell; CD4effector=CD4 effector T-cell.
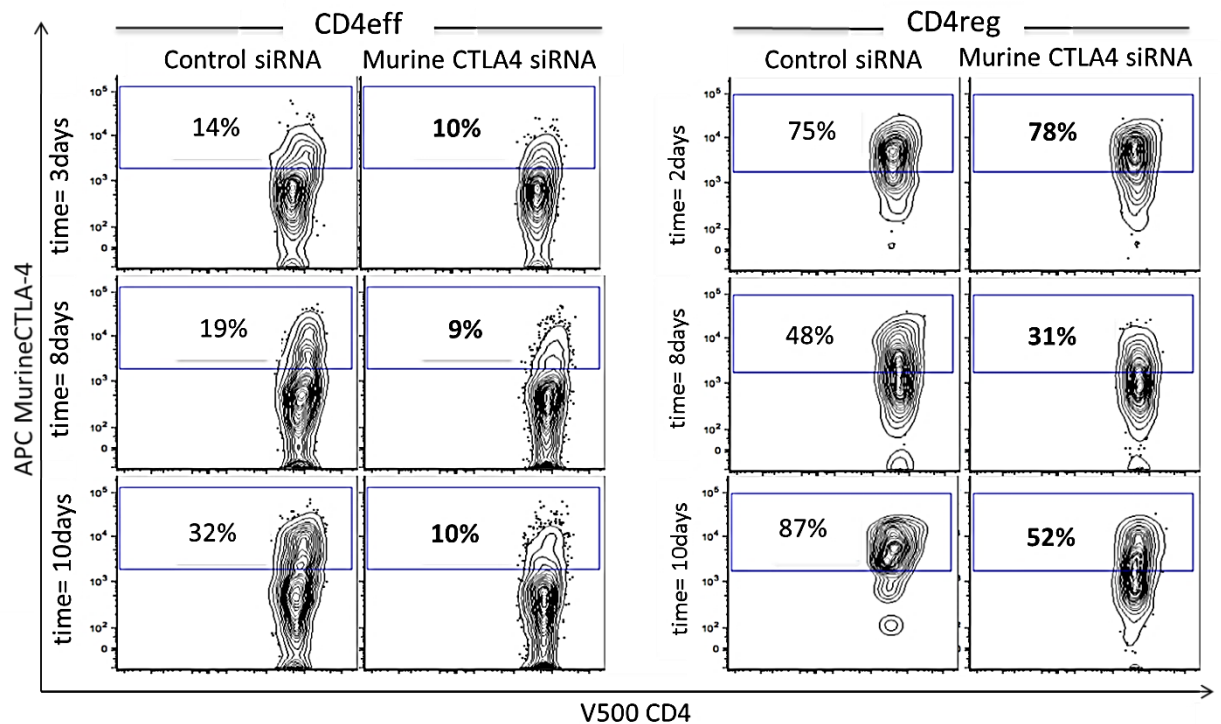
3.3   Discussion

The objective of Chapter 3 was to acquire a construct that could ablate CTLA-4 expression on the T cell surface, permit unchecked CD28 interaction with B7.1 and B7.2, and had the potential to enhance effector function, particularly with respect to tumour rejection.

We have generated human and murine CTLA-4 targeted siRNA constructs that can diminish cell surface expression of CTLA-4 in cell lines modified to overexpress CTLA-4 (figure 3.2b). We have shown that primary murine lymphocytes can be transduced with murine CTLA-4 siRNA at efficiencies approaching 50%. It is apparent that cell surface expression of CTLA-4 on primary murine lymphocytes is low so we elected to use intracellular CTLA-4 expression as a read-out for the potential efficacy of the siRNA constructs. Moving forward, there was no obvious reduction in CTLA-4 expression at 72 hours post-transduction in primary murine lymphocytes transduced with murine CTLA-4 siRNA (see figure 3.3a). We concluded that this may be due to

persistence of pre-existing intracytoplasmic CTLA-4 stores rather than a failure of the construct, and to address this we designed a time course experiment to run over 10 days.

Observation of murine siRNA transduced C57BL/6 lymphocytes over 10 days in vitro with rHuIL-2 restimulation at day 7 revealed a modest reduction in CTLA-4 expression at days 8 and 10 of culture (figure 3.3b). The potential physiological or therapeutic impact of partial knockdown is unclear. What we do know from the seminal paper describing the pSuperRetro vector system is that it is possible to achieve a 90% reduction in target protein with siRNA technology, with no appreciable detrimental effect on cell survival (82). The fact that murine CTLA-4 siRNA does not achieve this efficacy may reflect a limitation of the construct, and/or of the target. An additional consideration is that intracellular CTLA-4 expression may not reflect surface expression, and that modest reductions in intracellular CTLA-4 may translate into more meaningful cell surface reductions that have the potential to alter cell biology.

In vivo testing may be necessary to optimally test the CTLA-4 siRNA constructs. Passing CTLA-4 siRNA transduced tumour reactive T cells into irradiated tumour-bearing murine recipients might permit a protracted period of observation for a drop in CTLA-4, thus avoiding the timeframe issues and other limitations imposed by longer-term in vitro culture. Alternatively, as a short-term read-out of siRNA efficacy, RT-PCR for CTLA-4 mRNA could be informative of mRNA downregulation secondary to siRNA, and may be less complicated than the interpretation of (recirculating) intra/extracellular CTLA-4 protein levels (104). Whether this is meaningful in the presence of preserved protein levels observed by flow cytometry is pertinent.

In summary, it is possible that additional CTLA-4 siRNA experiments could define a construct worthy of downstream applications, but based on the in vitro lymphocyte data, we hypothesise that incomplete CTLA-4 knockdown is the likely outcome. It is possible that titres of CTLA-4 mRNA generated in the process of lymphocyte activation are too high to be susceptible to siRNA mediated silencing and essentially overwhelm the mechanism.

3.4 Future directions

The murine CTLA-4 siRNA constructs induce modest reductions in intracellular CTLA-4 in our hands. To date we have not defined a workable in vivo method for cell intrinsic CTLA-4 ablation.

We accept that the majority of published information on the anti-tumour effect of CTLA-4 blockade has been derived from studies of mAb-mediated receptor blockade rather than genetic absence of the receptor and as such there is not a huge precedent to support the potential efficacy of this approach in cancer immunotherapy.

We also acknowledge that a strong body of work is emerging to support a dominant extrinsic effector role for CTLA-4 whereby CTLA-4-replete T cells can abrogate CTLA-4$^{-/-}$ Teff expansion in a dose dependent fashion (26).

Given the lack of clear published data to compare the effect of T cell intrinsic CTLA-4 absence with mAb-mediated CTLA-4 blockade in a cancer model, we elected to test this in the well characterised B16/BL6 murine melanoma model in Chapter 4. The aim was to compare anti-tumour and immunological differences between adoptively transferred CTLA-4-replete and CTLA-4-depleted tumour reactive CD4 T cells with and without exogenous αCTLA-4 mAb therapy. This will clarify the relative value of genetic ablation of CTLA-4 versus mAb-mediated CTLA-4 blockade in tumour-reactive T cells in vivo, and help to delineate the risk posed by endogenous CTLA-4-replete populations acting in trans to abrogate the (potential) expansion of CTLA-4-depleted tumour reactive T cells.

The outcomes of these experiments will inform the decision to explore other avenues towards cell intrinsic CTLA-4 inhibition.

CHAPTER 4

4. INVESTIGATION OF CTLA-4 IN VIVO USING A CTLA-4 KNOCKOUT MOUSE

4.1 Introduction

4.1.1 CD4 T cells as an adoptive cell therapy (ACT) for cancer

Most research into ACT for cancer has focussed on autologous, tumour-derived, in vitro expanded CD8 T cells. These have been shown in clinical trials of metastatic melanoma and several EBV-driven tumours to confer a survival advantage in some patients, enhanced by prior lymphodepletion (25, 106, 107). One of the limitations of CD8 T cells in tumour immunotherapy is that responses can be incomplete and of limited duration. One biological weakness of CD8 T cells in this role is their dependence on functional tumour-cell-surface MHC Class 1 molecules. Genetic instability within tumour cells often renders MHC unable to present antigen, and lack of T cell co-stimulation and a high concentration of immunosuppressive cytokines results in suboptimal stimulation of CD8 T cells, anergy and failure to persist (108).

By convention, CD4 T helper (T_H) cells have been ascribed a supporting role in immunotherapy, augmenting priming, persistence and trafficking of CD8 T cells (72, 108). Some groups feel that they have several potential advantages over CD8 T cells as primary effectors of tumour rejection. Stimulated CD4 T_H cells can be directly cytotoxic, and recognise peptide presented on MHC Class II molecules. MHC Class ll is upregulated in response to IFNγ (108, 109) and autophagy promotes MHC Class ll restricted tumour-associated peptide display on the surface of tumour cells. CD4 T_H cells can augment anti-tumour immunity through licensing intratumoural APCs to provide costimulation to CD8 T cells, and through processing and presentation of exogenous and extracellular tumour antigens on MHC Class II. Innate and adaptive immune responses including NK cells and tumouricidal macrophages can also be recruited to target MHC-negative populations (108).

T_H17 cells are a subtype of CD4 Teff with immunotherapeutic potential. They are generated in response to TGFβ and IL-6, expanded in IL-23 and are involved in inflammation, recruitment of the innate immune system and tissue damage in autoimmunity. Using an in vivo B16/BL6 murine melanoma model, one group showed that T_H17 polarised tumour-specific CD4 T cells secrete IFNγ, acquire T_H1 characteristics post-adoptive transfer and are more effective in

rejecting tumour than T_H1 or T_H0 skewed cells in irradiated recipients. They suggest that T_H17 polarised TRP1 CD4 T cells persist beyond T_H1 cells, but with lesser proliferation, but this may be as a result of proliferation to exhaustion in the T_H1 subgroup (72).

Clinical experience using CD4 T_H cells as ACT is limited. The most compelling evidence for their utility in tumour rejection in humans derives from allogeneic stem cell transplantation data. CD4 T_H donor lymphocytes recognise MHC Class II expressed on BM derived cells, and are thought to help prevent outgrowth of MHC Class II expressing malignant haematopoietic clones (108).

Potential problems with CD4 T_H cells as adoptive tumour immunotherapy include a lack of well-established MHC Class II tumour-associated targets, and significant technical difficulty in obtaining sufficient CD4 T_H cell numbers for adoptive transfer (108, 110, 111).

4.1.2   The TRP1 CD4 T cell model in B16/BL6 melanoma- current paradigms

Recognising the potential of CD4 T_H cells as immunotherapeutic tools and the need for an appropriate model system in which to test them, Muranski et al generated the TRP1 mouse: a transgenic animal with an MHC Class ll restricted T cell receptor (TCR) targeting the endogenous melanocyte differentiation antigen TRP1 (gp75) expressed on melanoma tumours and normal melanocytes (71, 72).

Initial attempts to generate CD4 T cells reactive to TRP1 using immunised wild-type (WT) mice were unsuccessful, most likely due to tolerising mechanisms present in animals expressing endogenous TRP1 protein (71). The TRP1 TCR was ultimately derived from white-based-brown mutant cappuccino mice (B^w), in which an irradiation-induced-mutation results in complete absence of TRP1. Following backcrossing onto a C57BL/6 background, immunisation (and booster doses) with TRP1 vaccinia virus was performed prior to organ harvesting and hybridoma generation. The TCR most reactive for TRP1 protein/truncated peptides was identified by flow cytometry as Vβ16Vα3.2, which was sequenced and sub-cloned into a TCR cassette vector and co-injected into fertilised C57BL/6 embryos. The transgene inserted into the Y chromosome, and these male mice were successfully crossed into $RAG^{-/-}$ (black) mice to eliminate rearrangement of TRP1 TCR with endogenous TCR, and ultimately into the $RAG^{-/-}$ B^w (cappuccino) background to prevent autoimmune sequelae and to preserve the transgenic cells. It is thought that highly avid TRP1 reactive TCRs are deleted from the T cell repertoire in immune competent C57BL/6 mice (72).

TRP1 T cells mediate profound vitiligo and uveitis when infused into RAG$^{-/-}$ recipients, but animals survive to 12 months. Sublethally irradiated C57BL/6 mice receiving the same cells develop vitiligo and a less severe uveitis, with preserved longevity. Of note, TRP1 CD4 T cell replete RAG$^{-/-}$ mice were not protected from B16/BL6 tumour challenge, thought to be due to a lack of costimulation (72).

Adoptive transfer of TRP1 CD4 T cells into B16/BL6 murine melanoma bearing immune-competent C57BL/6 hosts results in tumour rejection and in some cases protection on tumour rechallenge. This is dependent upon IFNγ through myriad effects on T cell cytotoxic function, pro-apoptotic and anti-angiogenic effects, recruitment of the innate immune system, and upregulation of MHC expression on tumour cells mediating immune lysis (46, 72).

Quezada and Peggs demonstrated that tumour eradication and long-term tumour protection was achieved in lymphodepleted B16/BL6-bearing animals treated with TRP1 T cells and α-CTLA-4 mAb (46). 60% of tumours recrudesced in the cellular monotherapy group. At the cellular level, α-CTLA-4 mAb was associated with an intratumoural reduction in TRP1 and endogenous CD4 Tregs and an increase in TRP1 CD4eff and serum inflammatory cytokines such as IFNγ. In the lymphopenic environment, priming of tumour-reactive TRP1 T cells occurs in vivo to generate T$_H$1-like cells capable of granzyme B production (46), and blockade of granzyme B and perforin in vitro prevented lysis of tumour cell targets. Granzyme B is likely to be critical to the tumour cytolytic ability of TRP1 CD4 T cells.

4.1.3 The TRP1 CTLA-4 knockout (TRP1 CTLA-4$^{-/-}$) mouse

The CD45.1$^{+/+}$ B^W RAG$^{-/-}$ TRP1 CTLA-4$^{-/-}$ CD4 T cell transgenic mouse was generated at UCL by crossing B^W RAG$^{-/-}$ TRP1 transgenic mice (72) to CD45.1 expressing B6.SJL mice (Jackson labs) and then to CTLA-4$^{-/-}$ mice (42). Using these in tandem with CTLA-4 replete CD45.1$^{+/+}$ B^W RAG$^{-/-}$ TRP1 mice which we will refer to from now on as 'wild type' (WT), we conducted a series of experiments to explore the biological impact of complete absence of CTLA-4 on tumour-reactive T cells compared with a CTLA-4-replete T cell product, and additionally to discern whether ablating CTLA-4 'in cis' is fundamentally different to blocking CTLA-4 'in trans' using a blocking antibody/fragment. This question becomes increasingly relevant in light of work showing that CTLA-4 can sequester B7.1 and B7.2 from APC membranes in a cell extrinsic manner and that this mechanism is not restricted to Tregs (9, 26). This has implications for T cell intrinsic CTLA-4 ablation strategies for use in adoptive transfer models, as CTLA-4-replete host T cells could technically dampen the immune response evoked by CTLA-4$^{-/-}$ transferred

cells by providing a reservoir of endogenous CTLA-4 to act 'in trans' around the CTLA-4 negative cell product. This has the potential to switch off stromal costimulatory signals, augment production of intra-tumoural immuosuppressive cytokines (9, 26) and adversely impact upon the adoptively transferred cell product.

4.1.4   Mechanism of action of α-CTLA-4 mAb

Traditionally, blockade of the inhibitory activity of CTLA-4 on Teff and Treg was thought to underlie the anti-tumour effect of α-CTLA-4 mAb, but a recent publication has elucidated a novel mechanism. Simpson and Quezada show that there is a selective depletion 'in trans' of (CTLA-4^{hi}) Tregs within the tumour microenviroment and that it is dependent upon the presence of Fcγ-receptor expressing macrophages to effect ADCC (67). We will explore this in more detail in the TRP1 CTLA-4$^{-/-}$ setting.

4.2   Results

4.2.1   Baseline characteristics of TRP1 CTLA-4$^{-/-}$ mouse

The absence of CTLA-4 on transgenic effector T cells does not confer a survival advantage in cognate antigen poor, naïve mice, but neither does it disadvantage them, and baseline markers of murine wellbeing and longevity indicate that their weight, lifespan, breeding patterns and feeding habits are broadly comparable to wild type (WT TRP1) transgenic animals. To define the baseline characteristics of the TRP1 CTLA-4$^{-/-}$ transgenic mouse, we compared lymph nodes from naive C57BL/6, WT TRP1 and TRP1 CTLA-4$^{-/-}$ mice (see Chapter 2.4.1 for detail on murine strains).

Figure 4.1 shows that naïve TRP1 CTLA-4$^{-/-}$ mice have the highest proportion of Tregs of the three strains comprising 33.7% of total T cells compared with 12.3% in the C57BL/6 mouse and 7.06% in the WT TRP1 mouse. This is explained by a higher Ki67 proliferative index on TRP1 Tregs than the other strains (34.8% compared with 25.01% on the C57BL/6 mouse and 5.09% on the WT TRP1 mouse). Low WT TRP1 CD4+ FoxP3+ T cell numbers have been observed in other experiments but increase promptly with TRP1 peptide and IL-2 (data not shown).

WT TRP1 mice have the highest proportion of TRP1 Teff (92.6% of total T cells), followed by the C57BL/6 mouse at 86.9% and the TRP1 CTLA-4$^{-/-}$ mouse at 66.1%. Again, this is reflected in a

higher Ki67 proliferative index, with 30.9% on WT TRP1 Teff compared with 20.78% on TRP1 CTLA-4$^{-/-}$ Teff and 7.05% on C57BL/6 CD4 Teff.

Figure 4.1: comparison of Teff and Tregs between different murine strains at the point of cell isolation with assessment of proliferative (Ki67) and activation status (CD25 expression) on lymph node preparations. CTLA-4$^{-/-}$ TRP1 Treg are more proliferative than WT TRP1 Treg, but CTLA-4$^{-/-}$ TRP1 Teff are less proliferative than WT TRP1eff. **Key:** CD4 eff=CD4 Teffector cells; CD4 Treg=CD4 Tregulatory cells; FSC=forward scatter; WT=wild type. Experiment repeated in duplicate.
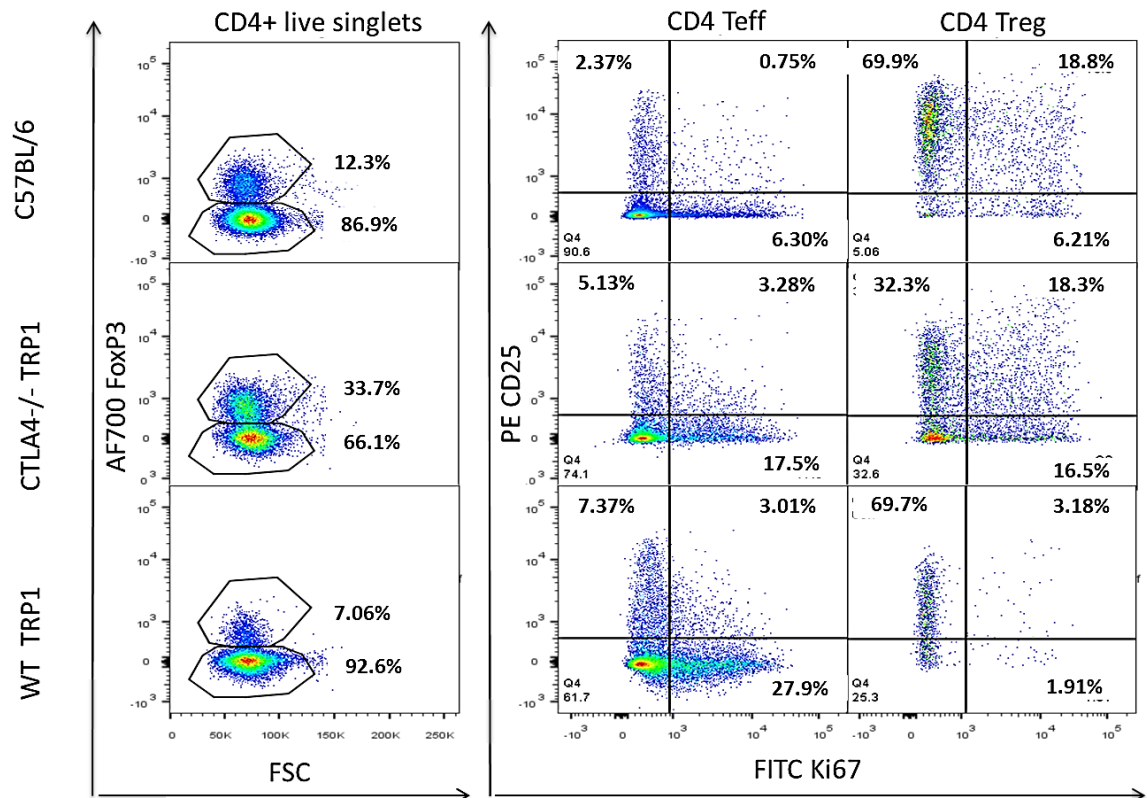
CD25 is found on activated T and B cells, and associates with CD122 to form a heterodimer that acts as a high-affinity receptor for IL-2. It has been used as a marker of CD4+FoxP3+ regulatory T cells in mice (34). CD25 and IL-2 are upregulated in an autocrine loop in response to activation through TCR signalling and are important to Treg development, function and homeostasis. Loss of CD25 on Tregs adversely affects their survival and expansion in the peripheral circulation, but their suppressive function remains intact (34). In excess, Tregs can act as cytokine sinks, preferentially binding and sequestering cytokines such as IL-2 (35).

In this experiment, CD25 expression is higher on CD4 Teff in WT TRP1 and TRP1 CTLA-4$^{-/-}$ mice (10.38% and 8.41% respectively) than on C57BL/6 (3.12%) mice, but on CD4 Treg, there is lower expression of CD25 on the TRP1 CTLA-4$^{-/-}$ mouse (50.6% CD25+ compared with 72.88% on the WT TRP1 and 88.7% on the C57BL/6 mouse).

4.2.2. TRP1 CTLA-4$^{-/-}$ T cell transfer into immunocompetent hosts

WT TRP1 CD4+ T cells can prevent outgrowth of B16/BL6 murine melanoma in immunocompetent recipients when co-administered with Gvax and systemic αCTLA-4 mAb (9H10 clone). This is associated with an intratumoural reduction in TRP1 Tregs and increased IFNγ secretion from TRP1 Teff [67].

Informed by the above and work described by Simpson et al [68] of adoptively transferred WT TRP1 T cells, we elected to recapitulate their experimental format with 2 additional groups receiving TRP1 CTLA-4$^{-/-}$ T cells with and without systemically administered αCTLA-4 mAb (see figure 4.2 for experimental layout). The experimental aims/endpoints were to determine whether the absence of CTLA-4 on TRP1 CD4 T cells impacts upon TRP1 Treg numbers intratumourally between groups within the 10 day experimental time frame [68], and whether the absence of CTLA-4 on TRP1 Teff in this model parallels the previously described anti-tumour effects of CTLA-4 blockade using exogenous αCTLA-4 mAb.

Figure 4.2: adoptive transfer of CTLA-4$^{-/-}$ TRP1 T cells is compared with transfer of WT TRP1 T cells into immunocompetent B16/BL6 murine melanoma bearing C57BL/6 recipients. Adjuvant Gvax therapy is required to promote TRP1 T cell numbers and infiltration into tumour. **Key:** Trp1= tyrosinase related protein 1; WT=wild type; 250k=250 thousand; i.d=intradermal; Gvax=GM-CSF secreting cellular vaccine; αCTLA-4=anti-murine CTLA-4 mAb (9H10 clone); LN=lymph node; TIL=tumour/tumour infiltrating lymphocytes; data represents 3 separate experiments.
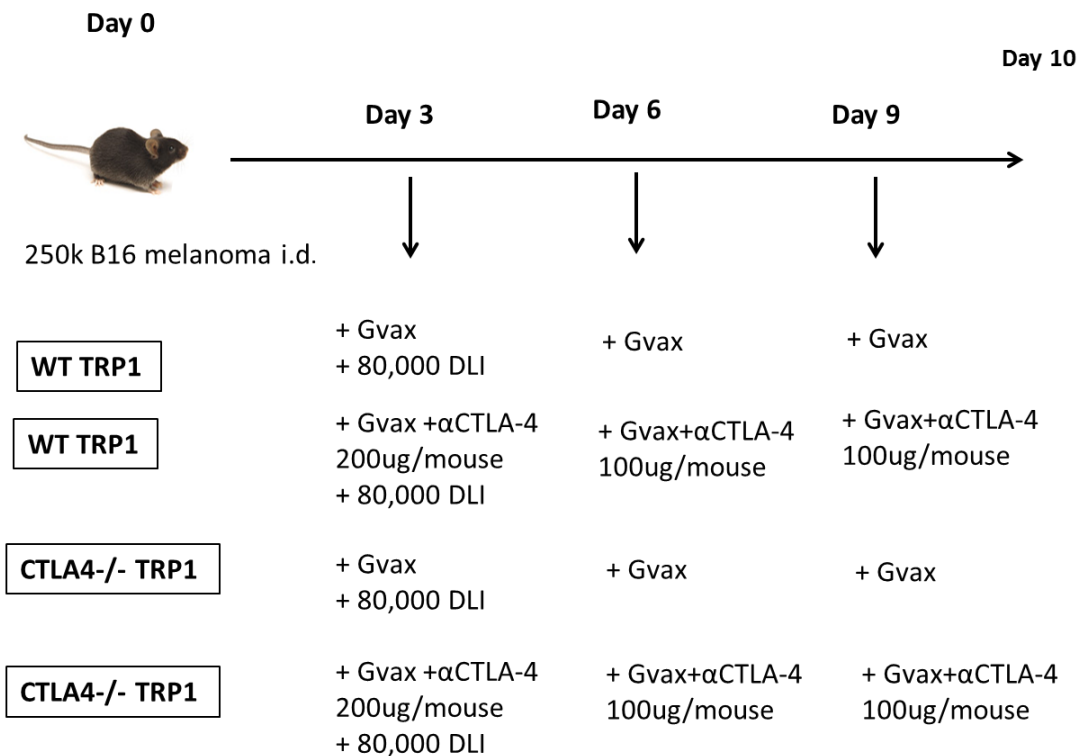
We elected to use conservative mouse numbers in the first instance (3 mice per group), as published data using the model had demonstrated a definitive treatment effect in the WT TRP1 setting with a reproducible, complete absence of TRP1 Tregs intratumourally by Day 10 (67).

On day 3, WT TRP1 and CTLA-4$^{-/-}$ TRP1 donor LN and spleen harvests underwent CD4 positive selection (Miltenyi Biotech, CliniMACS® cell sorting, Auburn, CA), yielding CD4+Vβ14+ purities of 58.4% and 63.5% respectively (figure 4.3). 50% of the mice received WT TRP1 T cells, and 50% received CTLA4$^{-/-}$ TRP1 T cells. All animals received adjuvant GM-CSF secreting cellular vaccine (Gvax) to promote TRP1 T cell expansion and tumour infiltration. Subgroups of each cohort received αCTLA-4 mAb (9H10 clone) at days 3, 6 and 9 (see Chapters 2.2.4 and 2.4.7 for experimental details).

Figure 4.3: purity of CD4 selected WT TRP1 and CTLA-4$^{-/-}$ TRP1 cells for adoptive transfer into B16/BL6-bearing C57BL/6 recipients. There was limited loss of cells to the column. Gated on live singlets. **Key:** WT=wild type; Vb14=β chain of the monoclonal TCR expressed in TRP1 mice.
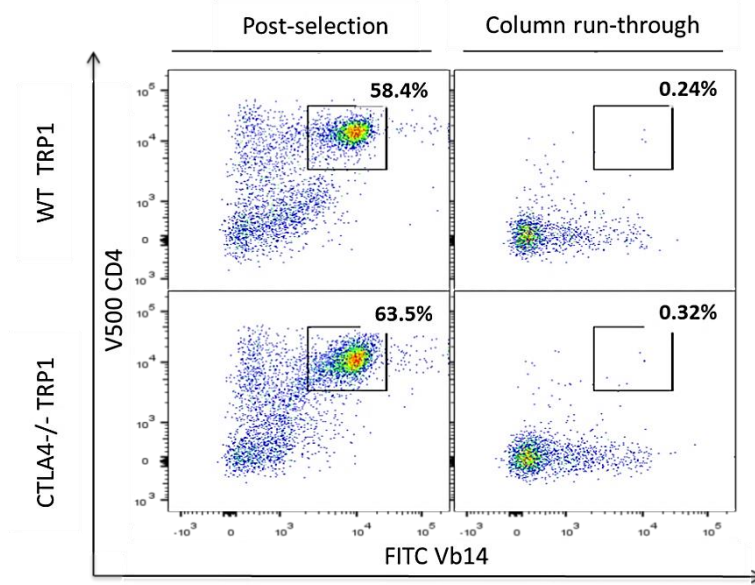
Figure 4.4a: tumour weight at day 10 in immunocompetent B16/BL6 tumour-bearing C57BL/6 recipients shows no significant difference between groups. Key: TRP1= tyrosinase related protein 1; Gvax=GM-CSF secreting cellular vaccine; αCTLA4=anti-murine CTLA-4 monoclonal antibody (9H10 clone); mg=milligrams; ns=non-significant. Horizontal bars represent mean values and vertical bars represent the standard error of the mean (SEM). Statistical tests: one-way analysis of variance and multiple comparisons test.
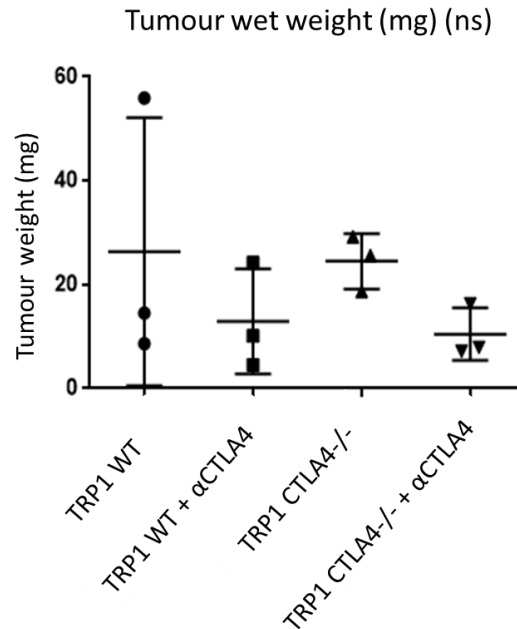
Figure 4.4b: WT TRP1 Tregs (but not TRP1 CTLA4$^{-/-}$ Treg) are depleted intratumourally by the addition of αCTLA-4 mAb. αCTLA-4 mAb associated reduction in TRP1 Tregs is not apparent in LN. All groups received Gvax at days 3, 6 and 9. **Key:** Trp1= tyrosinase related protein 1; Gvax=GM-CSF secreting cellular vaccine; αCTLA4=anti-murine CTLA-4 mAb (9H10 clone); CD45.1=congenic marker of TRP1 T cells; LN=lymph node; TIL=tumour/tumour-infiltrating lymphocytes.
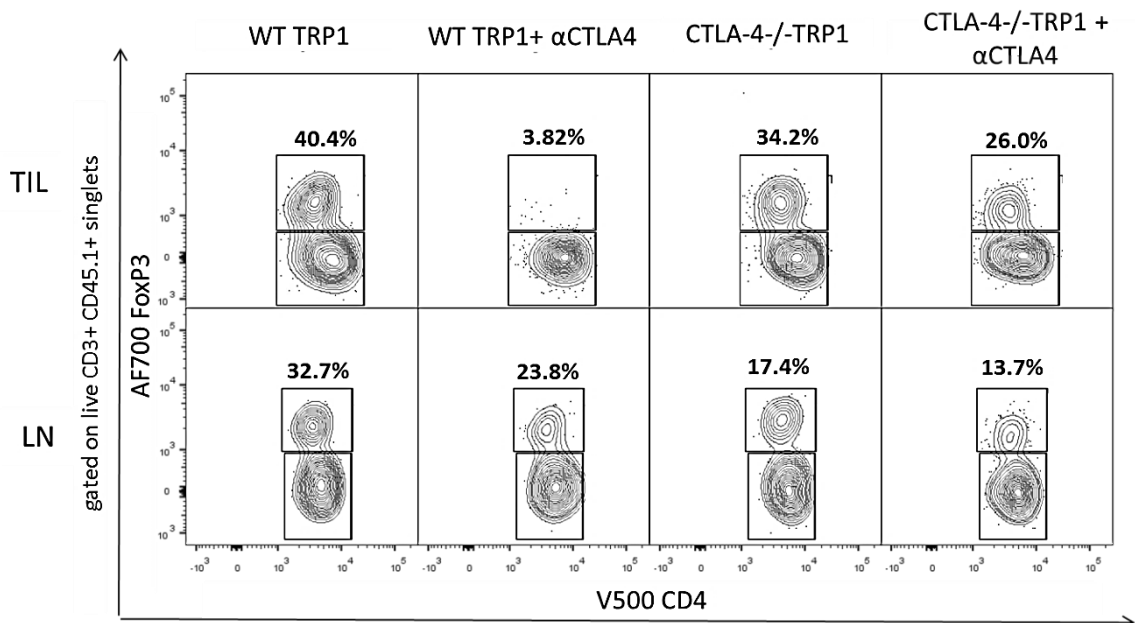
Figure 4.4c: absolute numbers of TRP1 CTLA4$^{-/-}$ **Teff are significantly higher in LN when co-administered with αCTLA4 mAb (clone 9H10) than in other groups.** Intratumoural WT TRP1 Tregs, but not CTLA4$^{-/-}$ TRP1 Tregs, are (non-significantly) lower with αCTLA4 mAb. **Key:** WT=wild type; Gvax=GMCSF secreting cellular vaccine; αCTLA4=anti-murine CTLA-4 mAb (9H10 clone) ;mg=milligrams. Horizontal bars represent mean values and vertical bars represent SEM. Statistical tests: one-way analysis of variance and multiple comparisons test.
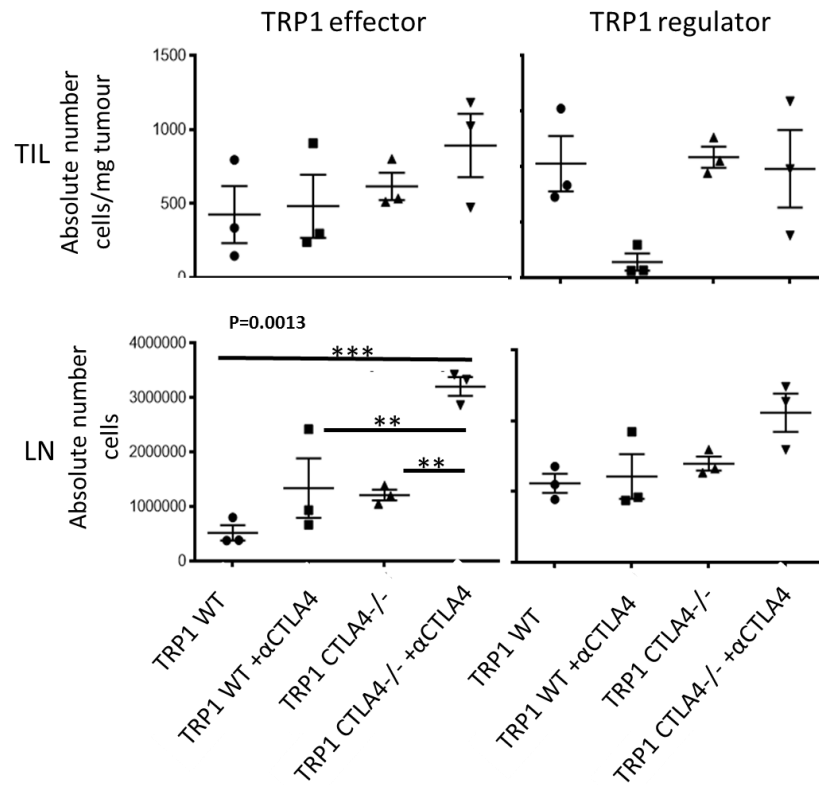
Figure 4.4a shows that tumour size is statistically equivalent between groups by Day 10 with no definitive early indicators of improved anti-tumour efficacy with TRP1 CTLA-4$^{-/-}$ cells. There is a trend towards lower tumour weights in the groups receiving concurrent exogenous αCTLA-4 mAb, but this does not reach statistical significance. Consistent with what is published (46), figures 4.4b shows a reduction in intratumoural WT TRP1 Tregs in the group treated with αCTLA-4 mAb (46, 67), but resistance to this effect is observed amongst intratumoural TRP1 CTLA-4$^{-/-}$ Tregs. TRP1 Tregs in the LN are also protected from this effect.

Quantitation of absolute cell numbers in figure 4.4c confirms an intratumoural drop in WT TRP1 Tregs (but not TRP1 CTLA-4$^{-/-}$ Tregs) with αCTLA-4 mAb that is not explained by a reduction in Ki67 expression (figure 4.4d). This supports the hypothesis of αCTLA-4 mAb directed CTLA-4^{hi} target cell depletion (67), as cells lacking the antibody target (TRP1 CTLA-4$^{-/-}$ Tregs) are unaffected. CTLA-4-replete TRP1 Tregs in the LN are also unaffected.

There is a trend in LN and tumour towards higher absolute numbers of CTLA-4$^{-/-}$ TRP1 Teff compared with WT TRP1 Teff, but this only reaches significance in the lymph node with co-administered αCTLA-4 mAb. CTLA-4$^{-/-}$ TRP1 Teff are more proliferative than WT TRP1 Teff alone (without αCTLA-4 mAb) in LN and tumour, but the significant increase in CTLA-4$^{-/-}$ TRP1 Teff cell numbers with αCTLA-4 mAb is not fully explained by the Ki67 expression observed.

It is possible that αCTLA-4 mAb-mediated diminution of endogenous CD4 Treg numbers may contribute to the effector expansion in the tumour (figure 4.4e), whereas in the LN where the density of effectors for ADCC is lower, αCTLA-4 mAb may fulfil a receptor blocking role resulting in activation and expansion(46).

Figure 4.4d: TRP1 CTLA-4$^{-/-}$ Tregs and Teff are more proliferative (high Ki67) in the LN compared with WT TRP1 T cells (p<0.05). This effect is lost in the TIL. Key: TIL=tumour/tumour infiltrating lymphocytes; LN=lymph node; mg=milligrams; WT=wild type; Gvax=GMCSF secreting cellular vaccine; αCTLA4=anti-murine CTLA-4 mAb (9H10 clone); ns=non-significant. Vertical bars represent SEM. Statistical tests: one-way analysis of variance and multiple comparisons test.
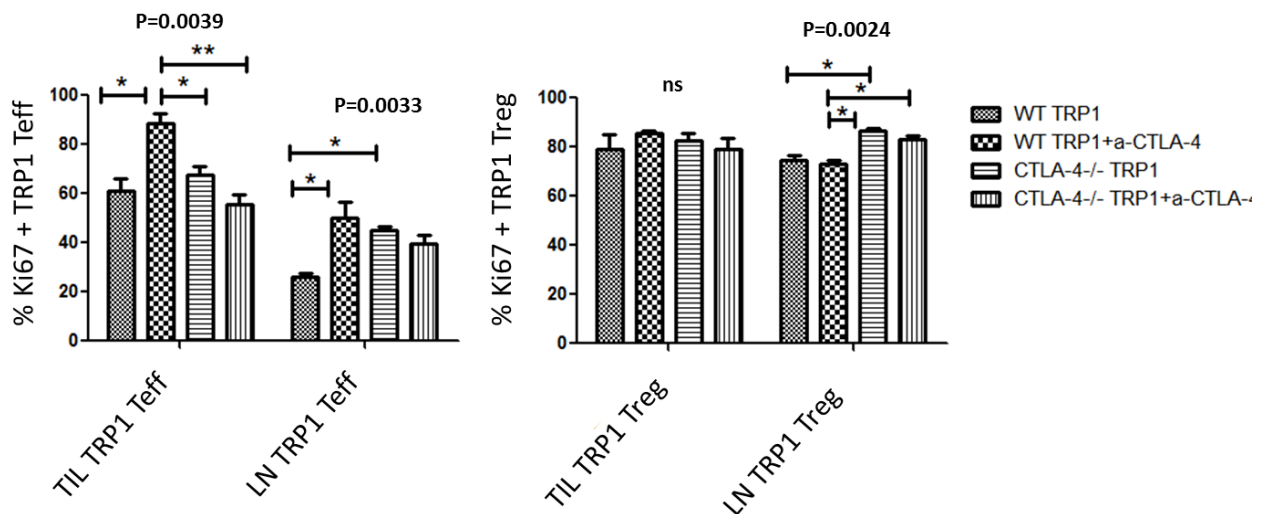
Figure 4.4e: αCTLA4 mAb is associated with a significant reduction in endogenous CD4 Tregs intratumourally, but not in the LN (p<0.05). Key: TIL=tumour/tumour infiltrating lymphocytes; LN=lymph node; mg=milligrams; WT=wild type; Gvax=GMCSF secreting cellular vaccine; αCTLA4=anti-murine CTLA-4 mAb (9H10 clone). Horizontal bars represent mean values and vertical bars represent SEM. Statistical tests: one-way analysis of variance and multiple comparisons test.
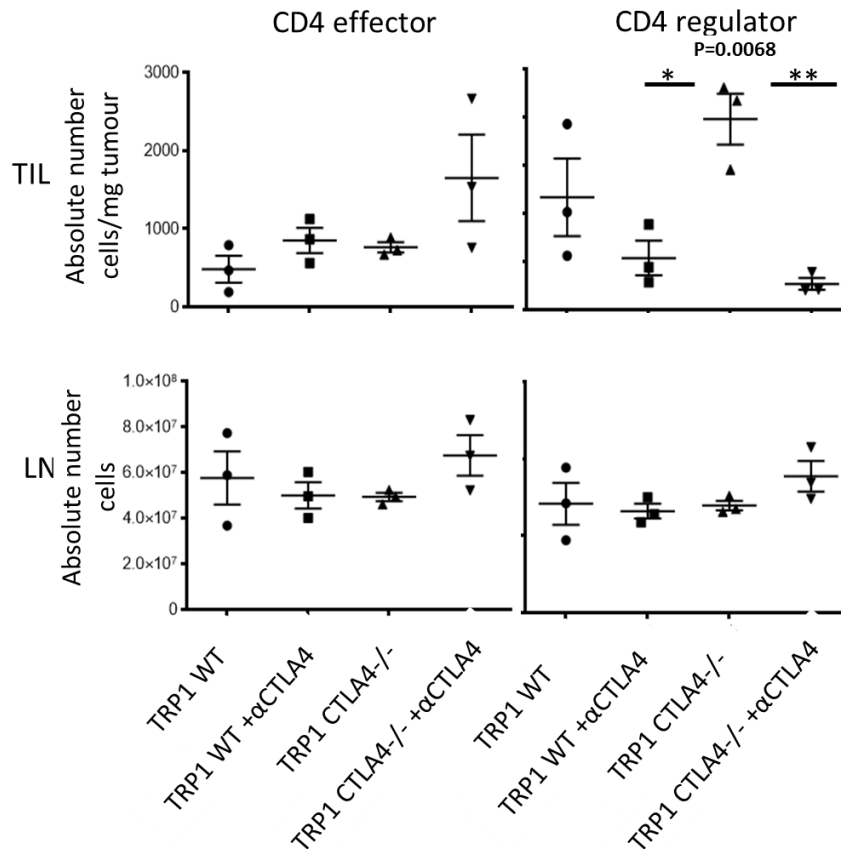
TRP1 Tregs and endogenous CD4 Tregs are heavily depleted by αCTLA-4 mAb in the tumour but not the LN (figures 4.4c and 4.4e). TRP1 CTLA-4$^{-/-}$ Tregs are resistant to the effects of αCTLA-4 mAb. Figures 4.4f and 4.4g show that CTLA-4 expression on endogenous and TRP1 CD4 T cells is substantially higher in the tumour compared to the LN. In the tumour, αCTLA-4 mAb ablates CTLA-4 expression on Tregs.

This reproducible dataset supports previously published work (46, 67) of a direct toxic effect of αCTLA-4 mAb to CTLA-4^{hi} cells. The underlying mechanism is proposed to be antibody-directed deletion via ADCC of CTLA-4^{hi} targets (67), and our data provides further evidence for this mechanism showing that absence of CTLA-4 from Tregs seems to protect them from depletion. Mean fluorescence intensity (MFI) of CTLA-4 on endogenous and TRP1 Tregs is brighter in the tumour than in the LN, and may explain why depletion is more apparent in the tumour.

Figure 4.4f: αCTLA4 mAb therapy is associated with a reduction in CTLA-4 expression in endogenous and WT TRP1 Tregs in the tumour. TRP1 CTLA-4$^{-/-}$ Tregs are relatively unaffected. **Key:** WT=wild type; αCTLA4=anti-murine CTLA-4 mAb (9H10 clone); Gvax=GMCSF secreting cellular vaccine.
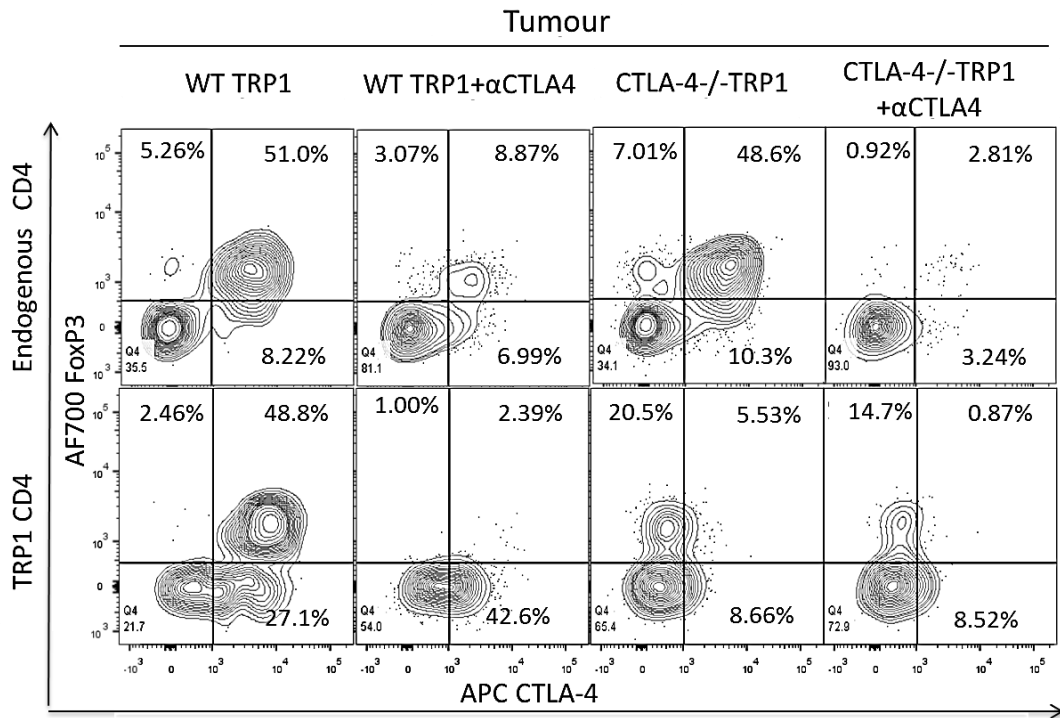
Tumour

Figure 4.4g: CTLA-4 expression on endogenous and TRP1 Tregs in the lymph node is lower than in the tumour and αCTLA4 mAb therapy is associated with a minor reduction in CTLA-4 expression on WT TRP1 Tregs. **Key:** WT=wild type; αCTLA4=anti-murine CTLA-4 mAb (9H10 clone); Gvax=GMCSF secreting cellular vaccine.

LN
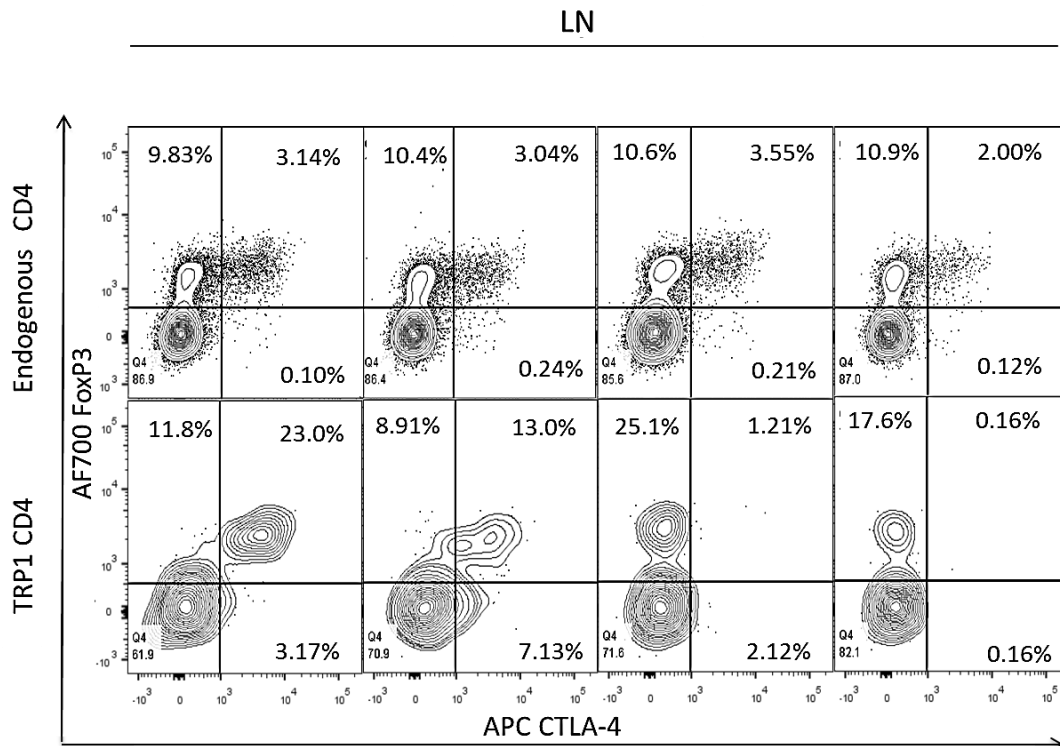
Figure 4.4h: CD25 expression is significantly reduced on intratumoural TRP1 CTLA-4$^{-/-}$ Teff compared with WT TRP1 Teff. **Key:** Teff=CD4 T-effector cells; TIL=tumour/tumour infiltrating lymphocytes; WT=wild type; Gvax=GMCSF secreting cellular vaccine; αCTLA4=anti-murine CTLA-4 mAb (9H10 clone). Vertical bars represent SEM. Statistical tests: one-way analysis of variance and multiple comparisons test.
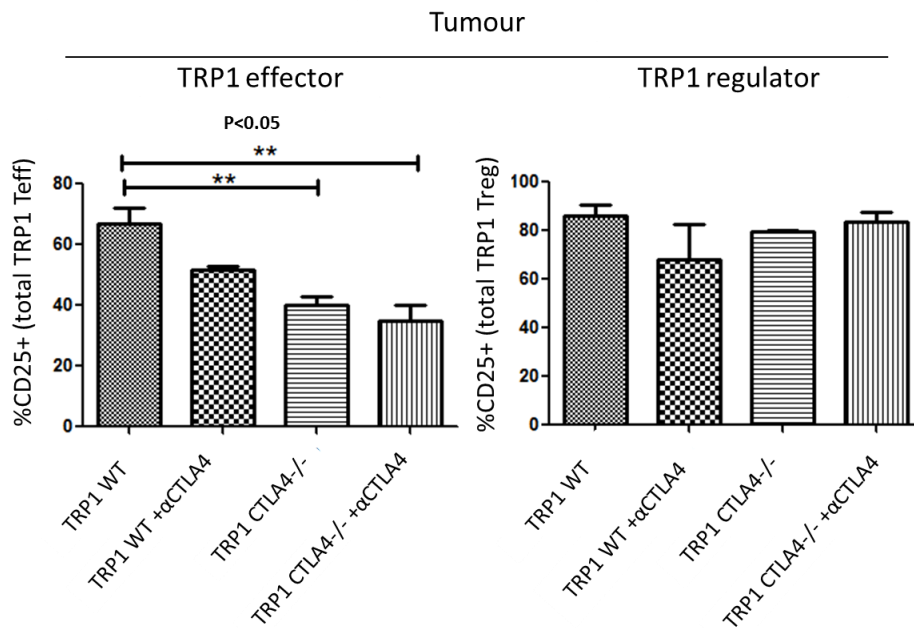

Naïve (unmanipulated, pre-adoptive transfer) TRP1 CTLA-4$^{-/-}$ Tregs and to a lesser extent Teff express less CD25 than naive WT TRP1 Tregs (figure 4.2), but following adoptive transfer into

immunocompetent tumour bearing hosts, CD25 expression on Tregs (WT and CTLA-4$^{-/-}$) increases such that it is high across all groups (between 75-85%)(figure 4.4h).

Intratumoural TRP1 CTLA-4$^{-/-}$ Teff express lower CD25 compared with WT TRP1 Teff (which is not observed in the LN) without an obvious associated drop in Ki67 (figure 4.4d) . It is recognised that Tregs are associated with significant downregulation of IL-2 mRNA in Teff in vitro and that competition for IL-2 drives Tregs to upregulate CD25 (a process that is dependent on IL-2) where Teff cannot as they are (relatively) IL-2 deprived from cytokine sequestration by Tregs (112). In fact, Tregs are dependent on an exogenous supply of gamma chain cytokines (35).

IL-2 was not observed on TRP1 Teff at in vitro restimulation but figure 4.4i shows that IL-2 expression is increased on endogenous CD4 Teff in the tumour (but not the LN) with αCTLA-4 mAb and would support the hypothesis that absence of Tregs permits upregulation of IL-2 transcription in Teff. Lower expression of CD25 and a lack of staining for IL-2 on CTLA-4$^{-/-}$ TRP1 Teff in the tumour (or a lack of appropriate CD25 upregulation in the context of inflammation) should confer a survival disadvantage. However, given the increase in absolute CTLA-4 $^{-/-}$ TRP1

Teff numbers, it may be this drop in CD25 simply represents a homeostatic adaptation to control T cell populations.

Figure 4.4i: IL-2 expression is increased on endogenous CD4 Teff in the tumour (but not the LN) with αCTLA-4 mAb and would support the hypothesis that absence of Tregs permits upregulation of IL-2 transcription in Teff. Gated on live, CD4+, CD45.1-, FoxP3- singlets. **Key:** WT=wild type; Gvax=GMCSF secreting cellular vaccine; αCTLA4=anti-murine CTLA-4 mAb (9H10 clone).
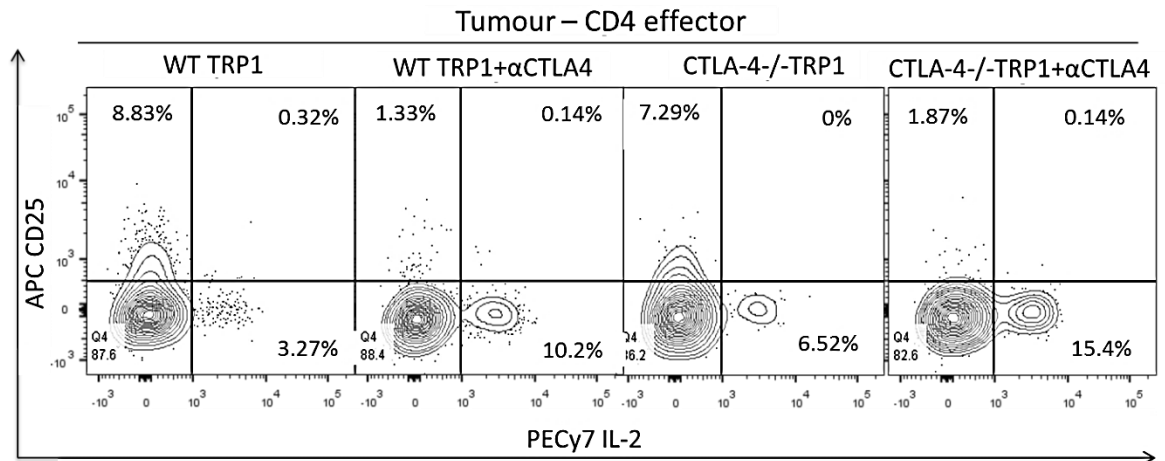
Figure 4.4j: Granzyme B expression is increased on intratumoural TRP1 CTLA-4$^{-/-}$ T-eff compared with WT TRP1 T-eff. αCTLA-4 mAb appears to increase granzyme B expression in WT and CTLA-4$^{-/-}$ transgenic Teff. All animals received Gvax. Minimal granzyme B is observed in the LN. **Key:** TIL=tumour/tumour infiltrating lymphocytes; LN= lymph node; WT=wild type; αCTLA4=anti-murine CTLA-4 mAb (9H10 clone).
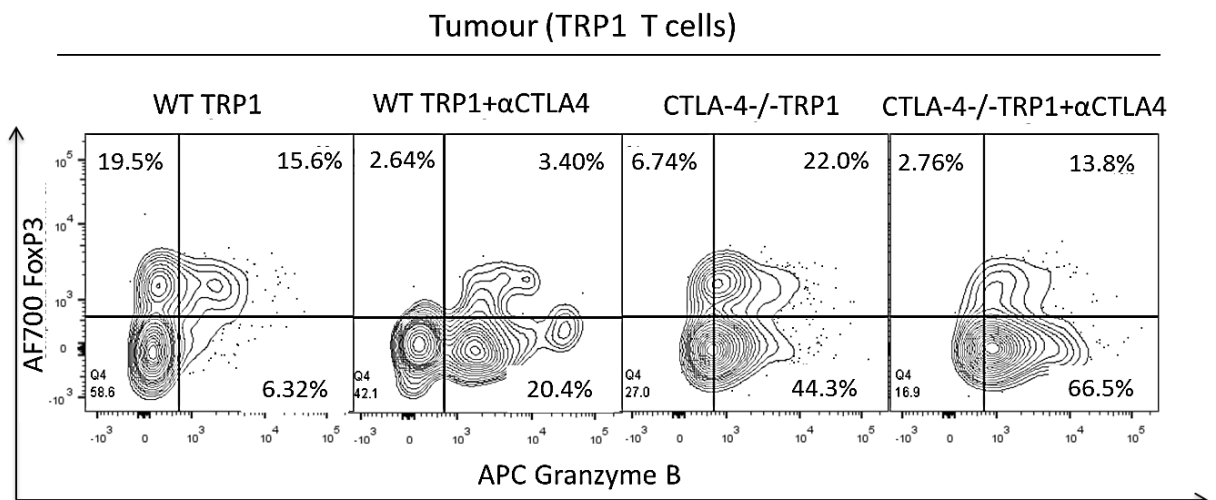
Assessment of of TRP1 CTLA-4$^{-/-}$ Teff function shows enhanced granzyme B expression compared with WT TRP1 Teff (figure 4.4j) but there is no significant difference in IFNγ expression on a restimulation assay (see Chapter 2.4.8 for assay details) (data not shown).

Summary

A fundamental question underlining these experiments is whether CTLA-4 ablation on tumour reactive T cells is functionally and therapeutically equivalent to the administration of exogenous αCTLA-4 mAb in an immunocompetent murine model of cancer.

What is apparent from recently published work and supported by this data is that exogenous αCTLA-4 mAb has a powerful biological effect in the tumour, targeting CTLA-4^{hi} cells for depletion by ADCC (67). Figures 4.4b and 4.4c show αCTLA-4 mAb mediated depletion of WT TRP1 Tregs in the tumour (but not the LN) with sparing of TRP1 CTLA-4$^{-/-}$ Tregs which lack the target receptor. Figure 4.4e shows that intratumoural endogenous CD4 Tregs are similarly vulnerable to depletion.

Expression profiles of CTLA-4 across endogenous and transferred CD4 compartments in LN and tumour are shown in figures 4.4f and 4.4g. CTLA-4 expression is substantially higher in endogenous and TRP1 Tregs in the tumour compared with the LN and expression drops markedly in CTLA-4-replete cells treated with αCTLA-4 mAb. This suggests that one of the reasons for the more extensive Treg depletion seen with αCTLA-4 mAb in the tumour compared with LN is the high expression of target antigen defined by mean fluorescence intensity (MFI). It is possible that other factors such as availability of ADCC-competent effector cells also influence this.

TRP1 CTLA-4$^{-/-}$ T cells do not offer a clear anti-tumour advantage compared with αCTLA-4 mAb by experimental day 10, as tumour weights are broadly equivalent between groups. Rather there is a trend towards lower tumour weight in groups receiving exogenous αCTLA-4 mAb.

The failure of TRP1 CTLA-4$^{-/-}$ T-cells to demonstrate a significant anti-tumour advantage here is probably multifactorial. It is possible that assessment at day 10 of tumour growth is too early to demonstrate a clear difference in effect between TRP1 WT and TRP1 CTLA-4$^{-/-}$ T-cells. However, it may also be that the treatment effect is diluted by small experimental groups. Power analysis indicates the sample size required to ensure that statistical judgments are precise and reliable and incorporates several factors: the type of statistical test being

performed, the sample size (bigger sample usually means greater power), the effect size, and the degree of experimental measurement error. For future experiments we plan to incorporate power analysis based on our own preliminary data on effect size. From this we can determine the minimum sample size required to demonstrate a statistically significant anti-tumour effect. We also propose a tumour time course experiment to establish the optimal point at which to terminate the experiment with this endpoint of tumour growth in mind.

Biologically with respect to anti-tumour effect, it is probable that CTLA-4 on endogenous Tregs acts 'in trans' to prevent full TRP1 CTLA-4$^{-/-}$ Teff expansion, evidenced by the increase in absolute numbers obtained with concurrent αCTLA-4 mAb treatment. In an attempt to minimise the impact of the endogenous compartment, we plan to repeat the experiment in lymphodepleted tumour-bearing recipients.

That said, there are several features that make TRP1 CTLA-4$^{-/-}$ T cells a potentially attractive ACT option. They are more proliferative than WT TRP1 T cells (figure 4.4d) and there is a clear trend towards higher Teff numbers, reaching significance in the LN with concurrent administration of αCTLA-4 mAb (figure 4.4c). They are also potentially more cytotoxic than WT TRP1 Teff, producing higher levels of granzyme B in the tumour.

These perceived advantages may be partly due to functionally compromised co-transferred TRP1 CTLA-4$^{-/-}$ Tregs. It is widely accepted that Tregs lacking CTLA-4 cannot negatively regulate Teff expansion in the same way as CTLA-4-replete Tregs, and over the longer term this can lead to lymphoproliferation in mice[43]. In some ways, the CTLA-4-ablated TRP1 cell product is akin to a WT TRP1 cell product that has been purged of functional antigen-specific Tregs. Either way, if the net result of CTLA-4 ablation on tumour specific T cells is to promote a dominant effector phenotype that is maintained in the tumour, then it has potential value as a therapeutic tool.

4.2.3   TRP1 CTLA-4$^{-/-}$ T cell transfer into lymphodepleted hosts

Published data confirms that WT TRP1 T cell adoptive transfer in combination with lymphodepletion + αCTLA-4 mAb into the B16/BL6 murine melanoma model results in lower tumour weight, higher intratumoural TRP1 Teff/Treg ratios and higher granzyme B expression in tumour reactive T effectors when compared with transfer of WT TRP1 T cells and lymphodepletion alone (46). We repeated the experiment detailed in Chapter 4.2.2 in a cohort of irradiated C57BL/6 recipients (figure 4.5). Sub-lethal irradiation is described in Chapter 2.4.12. T cell isolation and purification was performed using a murine CD4 positive bead/column selection kit (Miltenyi Biotech, CliniMACS® cell sorting, Auburn, CA) and 50 x 10^4 CD4+Vβ14+ cells/mouse were infused.

Figure 4.5: experimental set-up for testing of TRP1 CTLA-4$^{-/-}$ T cells in LYMPHODEPLETED B16/BL6 murine melanoma bearing C57BL/6 recipients. Adjuvant Gvax is not required. **Key:** Trp1= tyrosinase related protein 1; WT=wild type; 250k=250 thousand; i.d.=intradermal; αCTLA-4=anti-murine CTLA-4 mAb (9H10 clone); LN=lymph node; TIL=tumour/tumour infiltrating lymphocytes. Experiment repeated in duplicate.
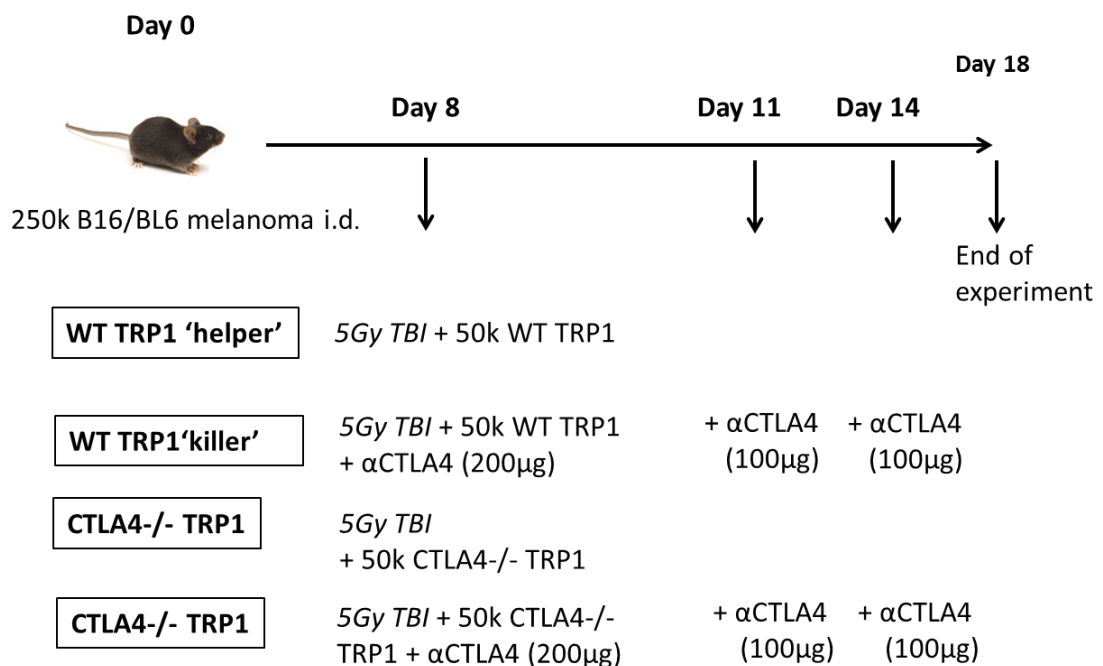
Figure 4.6a: WT TRP1 Tregs are proportionally lower than CTLA-4$^{-/-}$ TRP1 Tregs post CD4 selection and pre-adoptive transfer. Key: WT=wild type; Vβ14=β chain of the monoclonal TCR expressed in TRP1 mice.
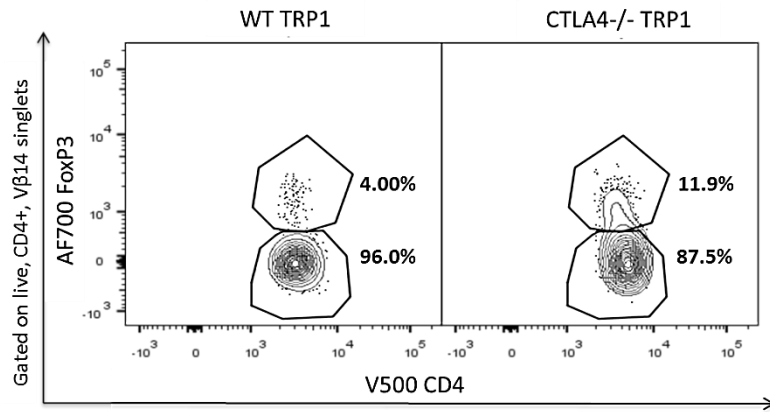
In the naïve state, WT TRP1 Tregs are proportionally low compared with CTLA-4$^{-/-}$ TRP1 Tregs (figure 4.1). Figure 4.6a confirms this finding in post-CD4 selection, pre-adoptive transfer FACS analysis.

Other groups have identified human CTLA-4 on melanoma cell lines in vitro (113) which could theoretically act 'in trans' to compromise the effect of CTLA-4 ablation on tumour reactive T cells. In tumour samples harvested during our TRP1 T cell transfer experiments, B16/BL6 murine melanoma does not appear to express CTLA-4 (live, non CD3+ singlets are negative for CTLA-4) (figure 4.6b).

Figure 4.6b: CTLA-4 is not expressed on B16/BL6 melanoma.. Key: WT=wild type; SSC=side scatter; FSC=forward scatter; SSW=side scatter width.
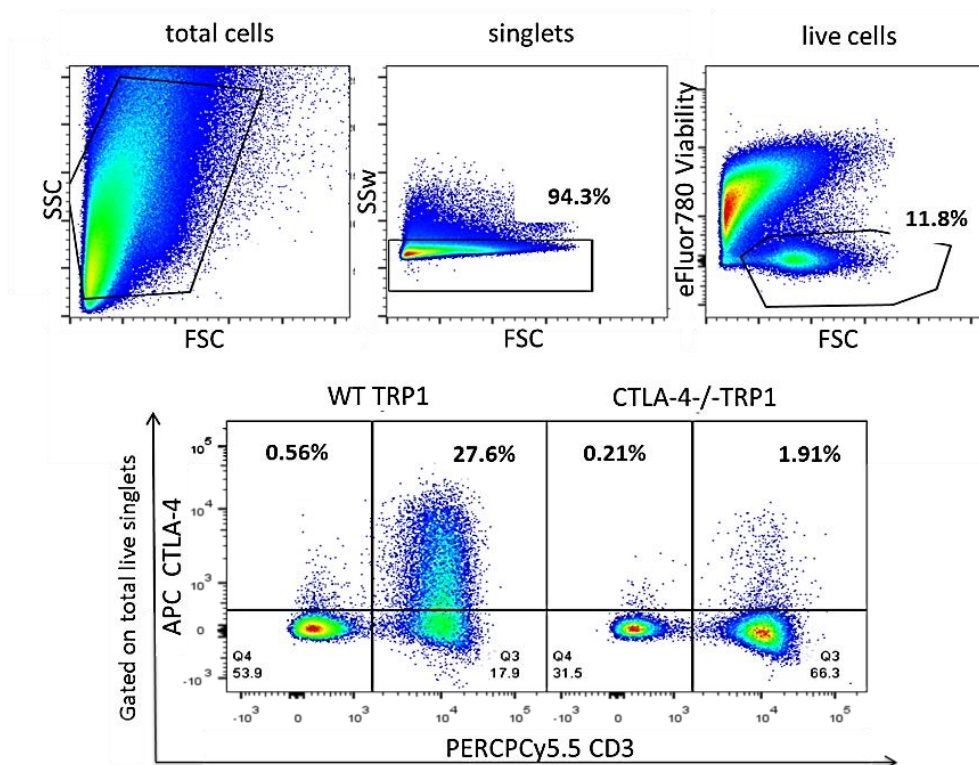
Figure 4.7a: tumour weight at day 18 in lymphodepleted B16/BL6 tumour-bearing C57BL/6 mice shows a non-significant trend towards lower tumour weight in TRP1 CTLA-4$^{-/-}$ T cell recipients compared with WT TRP1 recipients, irrespective of αCTLA4 mAb therapy. Key: TRP1= tyrosinase related protein 1; αCTLA4=anti-murine CTLA-4 monoclonal antibody (9H10 clone); mg=milligrams; ns=non-significant. Horizontal bars represent mean values and vertical bars represent SEM.
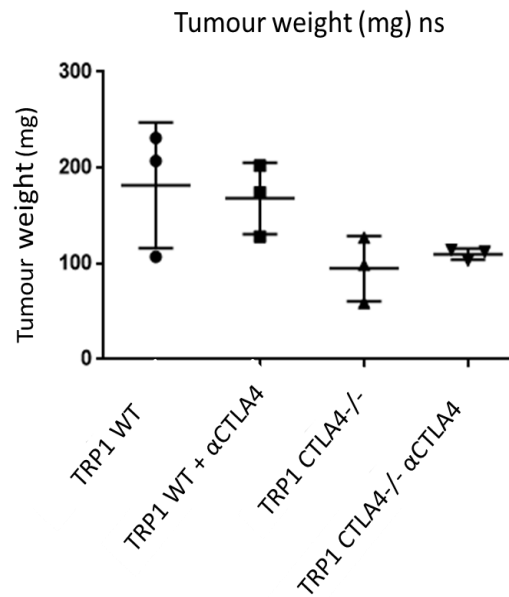
Figure 4.7b: αCTLA4 mAb is associated with a significant reduction in absolute numbers of endogenous CD4reg in the tumour, not apparent in the LN. Key: LN=lymph node; TIL=tumour/tumour infiltrating lymphocytes; mg=milligrams; WT=wild type; αCTLA4=anti-murine CTLA-4 mAb (9H10 clone). Horizontal bars represent mean values and vertical bars represent SEM. Statistical tests: one-way analysis of variance and multiple comparisons test.
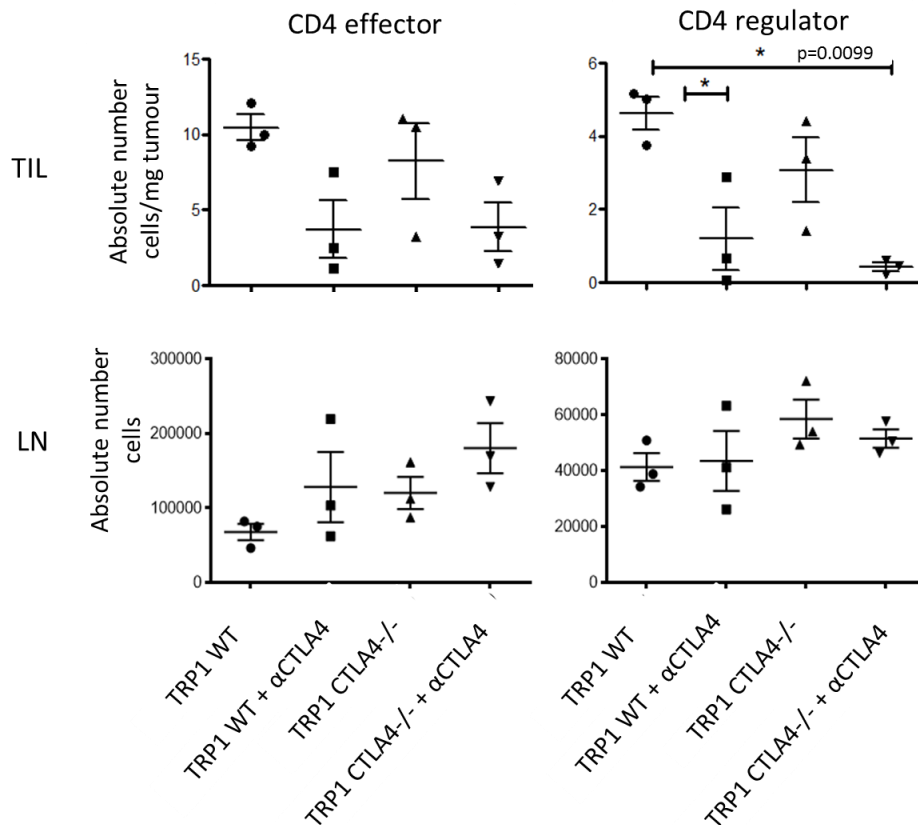
Figure 4.7c: CTLA-4 expression on endogenous CD4 Teff and Tregs is higher in the tumour than the LN and expression is lost in the tumour on exposure to αCTLA4 mAb. This supports the hypothesis of CTLA-4 targeted depletion of CTLA-4^{hi} targets by αCTLA4 mAb and would explain the reduction in absolute numbers of intratumoural CD4regs observed in figure 4.7b. Key: αCTLA4=anti-murine CTLA-4 mAb (9H10 clone); WT=wild type TRP1.
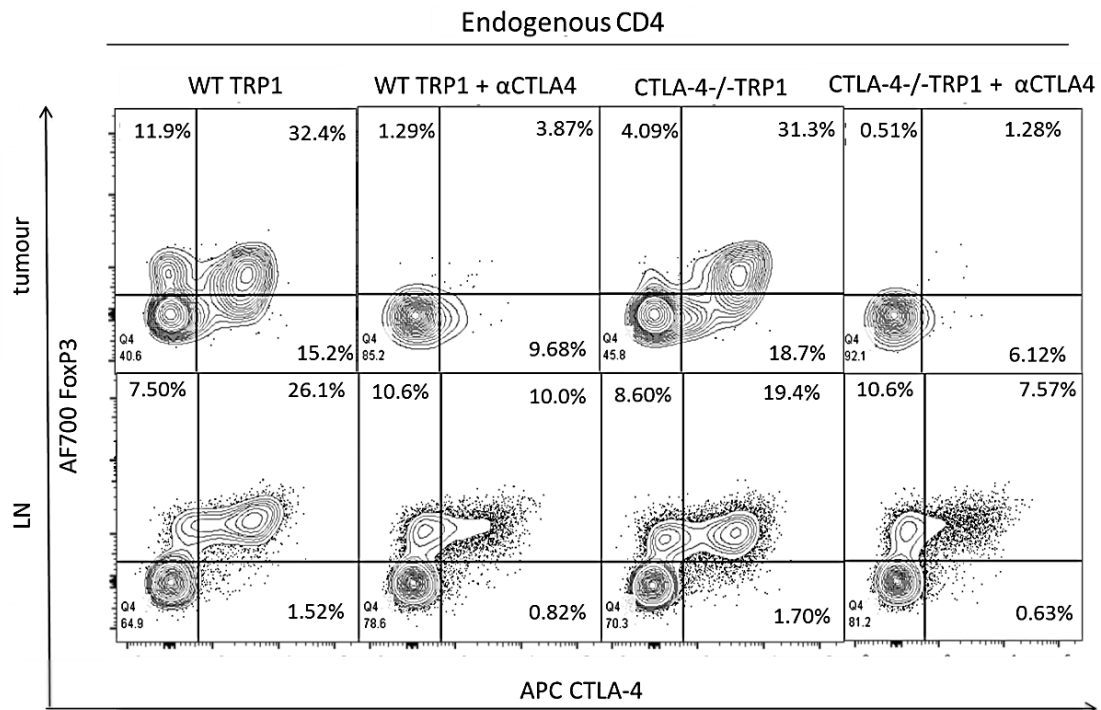
Figure 4.7a demonstrates a non-significant trend towards lower tumour weight in TRP1 CTLA-4$^{-/-}$ T cell recipients. In the tumour, there is a significant reduction in absolute numbers of endogenous CD4 Treg, and a trend towards lower CD4eff numbers and lower WT TRP1 Treg numbers with αCTLA-4 mAb therapy (figures 4.7b and 4.7d). One potential mechanism could be depletion of CTLA-4^{hi} targets by ADCC-competent αCTLA-4 mAb (see figure 4.7c for endogenous LN and tumour CTLA-4 profiles)(67).

Absolute TRP1 CTLA-4$^{-/-}$ Teff numbers are increased compared with WT TRP1 Teff numbers in the LN and the tumour, reaching significance when co-administered with αCTLA-4 mAb (figure 4.7d). TRP1 CTLA-4$^{-/-}$ Treg numbers are surprisingly low in tumour and LN, comparable to WT TRP1 Treg numbers following depletion by α-CTLA4 mAb. This was not apparent in experiments conducted in immunocompetent recipients (figure 4.4c). These changes result in an increased TRP1 CTLA-4$^{-/-}$ Teff/Treg ratio which we know to be associated with lower tumour weight (46).

Figure 4.7d: absolute numbers of TRP1 CTLA-4^{-/-} Teff are increased in the LN and tumour compared with WT TRP1 Teff. This is further enhanced by αCTLA4 mAb (clone 9H10). TRP1 CTLA-4^{-/-} Tregs are low in the tumour and LN, comparable to WT TRP1 Treg levels in tumour following depletion by αCTLA4 mAb (clone 9H10). **Key:** mg=milligrams; WT=wild type; αCTLA4=anti-murine CTLA-4 mAb (9H10 clone). Horizontal bars represent mean values and vertical bars represent SEM. Statistical tests: one-way analysis of variance and multiple comparisons test.
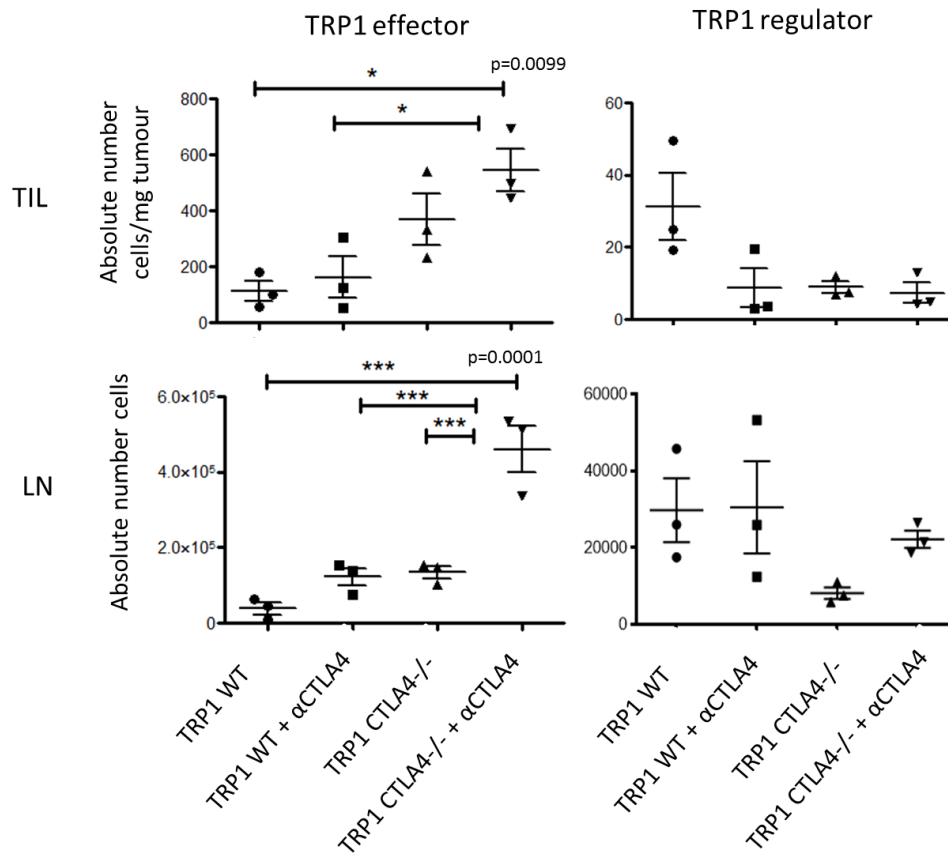
Figure 4.7e: TRP1 CTLA-4^{-/-} Tregs are significantly less proliferative than WT TRP1 Teff in the LN and tumour and may explain the low absolute TRP1 CTLA-4^{-/-} Tregs numbers observed in figure 4.7d. There is a trend towards lower Ki67 expression on TRP1 CTLA-4^{-/-} Teff in the LN which reaches significance with αCTLA4 mAb. **Key:** LN=lymph node; WT=wild type; αCTLA4=anti-murine CTLA-4 mAb (9H10 clone). Vertical bars represent SEM. Statistical tests: one-way analysis of variance and multiple comparisons test.
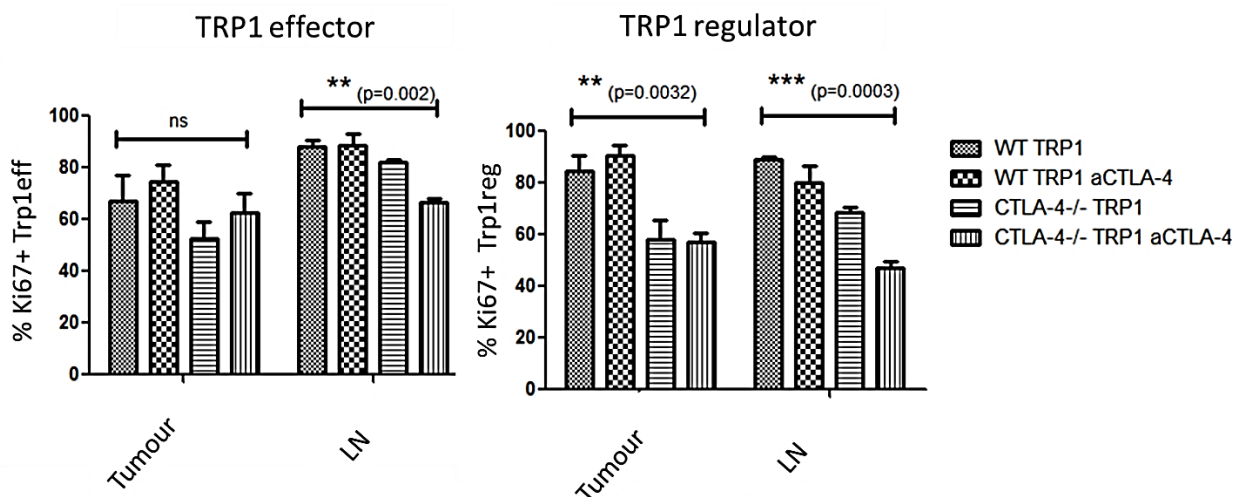
The reduction in TRP1 CTLA-4$^{-/-}$ Treg numbers may be explained by significantly lower Ki67 expression in these populations in LN and TIL compared with WT TRP1 (figure 4.7e). There is no clear correlation with CD25 expression on Tregs in this experiment, and the proportion of FoxP3+ cells infused was comparable between groups at the point of cell transfer (figure 4.6a). Genetic ablation of CTLA-4 on Tregs transferred into irradiated hosts appears to confer a proliferative disadvantage compared with WT TRP1 Tregs that is not obviously explained by altered CD25 expression. It is recognised that in lymphopenic mice, Tregs prevent CD25 upregulation on co-transferred naive T cells while increasing their own CD25 expression and sequestering IL-2 to enable their differentiation to IL-10 production (112). It is conceivable that the naïve TRP1 CTLA-4$^{-/-}$ T cells at the point of transfer were disadvantaged by endogenous CD4regs in the context of homeostatic peripheral expansion (HPE). HPE is the early period of immune reconstitution post lymphodepletion which is cytokine dependent and sees a proportional increase in Tregs (114). It is not clear why the same effect was not observed in the WT TRP1 group.

Despite high absolute numbers of Trp1 CTLA-4$^{-/-}$ Teffs in LN (and tumour), CD25 expression on this subset is lower than on WT TRP1 in the LN (data not shown) and is consistent with lower Ki67 expression (figure 4.7e). It is possible that a drop in Ki67/CD25 on these cells reflects a competitive environment in the LN where Treg-mediated sequestration of IL-2 predominates. Equally, there may be an alternative mechanism to explain the high cell numbers and lower Ki67/CD25, such as improved cell persistence/reduced apoptosis in this subset that requires further investigation.

Figure 4.7f: TRP1 CTLA-4$^{-/-}$ Tregs express higher granzyme B and Eomes than WT TRP1 T cells in the LN, but any significant differences in expression are lost in the tumour. Key: LN=lymph node; WT=wild type; αCTLA4=anti-murine CTLA-4 mAb (9H10 clone). Vertical bars represent SEM. Statistical tests: one-way analysis of variance and multiple comparisons test.

TRP1 effector
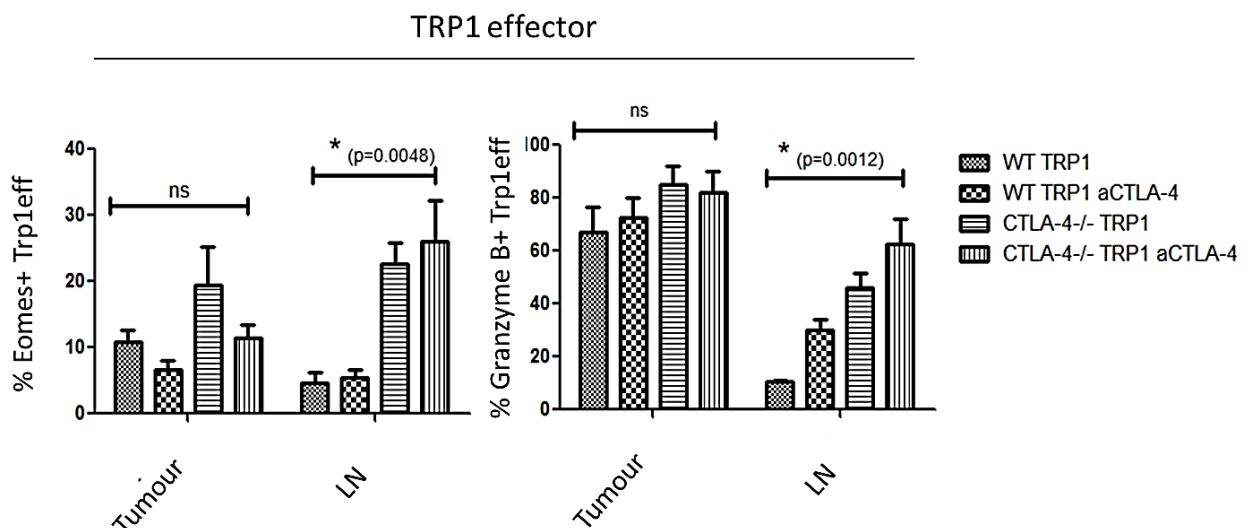
Eomes is a transcription factor of the T-box family, involved in programming cytotoxic CD8 T cell functions via the perforin/granzyme and Fas-FasL pathways (115). Figure 4.7f shows that in the LN, CTLA-4$^{-/-}$ TRP1 Teff express higher granzyme B and Eomes than WT TRP1 T cells, but any significant differences are lost in the tumour with the assumption that cytotoxic activity within the tumour is equivalent between groups. It is conceivable that higher granzyme B expression in the LN is undesirable and may be associated with symptoms of immune toxicity. CTLA-4 ablation on TRP1 Teff appears to potentiate their baseline (LN) cytotoxic phenotype which may be related to the non-functional TRP1 CTLA-4$^{-/-}$ Tregs promoting a dominant effector phenotype.

IFNγ and TNFα production by CTLA-4$^{-/-}$ TRP1 T cells was equivalent to that of WT TRP1 T cells (data not shown).

Summary

Our aim was to explore the anti-tumour and functional properties of TRP1 Teff ablated for CTLA-4 in a lymphodepleted model to minimise endogenous T cell expression of CTLA-4.

Host lymphodepletion does not clearly 'release the brakes' on adoptively transferred TRP1 CTLA-4$^{-/-}$ T cells in terms of tumour eradication, with only a non-significant downward trend in tumour weight noted at day 18 when the experiment ended (figure 4.7a). In terms of functionality, there is some evidence that absence of CTLA-4 promotes a more cytotoxic phenotype, evidenced by higher granzyme B and eomes expression in the LN, but this significance is lost in the tumour (figure 4.8). TRP1 CTLA-4$^{-/-}$ Teff do not significantly upregulate IFNγ or TNFα secretion beyond that of WT TRP1 Teff.

TRP1 CTLA-4$^{-/-}$ Teff cells are increased in absolute number in LN and tumour, potentiated by the addition of αCTLA-4 mAb. We believe that this represents the effect of comprehensive CTLA-4 blockade on the endogenous compartment (with no dilution of the effect on TRP1 T cell). Irradiation alone permits a small (non-significant) expansion of TRP1 CTLA-4$^{-/-}$ Teff compared with WT TRP1 Teff in the absence of exogenous mAb and despite equivalent/lower Ki67 and CD25 expression than WT TRP1 Teff. It is likely that this is partly explained by TRP1 CTLA-4$^{-/-}$ Treg which in the context of the current experiment are low in absolute number and Ki67 expression, but are also generally accepted to be functionally compromised by the lack of CTLA-4 (note that specific deletion of CTLA-4 on Tregs resulted in systemic lymphoproliferation in mice)(43).

TRP1 CTLA-4$^{-/-}$ Teff cells have some potential advantages as ACT. We have shown that they are inherently more proliferative than WT CTLA-4-replete TRP1 Teffs and have a more cytotoxic phenotype in the LN. The reason for the Teff advantage may be the poor engraftment/survival of CTLA-4$^{-/-}$ TRP1 Tregs promoting a dominant effector phenotype, but this may still offer an advantage in the setting of ACT for cancer, albeit the possible autoimmune toxicity of this approach may be concept-limiting.

These experiments demonstrate that TRP1 CTLA-4$^{-/-}$ T cells can evoke an anti-B16/BL6 melanoma effect in lymphodepleted recipients at day 18 post tumour induction. We would like to establish that TRP1 CTLA-4$^{-/-}$ T cells can fully reject and prevent recrudescence of tumour over a protracted in vivo time-course to the same extent as WT TRP1 T cells, and to investigate whether this is independent of exogenous αCTLA-4 mAb.

4.2.4. TRP1 CTLA-4$^{-/-}$ T-cells in the lymphodepleted host: protection experiment

In the TRP1 ACT model of murine melanoma, it is accepted that the 'killer' condition (TRP1 T cells + lymphodepletion + αCTLA-4 mAb) is associated with tumour eradication and protection from recurrence, and that the 'helper' condition (TRP1 T cells + lymphodepletion alone) is capable of eradication, but not long-term protection (46). We used the experimental set-up illustrated in figure 4.5 to compare the end-points listed above in CTLA-4$^{-/-}$ TRP1 and WT TRP1 T cells.

Between days 17-25 post induction of tumour, all murine recipients showed signs of uveitis, reduced activity and dishevelled fur. There was significant mortality observed in all treatment groups which was not related to tumour progression. Beyond day 25, mice in all groups started to lose pigment, particularly around the tumour site, which was progressive throughout the period of observation.

Figure 4.8 shows how all groups completely reject B16/BL6 tumour at similar rates between days 20-30 post tumour inoculation. Surviving mice were observed over a period of 100 days and tumour recrudescence did not occur in any of the treatment groups (data not shown).

The experiment was completed after 100 days and TRP1 T cells were detectable in all groups from blood, lymph node and spleen. Figure 4.11 shows persistence of congenically marked Trp1 T cells in LN specimens. Surprisingly, CTLA-4$^{-/-}$ TRP1 Tregs are absent in the group that received αCTLA-4 mAb at days 8, 11 and 14 post-tumour induction. This is not seen in the WT TRP1 group that received αCTLA-4 mAb. It is possible that the irradiated environment together with αCTLA-4 mAb skewed the expansion of CTLA-4$^{-/-}$ TRP1 T cells to become dominated by TRP1 Teff with low TRP1 Treg engraftment.

Figure 4.8: in the context of a protection experiment, all groups rejected B16/BL6 melanoma over a similar time frame. Key: WT=wild type; αCTLA4=anti-murine CTLA-4 mAb (9H10 clone); ACT=adoptive cellular therapy. Data represents a single experiment.
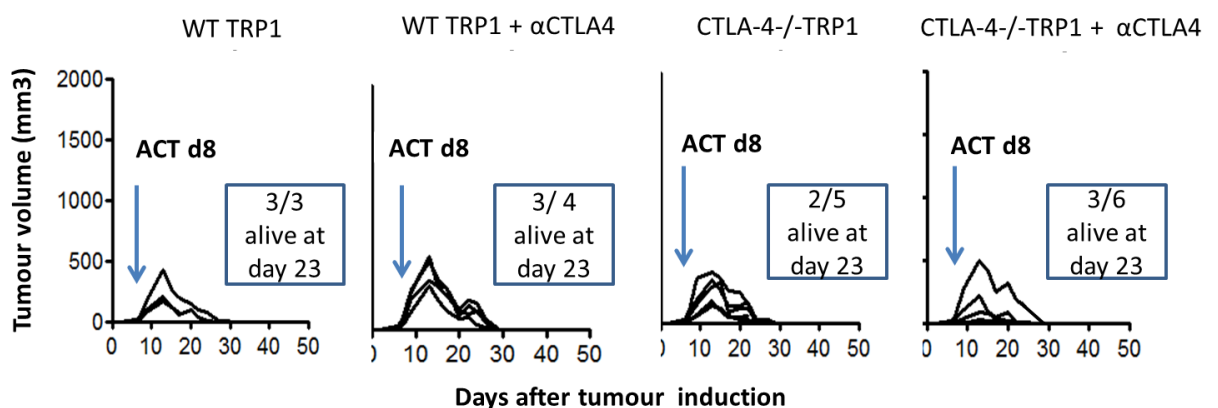
Figure 4.9: Lymph Node (LN) preparation at 100 days post ACT demonstrates persistence of transferred congenically marked cells. Repopulation with TRP1 Tregs is strongest in the WT TRP1+RT setting, and absent in CTLA-4$^{-/-}$ TRP1 treated with αCTLA-4 mAb. Functionally, CTLA-4$^{-/-}$ T cells produce granzyme B and Eomes. Key: WT=wild type; αCTLA4=anti-murine CTLA-4 mAb (9H10 clone); ACT=adoptive cellular therapy.
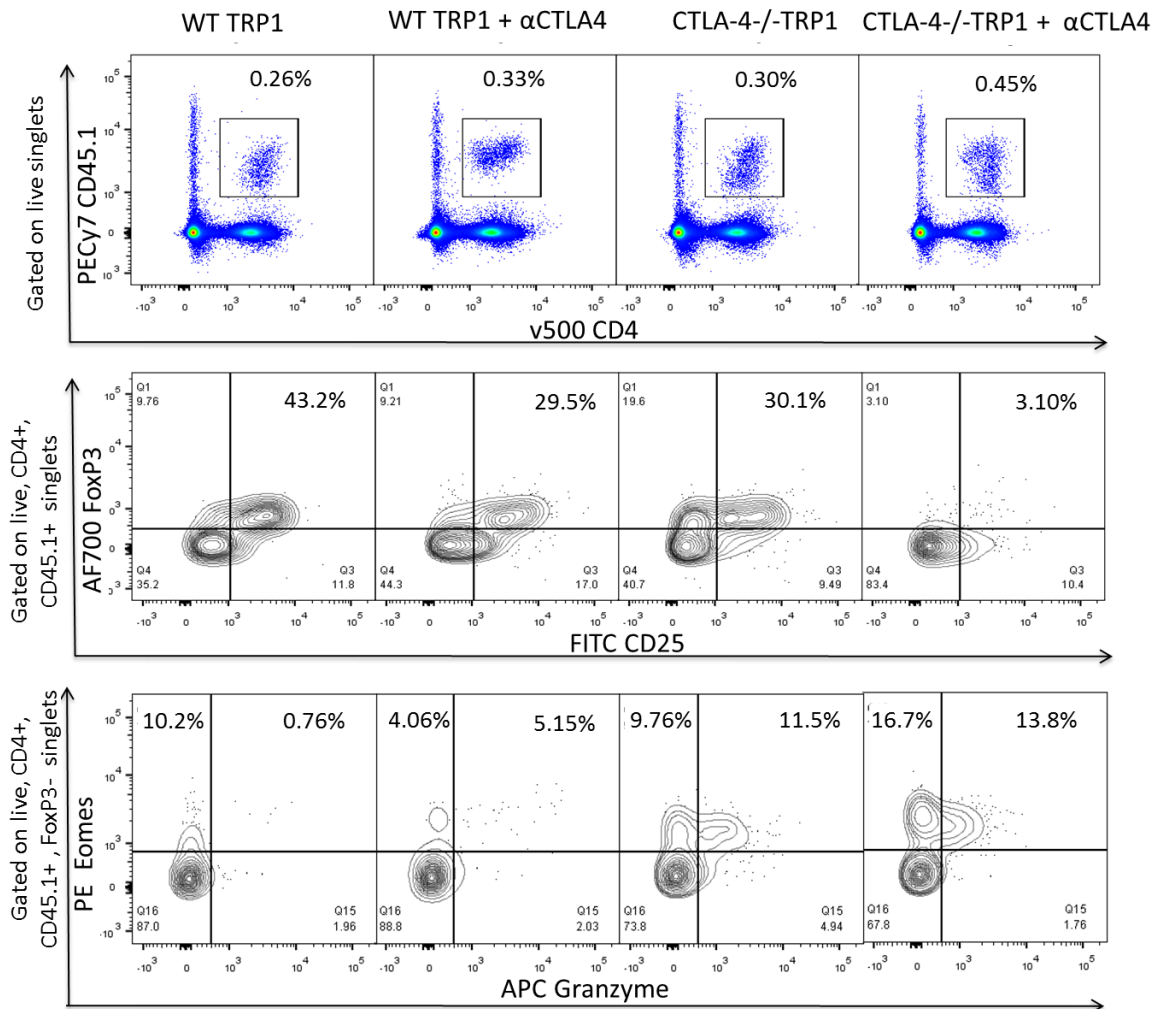
On a functional level, CTLA-4$^{-/-}$ TRP1 T cells produced more granzyme B and eomes than WT TRP1 T cells, even with prior αCTLA-4 mAb treatment (figure 4.9). IFNγ expression was noted to be lower in the group treated with irradiation plus TRP1 T cells alone, compared with the other groups that lacked CTLA-4 or were subject to blockade (figure 4.10).

CD25 expression was lower on CTLA-4$^{-/-}$ TRP1 Teff as seen in previous experiments, and there was an inverse correlation with IL-2 which supports the hypothesis of an autocrine feedback loop (figure 4.10).

Figure 4.10: Analysis of TRP1 Teff from LN at 100 days post tumour initiation. CD25 expression is non significantly lower on CTLA-4$^{-/-}$ TRP1 Teff and there is an inverse correlation with IL-2, suggestive of an autocrine feedback loop. IFNγ expression is significantly higher in CTLA-4$^{-/-}$ TRP1 T cells previously treated with αCTLA-4 mAb**. All groups received 5Gy of irradiation at day 8. **Key:** WT=wild type; αCTLA4=anti-murine CTLA-4 mAb (9H10 clone); ACT=adoptive cellular therapy. Horizontal bars represent mean values. Statistical tests: one-way analysis of variance and multiple comparisons test.
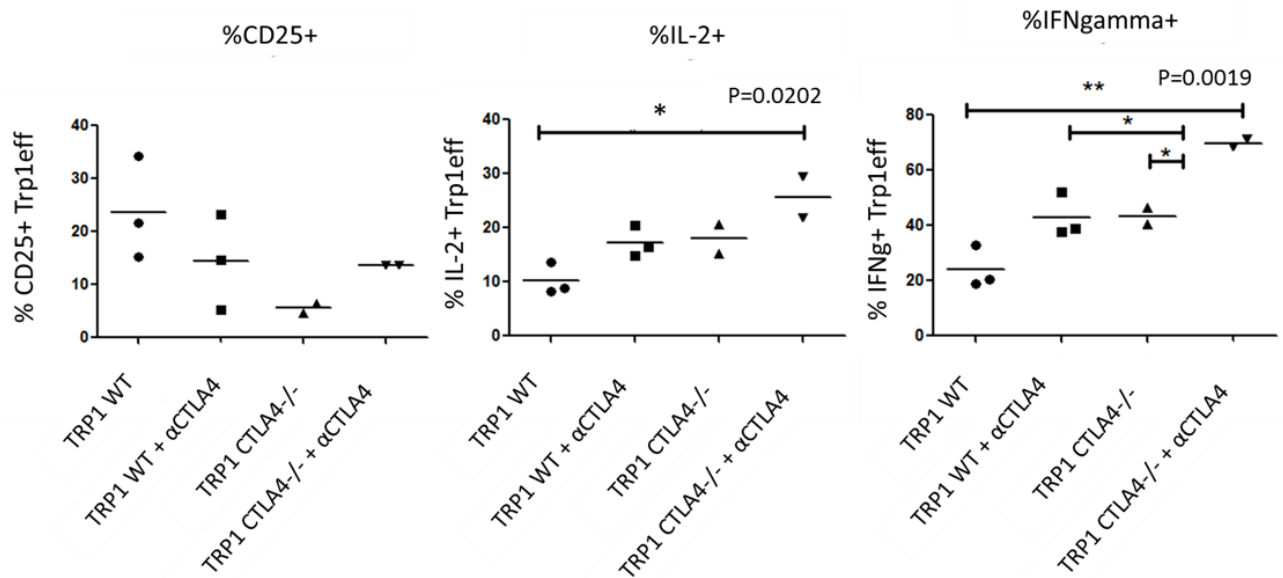
4.3   Discussion

The TRP1 T cell ACT model in B16/BL6 murine melanoma has given huge insights into the potential of immune modulatory therapies in cancer immunotherapeutics. It has been previously demonstrated that the 'killer' condition (TRP1 T cells + lymphodepletion + αCTLA-4 mAb) is associated with B16/BL6 tumour eradication and protection from recurrence, and that the 'helper' condition (TRP1 T cells + lymphodepletion alone) is capable of tumour eradication, but not long-term protection (46). This work underlines the importance of CTLA-4 blockade in establishing complete, durable immune-mediated anti-tumour responses to ACT.

One of our aims has been to determine whether genetic absence of CTLA-4 on tumour-reactive T cells is a surrogate for the systemic administration of αCTLA-4 mAb in terms of outcome measures such as tumour eradication, promotion of high intratumoural Teff/Treg ratios and enhanced cytotoxic potential, but with lesser incidence of autoimmune toxicity.

There is no significant reduction in tumour weight compared with WT TRP1 T cells, but a downward trend is observed with TRP1 CTLA-4$^{-/-}$ T cell ACT in the lymphodepleted setting. In the protection experiment, all animals rejected tumour over a similar time-frame and there

was no evidence of recrudescence or of susceptibility to tumour rechallenge in any of the groups. The data from the protection experiment requires validation with a larger scale repeat.

We can conclude from these experiments that TRP1 CTLA-4$^{-/-}$ Teff are more proliferative than WT TRP1 Teff and have a more cytotoxic phenotype in the LN which is less obvious in the tumour (figure 4.8). Part of the explanation for this may be that TRP1 CTLA-4$^{-/-}$ Treg are (likely to be) functionally impaired compared to WT TRP1 Tregs, despite appearing normal in number on quantitative analysis, allowing unopposed proliferation of TRP1 Teff (43).

The low numbers of TRP1 CTLA-4$^{-/-}$ Tregs obtained at the end of the experiment in LN and TIL was unexpected. A similar phenomenon was observed in the protection experiment, where mice receiving TRP1 CTLA-4$^{-/-}$ T cells + αCTLA-4 mAb had complete absence of (transgenic) Tregs in the LN at 100 days post tumour inoculation, which was not observed on the other groups (figure 4.9). Possible explanations include cytokine deprivation and Treg reprogramming into Teffs (53). This area requires further investigaton.

There are potential advantages of using these cells for ACT: TRP1 CTLA-4$^{-/-}$ Teff are more proliferative, have a more cytotoxic phenotype in the LN (see figure 4.8) and TRP1 CTLA-4$^{-/-}$ Tregs are at a proliferative/survival disadvantage in the lymphodepleted host. The possible autoimmune toxicity of this approach should also be explored.

Based on this set of experiments, genetic ablation of CTLA-4 on tumour-reactive cells may offer an equivalent, valid alternative to αCTLA-4 mAb in terms of therapeutic effect and biological impact in vivo. It is conceivable that concurrent administration of αCTLA-4 mAb could potentiate these features to good effect. This observation supports the theory of CTLA-4 acting 'in trans' to create an immune-suppressive environment, presumably by sequestering B7.1 and B7.2 amongst other APC inhibitory effects. B16/BL6 data confirms that it is not a tumour-based CTLA-4 reservoir contributing to this. A major concern would be if the tumour antigen target were not restricted, then CTLA-4-ablated T cells administered with αCTLA-4 mAb would pose a significant toxicity risk.

4.4   Future directions

It is clear that repetition of the protection experiment is needed not only to investigate the anti-tumour biology of TRP1 CTLA-4$^{-/-}$ T cells compared with WT TRP1 T cells, but also to explore potential toxicities in more detail using cytokine bead arrays, transcription factor analysis and autoantibody levels. There has also been discussion of running a microarray on the TRP1 CTLA-4$^{-/-}$ T cells to establish whether they share any clear trancriptomic features with WT TRP1 T cells.

Overall, Chapter 4 allows us to compare the engraftment, expansion and trafficking of TRP1 CTLA-4$^{-/-}$ T cells with WT TRP1 T cells, and illustrates the impact of concurrent αCTLA-4 mAb. However, there remain several unanswered questions. Definitive characterisation of functionality (cytotoxicity and cytokine secretion) of TRP1 CTLA-4$^{-/-}$ T cells is required to fully determine their potential for therapeutic efficacy upon adoptive transfer. Preliminary work can be performed in vitro. We propose to use a FACS-based cytotoxicity assay to compare the inherent cytotoxic potential of TRP1 CTLA-4$^{-/-}$ T cells with WT TRP1 T cells directed against GFP-expressing B16/BL6 murine melanoma targets. Supernatant from these cultures will be used to run ELISAs testing for IL-2 and IFNγ.

Conventional T cell killing assay and cytokine data will be supplemented with a TRP1 CTLA-4$^{-/-}$ T cell degranulation assay. Staining for CD107a and CD107b following incubation of transgenic T cells with B16/BL6 murine melanoma TRP1-expressing targets will give further information regarding cytotoxic potential (and specificity) of the transgenic cells.

We plan to conduct a formal assessment of proliferative potential of the transgenic cells over a 7 day co-culture with irradiated TRP1 antigen positive and negative targets. This will give numerical data on T cell expansion as well as additional cytokine data. To date, we have used Ki67 expression as a barometer of proliferation, but we appreciate the need to supplement this with more robust numeric data. It is our intention to conduct an extended cytokine bead array (CBA) once we have generated primary data by ELISA.

We additionally plan to assess the transgenic cells for expression of T cell exhaustion markers (e.g. programmed cell death 1 (PD-1), TIM-3 and LAG-3) which can render T cells sensitive to potent immunosuppressive ligands in vivo and potentially compromise biological function (147). We also hope to determine the relative proportions of memory and effector T cell populations across the different TRP1 genotypes with and without αCTLA-4 mAb. Broadly, T cell maturation status is proposed to impact upon expansion and persistence of adoptive cells

in vivo and a stem-cell-like phenotype may be an advantage in this setting (135, 146). We will compare these features between the TRP1 genotypes.

CHAPTER 5

5. GENERATION AND INVESTIGATION OF HUMAN ANTI-CTLA-4 ANTIBODY

5.1 Introduction

There is a large body of evidence to support the anti-tumour efficacy of CTLA-4 blockade in models of cancer (46, 72) and in clinical trials (49). Ipilimumab is a fully humanised αCTLA-4 mAb which has been licensed to treat metastatic melanoma in humans, but systemic administration and interaction with polyclonal T cells engenders it with immune-mediated toxicity. One of the aims of this project is to devise a strategy to target CTLA-4 inhibition specifically to the tumour to concentrate the therapeutic anti-tumour effect in the tumour whilst reducing the risk of widespread polyclonal T cell activation. We proposed to approach this in two ways: by ablating CTLA-4 from tumour reactive T cells prior to adoptive transfer, and by genetically modifying tumour reactive T cells to secrete functional αCTLA-4 mAb or scFv enabling a 'payload' delivery of αCTLA-4 mAb intratumourally.

In order to define the method that will best achieve the aim of tumour-specificity of effect, we directly compared the absence of CTLA-4 on tumour reactive T cells with the effect of systemically administered exogenous αCTLA-4 mAb on (co-transferred) tumour-reactive T cells using a transgenic mouse model developed at UCL and described in Chapter 4, sections 4.1.3 and 4.2.1.

Chapter 4 concludes that there are biological differences between TRP1 CTLA-4$^{-/-}$ T cells and WT TRP1 T cells beyond differential expression of CTLA-4. In order to realise the potential advantages of these, host lymphodepletion or concurrent administration of exogenous αCTLA-4 mAb may be required to reduce the reservoir of endogenous T cell CTLA-4 which can act in trans to inhibit effector function (9, 26). In cohorts of irradiated recipients, transferred TRP1 CTLA-4$^{-/-}$ Teffs comprised significantly higher total numbers in the tumour, were associated with (non-significantly) lower tumour mass at day 18 and higher expression of granzyme B and eomes in the LN (significant) and tumour (non-significant) than WT TRP1 T cells. TRP1 CTLA-4$^{-/-}$ T cells permitted complete eradication of tumour, displayed a more cytotoxic phenotype in the LN and offered protection from tumour recrudescence at 100 days post tumour challenge. All of these effects were potentiated further by the addition of αCTLA-4 mAb and its impact on the endogenous compartment.

An important mechanism of αCTLA-4 mAb anti-tumour activity has been recently described by Simpson and Quezada(67). In essence αCTLA-4 mAb can label CTLA-4^{hi} targets for ADCC-mediated depletion by the innate immune system, and this effect is dependent on the mAb isotype, the presence of effector (macrophages) and the density of expression of the antigenic target. This partly explains the results obtained in Chapter 4, namely that CTLA-4^{hi} Treg would appear to be depleted by αCTLA-4 mAb in the tumour (less so in the LN) by virtue of their dense expression of CTLA-4 and the presence of activated effectors. The net result is potentiation of effector numbers, permitting an anti-tumour response. Taking this forward, any approach which can effect an increase in the Teff/Treg ratio could offer the same outcome as systemic αCTLA-4 mAb.

The aim of Chapter 5 is to manipulate tumour-reactive T cells to secrete anti-human CTLA-4 mAb in a payload manner on engaging cognate antigen, such that CTLA-4 is targeted in the tumour, but only minimally engaged in the periphery (49).

5.1.1 9H10 as the paradigm for CTLA-4 blockade in murine models of melanoma

9H10 anti-murine CTLA-4 antibody was first described in 1995 (116). Syrian hamsters were immunised with heat-killed Staphylococcus A bacteria coated with 100µg of CTLA-4 immunoglobulin (Ig) (117). Lymphocytes underwent polyethylene glycol fusion with a myeloma cell line, and hybridomas obtained were cloned by limiting dilution in the presence of irradiated mouse thymocyte feeders and tested for reactivity against CTLA-4 Ig. Antibody 9H10 was selected on the strength of its binding to CTLA-4, its ability to block B7 binding by CTLA-4-immunoglobulin (CTLA-4 Ig), and its ability to stain activated, but not freshly isolated T cells (1).

Originally, 9H10 was used in experiments to determine the biological role of CTLA-4, but more recently it has been extensively used in pre-clinical evaluation of CTLA-4 blockade in tumour immunotherapy. Unpublished work by Quezada et al demonstrates an enhancement of anti-tumour CD4 T cell activity when 9H10 and Gvax are co-administered into a non-irradiated B16/BL6 melanoma model. It is apparent that 9H10 has no anti-tumour effect as a monotherapy, but potentiates the impact of tumour-reactive CD4 T cells when used as part of a combinatorial strategy.

In adoptive transfer models where tumour-reactive TRP1 CD4 T cells are transferred into irradiated B16/BL6 melanoma bearing C57BL/6 recipients, the addition of 9H10 has been

shown to prevent tumour recrudescence compared with transfer of cells alone, suggesting an important role for CTLA-4 blockade in tumour protection and longer term immunity(46).

5.1.2   10D1 anti-human CTLA-4 mAb

10D1 is an anti-human CTLA-4 antibody designed by Alan Korman (patent US2010047244 (A1). It was first described in 2003 to help elucidate the full potential of CTLA-4 blockade in humans. Extensive prior murine work had confirmed anti-tumour immune responses with antibody-mediated CTLA-4 blockade, but evidence of a similar anti-tumour effect in humans was lacking. To that point, epidemiological data on CTLA-4 polymorphisms in autoimmunity was suggestive of an immune modulatory role for anti-CTLA-4 antibody (58, 118).

Anti-human CTLA-4 mAbs were generated in transgenic HC2/KCo7 mice. These mice possess introduced human Heavy (H) and Light (L) chain transgenes that undergo class switching and somatic mutation to produce human IgG1k and IgG3k antibodies (119). The mice were immunised with B^WCTLA-4/CD3δ, and single cell suspensions of splenic lymphocytes were then hybridised with a murine myeloma cell line and screened for human IgG1k production by ELISA. Specificity was then confirmed by flow cytometry for CTLA-4 binding, and resulted in the generation of 10D1(80).

10D1 is a high affinity anti-human CTLA-4 mAb that blocks binding of human CTLA-4 to human B7-1 and B7-2 with no cross species reactivity. In vivo testing of 10D1-induced CTLA-4 blockade in macaques was associated with a potentiated antibody response to hepatitis B surface antigen and human melanoma cell vaccines(80).

Chronic administration of 10D1 alone into macaques did not induce polyclonal T cell activation or significantly alter the repertoire of lymphocyte subsets, and was not associated with measurable autoimmunity. Anti-self-responses were only detectable by ELISA if vaccine and 10D1 were co-administered (80). Anti-self-responses have also been identified in murine models of cancer, as measured by the production of autoimmunity-associated antibodies (59).

We obtained the patent for 10D1 to generate an anti-human CTLA-4 antibody as an isotype control for anti-murine CTLA-4, and for direct testing in human CTLA-4 transgenic mice, described in more detail in Chapter 2.4.1.2.

5.1.3   Single chain Fv versus full length antibody

The generation of scFv is a standard molecular immunological technique, and a cornerstone in the emerging field of chimeric antigen receptor redirected T cells to treat cancer (120, 121). Blockade of CTLA-4 with soluble intact anti-CTLA-4 mAb and its F'ab fragments can enhance T cell proliferation (8). We initiated this project with 10D1 scFv with the expectation that this would promote T cell proliferation.

5.1.4   Human-CTLA-4 (Hu152Tg) BACS transgenic line

Pre-clinical testing of 10D1 anti-human CTLA-4 mAb requires an appropriate model system in which to demonstrate anti-cancer immunity. In-vitro work on human T cell lines is limited by the fact that a single αCTLA-4 mAb can have opposite effects on different cell lines (122). We are fortunate to have access to a human CTLA-4 transgenic murine model (Hu152Tg) (48). These mice express a chimeric 17 –kb DNA construct comprising the human extracellular domain (exon 2) and the mouse transmembrane and cytoplasmic domains of CTLA-4. Due to inter-species conservation, human CTLA-4 interacts normally with murine B7.1 and B7.2 (see Chapter 2.4.1.2 for more details).

5.1.5   UC10-4F10 anti-murine CTLA-4 mAb

We required a control, isotype-matched, non-target binding antibody to test against 10D1 anti-human CTLA-4 mAb in the Hu152Tg model. Jeffrey Bluestone created UC10-4F10 anti-murine CTLA-4 mAb and kindly supplied the scFv sequence (10, 81, 123). Originally, the antibody was generated by immunising Armenian hamsters with an extracellular portion of murine CTLA-4 fused to murine IgG2a. Subclones were obtained by limiting dilution, and tested for reactivity to murine CTLA-4-Ig by ELISA.

UC10-4F10 αCTLA-4 mAb has been shown to reduce intra-tumoural CD4 Tregs in vivo in a similar manner to that observed with 9H10 mAb (46, 67).

5.2   Results

5.2.1   Generating CTLA-4 high cell lines as 'targets' to test constructs

This is described in detail in Chapter 3.2.1. In brief, we generated SFG plasmids coding for human and murine CTLA-4 (Chapter 3, figure 3.1a: plasmid maps) then stably transduced and positively selected (using the human CD34 marker protein) 293T cells and SupT1 cells (Chapter 3, figures 3.1b and 3.1c).

5.2.2   Generation of 10D1 and UC10-4F10 αCTLA-4 scFv surface-linked constructs

The 10D1 anti-human CTLA-4 mAb sequence was obtained from a patent filed by Medarex (patent US2010047244 (A1) and was adapted by Martin Pule into a scFv which was constructed by oligonucleotide assembly (see Chapter 2.1.6 for details). Expression testing as a cell surface-linked construct (in chimeric antigen receptor (CAR) format (see Figure 5.1a) was by transfection into 293T cells followed by staining for anti-Human-Fc at 72 hours and flow cytometric analysis. Sequences were verified prior to downstream applications (data not shown).

The UC10-4F10 anti-murine CTLA-4 scFv sequence was kindly supplied by Jeffrey Bluestone (10, 81) and was generated and validated as for 10D1. See Figure 5.1a for the general structure of full length IgG, single-chain Fv (scFv) and membrane-bound scFv in chimeric antigen receptor (CAR) format.

5.2.3   Secretory version of 10D1 scFv and in vitro testing

To establish that 10D1 αCTLA-4-scFv could bind human CTLA-4 we subcloned 10D1-scFv into a construct capable of scFv secretion (see Chapter 2.3.2 for details).

Testing the secretory 10D1 construct was by transient transfection of 293T cells with (sec)-10D1-scFv and (sec)-UC10-4F10-scFv as a control using the protocol outlined in Chapter 2.2.6. At 72 hours post-transfection, antibody-rich 293T cell culture supernatants were incubated with CTLA-4^{hi} SupT1 cells for 30 minutes at 4∘C in the dark, followed by a secondary α-human-

Fc stain (30 min/ 4∘C/dark). Figure 5.1b demonstrates that (sec)-10D1-scFv (αhuman-CTLA-4) binds human CTLA-4 in a species-specific manner.

Figure 5.1a: general structure of full length IgG, scFv and membrane-bound scFv to illustrate the range of constructs generated for use in Chapter 5. Key: IgG= Immunoglobulin G; scFV=single chain variable fragment; Vh=variable heavy chain; Vl=variable light chain; CH=constant heavy chain; Cl= constant light chain; CD3Z=CD3 zeta chain.
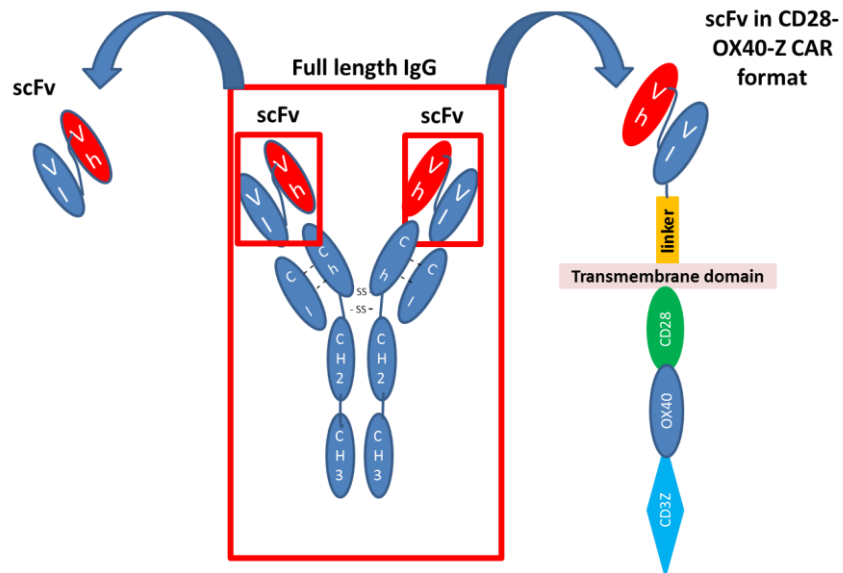
Figure 5.1b: secreted 10D1 anti-human CTLA-4-scFv binds human CTLA-4 in a species-specific manner. Control UC10-4F10 anti-murine CTLA-4-scFv does not bind murine CTLA-4. Key: 10D1 anti-CTLA-4= anti-human-CTLA-4; 4F10 anti-CTLA-4=UC10-4F10 anti-murine-CTLA-4; human CD34=transduction marker gene/protein indicating CTLA-4 transduced cells; anti-Human Fc= secondary antibody stain.
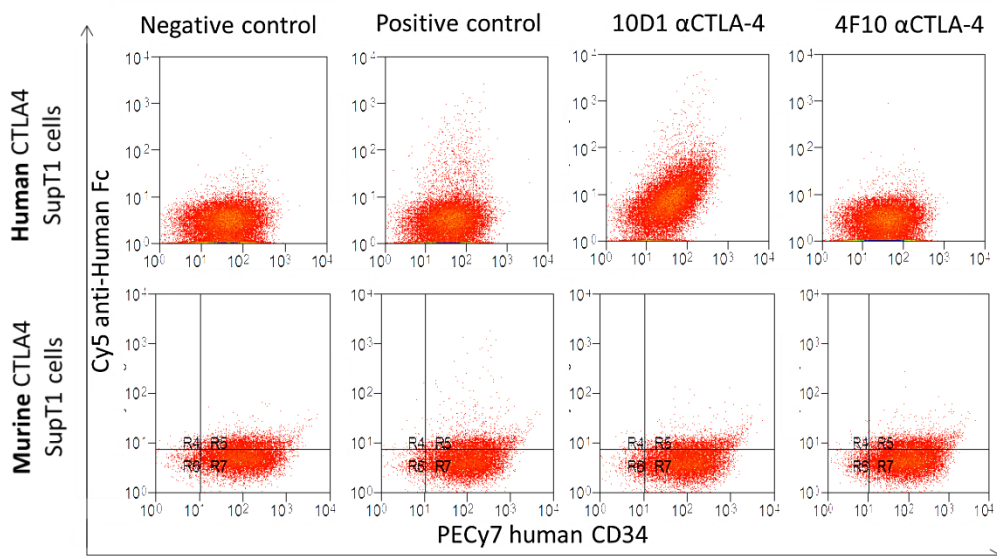
Control UC10-4F10-scFv-secretory α-murine-CTLA-4 did not bind murine CTLA-4. Transfected 293T cells expressed eBFP as a marker of transfection, and intracellular staining for anti-Human-Fc following Brefeldin A treatment revealed the presence of intracytoplasmic Fc (data not shown). Target SupT1 cells were strongly positive for murine CTLA-4 (see figure 3.1c). There were concerns that this could represent aberrant folding of scFv and we decided to adapt UC10-4F10 scFv into a full-length (F/L) construct with the expectation that this could overcome any issues of scFv misfolding. In addition, novel mechanistic insights into the mode of activity of αCTLA-4 mAb (Fc-mediated ADCC of CTLA-4^{hi} targets intratumourally (67) and developments in antibody engineering, gives a clear rationale for using F/L constructs to exploit the effector functions afforded by Fc expression. We thus generated F/L antibody constructs for 10D1 and UC10-4F10 in IgG1 and IgG2a isotype.

5.2.4   Full length (F/L) 10D1 and in vitro testing

To test binding of F/L αCTLA-4 mAbs destined for secretion by cells is to dual-transfect 293T cells with separate constructs coding for corresponding heavy and light chains, to collect and 0.22µm filter transfectant supernatant at 72 hours, and then apply this to target cells. Secondary anti-Fc staining as described in Chapter 2.2.6 demonstrates that F/L- 10D1 binds CTLA-4 in a species-specific manner with no cross-reactivity (figure 5.2).

Figure 5.2: Full length (F/L)-10D1 anti-human CTLA-4 mAb and (F/L)-UC10-4F10 anti-murine CTLA-4 mAb bind CTLA-4 in a species-specific manner with no cross-reactivity. Key: 10D1 anti-CTLA-4= anti-human-CTLA-4; 4F10 anti-CTLA-4=anti-murine-CTLA-4; human CD34=transduction marker gene/protein of CTLA-4 expressing SupT1 target cells.
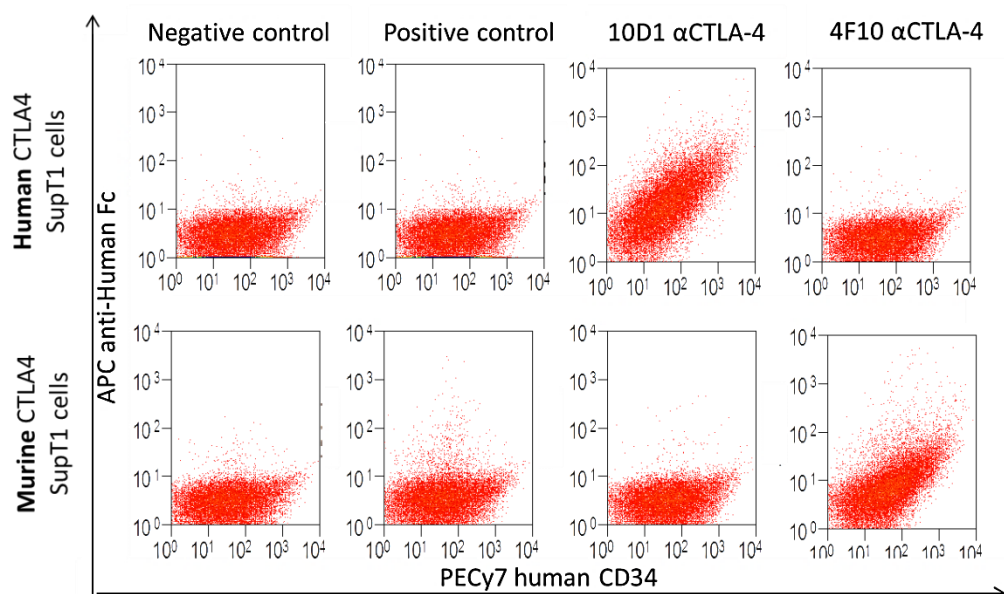
The aim is to translate this cell line work into primary murine lymphocytes. To generate a single construct for transduction purposes, Martin Pule designed tricistronic vectors to incorporate light chain linked by TaV-2A to heavy chain, linked by IRES to marker protein (figure 5.3: plasmid maps).

It had become apparent during attempts to saponify transduced cells that fluorescent marker proteins were unable to robustly survive the cell fixation process. For this reason we generated a truncated version of murine CD19 as a marker of transduction to use in place of eBFP. Truncated murine CD19 is surface fixed, non-immunogenic, unable to transmit an intracellular signal, and enables cell selection using a commercially available column/magnetic bead kit (Miltenyi Biotech, CliniMACS® cell sorting, Auburn, CA).

There were concerns that the complexity of tricistronic constructs would limit cell transfection or transduction efficiency. Initial testing in 293T cells showed this not to be the case, and filtered transfectant supernatant bound target SupT1 cells (data not shown).

Figure 5.3: plasmid maps for tricistronic IgG1 and IgG2a 10D1 anti-human CTLA-4 vectors. Key: LTR=long terminal repeats; 10D1-LC-mKappa= 10D1 light chain (kappa); 10D1-HC-mIgG1= 10D1 murine IgG1 heavy chain; 10D1-HC-mIgG2a= 10D1 murine IgG2a heavy chain; 2A= FMD 2A sequence; IRES=internal ribosomal entry site; dMuCD19=truncated murine CD19;SD=splice donor;SA=splice acceptor.
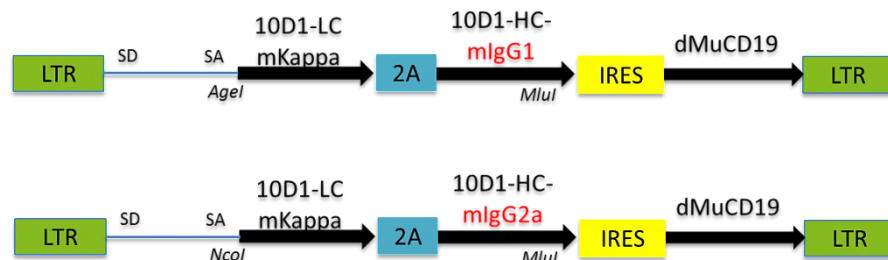
5.2.5 Testing constructs in polyclonal primary lymphocytes in vitro

Retroviral transduction of C57BL/6 lymphocytes was conducted as per Chapter 2.4.5.1 with ConA + IL-7 stimulation. Mean T cell transduction efficiency (CD19 expression at 72 hours post activation) was 40-50% and transduced CD8 T cells were capable of granzyme B and IFNγ secretion at 72 hours in vitro (figure 5.4a) to the same degree as mock transduced cells.

Figure 5.4a: retroviral transduction efficiency of F/L 10D1 anti-human CTLA-4 IgG2a and F/L UC10-4F10 anti-murine CTLA-4 IgG2a constructs in C57BL/6 CD8 T cells is between 40-50% and transduced cells can secrete Granzyme B at 72 hours post stimulation. Key: FSC=forward scatter; F/L-10D1 IgG2a= α-human-CTLA-4; F/L-UC10-4F10 IgG2a = α-murine-CTLA-4.
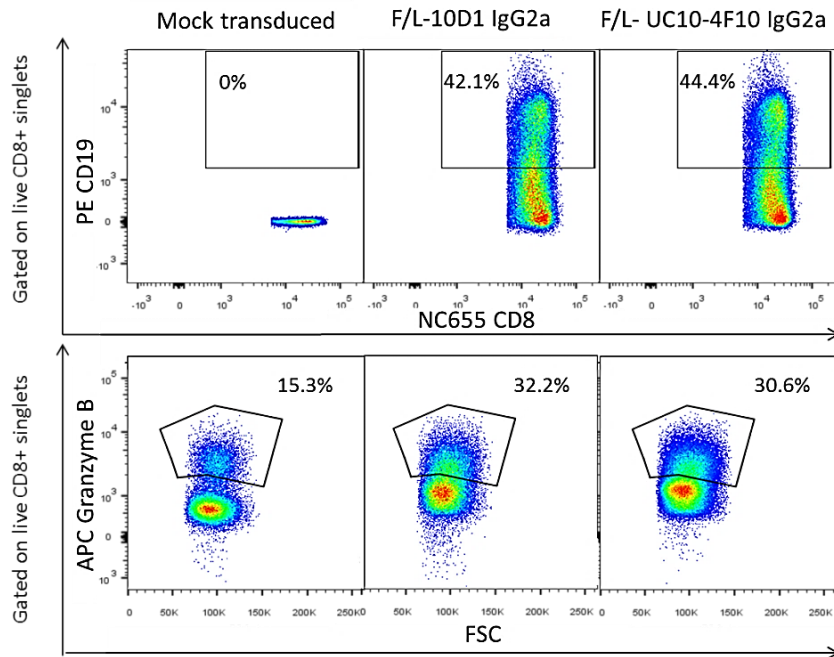
Figure 5.4b: tricistronic vector transduced C57BL/6 lymphocytes secrete F/L-10D1 anti-human CTLA-4 IgG2a and F/L-UC10-4F10 anti-murine CTLA-4 IgG2a which bind CTLA-4 transduced SupT1 cells in a species-specific manner. Key: FL=full length; 10D1 anti-CTLA-4= anti-human-CTLA-4; 4F10 anti-CTLA-4=anti-murine-CTLA-4; human CD34=transduction marker gene/protein; mAb=monoclonal antibody; FSC=forward scatter; anti-murine-Fc=secondary antibody staining to detect secreted antibody (pan isotype).
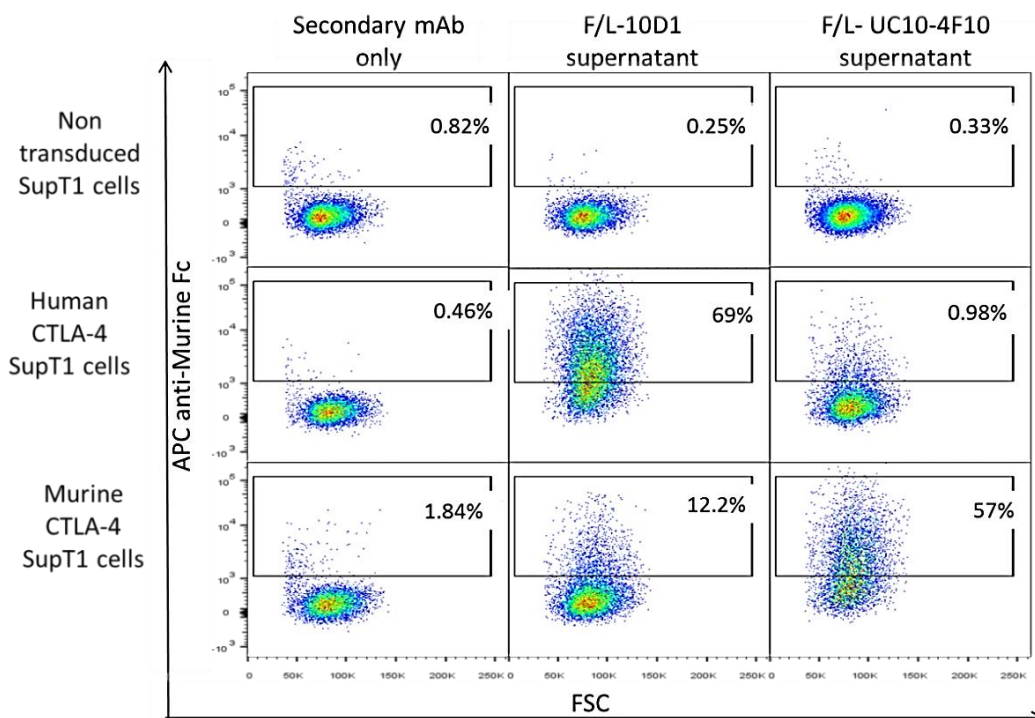
Supernatant collected from activated, transduced polyclonal murine T cell cultures contained antibody which bound CTLA-4 target cells in a species specific manner (figure 5.4b).

5.2.6 Testing constructs in monoclonal TRP1 CD4 T lymphocytes in vitro

We wanted to establish a method for selective expansion of tumour-reactive cells from within a mixed culture, as we ultimately hope to be able to extract tumour-infiltrating lymphocytes (TILs) from tumours/draining-lymph nodes for expansion and transduction. In addition, we need to be able to expand transgenic TRP1 T cells to adequate numbers for adoptive transfer. We explored several modes of T cell stimulation and expansion. Details of the methods are discussed in Chapter 2.4.5.

ConA+IL-7 stimulation induces excellent polyclonal T cell expansion to enable retroviral transduction of C57BL/6 primary T cells (figure 5.4a). TRP1 B^{W}RAG$^{-/-}$ transgenic mice express an avid monoclonal TCR directed against a peptide derived from TRP1 and presented on I-Ab (30). Given the monoclonal TCR, we suspected that TRP1 T cells would expand better with antigen-specific stimulation. We compared ConA+IL-7 to TRP1 peptide + polyclonal dendritic cells (DCs) in a culture derived from tumour-draining LN of a B16/BL6-bearing C57/BL6 mouse following adoptive transfer of WT TRP1 T cells 10 days prior to organ harvesting. This was to recreate the scenario of antigen specific TIL extraction from tumour/tumour draining lymph node.

Figure 5.5a: TRP1 peptide is superior to ConA+IL-7 for proportional in vitro enrichment of TRP1 CD4 T cells in a mixed cell culture. Key: ConA=concanavalin A; IL-7=interleukin 7; TCR Vbeta14=T-cell receptor Vβ14 expressed by TRP1 T cells; DC=dendritic cells; CD45.1=congenic marker of TRP1 transgenic strain; Trp1 peptide=tyrosinase related protein 1.
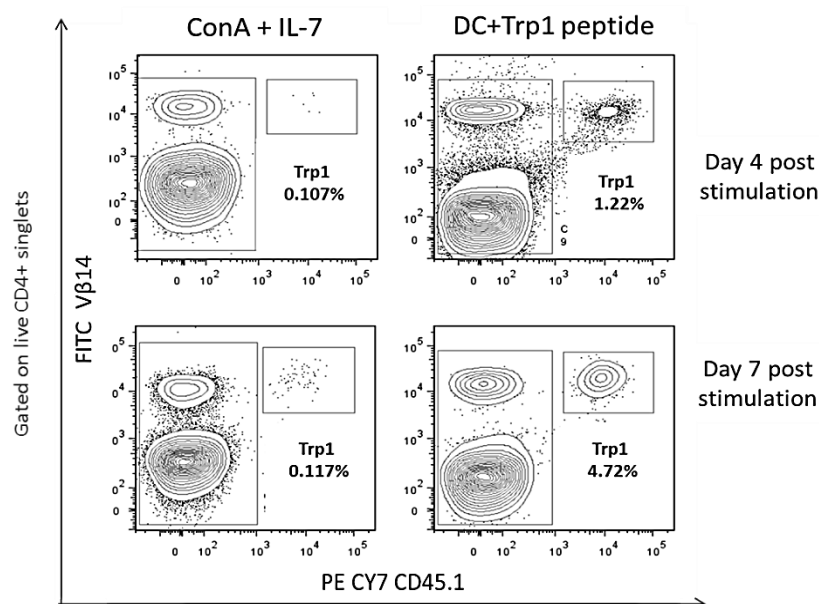
Figure 5.5b: TRP1 peptide is superior to ConA+IL-7 for preferentially expanding TRP1 CD4 T cells for transduction in a mixed culture. Key: CD19=transduction marker gene/protein; F/L 10D1 IgG2a= anti-human-CTLA-4; ConA=concanavalin A; IL7=interleukin 7; DC=dendritic cells; Trp1 peptide=tyrosinase related protein 1; TRP1= TRP1 CD4 T cell; Endog=endogenous CD4 T cells; Vβ14=TCR β chain.
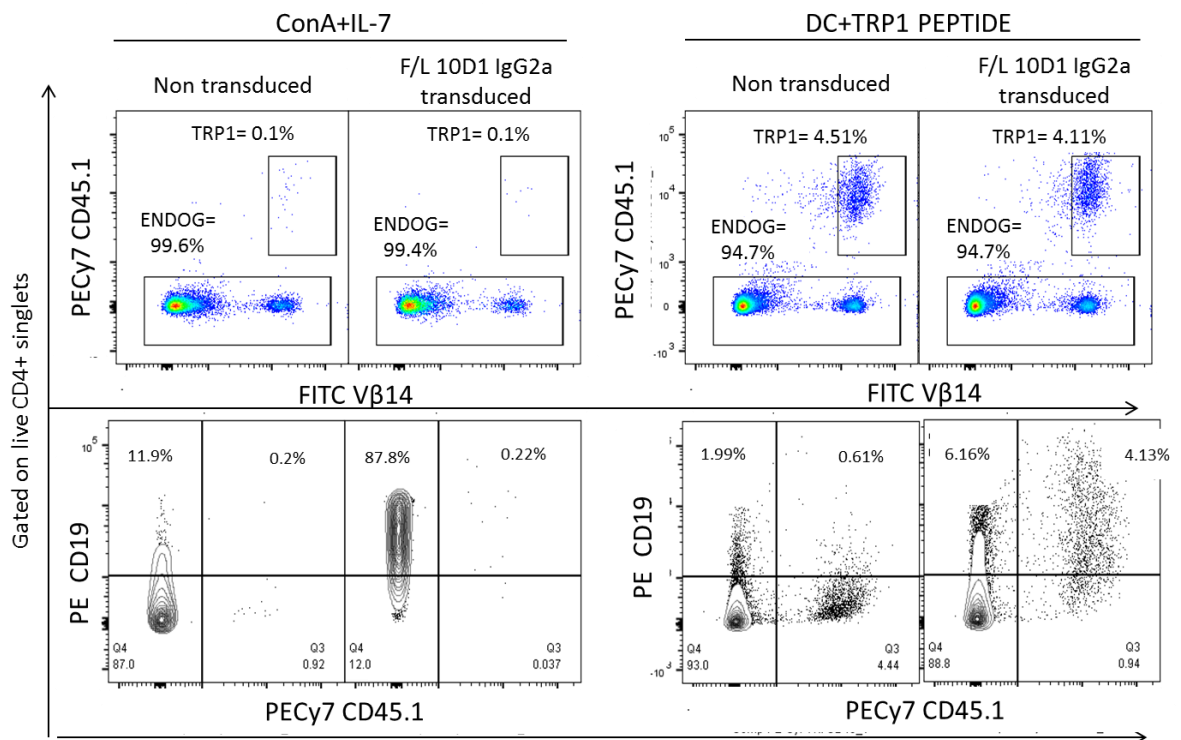
Figures 5.5a & 5.5b show enrichment of TRP1 tumour-reactive T cells in a mixed cell culture at 72 hours in vitro with TRP1 peptide+DCs compared with ConA+IL-7. In the latter condition the expansion of TRP1 T cells was very poor. DC+ TRP1 peptide was also found to expand pure naïve TRP1 CD4 T cells better than ConA+IL-7 (data not shown) and for this reason was selected to be used in all downstream experiments.

5.2.7   Biological functions of 10D1 IgG1 and IgG2a – ADCC assays

Based on the hypothesis that αCTLA-4 mAb can deplete CD4 Tregs in the tumour via an Fc-directed mechanism (67), we set up an ADCC assay to simulate this in vitro to test whether 10D1 IgG2a αCTLA-4 mAb can deplete CFSE-labelled human CTLA-4 transduced SupT1 cell targets when co-incubated with bone marrow (BM)-derived macrophage effectors. The experimental outline is described in detail in Chapter 2.4.8, CFSE labelling in Chapter 2.4.9, and production of mature-lipopolysaccharide (LPS)-treated BM-derived macrophages in Chapter

2.4.3. Pre-assay flow cytometric analysis of BM-derived macrophages revealed a population of CD11b^{hi}, CD11c^{int} cells with high iNOS and FcγR IV expression (figure 5.6a).

Figure 5.6a: BM-derived macrophages are CD11b^{hi}, CD11c^{int} and co-express iNOS and FcγR IV and fulfil an effector function in this ADCC assay. Gated on live singlets. **Key:** iNOS=inducible nitric oxide synthetase; FcγR IV=expressed on CD11b high macrophages and involved in ADCC.
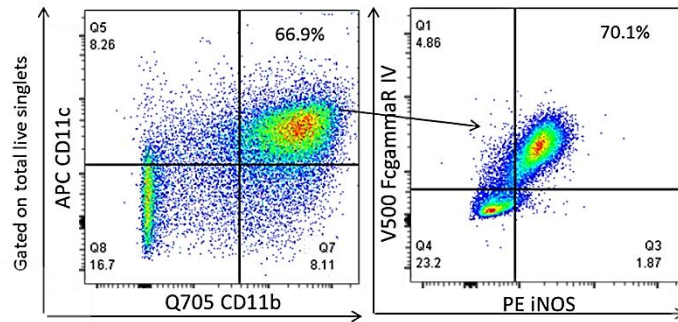
Full length 10D1 αCTLA-4 IgG1 and IgG2a mAbs for ADCC testing were obtained from 293T cell transfection supernatants, polyclonal murine T cell transfection supernatants and TRP1 CD4 T cell transfection supernatants. The supernatants were 0.22µm filtered, and quantitated by Ready-Steady-Go ELISA (affymetrix, eBioscience). This is described in more detail in Chapter 2.5.10. Control antibody was isotype matched, but had no corresponding target antigen on CFSE-labelled SupT1 cells. We used anti-murine CD25 (PC61 clone). Antibody-containing supernatants were tested in triplicate with the following effector(e) to target(t) ratios: 10e:1t, 5e:1t and 0.5e:1t and controls (target cells+antibody (no effectors). See figure 5.6b for the full experimental layout.

Figure 5.6b: ADCC assay layout for testing full length 10D1 IgG1 and IgG2a. Supernatants were tested in triplicate against CFSE-labelled SupT1 target cells incubated with LPS-matured BM-derived macrophages for 16 hours at concentrations of 10e:1t, 5e:1t, 0.5e:1t. **Key:** 10D1 IgG2a (or IgG1)=10D1 anti-human CTLA-4; LPS=lipopolysaccharide; BM=bone marrow; e=effector; t=target; Isotype control= non-binding mAb (αMurineCD25 (PC61 clone).

Figure 5.6c: **F/L 10D1 anti-human CTLA-4 IgG2a shows higher target cell killing at ratios of 10e:1t and 5e:1t than F/L 10D1 IgG1 or isotype control in a 16 hour ADCC assay. Key:** 10D1=10D1 anti-human-CTLA-4 mAb; e=effector; t=target; CD25=isotype control. Vertical bars represent SEM. Statistical tests performed on triplicate samples: one-way analysis of variance and multiple comparisons test. Data is representative of 2 independent experiments.
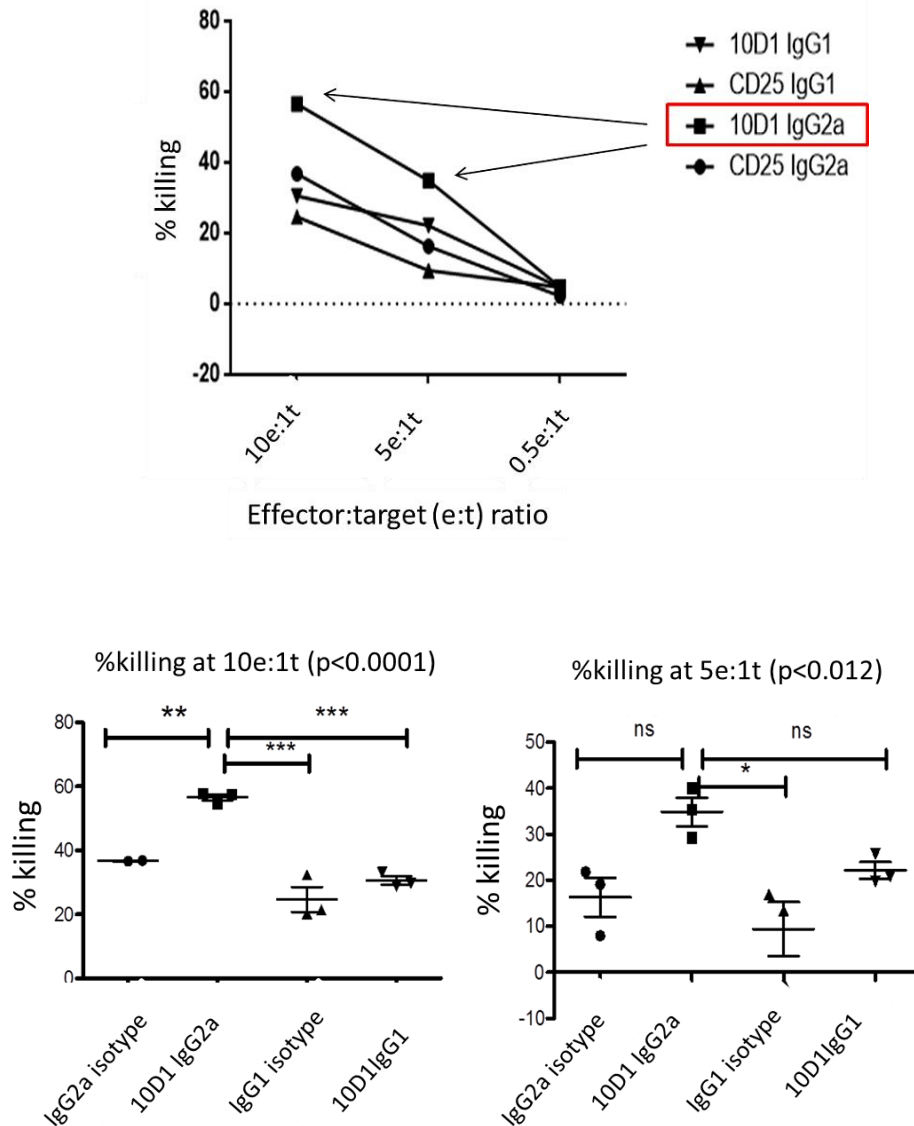
Compared with isotype control and with 10D1-IgG1, 10D1-IgG2a is associated with significantly higher depletion of human CTLA-4 expressing SupT1 targets at 10e:1t and 5e:1t (figure 5.6c).

Full-length UC10-4F10 anti-murine CTLA-4 antibody was also tested in an ADCC assay (figure 5.6d) and was associated with significantly higher depletion of murine CTLA-4 expressing SupT1 targets at 10e:1t and 5e:1t compared with isotype control and UC10-4F10-IgG1 when tested in triplicate.

Figure 5.6d: full length UC10-4F10 α-murine-CTLA-4 IgG2a shows significantly higher target cell killing at ratios of 10e:1t and 5e:1t than F/L UC10-4F10-IgG1 and isotype controls in an ADCC assay (p<0.0001). Target cells are murine CTLA-4 expressing SupT1 cells. **Key:** UC10-4F10=4F10 anti-murine-CTLA-4; mAb=monoclonal antibody; e=effector; t=target; CD25=isotype control. Vertical bars represent SEM. Statistical tests performed on triplicate samples: one-way analysis of variance and multiple comparisons test. Data is representative of 2 independent experiments.
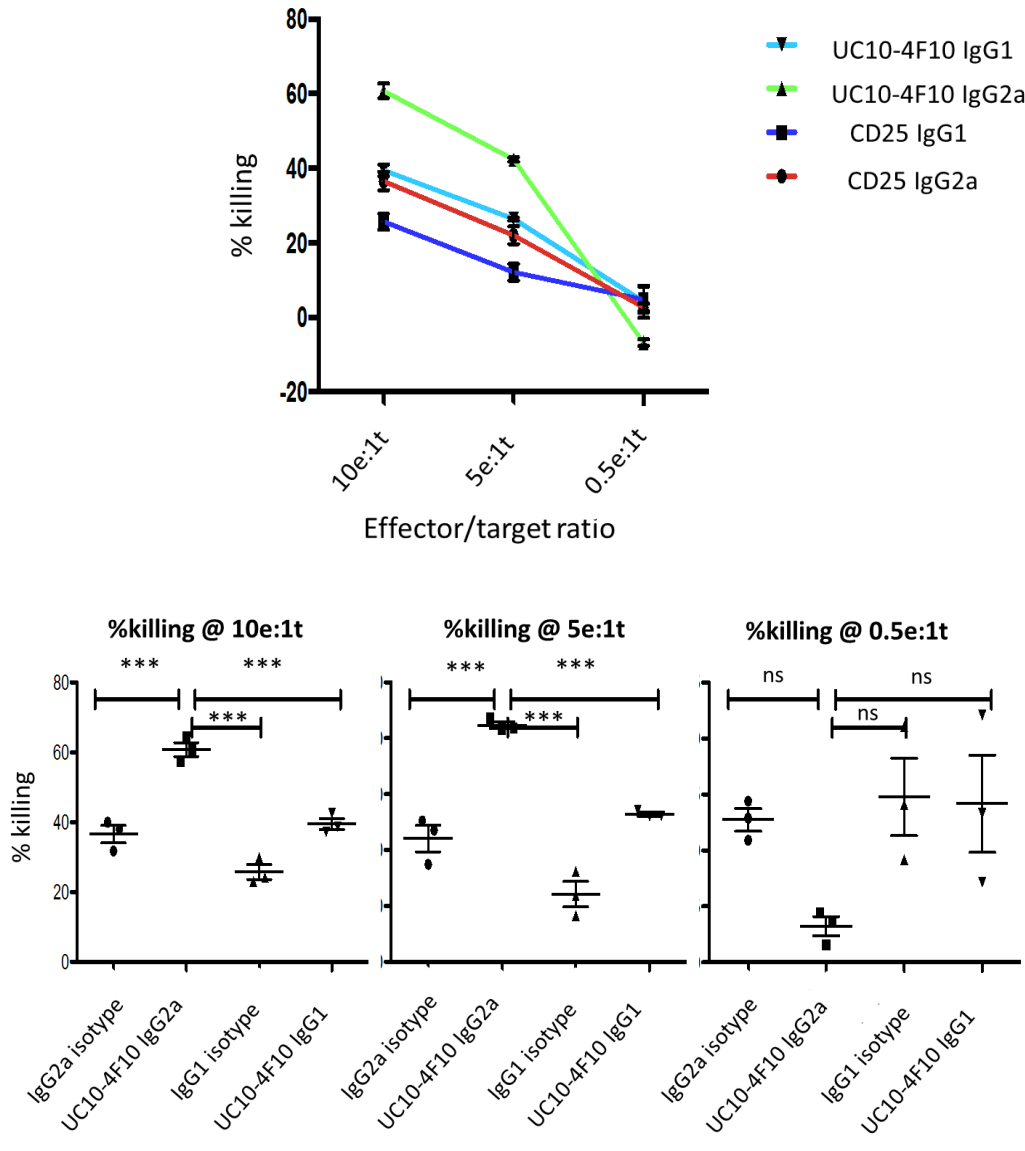
5.2.8 Testing constructs in vivo: 10D1 in the Hu152Tg mouse (Trp1 CTLA4$^{-/-}$ T cell transfer)

We have generated 10D1 α-human CTLA-4 mAb which can bind human CTLA-4 in a species-specific manner, can mediate ADCC of CTLA-4^{hi} targets in an ADCC assay in vitro and can be secreted from polyclonal and monoclonal primary T cells using retroviral transduction methods. The next objective is to adoptively transfer 10D1 αHuman-CTLA-4 IgG2a secreting tumour-reactive transgenic T cells into a B16/BL6 melanoma tumour model to observe whether the antibody is biologically active in vivo. The experimental setup is illustrated in figure 5.7.

Figure 5.7: experimental model to compare 10D1-α-Human CTLA-4-IgG2a transduced DLI to mock transduced DLI (+/- exogenous 10D1 administered intraperitoneally at days 8, 11 and 14) and UC10-4F10 α-murine CTLA-4-IgG2a transduced DLI. Recipients are irradiated B16/BL6 melanoma-bearing Hu152Tg mice. DLI donors are TRP1 CTLA4$^{-/-}$ mice. **Key:** 250k=250,000 cells; Hu152Tg= transgenic mice expressing exon 2 of human-CTLA-4; 5Gy TBI= 5 Gray of total body irradiation; DLI=donor lymphocyte infusion; αCTLA-4= exogenous 10D1 anti-CTLA-4 antibody; UC10-4F10-IgG2a-DLI = UC10-4F10 IgG2a anti-murine-CTLA-4 secreting DLI; 10D1-IgG2a-DLI= 10D1 IgG2a anti-human-CTLA-4 secreting DLI; data represents two independent experiments.
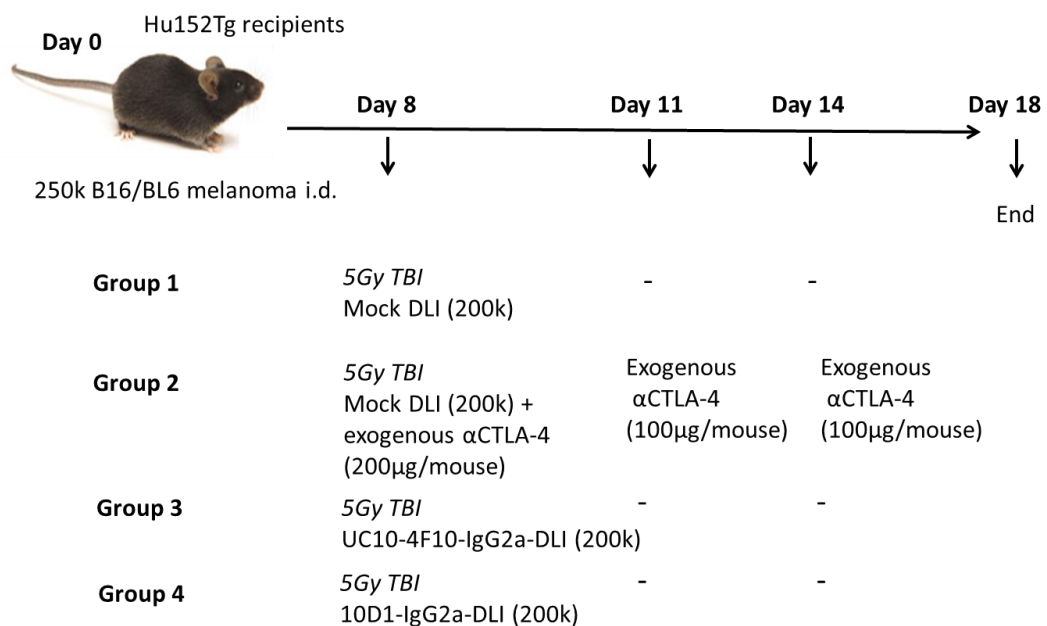
Irradiated (5Gy TBI) human CTLA-4 transgenic (Hu152Tg) mice bearing B16/BL6 melanoma tumours were treated at day 8 post tumour induction with a TRP1 CTLA4$^{-/-}$ cell product transduced to express 10D1 α-human-CTLA-4-IgG2a, UC10-4F10-α-Murine CTLA-4-IgG2a or mock transduced cells with and without systemically administered exogenous 10D1 α-human-CTLA-4 mAb.

We elected to use TRP1 CTLA-4$^{-/-}$ murine cells as they have better viability and growth in vitro, and permit us to use UC10-4F10 α-Murine CTLA-4-IgG2a as a control in this experiment. The biological impact of secreted 10D1 αCTLA-4 mAb should be visible in the endogenous T cell compartment only.

Cells underwent retroviral transduction according to the protocol described in Chapter 2.4.5.2, and at 72 hours post-stimulation, transduction efficiency was determined to be 40-50%. Supernatant from TRP1 T cell culture at 72h was tested in the ADCC assay described in Section 5.2.7 and the same pattern of results was obtained, namely that 10D1 IgG2a-containing supernatant preferentially depleted human CTLA-4 expressing targets at e:t ratios of 10:1 and 5:1 compared with 10D1 IgG1 and isotype control supernatants.

A commercially available murine CD19 magnetic bead/column sorting kit (Miltenyi Biotech, Auburn, CA) gave a post-selection purity of >95% for the transduction marker murine CD19 on live CD4+ singlets (figure 5.8). There is some loss of transduced cells in the selection process which we established by staining the column run-through in tandem with the selected fraction for flow cytometry.

Figure 5.8: CD19 magnetic bead/column selection at 48 hours post-transduction gives a pre-injection CD19+ CD4+ live singlet purity of >95% for F/L 10D1 IgG2a and F/L UC10-4F10 IgG2a. There is some loss of transduced cells to the column. **Key:** FL/UC10-4F10 = full length UC10-4F10 IgG2a anti-murine-CTLA-4; FL/10D1 = full length 10D1 IgG2a anti-human-CTLA-4; CD19=marker of transduction; Vβ14= TCR beta chain subunit.
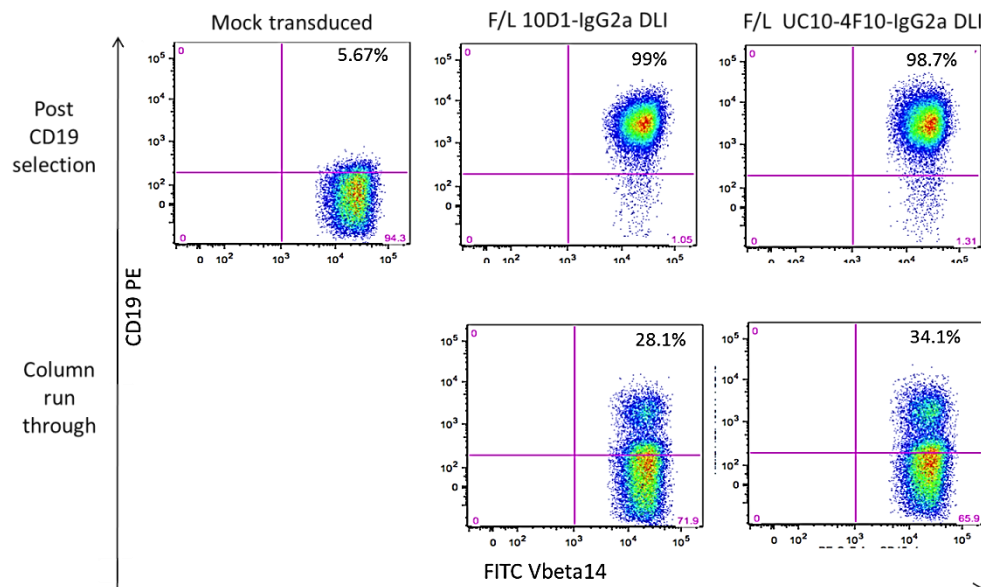
Tumour weight at day 18 showed a higher (but non-significant) increase in tumour mass in the 10D1-IgG2a-DLI cohort compared with the control groups (figure 5.9a).

Figure 5.9a: 10D1-IgG2a-transduced TRP1 CTLA-4$^{-/-}$ T cells are associated with a (non-significantly) higher tumour weight than controls. Key: UC10-4F10-IgG2a= α-murine-CTLA-4; 10D1-IgG2a= α-human-CTLA-4; DLI= donor lymphocyte infusion; exog-10D1=exogenous 10D1 monoclonal antibody; mg=milligrams. Horizontal bars represent mean values and vertical bars represent SEM.
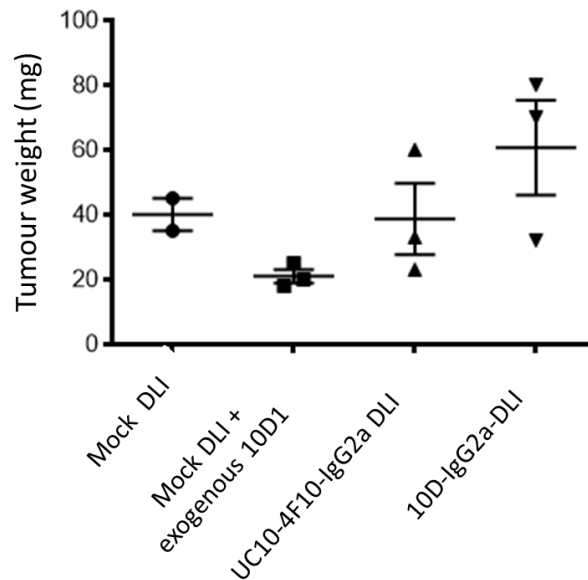
Engraftment and persistence of transduced DLI is shown in figure 5.9b. Lower expression of the marker protein CD19 was observed at the end of the experiment compared to day 8/ adoptive transfer. A drop in expression of the section of transgene beyond IRES in the cassette is common (148) and can be recovered by a period of in vitro stimulation (data not shown). To define the transduction population we instead used intracellular murine-Fc staining after a short in vitro restimulation with TRP1 peptide+B16-pulsed DCs+brefeldin A (methods described in Chapter 2.4.8). Figure 5.9b shows that transduced, tumour-reactive TRP1 T cells are present in higher concentration in the tumour compared to the LN. This supports the idea that tumour-reactive T cells could be good vehicles for the delivery of antibody into the tumour with lesser peripheral exposure to α-CTLA-4 mAb.

Quantitation of absolute numbers of TRP1 CTLA-4$^{-/-}$ Teff and Treg shows no significant differences between groups (data not shown). There is no significant difference in granzyme B production or Ki67 expression in 10D1-IgG2a transduced TRP1 CTLA-4$^{-/-}$ Teff compared with controls, indicating that transduced cells are still capable of effector function and proliferation (figure 5.9c).

Figure 5.9b: 10D1-IgG2a transduced cells are present at high concentration in the tumour compared with the LN and stain strongly for αmurine-Fc. Key: UC10-4F10-IgG2a-DLI= anti-murine-CTLA-4;10D1-IgG2a-DLI=anti-human-CTLA-4; DLI=donor lymphocyte infusion; αCTLA-4=exogenous 10D1 anti-human-CTLA-4 mAb; TIL=tumour/tumour-infiltrating lymphocyte; LN= lymph node; anti-MuFc=anti-murine Fc antibody (secondary stain); CD19=transduction marker gene/protein.
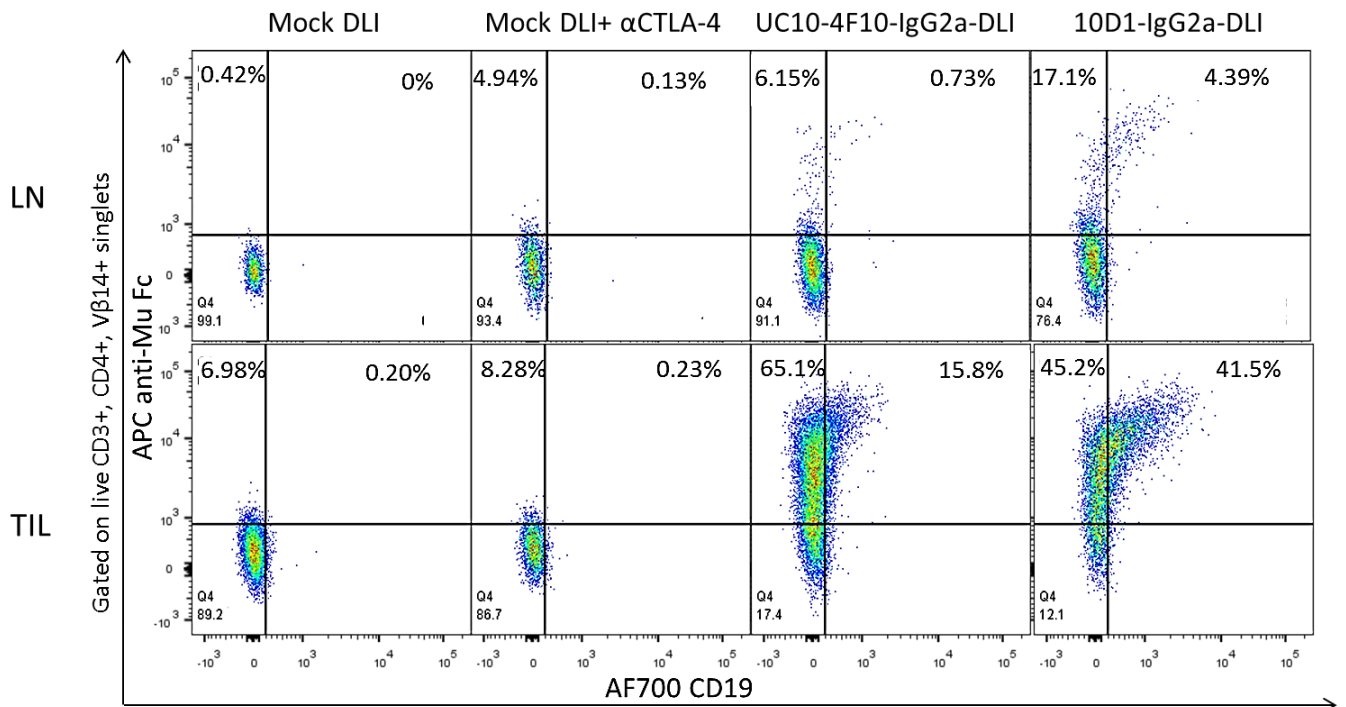
Figure 5.9c: proliferative capacity and features of effector function (granzyme b production) are preserved in transgenic TRP1 T cells transduced to secrete αCTLA-4 mAb. Key: UC10-4F10 DLI = α-murine-CTLA-4 transduced DLI;10D1 DLI = 10D1 IgG2a anti-human-CTLA-4 transduced DLI; DLI=donor lymphocyte infusion; aCTLA-4=exogenous, systemically administered (10D1) monoclonal antibody; LN=lymph node. Vertical bars represent SEM. Statistical tests: one-way analysis of variance and multiple comparisons test.
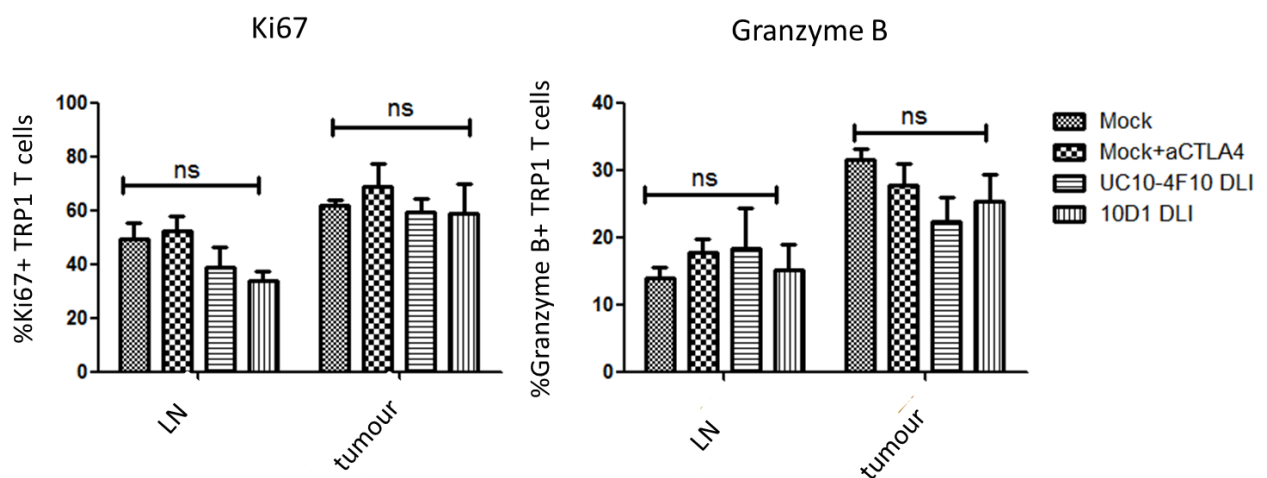
There is a clear trend towards lower absolute numbers of endogenous T cells in the tumour (but not the LN) of the 10D1-IgG2a-DLI condition compared with controls (figure 5.9d). To a lesser extent, this pattern is mirrored in the mock DLI plus exogenous α-human-CTLA-4 group. The apparent toxicity of 10D1-IgG2a-secreting DLI to the whole endogenous T cell compartment within the tumour microenvironment may be explained by unexpectedly high intratumoural CTLA-4 expression in the Hu152Tg model across lymphocyte subsets. Figure 5.9e compares CTLA-4 expression between B16/BL6 melanoma-bearing Hu152Tg and C57BL/6 mice and shows that in the Hu152Tg model, 29% of CD8 T cells and 24% of CD4 T cells in the tumour express CTLA-4 compared with 1.02% and 10% respectively in the C57BL/6 mouse. In the Hu152Tg LN, CTLA-4 expression is lower than in the tumour, but still higher than in the control C57BL/6 mouse. This potentially supports the hypothesis of targeted toxicity of α-CTLA-4 mAb towards CTLA-4^{hi} subsets outlined in Chapter 4 (67).

Figure 5.9d: 10D1-IgG2a-DLI and to a lesser extent Mock DLI+ exogenous 10D1 are associated with an intratumoural reduction in all endogenous T cell compartments. This is not apparent in the LN. **Key:** UC10-4F10-IgG2a= UC10-4F10 IgG2a anti-murine-CTLA-4;10D-IgG2a= 10D1 IgG2a anti-human-CTLA-4; DLI=donor lymphocyte infusion; aCTLA-4=exogenous, systemically administered (10D1) monoclonal antibody; TIL=tumour/tumour-infiltrating lymphocyte; LN=lymph node. Horizontal bars represent mean values and vertical bars represent SEM. Statistical tests: one-way analysis of variance and multiple comparisons test.
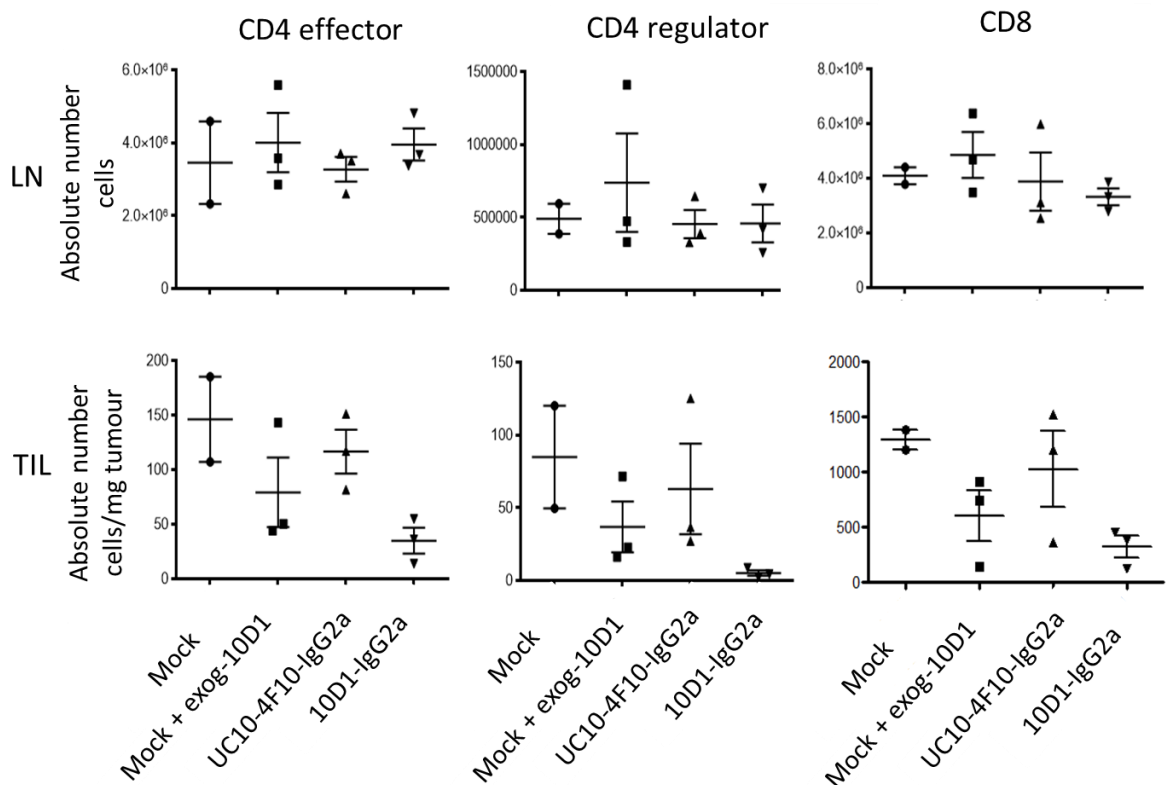
Figure 5.9e: endogenous Hu152Tg CD4regs, CD4eff and CD8eff all show high levels of CTLA-4 expression in the tumour compared with the LN and compared with the tumour of a B16/BL6 bearing C57BL/6 mouse. This may explain the drop in endogenous T cell numbers intratumourally in groups exposed to 10D1 αHumanCTLA-4 mAb. **Key:** TIL=tumour/tumour-infiltrating lymphocyte; LN=lymph node.
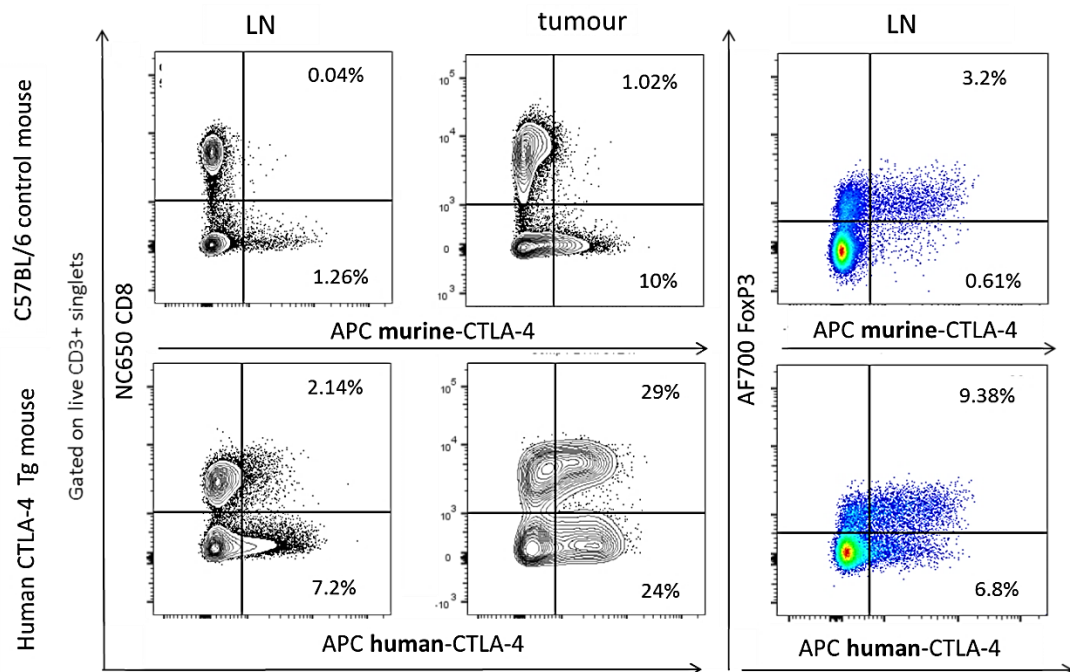
It is interesting to consider why the intratumoural reduction in endogenous T cells is more profound in the 10D1-IgG2a-DLI cohort compared with the mock transduced + exogenous 10D1 αCTLA-4 mAb control group. It is possible that local delivery of biologically active antibody from tumour reactive transduced cells as a payload results in a more concentrated mAb effect in the tumour compared with systemic delivery. This could offer an anti-tumour benefit provided that there is a clear magnitude of difference in CTLA-4 expression levels between Tregs and Teffs, otherwise Teffs will be vulnerable to depletion as was observed in the Hu152Tg mouse model. In future experiments we hope to be able to check serum levels of αCTLA-4 mAb to be able to further explore this hypothesis.

Figure 5.9f: 10D1-IgG2a-DLI is associated with a reduction in CTLA-4 expression on endogenous CD4 T cells in the tumour (but not the LN) and a depletion of Tregs that is not seen in the UC10-4F10-DLI cohort. This supports a targeted anti-CTLA-4 mAb mediated effect. Key: UC10-4F10-IgG2a= UC10-4F10 IgG2a anti-murine-CTLA-4;10D-IgG2a= 10D1 IgG2a anti-human-CTLA-4; DLI=donor lymphocyte infusion; aCTLA-4=exogenous, systemically administered (10D1) monoclonal antibody; TIL=tumour/tumour-infiltrating lymphocyte; LN=lymph node.
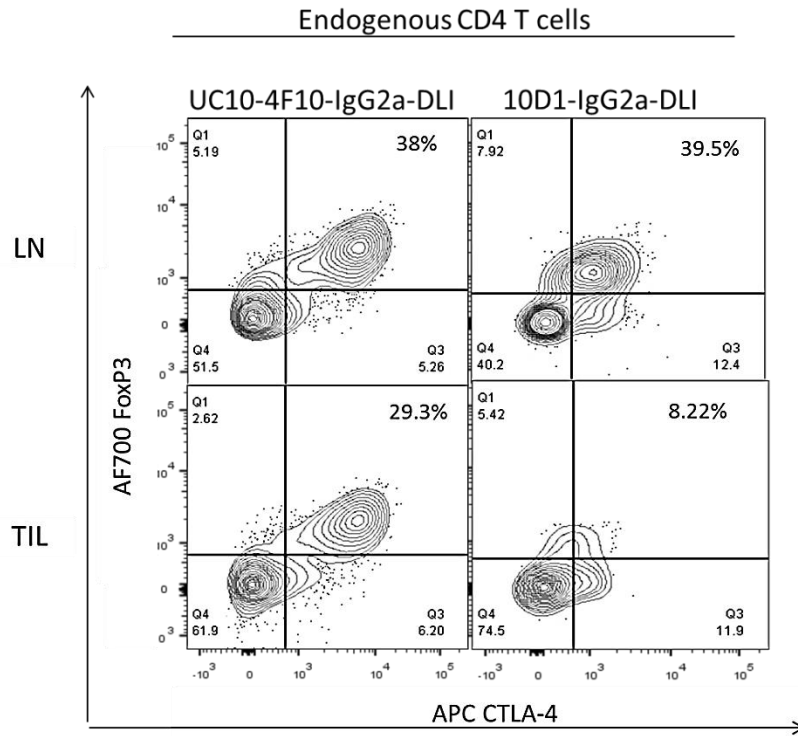
5.3   Discussion

Broadly, these experiments gave us significant insights into adoptive cell transfer. TRP1 CTLA-4$^{-/-}$ T cells are a good vehicle for genetic manipulation to secrete αCTLA-4, as they permit an effect on endogenous T cells without significantly compromising themselves in the process.

It was valuable to run the exogenous 10D1 αCTLA-4 mAb control in tandem with DLI transduced to secrete 10D1, as it defined what we should expect biologically from 10D1and enabled us to identify and comment upon differences in secreted versus systemically administered antibody.

Building on the findings from Chapter 4, these experiments in Hu152Tg recipients show how αCTLA-4 mAb targets CTLA-4^{hi} cells for depletion in the tumour, reflected in a drop in absolute cell numbers. This depletion is not evident in the LN, and part of the reason for this is likely to be simply that the CTLA-4 expression levels in LN are much lower than in the tumour, and that the tumour-reactive T cells secreting αCTLA-4 mAb preferentially migrate to the tumour, concentrating the antibody effect there and sparing the peripheral Tregs. This is a potentially attractive option to minimise peripheral toxicity from CTLA-4 blockade.

Manipulating T-cells to secrete αCTLA-4 mAb which exerts its effect through deletion of CTLA-4^{hi} cells in the tumour microenvironment, poses a significant risk to CTLA-4-replete populations used for adoptive transfer, both in vivo and potentially in vitro, where local secretion of antibody into a mixed cell culture (incorporating APCs) could potentially lead to Fc-mediated cell deletion even prior to selection, and this requires further investigation.

5.4   Future plans

The expression level of CTLA-4 in the Hu152Tg mouse is not representative of that of a C57BL/6 mouse or that of a human. As such, interpretation of these experimental findings has limited application beyond this model. We plan to conduct testing of anti-murine CTLA-4 mAb constructs in C57BL/6 recipients in which the distribution of CTLA-4 is well established.

It is possible that at the root of the aberrant expression of CTLA-4 across all T cell subsets in this transgenic model is the BACS methodology used to generate the model. The proximal CTLA-4 gene promoter is incorporated into the transgene, but random integration of the construct into the genome could have had a potential impact upon the normal intranuclear and intracytoplasmic regulatory mechanisms governing CTLA-4 gene expression in its native

state. The normal transcriptional regulation of CTLA-4 is discussed in more detail in Chapter 1.2.2.

In retrospect, additional in vitro characterisation of transduced transgenic CD4 T cell functionality (cytotoxicity and cytokine secretion) would have been extremely interesting to further understand the tumour growth observed in Figure 5.9a and to verify that the additional transcriptomic burden of F/L αCTLA-4 mAb generation and secretion by these transgenic cells does not compromise their inherent anti-tumour potential. For this reason we propose to conduct experiments similar to those described at the end of Chapter 4, including FACS-based cytotoxicity and a degranulation assay (staining stimulated T cells for CD107a and CD107b) to define the cytotoxic potential of the transduced TRP1 CD4 T cells. 7 day co-culture with irradiated TRP1 antigen positive and negative targets will deliver data on transduced T cell expansion as well as cytokine data, and we will complete in vitro testing with analysis of T cell exhaustion markers and maturation status (effector/memory skew). This will hopefully inform further in vivo work required to bring this project to its conclusion.

CHAPTER 6

6. GENERATION AND INVESTIGATION OF ANTI-MURINE CTLA-4 ANTIBODY

6.1 Introduction

6.1.1 9D9 anti-murine CTLA-4 mAb

In Chapter 5 we described the process of generating and testing constructs for 10D1 α-human-CTLA-4 and UC10-4F10-α-murine-CTLA-4, the latter developed as a control for testing the former. In the process we established that UC10-4F10 secreted from transduced cell lines and primary murine lymphocytes bound murine CTLA-4 in a species-specific manner (figure 5.4b) and that UC10-4F10-IgG2a isotype depleted murine CTLA-4 expressing targets at a significantly higher level than isotype control or UC10-4F10 IgG1 isotype in an ADCC assay (figure 5.6d).

The limiting issue with UC10-4F10 in our hands was low transduction efficiency of transgenic lymphocytes in vitro compared with 10D1 when run in identical conditions in parallel. This ultimately translated into higher murine donor requirements for animal experiments and prompted us to design an alternative anti-murine CTLA-4 monoclonal antibody (mAb) secreting construct.

The reason that we cannot proceed further with 10D1 anti-human CTLA-4 in the Hu152Tg mouse is that CTLA-4 expression on the Teff populations is much higher than is seen in other murine models and essentially leave the entire effector population as vulnerable to αCTLA-4 mediated depletion as the Treg population.

9D9 is an IgG2a α-murine-CTLA-4 mAb originally described by James Allison for which we located the patent and sequence online (US 2011/0044953A). Simpson and Quezada showed that 9D9 can promote the anti-tumour effect of WT TRP1 CD4 T cells in a manner akin to that of the well-described 9H10 α-murine-CTLA-4 mAb. Like 9H10, 9D9 can switch the balance of intratumoural effector to regulatory T-cells (67). 9D9 can also exert an anti- B16/BL6 melanoma effect in non-irradiated tumour-bearing recipients, when given as combinatorial therapy with Gvax (48).

Informed by previous experiments and a developing interest in the field of Fc modulation to achieve different biological effects in vivo, we proceeded directly to the generation of

tricistronic vectors coding for full length 9D9 antibody with the aim of testing IgG1 and IgG2a isotypes in parallel within experiments in an attempt to discern a possible difference in anti-tumour effect.

6.1.2   Modulation of mAb Fc and its impact on biological function

We know from published work that many therapeutic mAbs used in cancer can mediate their effects via antibody-dependent cellular cytotoxicity (ADCC) or complement dependent cytotoxicity (CDC). These mechanisms are governed by the Fc portion of the mAb and the corresponding Fc gamma receptor (FcγR) expression profiles of available effectors which can be microenvironment dependent (124-126). An overview of this subject can be found in a review by Furness et al (70).

FcγRs are expressed on B cells, dendritic cells, macrophages, mast cells, natural killer cells, and neutrophils (127). Functionally FcγRs are activating or inhibitory, but most cells (except B cells) co-express both types to permit tight control over cellular activation thresholds. Activating FcγRs have an intracytoplasmic immunoreceptor tyrosine-based activation motif (ITAM). Inhibitory receptors, the only example in the mouse setting being FcγRIIb, has an intracytoplasmic immunoreceptor tyrosine-based inhibition motif (ITIM)(128). In healthy mice, the highly expressed inhibitory receptor is predominant, with a high affinity for abundant antibody isotypes (127, 129), to preserve immunological tolerance. However, this skewed repertoire may adversely impact upon the efficacy of cancer-targeting therapeutic antibodies, such as those directed towards CTLA-4.

The capacity of mAbs to mediate ADCC depends upon their (isotypic) affinity for activating and inhibitory FcγR pairs. This can be quantified using the activating/inhibitory (A:I) ratio (130, 131). The A:I ratio is purported to correlate with therapeutic activity in vivo. For instance, murine IgG1 isotype antibodies have an A:I ratio of <1 meaning that they have a strong affinity for inhibitory FcγRIIb, and are thus only weakly associated with ADCC. On the other hand, IgG2a and IgG2b isotypes have A:I ratios as high as 70, are less regulated by FcγRIIb, and are more strongly associated with ADCC. In fact, they are recognised to be more efficient in tumour cell depletion than IgG1 and IgG3 subclasses (132). In summary, the IgG isotype of immunomodulatory antibodies may significantly impact upon effector function and clinical outcome, and should be a consideration in the generation of future therapies and has informed the direction of this project.

6.1.3 Aims

Our aim is to generate functional anti-murine CTLA-4 in tricistronic secretory format that lends itself to high efficiency transduction of primary murine lymphocytes. Consequent application to an in vivo melanoma model will enable us to determine whether intratumoural secretion of antibody effects tumour rejection, and whether the Fc portion of the secreted antibody impacts upon this in any way.

6.2 Results

6.2.1 Generation of full length IgG1 and IgG2a anti-murine CTLA-4 (9D9)

The sequence for 9D9 was taken from patent US 2011/0044953A and Martin Pule generated maps for gene synthesis by oligonucleotide assembly. PCR reactions were performed with High-Fidelity Phusion Polymerase (NEB, Ipswich, MA) as described in Chapter 2.1.6 in more detail, and verified sequences for secretory full length 9D9 were subcloned into IgG1 and IgG2a tricistronic backbones. See figure 6.1 for plasmid maps. The heavy and light chains are connected by a TaV 2A sequence to enable equimolar translation of both and joined by IRES to the truncated murine CD19 marker protein (dMuCD19).

Figure 6.1: plasmid maps for tricistronic, full length, secretory 9D9-anti-murine-CTLA-4-IgG1 and 9D9-anti-murine-CTLA-4-IgG2a vectors. The 9D9 scFv sequence was obtained from patent US2011/0044953 (J. Allison et al). **Key:** LTR=long terminal repeats; 9D9-LC-mKappa= 9D9 light chain (kappa); 9D9-HC-mIgG1= 9D9 murine IgG1 heavy chain; 9D9-HC-mIgG2a= 9D9 murine IgG2a heavy chain; 2A= FMD 2A sequence; IRES=internal ribosomal entry site; dMuCD19=truncated murine CD19;SD=splice donor;SA=splice acceptor.
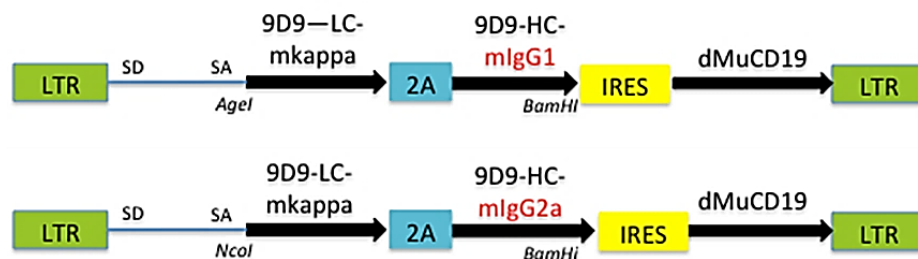
6.2.2 In vitro testing of 9D9 binding to murine CTLA-4

293T cells were transfected according to the method described in Chapter 2.2.6 with 9D9 IgG1 and IgG2a tricistronic constructs. At 72 hours post transfection, supernatant was collected from transfected 293T cells and filtered through a 0.22µm filter as per Chapter 2.2.7, prior to incubation with human or murine CTLA-4 high SupT1 cells. Secondary staining with anti-murine Fc mAb (pan-isotype) demonstrated species-specific target binding of 9D9 (data not shown). Staining with isotype specific anti-Fc mAb distinguished 9D9 IgG1 from IgG2a with no cross-reactivity (figure 6.2).

Figure 6.2: 9D9 IgG1 and IgG2a in supernatant from transfected 293T cells bind murine CTLA-4 transduced SupT1 cells and are distinguishable in their isotype by isotype-specific-anti-Fc staining. Note 9D9 hybridoma generates IgG2a isotype mAb. Gated on live singlets. **Key:** anti-mu-Fc= anti-murine Fc only/secondary antibody staining only; FSC=forward scatter; data represents 3 independent experiments.
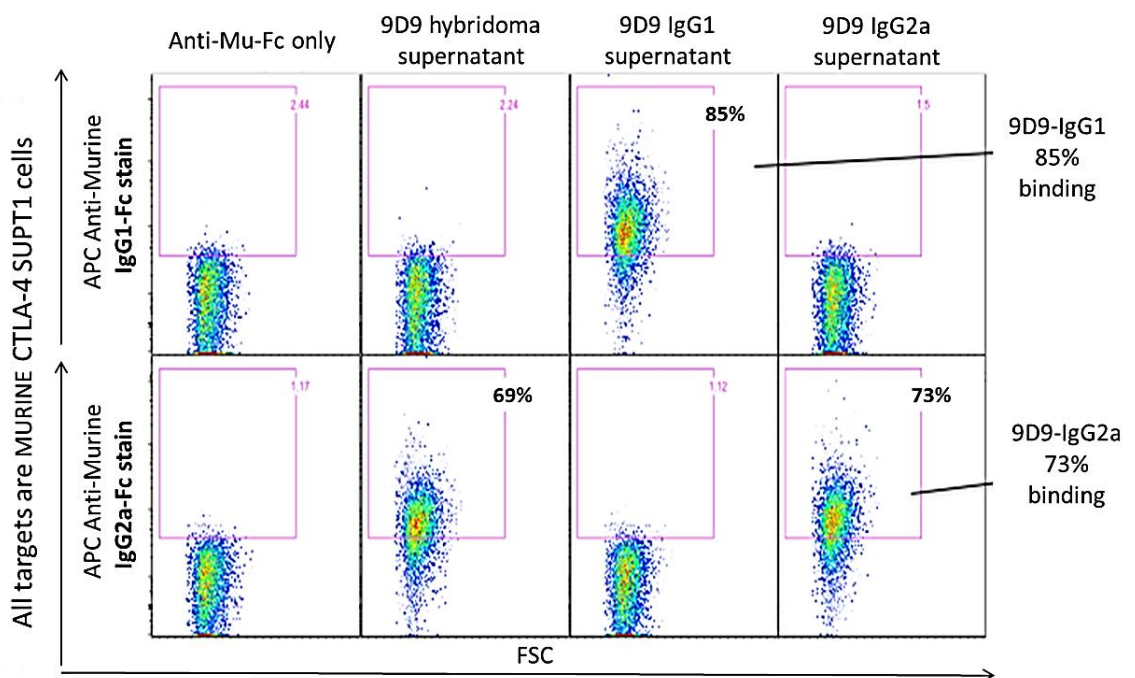
6.2.3 In vitro testing of antibody dependent cell-mediated cytotoxicity (ADCC)

Broadly the question to be answered is whether 0.22µm filtered 9D9-IgG2a containing transfectant supernatant can deplete CFSE-labelled murine CTLA-4 expressing targets when incubated with activated, M-CSF differentiated effector macrophages (figure 5.6a) in a 16 hour ADCC assay. The experimental outline is described in detail in Chapter 2.4.8, CFSE labelling in Chapter 2.4.9, and production of bone-marrow derived macrophages in Chapter 2.4.3.

Figure 6.3: full length 9D9 anti-murine CTLA-4 IgG2a and UC10-4F10 anti-murine CTLA-4 IgG2a demonstrate significantly increased target cell depletion of CFSE-labelled murine CTLA-4 expressing SupT1 cells compared with isotype control at e:t ratios of 10:1 (p<0.05) and 5:1 (p<0.05) in a 16 hour ADCC assay. Key: 9D9-IgG2a = anti-murine CTLA-4 mAb; CD25 IgG2a =anti-murine-CD25 IgG2a isotype control (PC10 clone); UC10=UC10-4F10 IgG2a anti-murine CTLA-4 mAb; e=effector (BM-derived macrophage); t=target (SupT1 transduced to express murine CTLA-4). Statistical tests performed on triplicate samples: one-way analysis of variance and multiple comparisons test. data represents 2 independent experiments.
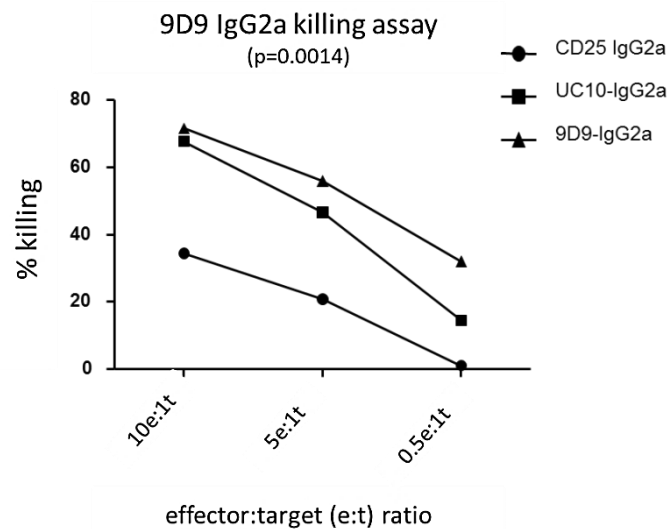
IgG2a 9D9 was tested in triplicate alongside IgG2a isotype control (anti-murine CD25 mAb/PC10 clone) and the positive control UC10-4F10 IgG2a (anti-murine CTLA-4 mAb). Effector(e) to target(t) ratios were 10e:1t, 5e:1t and 0.5e:1t with appropriate controls (target cells and antibody only, no effectors). Antibody quantitation in the supernatant was by secondary α-murine-Fc staining as described in chapter 2.2.6, or ELISA (described in Chapter 2.5.10) to ensure that antibody concentrations between supernatants were equivalent (data not shown). Figure 6.3 shows that 9D9 IgG2a and UC10-4F10 IgG2a show statistically increased depletion of murine CTLA-4 expressing SupT1 targets when compared with isotype control at ratios of 10e:1t and 5e:1t.

6.2.4   Transduction into primary murine lymphocytes

We have established that 9D9 IgG2a binds CTLA-4 in a species-specific manner and can deplete CTLA-4^{hi} targets in the presence of effector macrophages. We elected to proceed with primary murine lymphocyte transduction with a view to in vivo tumour-based experiments. Retroviral supernatant for 9D9 IgG1 and IgG2a constructs was generated according to Chapter 2.3.1 and validated by transduction of activated polyclonal C57BL/6 lymphocytes using the protocol outlined in chapter 2.4.5.1. Flow cytometric assessment confirmed transduction (CD4/CD19

double-staining) and 0.22µm filtered culture supernatant demonstrated murine CTLA-4 SupT1 cell binding by secondary antibody staining as described in Chapter 2.2.7 and ADCC-mediated killing of murine CTLA-4 expressing targets in a similar manner to that described in Chapter 6.2.3 (data not shown).

6.2.5   Testing constructs in vivo: 9D9 in the C57BL/6 mouse (Trp1 CTLA4$^{-/-}$ transfer)

We elected to use CTLA-4$^{-/-}$ TRP1 donors for these experiments as we know from Chapter 5 that these cells can be genetically modified in sufficient numbers for ACT experiments and should not be subject to autocrine deletion by anti-murine CTLA-4 by virtue of their complete genetic absence of CTLA-4.

In each experiment we used 4 recipient C57BL/6 mice per group, and all received an inoculation of 250x10^3 B16/BL6 cells intradermally on day 0. Donor CTLA-4$^{-/-}$ TRP1 LN and spleen were harvested and stimulated with TRP1 peptide and IL-2 on day 5, and underwent retroviral transduction on day 6 for adoptive transfer into irradiated tumour-bearing C57BL/6 mice on day 8. The experiments were ended on day 18 post tumour induction (figure 6.4a). Details of the protocols used are in Chapter 2, sections 2.3.1 and 2.4.

Figure 6.4a: experimental outline for in vivo testing of 9D9 IgG1 and IgG2a constructs using transduced TRP1 CTLA-4$^{-/-}$ T-cells as ACT in irradiated, B16/BL6 melanoma-bearing C57BL/6 recipients (4/group). Key: DLI=donor lymphocyte infusion; 250k=250,000 cells; B16/BL6=murine melanoma; 5Gy TBI= 5 Gray of total body irradiation; 9D9 IgG1 DLI=DLI transduced with 9D9 α-murine CTLA-4 IgG1; 9D9 IgG2a DLI=DLI transduced with 9D9 IgG2a; 10D1 IgG2a DLI=DLI transduced with α-human CTLA-4 IgG2a; LN=lymph node; TIL=tumour/tumour-infiltrating lymphocytes; data represents 2 independent experiments.

Day 0   250k B16/BL6 i.d. into C57BL/6 recipients

Day 8   Day 18

5Gy TBI
Group 1
9D9 IgG1 DLI (250k)   End of experiment

Group 2   *5Gy TBI*
9D9 IgG2a DLI (250k)

Group 3   *5Gy TBI*
10D1 (isotype control) IgG2a DLI (250k)
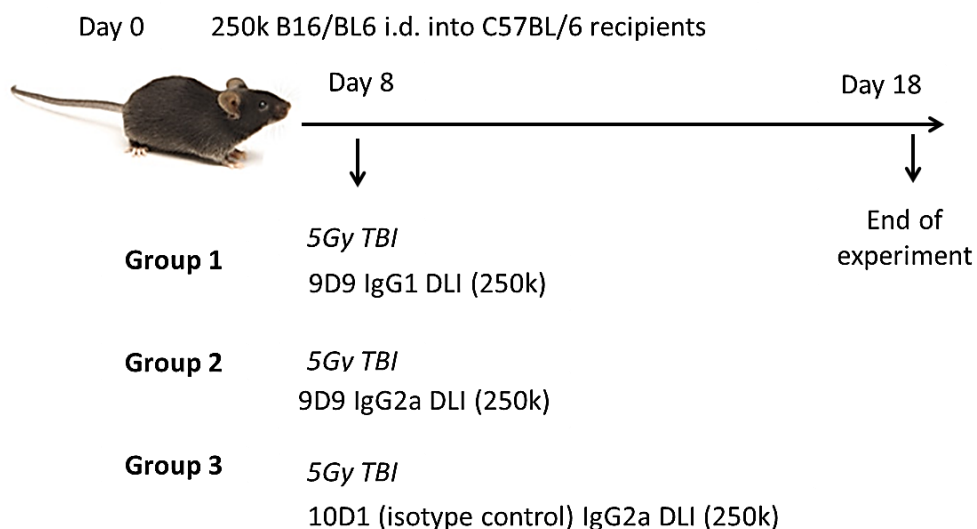
Transduction efficiency (defined by CD4+muCD19+ double positivity) at day 8 was between 40-50% of live TRP1 CD4 T cells. CD19 positive selection yielded 60-70% purity after a single column selection and 250 x 10³ transduced TRP1 T cells per mouse were transferred (data not shown). Incubation of 0.22µm-filtered cellular supernatants from in vitro transduced TRP1 CTLA4$^{-/-}$ cell cultures with CTLA-4^{hi} SupT1 cells followed by secondary anti-murine-Fc staining is shown in figure 6.4b and confirms that transduced cells secrete 9D9 mAb that binds target.

Figure 6.4b: cell culture supernatant from 9D9 transduced TRP1 CTLA-4$^{-/-}$ T cells contains secreted anti-murine CTLA-4 mAb which binds murine CTLA-4^{hi} SupT1 cell targets. Gated on live singlets. **Key:** anti-mu-Fc= anti-murine Fc only/secondary antibody staining only; FSC=forward scatter; 10D1 anti-Hu IgG2a= 10D1 anti-human CTLA-4 IgG2a mAb containing supernatant.
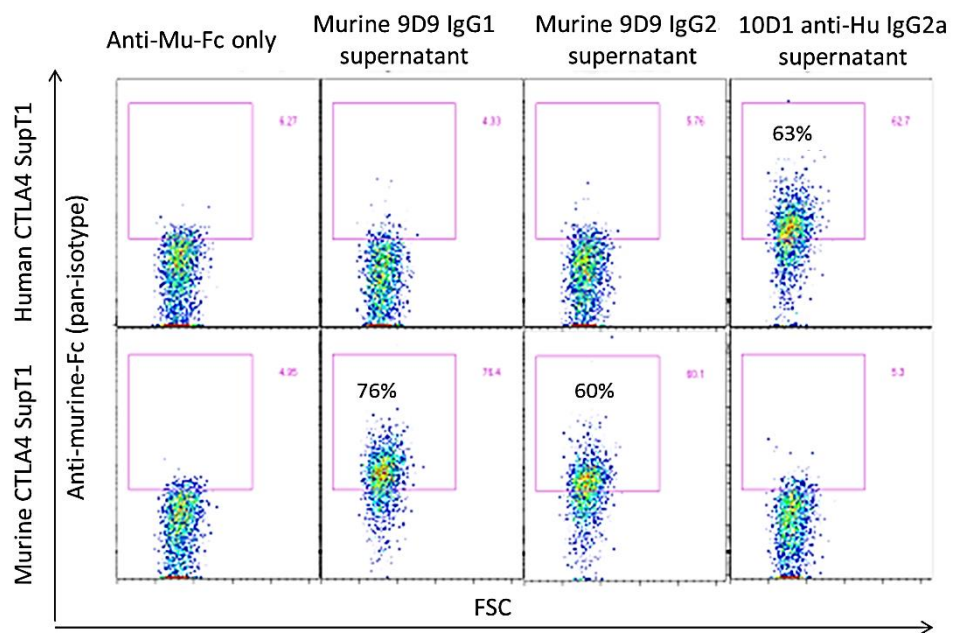
Figure 6.5a: B16/BL6 melanoma weight is not significantly different between experimental groups Key: DLI= donor lymphocyte infusion; 9D9 IgG1 =DLI transduced with 9D9 IgG1; 9D9 IgG2a =DLI transduced with 9D9 IgG2a; 10D1 IgG2a =DLI transduced with anti-human CTLA-4 IgG2a: ns=non-significant; mg=milligrams. Vertical bars represent SEM.
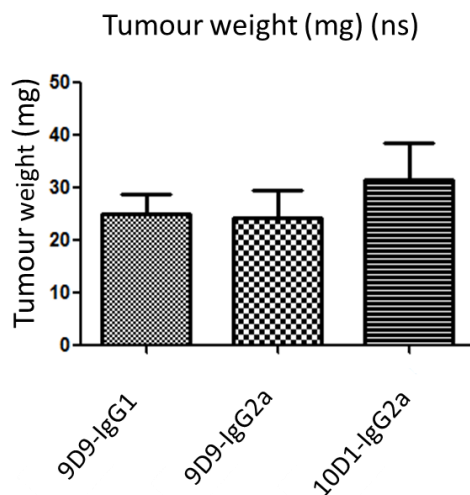
Figure 6.5b: transduced TRP1 CTLA-4$^{-/-}$ CD4 T cells engraft following adoptive transfer into irradiated, B16/BL6 tumour-bearing C57BL/6 hosts and are identified by intracellular staining for α-murine-Fc on T cells. Key: LN=lymph node; TIL=tumour/tumour-infiltrating lymphocytes; FSC=forward scatter.
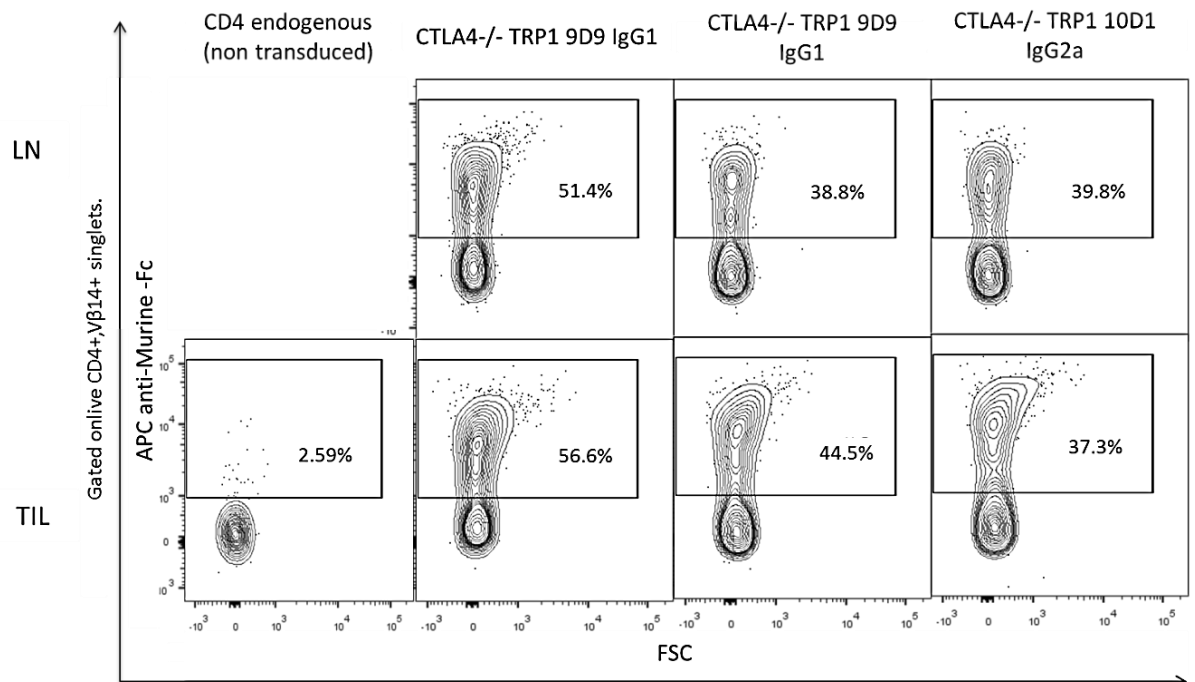
Tumour and LN were harvested 10 days following cell transfer. Tumour weight was not significantly different between groups at day 18 (figure 6.5a). Restimulation and intracellular staining for α-murine-Fc on T cells (see Chapter 2.4.7 for details) confirmed engraftment and persistence of transduced populations (figure 6.5b).

Absolute numbers of endogenous CD4 Teff and Tregs are significantly lower in the 9D9-IgG2a-DLI group compared with the 9D9-IgG1-DLI group in the tumour, but not in the LN (figure 6.5c).

The significant drop in absolute numbers of endogenous CD4 Tregs in the tumour (figure 6.6c) is consistent with the hypothesis of CTLA-4^{hi} cell depletion by α-CTLA-4 IgG2a (figure 6.5d). CTLA-4 expression on intratumoural endogenous CD4 T cells is non-significantly lower in the 9D9-IgG2a-DLI cohort compared to the other cohorts and compared to itself in the LN (figures 6.5d and 6.5e). The significant drop in Teff numbers in the tumour may reflect an effect of depletion of CTLA-4^{hi} populations and is possibly due to a non-specific macrophage mediated toxicity. Of note, non-specific macrophage killing activity is a feature of our in vitro ADCC assay. The other possibility is an off-target mAb-mediated effect. It has been reported that non-specific mAb binding can be observed at very high concentrations.

Figure 6.5c: 9D9-IgG2a-DLI is associated with an significant reduction in absolute numbers of endogenous CD4 Teff and Tregs in the tumour, but not the LN when compared with 9D9 IgG1 DLI (p<0.05). Key: DLI= donor lymphocyte infusion; 9D9= anti-murine CTLA-4; 10D1= anti-human CTLA-4; mg=milligrams; LN=lymph node; TIL= tumour/tumour-infiltrating lymphocytes. Horizontal bars represent mean values and vertical bars represent SEM. Statistical tests: one-way analysis of variance and multiple comparisons test.
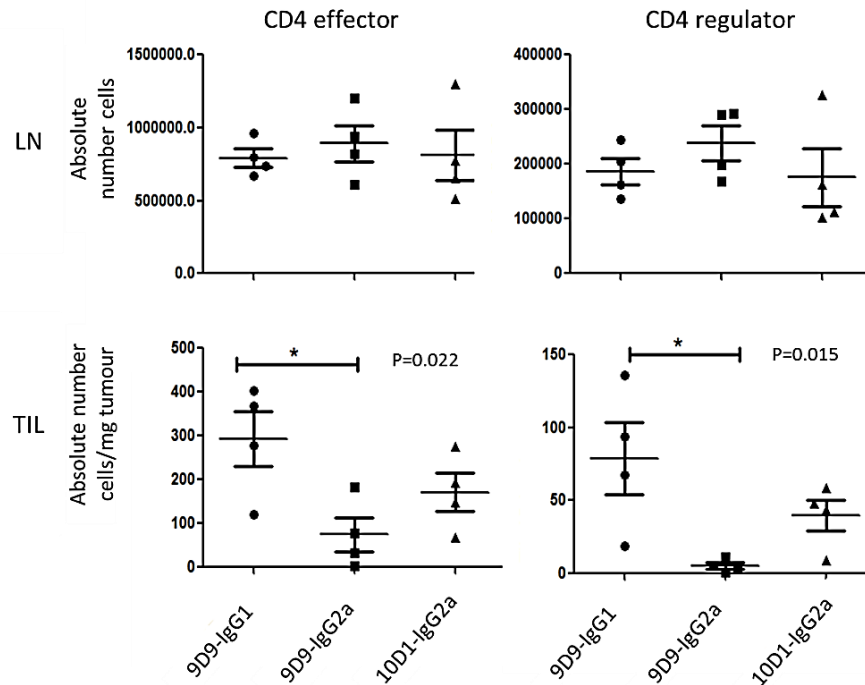
Figure 6.5d: 9D9-IgG2a-DLI is associated with reduced CTLA-4 expression and a proportional drop in endogenous CD4 Teff and Tregs in the tumour, but not the LN. TRP1 CTLA-4$^{-/-}$ T cells do not stain for CTLA-4. **Key:** LN=lymph node; TIL= tumour/tumour-infiltrating lymphocytes; 9D9 IgG1= anti-murine CTLA-4 IgG1; 9D9 IgG2a =anti-murine CTLA-4 IgG2a; 10D1 IgG2a = anti-human CTLA-4 IgG2a.
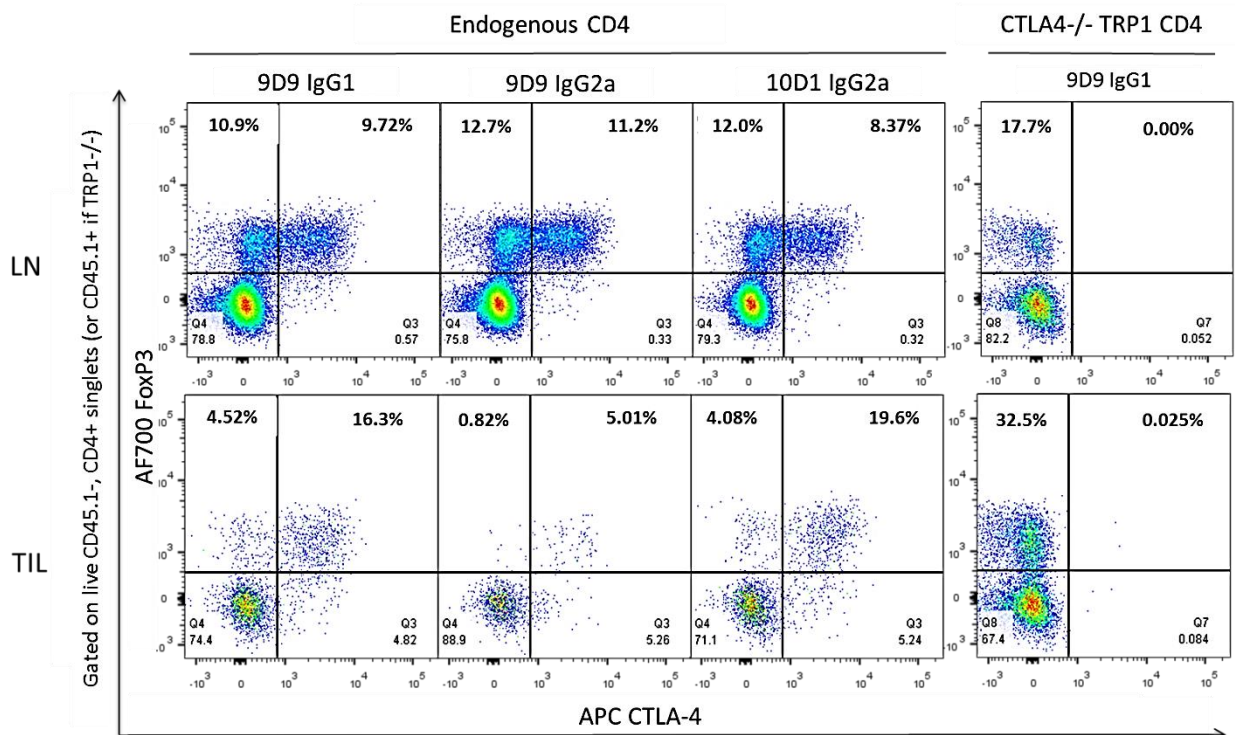
Figure 6.5e: 9D9 IgG2a DLI is associated with a trend towards lower CTLA-4 expression on endogenous CD4 T cells within the tumour but not the LN. Key: as per figure 6.6d; ns=non-significant. Vertical bars represent SEM. Statistical tests: one-way analysis of variance and multiple comparisons test.

TIL- total endogenous CD4 T cells (ns)

LN- total endogenous CD4 T cells (ns)
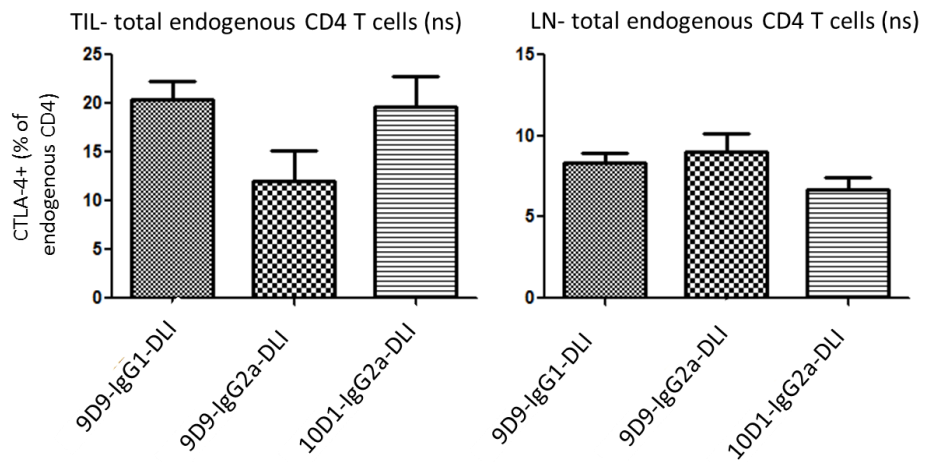
Figure 6.6: TRP1 CTLA-4$^{-/-}$ Tregs are significantly lower in absolute number in the tumour (but not the LN) in the 9D9 IgG2a DLI condition compared with the 9D9 IgG1 DLI condition and may be multifactorial: off-target toxicity from 9D9-IgG2a and/or improved cell survival with 9D9-IgG1 construct (p=0.014). Key: DLI= donor lymphocyte infusion; mg=milligrams; LN=lymph node; TIL= tumour/tumour-infiltrating lymphocytes. Horizontal bars represent mean values and vertical bars represent SEM. Statistical tests: one-way analysis of variance and multiple comparisons test.

TRP1 effector   TRP1regulator
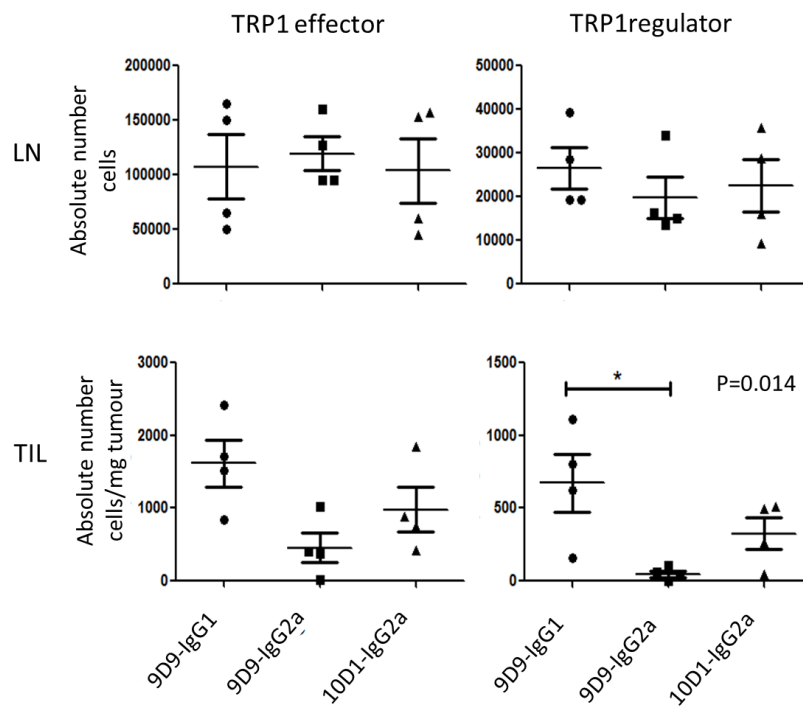
Quantitation of absolute numbers of transferred TRP1 CTLA-4$^{-/-}$ T cells shows that TRP1 Tregs are significantly lower in the 9D9-IgG2a-DLI group than in the 9D9-IgG1-DLI group within the tumour (but not the LN) (figure 6.6). There is a non-significant reduction in TRP1 Teff in the

9D9-IgG2a cohort within the tumour. To try to explain this we made an assessment of proliferative status of endogenous and TRP1 CTLA-4$^{-/-}$ populations in LN and tumour using Ki67 staining, but showed no significant differences between cohorts. The mechanism riving the difference in absolute numbers between 9D9 isotypes may be multifactorial: off-target toxicity from 9D9-IgG2a combined with improved cell survival with the 9D9-IgG1 construct. We have previously observed in Chapter 4 that TRP1 CTLA-4$^{-/-}$ Tregs are often low in tumour and lymph node in the context of lymphodepleted hosts, and it may be that they are more vulnerable to cytokine-deprivation-induced apoptosis than CTLA-replete WT TRP1 Tregs. Equally, the inflammatory environment generated by a functional ADCC-capable IgG2a could result in bystander toxicity in this model.

Summary

TRP1 CTLA-4$^{-/-}$ T cells can be genetically manipulated by retroviral transduction to secrete full length antibody that can bind target, deplete target cells in the context of an in vitro ADCC assay and secrete functional antibody in vivo to biological effect (a reduction in in total endogenous Treg numbers in the tumour).

The impact of Fc isotype is suggested by this experiment, namely that secretion of 9D9-IgG2a-DLI is associated with a drop in CTLA-4^{hi} cell populations in keeping with an ADCC role, and for 9D9-IgG1-DLI this is not the case. Rather, IgG1 may be associated with an increase in cell numbers. There was no significant impact upon tumour growth/eradication by day 18 of the experiment. It is clear that Tregs are vulnerable to IgG2a-mediated-depletion in the tumour (and less so the LN) for reasons that may include higher expression of target antigen (as demonstrated by MFI on flow cytometry) (figure 6.7a) and densely concentrated tumour associated macrophages (TAM) to act as ADCC effectors (133). CTLA-4 expression observed in these experiments is based on intracellular staining and most certainly over-represents true cell surface CTLA-4 expression.

There is a significant reduction in TRP1 Tregs intratumourally in the 9D9-IgG2a-DLI condition compared with the 9D9-IgG1-DLI condition despite the absence of target CTLA-4 on these cells. It is possible that part of the disparity in absolute numbers between groups is due to 9D9 IgG1 conferring a survival advantage. IgG1 isotype can bind endogenous Teffs and Tregs within the tumour allowing expansion and cytokine generation. Cytokine withdrawal from T cells can lead to Bim-mediated apoptosis (28). However, of more concern is the possibility of toxicity directly mediated by high concentrations of 9D9-IgG2a.

In summary, we have established that ACT using transduced TRP1 CTLA-4$^{-/-}$ T cells resulted in engraftment and secretion of mAb to target the endogenous T cell compartment. To bring the project a step closer to a translation, it is imperative to test the constructs in CTLA-4-replete TRP1 donors such that the secreted antibody can impact directly upon the tumour-specific effector T cells. The anticipated biological effects of 9D9-IgG2a secreted from CTLA-4-replete TRP1 T cells would be intratumoural Treg depletion with a resulting skew in the Teff/Treg ratio towards effector dominance and a consequent enhanced anti-tumour effect.

6.2.6   Transduction of WT TRP1 CD4 T-cells

There are hypothetical concerns that secretion of 9D9 αCTLA-4 IgG2a mAb from CTLA-4-replete T cells could compromise their persistence and longevity in vivo due to autocrine deletion. Ultimately this would compromise a major project goal of transducing TILs (CTLA-4^{hi}) with α-CTLA-4 mAb for adoptive transfer. In an attempt to answer this, we transduced WT (CTLA-4-replete) TRP1 CD4 T cells with the 9D9 α-murine-CTLA-4 constructs and transferred them into the murine B16/BL6 melanoma model discussed in Chapter 6.2.5.

Early attempts to obtain sufficient WT TRP1 cell numbers for adoptive therapy using protocols outlined in Chapter 2.4.5.2 were unsuccessful. After a period of optimisation we elected to augment harvested CD4 T cell numbers through vaccination of WT TRP1 donors with 2 doses of (irradiated) Gvax 1x10^6 cells/dose on days 1 and 3 followed by harvesting and stimulation on day 6 for transduction on day 7. Three mice received Gvax as described and three remained unvaccinated.

Figure 6.7a: vaccination of WT TRP1 donor mice with GM-CSF secreting cellular vaccine (Gvax) prior to organ harvest is associated with CD4 enrichment and improved overall cell viability compared with unvaccinated animals before and 24 hours after stimulation in vitro with TRP1 peptide. Gated on live singlets. **Key:** FSC=forward scatter.
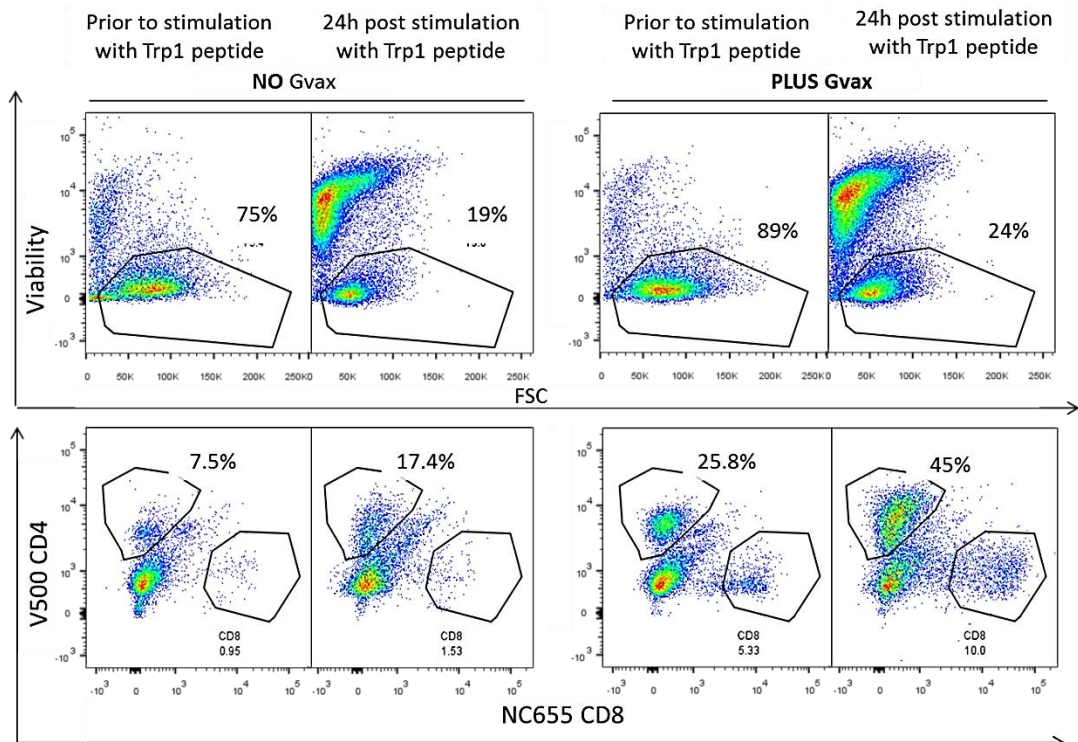
At day 6, vaccinated mice were well with no signs of distress compared to the control group. In the vaccinated cohort, LN/spleen were observed to be larger than for unvaccinated mice and gave a 5-fold higher total cell yield of 75 x 10^6 live cells (viability 84%) compared with 14x10^6 live cells (viability 84%) from unvaccinated controls (see figure 6.7a). Cell viability dropped after 24 hours of in vitro stimulation in both cohorts (see Chapter 2.4.5.2 for methods), but TRP1 CD4 T cells were enriched, to a greater extent in the vaccinated cohort (45% of total live cells compared with 17.4% in the unvaccinated group). Of note, the vaccinated cohort had a small population of CD8+Vβ14+ T cells pre- and post-stimulation.

An assessment of the myeloid populations present between cohorts by flow cytometry at 24 hours post-stimulation with TRP1 peptide revealed a population of CD11b^{hi}/CD11c^{int} cells positive for F4_80 and MHC Class II in the vaccinated donor cohort (data not shown). This phenotype is associated with in vitro depletion of antibody-labelled targets in the context of ADCC (see Chapter 2.4.8 for details on ADCC assays used in this project) and poses a theoretical risk to transduced α-CTLA-4 IgG2a secreting CTLA-4 replete cells in vitro.

One of the main concerns of using vaccinated donor mice for ACT is the potentially detrimental impact of antigen experience on persistence following in vivo transfer. Evidence suggests that naïve/stem-cell memory T cells (T$_{SC}$) (CD62L^{hi}, CD44^{low}) and central memory T cells (T$_{CM}$) (CD62L^{hi}, CD44^{hi}) are preferable to effector-memory T cells (T$_{EM}$) (CD62L^{low}, CD44^{hi}) for adoptive transfer (134). Figure 6.7b compares the maturation profiles for vaccinated and unvaccinated donor mice at the point of cell isolation and after 24 hours of in vitro stimulation with cognate antigen. Vaccination drives T cells towards the T$_{EM}$ phenotype compared with unvaccinated specimens prior to stimulation in vitro with TRP1 peptide (50.5% compared with 21.5% of total T cells). In vitro stimulation further enriches the T$_{EM}$ populations in both groups, more marked in the vaccinated group (74.5% compared with 54.5%). It is possible that this profile could compromise their half-life in vivo and their utility as ACT. Interestingly, TRP1 Teff from vaccinated donors expressed granzyme B after 24 hours in vitro, confirming an effector phenotype. This was not observed in the unvaccinated cohort (data not shown).

We know that Gvax treatment of WT TRP1 donor mice results in a higher number of viable CD4 T cells than unvaccinated controls (figure 6.7a), and testing of retroviral transduction demonstrated a transduction efficiency of 50-60% in this population, broadly comparable to that of TRP1 CTLA-4$^{-/-}$ donors (data not shown). Using this method, we elected to proceed with in vivo experiments to assess the persistence and viability of cells isolated from Gvax-treated donors in melanoma-bearing hosts.

Figure 6.7b: vaccination of WT TRP1 donors with Gvax is strongly associated with differentiation into T$_{EM}$ cells compared with unvaccinated donors. In vitro stimulation with cognate antigen for 24 hours enriches the T$_{EM}$ population in both groups. Key: Tem= effector-memory T cells; Tcm= central memory T cells; Tsc= stem-cell-memory T cells; Gvax= GMCSF secreting cellular vaccine.
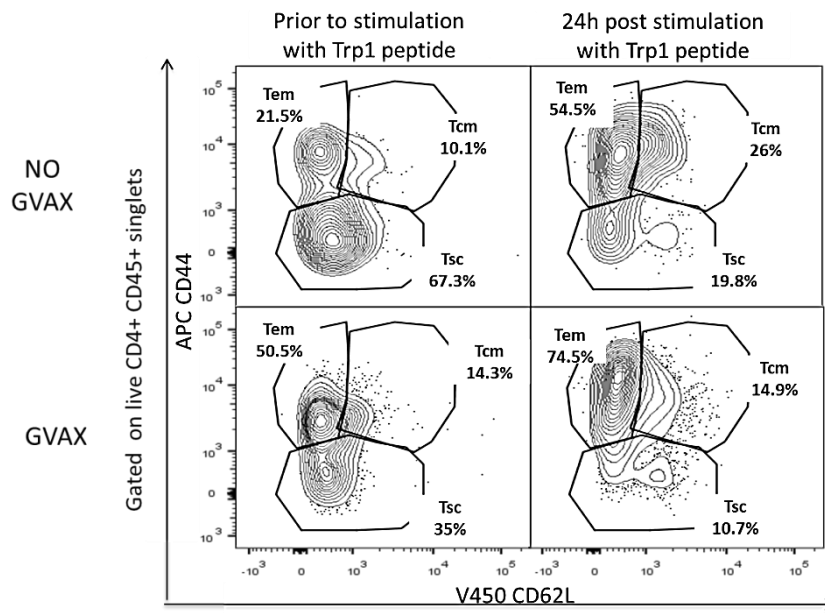
6.2.7 Testing constructs in vivo: 9D9 in the C57BL/6 mouse (WT TRP1 transfer)

Figure 6.8a: experimental outline for in vivo testing of 9D9 IgG1 and IgG2a constructs using transduced Gvax-treated WT TRP1 donor T-cells as ACT in lymphodepleted B16/BL6 melanoma-bearing C57BL/6 recipients. Key: 250k=250,000 cells; B16/BL6=murine melanoma; 5Gy RT= 5 Gray of irradiation; DLI=donor lymphocyte infusion; 9D9 IgG1 DLI= DLI transduced with 9D9 IgG1; 9D9 IgG2a DLI=DLI transduced with 9D9 IgG2a; LN=lymph node; TIL=tumour/tumour-infiltrating lymphocytes; data represents a single experiment.
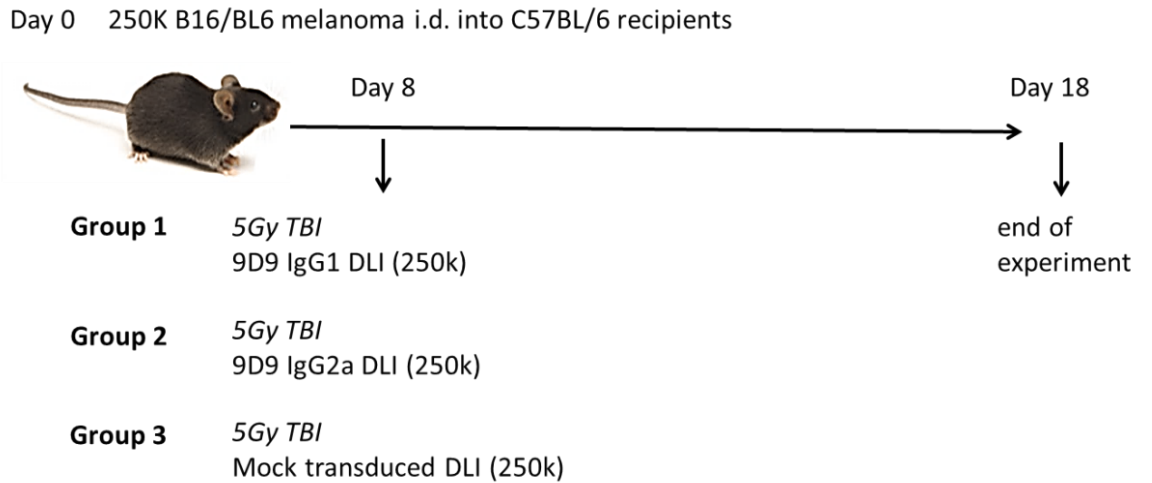
Figure 6.8b: CD19 selection of transduced Trp1 CD4 lymphocytes enriches transduced cells for adoptive transfer into sublethally irradiated B16/BL6 tumour-bearing C57BL/6 recipients. Gated on live CD4+ singlets. **Key:** DLI=donor lymphocyte infusion; 9D9 IgG1 DLI= DLI transduced with 9D9 IgG1; 9D9 IgG2a DLI=DLI transduced with 9D9 IgG2a.
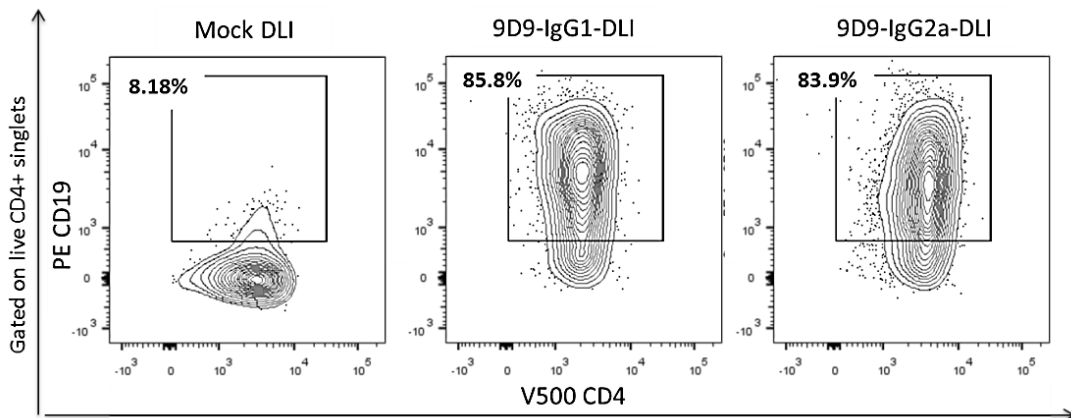
We used 5 irradiated B16/BL6 tumour-bearing C57BL/6 recipients per group (see figure 6.8a). Transduction of Gvax treated WT TRP1 donor T cells was performed according to the protocol outlined in Chapter 2.4.5.2 with no baseline CD4 selection step. Transduced populations were CD19 column-purified (figure 6.8b) prior to adoptive transfer. Given the in vitro finding of

128

CD8+Vβ14+ cells contaminating Gvax treated donor isolates (figure 6.7a), we screened transduced samples pre- and post-CD19 selection and found that CD4+ Vβ14+ purity in our culture system was in the order of 96-98% of total live singlets (figure 6.8c). Transfectant supernatant bound CTLA-4^{hi} SupT1 cell targets (data not shown).

Figure 6.8c: there is negligible contamination with CD8 T cells in WT TRP1 T cell populations selected for the transduction marker dMuCD19 despite prior Gvax administration. Key: DLI=donor lymphocyte infusion; 9D9 IgG1 DLI= DLI transduced with 9D9 IgG1; 9D9 IgG2a DLI=DLI transduced with 9D9 IgG2a.
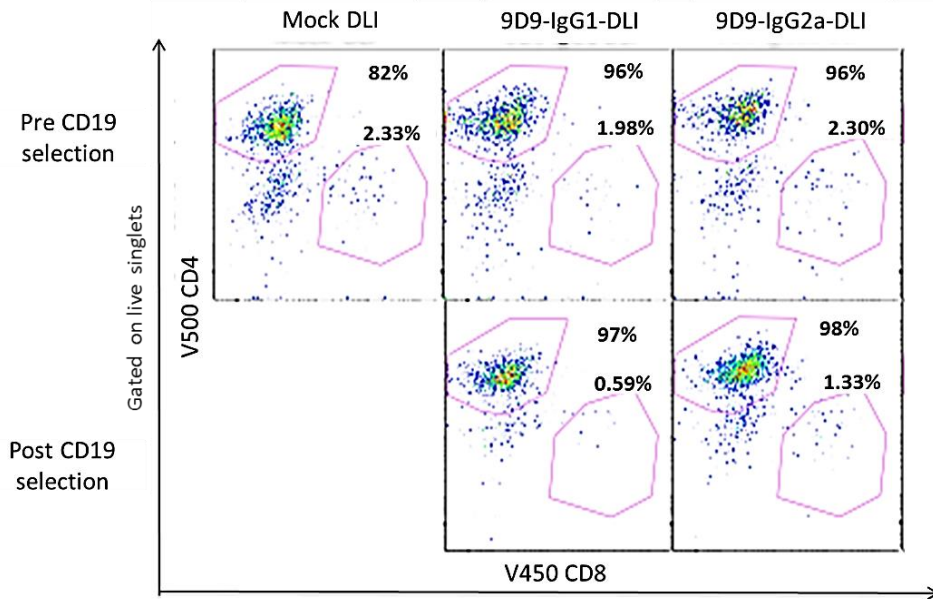
Figure 6.9a: tumour weight is significantly higher in the 9D9 IgG2a DLI group compared with the 9D9 IgG1 DLI and Mock DLI groups. Key: DLI=donor lymphocyte infusion; 9D9 IgG1 DLI= DLI transduced with 9D9 IgG1; 9D9 IgG2a DLI=DLI transduced with 9D9 IgG2a; mg=milligrams. Horizontal bars represent mean values and vertical bars represent SEM. Statistical tests: one-way analysis of variance and multiple comparisons test.
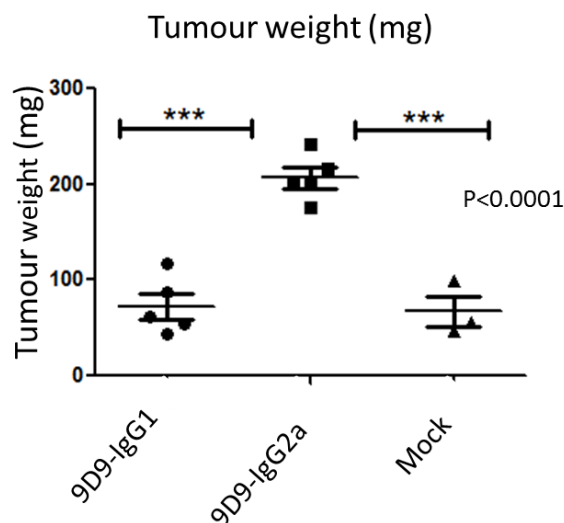
Figure 6.9b: 9D9-IgG2a-DLI is associated with a significant reduction in absolute numbers of TRP1 Teff and Treg within the tumour compared with 9D9-IgG1-DLI. There is a significant increase in TRP1 Tregs in the 9D9-IgG1 cohort in the LN compared with the other cohorts, and this may represent a survival advantage. Key: DLI=donor lymphocyte infusion; 9D9 IgG1 DLI= DLI transduced with 9D9 IgG1; 9D9 IgG2a DLI=DLI transduced with 9D9 IgG2a; mg=milligrams. Horizontal bars represent mean values and vertical bars represent SEM. Statistical tests: one-way analysis of variance and multiple comparisons test.
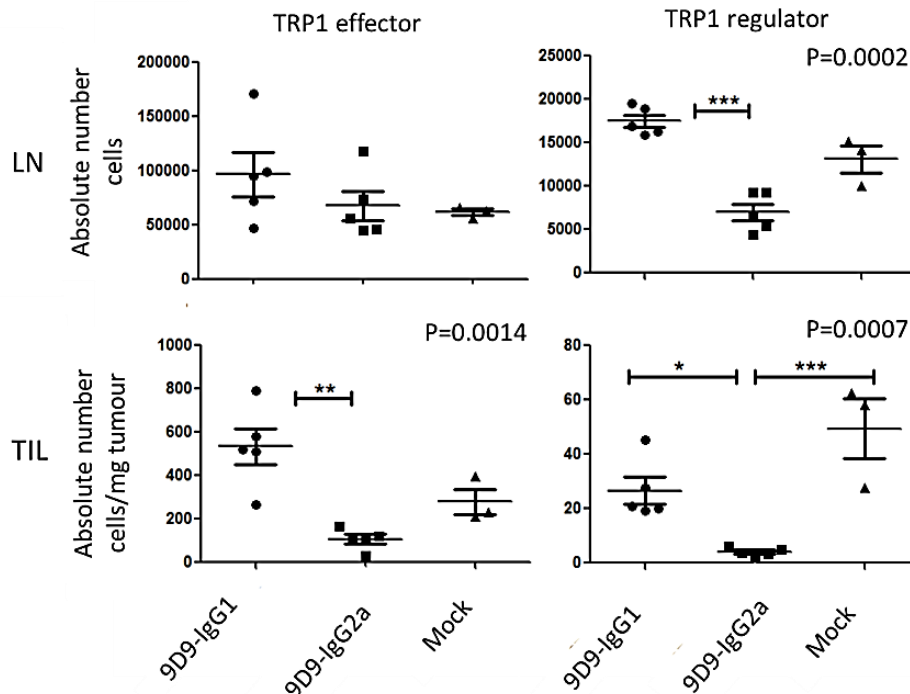
Tumour weight is significantly higher at day 18 in the 9D9-IgG2a-DLI cohort compared with the controls (figure 6.9a). It is likely that this relates to a significant reduction in intratumoural TRP1eff in this group (figure 6.10b) not seen in the LN. TRP1 Tregs are significantly lower in tumour and LN in the 9D9-IgG2a cohort compared with 9D9-IgG1. We had not observed this effect in the LN in other experiments using TRP1 CTLA-4$^{-/-}$ cells as vehicles for transfer of 9D9-IgG2a and this would support the hypothesis that high expression of CTLA-4 on Tregs renders them susceptible to lysis by IgG2a isotype mAb and that this effect is not exclusively limited to the tumour microenvironment. It is also likely that 9D9-IgG1 confers a survival advantage on the WT TRP1 Tregs as levels are significantly higher than in the other conditions.

Quantitation of CTLA-4 expression on TRP1 Teff and Treg as a percentage of parent cells is significantly higher in the LN and tumour of Mock DLI recipients compared with both 9D9 isotypes (diagnostic labelled mAb derives from a different clone to 9D9). TRP1 Tregs (but not TRP1 Teff) in the 9D9 IgG2a subgroup have significantly lower CTLA-4 expression in LN and tumour than the 9D9 IgG1 subgroup. We suggest that this reflects depletion of CTLA-4^{hi} targets by this isotype. The effect may not be as clear in the Teff populations as the level of

expression of CTLA-4 is much lower than in the tumour. For instance, under 10% of all TRP1 Teff in the LN express CTLA-4 compared with 30-55% in the tumour and compared with between 40-85% of TRP1 Tregs in LN and tumour. This helps to explain why the effect of depletion is limited in TRP1 Teff in the LN: surface expression (by MFI) of target is too low.

Figure 6.9c: CTLA-4 expression by MFI on the transferred cells is significantly higher in LN and tumour in the mock DLI group compared with both 9D9 DLI groups. Subgroup analysis shows a significant reduction in CTLA-4 expression on TRP1 Tregs in LN (p=0.0089) and tumour (p=0.0317) in the 9D9-IgG2a cohort compared with the 9D9 IgG1 cohort. **Key:** LN=lymph node; DLI=donor lymphocyte infusion. Vertical bars represent SEM. Statistical tests: one-way analysis of variance and multiple comparisons test.
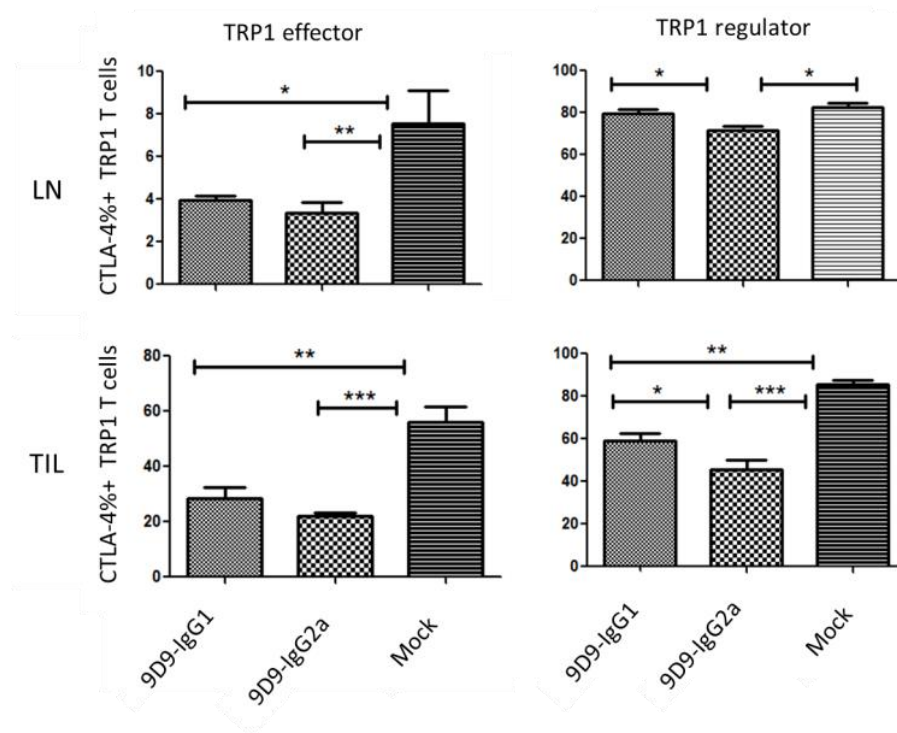
Despite a significantly higher tumour weight and a clear drop in CTLA-4 expression in the 9D9-IgG2a cohort, CD19 transduced cells were still evident at day 18 and were not proportionally significantly different between cohorts in the tumour (figure 6.9d). CD19 expression on Teff and Treg in the LN was proportionally higher in the 9D9-IgG1 group, and is suggestive of a conferred survival advantage in the LN. This is also supported by increased cell numbers in the 9D9-IgG1 cohort albeit this is not explained by differential Ki67 or CD25 staining (figure 6.9f).

9D9 IgG2a is associated with a reduction in CD19+CTLA-4+ TRP1 Tregs within the tumour and LN, but not TRP1 Teff (although there is a downward trend). This may represent autocrine deletion by 9D9-IgG2a (figure 6.9e).

Figure 6.9d: CD19+ expression on TRP1 T cells does not significantly differ between 9D9 IgG1 and 9D9 IgG2a treatment cohorts intratumourally but there is a significant reduction in the proportion of transduced cells in the LN. This pattern is confirmed by staining for intracellular Fc on T cells. This suggests that there may be a survival advantage of 9D9 IgG1 in the LN, supported by increased cell numbers (figure 6.10b). **Key:** LN= lymph node; TIL= tumour infiltrating lymphocytes. Vertical bars represent SEM. Statistical tests: one-way analysis of variance and multiple comparisons test.

CD19 expression on TRP1 T cells
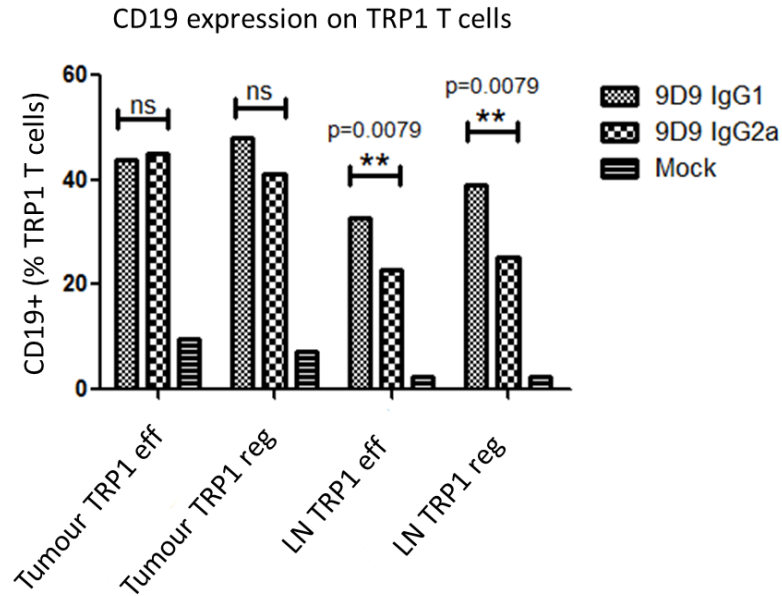
Figure 6.9e: 9D9 IgG2a is associated with a reduction in CD19+CTLA-4+ TRP1 Tregs within the tumour and LN, but not TRP1 Teff (although there is a downward trend). This may represent autocrine deletion by 9D9-IgG2a. Key: ns=non-significant; TIL=tumour/tumour-infiltrating lymphocytes; LN=lymph node. Horizontal bars represent mean values and vertical bars represent SEM. Statistical tests: one-way analysis of variance and multiple comparisons test.
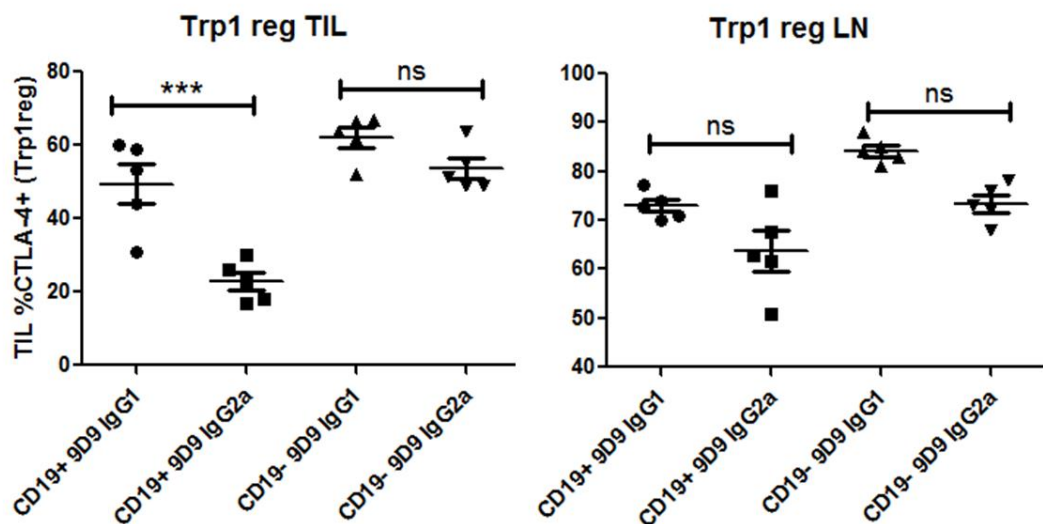
Figure 6.9f: there are no significant differences in Ki67 or CD25 expression on TRP1 T cells between groups. Vertical bars represent SEM. Statistical tests: one-way analysis of variance and multiple comparisons test.
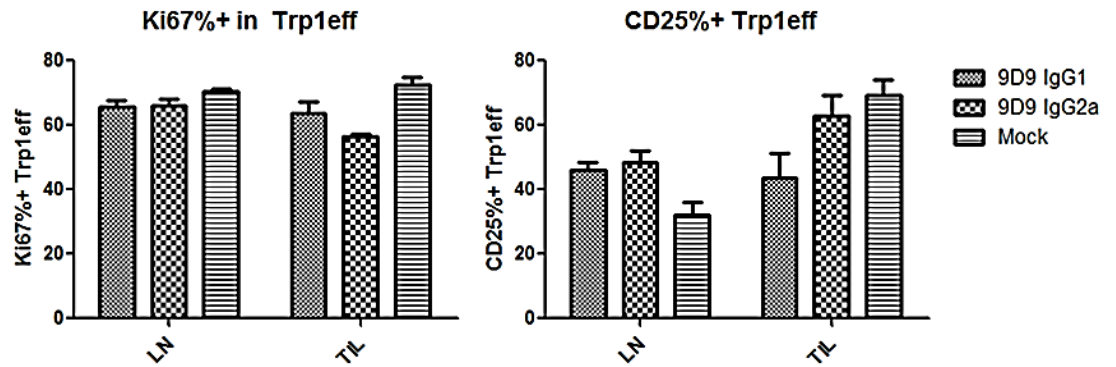
Figure 6.9g: there are no significant differences in absolute numbers of endogenous T cells between 9D9-IgG1 and -IgG2a isotypes within tumour or LN. Key: ns=non-significant; TIL=tumour/tumour-infiltrating lymphocytes; LN=lymph node. Horizontal bars represent mean values and vertical bars represent SEM. Statistical tests: one-way analysis of variance and multiple comparisons test.
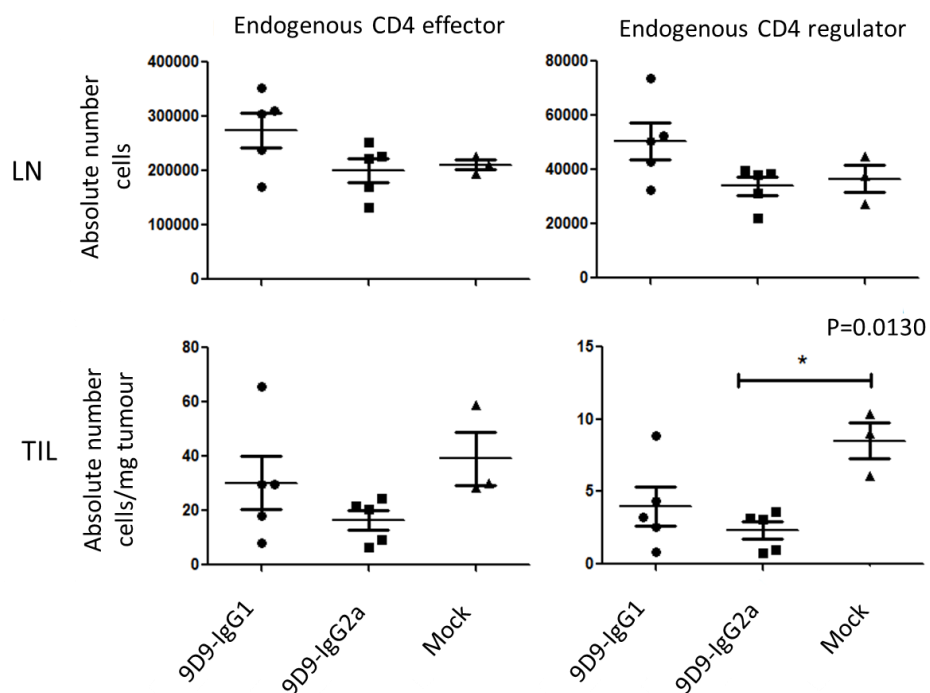

There are no significant differences in absolute numbers of endogenous T cells between 9D9-IgG1 and -IgG2a isotypes within tumour or LN (see figure 6.9g). The endogenous effector compartment was relatively unaffected within the tumour, supporting the accepted function of TRP1 T-cells in this model as primary mediators of B16/BL6 melanoma immune rejection, with endogenous cells fulfilling a support role(46).

Figure 6.9h: transferred TRP1 Teff are capable of effector functions, namely IFNγ and Granzyme B production. Key: ns=non-significant; TIL=tumour/tumour-infiltrating lymphocytes; CD45.1= congenic marker on TRP1 T cells; IFNγ= interferon gamma.
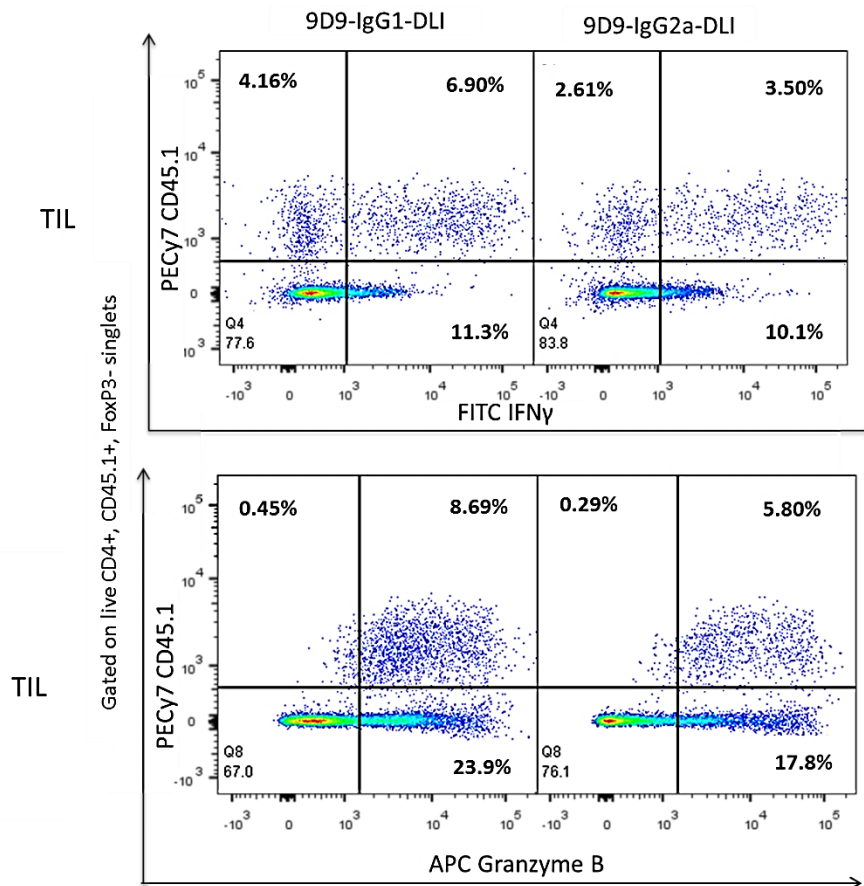
Critically, the transduced WT TRP1 T cells are capable of mAb secretion, but are also capable of effector function including granzyme B secretion and IFNγ secretion (figure 6.9h).

6.3 Conclusions

This final set of experiments has gone some way towards answering our original feasibility question, namely can transgenic T-cells be genetically modified to secrete an antibody that has the potential to augment anti-tumour immunity without inducing systemic autoimmune toxicity, and without posing a risk to their own survival?

In generating tricistronic vectors coding for 9D9 α-murine-CTLA-4 in IgG2a and IgG1 isotype, we have been able to move swiftly through a series of housekeeping experiments: proving that the antibody binds target specifically, that it can deplete target in an ADCC (in IgG2a but not IgG1 format) and that it can be used to successfully transduce tumour-reactive T-cells which can then act as intra-tumoural vehicles for therapeutic antibody secretion.

We know from experiments in Chapter 4 that systemically administered 9H10 anti-murine CTLA-4 selectively depletes CTLA-4^{hi} cells within the tumour and we know that Tregs are especially vulnerable due to their constitutively high expression levels of this receptor. What we have observed within the tumour in the first set of experiments using TRP1 CTLA-4$^{-/-}$ T cells as DLI is slightly different, in that the breadth of αCTLA-4-mediated depletion is widened, extending to endogenous CD4 Teff and even to CTLA-4$^{-/-}$ cells, raising the possibility that the inflammatory IgG2a-rich milieu can result in some off-target/bystander cell toxicity. Certainly, the mean intratumoural CTLA-4 expression on CD4 Teff is lower in the 9D9-IgG2a cohort than that seen in the control conditions, implying a degree of CTLA-4-directed depletion at the heart of the IgG2a effect. Rather than seeing a reduction in tumour burden in the 9D9-IgG2a-DLI group (as we had predicted at the outset), there is equivalence to control when TRP1 CTLA-4$^{-/-}$ cells are used, and this is likely attributable to a global reduction in Teff cells intratumourally, despite the effector:regulator ratios moving in the right direction.

Informed by these findings, we moved through a series of optimisation experiments to achieve transduction and ultimately transfer of CTLA-4-replete tumour-reactive T cells into B16/BL6-bearing irradiated C57/BL6 mice. Ultimately, the 9D9-IgG2a-DLI cohort had worse outcomes than 9D9-IgG1-DLI, with significantly higher tumour burden and evident depletion of TRP1 Teff and Tregs intra-tumourally. A significant reduction in CTLA-4 expression was observed on 9D9-IgG2a transduced TRP1 Tregs in the tumour and the LN compared with 9D9-IgG1, consistent with depletion of CTLA-4^{hi} cells. The unusual finding of lower absolute TRP1 Treg numbers in the LN in the 9D9 IgG2a cohort may be due to depletion in the LN (if sufficient ADCC-capable effectors are present). It is conceivable that the cells might be pre-labelled with lytic antibody in vitro (at the point where they are proportionally equivalent to the Treg numbers in the

other groups) and are then transferred in vivo where IgG2a-labelled TRP1 Tregs are destroyed intravascularly or in the reticuloendothelial system.

6.4   Future directions

There are challenges inherent in the transduction of WT CTLA-4 T cells and we are making efforts to resolve this in ongoing experiments within the lab. It may be that the use of Gvax to augment donor lymphocyte yields will in the long term be detrimental to engraftment and persistence, related to their CD44^{hi}/CD62^{lo} T$_{EM}$ status (134) and alternative strategies are being explored. Of note, stimulation with TRP1 peptide seems also to drive TRP1 cells towards CD44^{hi}/CD62L^{lo} status, so it may be worth looking at anti-CD3/28 as a more physiological method of stimulation for retroviral tranduction.

TRP1 CTLA-4$^{-/-}$ cells as donor lymphocytes offer a relative ease of transduction, with engraftment and persistence capability. We have shown that these cells can secrete αCTLA-4 mAb to biological effect with an observed CTLA-4-dependent depletion of endogenous Tregs.

In order to facilitate and support cell engraftment in this model we lymphodeplete recipient mice. Unlike the controlled administration of a pharmacokinetically and –dynamically predictable exogenous mAb, the transfer of a cell population that secretes mAb is more difficult to standardise. Variables such as expansion potential, survival and tissue infiltration are susceptible to biological variation and our concern in this set of experiments is that the extensive migration of transferred cells into the tumour results in activation, upregulated transcription of the transgene, and a payload secretion of therapeutic mAb. We accept that high mAb concentrations can result in off target and non-specific effects which may be the explanation for the marked drop in CTLA-4$^{-/-}$ TRP1 Tregs in the former experiments.   To mitigate for these effects, we would next like to repeat the experiment using transduced CTLA-4$^{-/-}$ TRP1 cells in an immunocompetent model, or to do a cell dose titration experiment to identify the point of optimal antibody secretion and lesser (possible) toxicity. It will be important to serially quantify mAb levels in the serum throughout the experiment and to make an attempt to discern whether blood levels reflect mAb concentration within the tumour. What is encouraging is that the transduction of tumour reactive T cells with immunomodulatory antibodies appears to concentrate the antibody effect within the tumour.

This could be an attractive approach for patients who have not responded to other systemically administered immunomodulatory treatments.

Prior to further in vivo work, and especially given the apparent detrimental impact of 9D9 IgG2a upon the transduced cells, we would like to take this opportunity to characterise these transduced cells further in vitro through a series of cytotoxicity, proliferation and cytokine secretion assays. We will additionally perform assessments of exhaustion markers and transduced T cell maturation status.

Over an extended in vitro culture we will aim to chart the viability of the transduced cells and the secretion of 9D9 IgG2a by sequential ELISAs to discern whether the same in vivo intratumoural disadvantages of 9D9 IgG2a secretion are borne out in vitro. It would be interesting to conduct an ADCC assay as previously described, but instead of SupT1 cells, using activated TRP1 T cells as targets to confirm that 9D9 IgG2a can deplete these in vitro. This would reinforce the hypothesis of 9D9 IgG2a-mediated autocrine depletion of transduced T cells.

In summary, 9D9 is an anti-murine CTLA-4 antibody, the sequence of which we have used to generate a retroviral vector for transduction of primary murine lymphocytes. We have shown that secreted 9D9 IgG2a can deplete antigen-expressing target cells in an ADCC assay. CTLA-4$^{-/-}$ TRP1 CD4 T cells can be genetically modified to secrete full length anti-CTLA-4 antibody, and can engraft and persist in lymphodepleted tumour-bearing hosts. In vivo, we have shown that the secreted antibody is capable of depletion of CTLA-4^{hi} target cells, rendering CD4 Tregs more susceptible to lysis than Teff cells. There are several questions arising from the data which inform the next phase of experiments to complete the project.

CHAPTER 7

7. FINAL DISCUSSION AND FUTURE DIRECTIONS

7.1 Summary and conclusions

This thesis explores the differences between cell intrinsic and cell extrinsic modes of CTLA-4 inhibition on tumour reactive T cells in an attempt to define whether targeted delivery of an effector product that is CTLA-4^{lo} or on which CTLA-4 is blocked by mAb is associated with improved tumour infiltration, expansion and ultimately augmented tumour rejection. The work is based on a solid foundation of pre-clinical and clinical data to support the efficacy of antibody-mediated CTLA-4 blockade in promoting tumour rejection and a first-in-class α-human CTLA-4 monoclonal antibody (Ipilimumab) that has been approved by the FDA and EMA for use in human melanoma (46, 49, 135). Limitations of Ipilimumab include low responder frequency and autoimmune toxicity which can lead to cessation of treatment and the need for high dose steroids. A method to improve response rates to αCTLA-4 mAb and to circumvent the development of adverse immune events from treatment would be of great clinical importance.

Cell intrinsic CTLA-4 deficiency has been investigated using transgenic murine models. The consequences of organism-wide failure to express CTLA-4 are polyclonal T cell expansion, overwhelming autoimmunity and premature death (41, 42). Milder phenotypes have been described in mice lacking CTLA-4 exclusively on CD4 Tregs (26, 43). CTLA-4 ablation on a specific population of tumour reactive effector T cells may help to prevent the toxicity seen with inhibition of the polyclonal T cell compartment. To my knowledge, there is no published work in tumour immunotherapy using cell intrinsic CTLA-4 knockdown.

Cell extrinsic CTLA-4 blockade can also potentially be targeted more specifically to the tumour. Previous work to generate a murine tumour cell vaccine modified to secrete α-murine-CTLA-4 mAb demonstrated tumour rejection that was equivalent to the administration of high-dose systemic α-murine-CTLA-4 mAb with lower recorded serum levels of α- CTLA-4 mAb and lower expression of serum markers of autoimmunity.

Our project goal is to define a genetic engineering strategy to target CTLA-4 blockade specifically to the tumour by modification of tumour specific T cells, with the translational objective to inform the development of TCR and CAR-T cell technologies in our institution. One

of the biggest barriers to success of these therapies is low engraftment and limited persistence of tumour specific gene-modified cells. We suggest that genetic modification to ablate/block co-inhibitory receptors on TCR or CAR-T cells could enhance their expansion and functionality in vivo.

This chapter summarises the main conclusions reached by the project, their practical implications for and directions for future research in this area.

7.2   Genetic ablation of CTLA-4 on tumour reactive T cells

In theory, cell-intrinsic CTLA-4 ablation from tumour-specific T cells offers the potential for a truly tumour targeted cell product with a reduced risk of systemic autoimmune toxicity (provided the tumour-associated antigenic target is uniquely expressed on tumour cells) and persistence of a highly activated effector population, resistant to this potent co-inhibitory pathway.

One potential problem relates to the evolving paradigms of effector extrinsic CTLA-4 co-inhibitory activity as the predominant mode of action of CTLA-4, mediated mainly (but not exclusively) by Tregs. During this process functional CTLA-4 dynamically and competitively sequesters B7 molecules on APCs, and prevents CD28 co-stimulatory signalling on Teff. As such, there is a risk that endogenous T cells (and their reservoir of CTLA-4 acting in trans) will limit the expansion of CTLA-4-ablated tumour-reactive T cells in vivo.

We must concede that the adoptive transfer experiments described in Chapter 4 support the above findings. In non-irradiated and irradiated recipients, TRP1 CTLA-4$^{-/-}$ Teff do not offer a significant advantage in rates of tumour rejection or prevention of recurrence than WT TRP1 Teff. There is a trend towards higher absolute TRP1 CTLA-4$^{-/-}$ Teff numbers and a more cytotoxic phenotype in the LN, but this only reaches significance upon the concurrent use of exogenous αCTLA-4 mAb. This illustrates the point that mAb-mediated blockade of the effector extrinsic endogenous CTLA-4^{hi} T cell pool is required to maximally expand TRP1 CTLA-4$^{-/-}$ Teff cells, and to drive them to full effector function (high granzyme B, eomes (in LN) and IFNγ expression).

There is a significant increase in the absolute numbers of TRP1 CTLA-4$^{-/-}$ Teff compared with WT TRP1 Teff on receipt of the same dosing schedule of αCTLA-4 mAb. This phenomenon is not a product of direct mAb binding to effectors (TRP1 CTLA-4$^{-/-}$ Teff lacks the target receptor). Rather, it is likely that complete CTLA-4 blockade is achieved with the TRP1 CTLA-4$^{-/-}$ T cell

group due to a lower frequency of CTLA-4^{hi} Treg targets and a more favourable antibody:antigen target ratio compared with the WT TRP1 T cell group. An additional pro-proliferative advantage conferred upon the TRP1 CTLA-4$^{-/-}$ T cell group is that co-transferred TRP1 CTLA-4$^{-/-}$ Tregs cannot negatively regulate Teff expansion in the same way as CTLA-4-replete Tregs. Despite normal absolute numbers by quantitative analysis, TRP1 CTLA-4$^{-/-}$ Treg will be functionally impaired (43). We plan to test this in a suppression assay using WT TRP1 Tregs as controls.

Absolute numbers of TRP1 CTLA-4$^{-/-}$ Tregs were significantly reduced at the end of the experiment following transfer into irradiated recipients (but not in the non-irradiated setting), with lower Ki67 expression than WT TRP1 Tregs run in parallel, and preservation of CD25 signal between groups. This was also observed in the protection experiment, where mice receiving TRP1 CTLA-4$^{-/-}$ T cells + αCTLA-4 mAb had complete absence of (transgenic) Tregs in the LN at 100 days post tumour inoculation, which was not observed in the other groups. It is possible that early administration of αCTLA-4 mAb following adoptive transfer of TRP1 CTLA-4$^{-/-}$ Tregs skews the host microenvironment through cytokine deprivation or even reprogramming of Tregs into Teffs (53).This requires further investigation. The 18 day experiments were performed in duplicate or triplicate, but the protection experiment was performed once, and repetition will be necessary to confirm these findings.

Based on this set of experiments, genetic ablation of CTLA-4 on tumour-reactive T cells in isolation may not offer a superior alternative to exogenous αCTLA-4 mAb in terms of tumour eradication and protection. However, concurrent administration of αCTLA-4 mAb potentiates the proliferative and cytotoxic properties of CTLA-4$^{-/-}$ Teff in vivo and may ultimately improve anti-tumour responses. This approach is at odds with the original aims of the project, namely to attempt to minimise toxicity from immune modulation and seek out alternatives to systemic αCTLA-4 mAb therapy. To address this, we propose further T cell modification to permit local/payload secretion of αCTLA-4 mAb into the tumour microenvironment to potentially limit systemic exposure. This is discussed in more detail in Chapter 7, section 7.3.

We did not make formal assessments of toxicity in these experiments, other than to observe mortality rates in the protection experiment and vitiligo that emerged in surviving mice as a consequence of TRP1-directed melanocyte destruction. We identified that in irradiated murine recipients, the period between days 7-19 post-TRP1 T cell transfer is the period of active tumour rejection and the period during which non-tumour related deaths were observed in the mice. The issue of toxicity is critical, and in future protection experiments we plan to serially monitor serum cytokines, autoantibody levels, perform transcription factor analysis on

adoptively transferred T cells and formally monitor murine weight from the point of TRP1 T cell infusion until the rejection of tumour, to explore the biological and functional differences between CTLA-4$^{-/-}$ TRP1 and WT TRP1 T cells.

One limitation of this study design is that assessment of the potential impact of cell intrinsic CTLA-4 ablation in tumour reactive T cells is based on findings from a transgenic mouse model. In order to ultimately translate this approach, we must identify a safe and efficacious gene editing strategy to enable CTLA-4-specific ablation from polyclonal T cells. Chapter 3 outlines the generation of human and murine CTLA-4 siRNA retroviral constructs, but these yielded disappointing results in primary murine lymphocytes, giving only incomplete CTLA-4 knockdown. TALEN and CRISPR/Cas technology are currently being explored in our laboratory.

7.3   αCTLA-4 mAb directed blockade of CTLA-4

The clinical relevance of αCTLA-4 mAb needs no introduction, but strategies to enhance its application are needed. An important publication in the field reports the mechanism underlying the anti-tumour activity of αCTLA-4 mAb to be ADCC-mediated depletion of αCTLA-4 mAb labelled CTLA-4^{hi} T cells by the innate immune system (67). In Chapter 4, we support this finding through the observation that αCTLA-4 mAb mediates depletion of CTLA-4^{hi} WT TRP1 Tregs in the tumour (but not the LN) with sparing of TRP1 CTLA-4$^{-/-}$ Tregs which lack the target receptor. Intratumoural endogenous CD4 Tregs are similarly vulnerable to depletion. CTLA-4 expression is substantially higher in the tumour compared to the LN, and higher in Tregs (endogenous and TRP1) compared with Teff. This partly explains the site-specific depletion observed in ours and others' work.

We have established that cell intrinsic CTLA-4 ablation does not confer significant anti-tumour or pro- T effector properties, likely due to endogenous reserves of CTLA-4 acting in trans. Co-administration of exogenous αCTLA-4 mAb with TRP1 CTLA-4$^{-/-}$ T cells increases absolute TRP1 CTLA-4$^{-/-}$ Teff numbers and enhances their cytotoxic profile. We hypothesise that CTLA-4 ablation on tumour-reactive T cells modified to secrete αCTLA-4 mAb could augment anti-tumour responses. Through payload secretion of mAb into a site that is densely packed with target antigen, we would hope to restrict mAb distribution and limit systemic effects.

We designed tricistronic vectors coding for full length human and murine αCTLA-4 mAb in (murine) IgG1 and IgG2a isotypes and tested them in vivo using tumour-reactive T cells as

intratumoural vehicles for payload secretion. IgG1 is associated with a blocking mode of action and IgG2a is associated with an ADCC/depletion effect. A theoretical risk of the IgG2a αCTLA-4 mAb construct is the potential for autocrine depletion of transduced T cells due to cell surface expression of CTLA-4. Teff in the non-stimulated state are CTLA-4^{lo}, but in the context of hyperstimulation for retroviral transduction and transgene incorporation, these cells drive up CTLA-4 expression at around the time that they begin to secrete mAb. Their cell-rich culture medium also contains an effector macrophage population which had originally been ascribed a role in antigen presentation, but could in theory deplete CTLA-4-replete transduced T cells in vitro, prior to adoptive transfer. It is also conceivable that CTLA-4^{hi} transduced cells may be pre-labelled with lytic antibody in vitro and on in vivo transfer are destroyed in the reticuloendothelial system.

We elected to test α-murine CTLA-4 (9D9 clone) in CTLA-4-replete TRP1 T cells in an irradiated B16 tumour model to assess the degree of toxicity of 9D9-IgG2a towards transferred cells. The impact of 9D9-Fc isotype is most evident in the tumour. Secretion of 9D9-IgG2a from transduced TRP1 CTLA-4$^{-/-}$ T cells is associated with a reduction in CTLA-4^{hi,} endogenous T cell populations in keeping with depletion, and secretion of 9D9-IgG1 from DLI is associated with an increase in endogenous T cell numbers, consistent with CTLA-4 blockade. There was an overall drop in TRP1 T cell numbers in the tumour encompassing both TRP1 Tregs (significant) and TRP1 Teff (non-significant) in the 9D9-IgG2a cohort, despite the absence of target CTLA-4 on these cells. This effect was not observed on the LN.

Part of the disparity in absolute numbers between groups may be due to 9D9 IgG1 conferring a survival advantage (28), but of more concern is the possibility of non-CTLA-4-directed toxicity directly mediated by 9D9-IgG2a in an inflammatory tumour microenvironment. Possible contributory factors include bystander activation of T cells which leads to high levels of apoptosis (136), M1 intratumoural macrophages acting in a non-Fc-directed manner leading to an 'off target-Fc' effect (133), and other interesting alternatives such as translocation of macrophage-mediated trogocytosed CTLA-4-mAb complexes onto adjacent cells resulting in their (accidental) depletion.

Non-F'ab targeted toxicity from excessively high concentrations of antibody is not clearly reported in the literature. However, in the setting of adoptive transfer experiments in the context of several unknowns, it becomes important to measure antibody concentration from serum, accepting that this may not be fully representative of actual tissue/tumour biodistribution (137-139).

The fact that T cells can be engineered to secrete full length biologically active antibody is a positive result. Of concern is the extent to which non-target expressing cells are reduced in number in this model, an as yet unexplained phenomenon which will inevitably compromise the efficacy of the technology if left unaddressed. Mechanistically this requires further investigation, and future experiments will require additional control conditions to help explain these observations. These could include a 10D1-IgG1-DLI isotype condition (mAb with no demonstrable target in this model) to compare with the 10D1-IgG2a-DLI condition, to quantify the depth of macrophage-mediated cell damage in the presence of non-binding IgG2a. It would be useful to compare intratumoural secretion with systemic exogenous administration of αCTLA-4 mAb in order to establish baseline expression against which to assess the transgenic conditions. Further characterisation of the tumour microenvironment would be desirable, with an incorporated elegant test of the depletion hypothesis using FcγRIV blockade. FcγRIV is expressed on murine tumour associated macrophages and is implicated in αCTLA-4 mAb-mediated ADCC of CTLA-4^{hi} targets. Blockade of FcγRIV with a monoclonal antibody, or the incorporation of FcγRIV$^{-/-}$ murine recipients into an adoptive transfer model of 9D9 (both isotypes) would be expected to show a neutralisation of 9D9-IgG2a-mediated depletion.

It is possible that the toxicity observed in this model reflects the transfer of an excessive dose of transduced cells and/or the accumulation of supraphysiological concentrations of mAb, resulting in non-specific off target effects. In order to address this concern, a titration experiment to identify the cell dose at which optimal antibody secretion and efficacy (with lesser toxicity) is necessary. Serial quantitation of serum mAb levels throughout the experiment may facilitate a comparison of blood titres versus end of experiment cell numbers to discern whether blood levels reflect antibody enrichment within the tumour.

7.4   Summary

The object of our project has been to establish a method to target inhibition of CTLA-4 to the tumour microenvironment. Results confirm that the first approach, ablation of CTLA-4 on tumour reactive T cells, does not obviously lead to improved tumour rejection compared with controls. Evidence to support an effector extrinsic mode of CTLA-4 activity explains why this could not work as a single intervention (26, 140).

The second approach was determined by the emergence of a novel mechanism to explain the drop in Treg numbers intratumourally following αCTLA-4 mAb, namely ADCC-mediated depletion of CTLA-4^{hi} cell targets (67, 69). Local intratumoural secretion of 9D9-IgG2a from CTLA-4-replete transferred cells was hypothesised to preferentially target CTLA-4hi Tregs for depletion. In reality, Teff were also depleted by virtue of having upregulated CTLA-4 expression following hyperstimulation in vitro to incorporate retroviral transgene. Comparatively, 9D9-IgG1 transduced CTLA-4-replete transferred cells were associated with engraftment and persistence within the tumour and LN, but did not appear to offer an anti-tumour advantage compared with the mock transduced condition.

The toxicity of 9D9-IgG2a to WT TRP1 T cells was ameliorated through the use of TRP1 CTLA-4$^{-/-}$ T cells for transduction, which improved 9D9-IgG2a-DLI engraftment and persistence in tumour and LN, but at levels below those observed in the control 9D9-IgG1 condition, suggesting the presence of an 'off target' toxicity from 9D9-IgG2a or the macrophage-driven ADCC mechanism.

7.5   Limitations of the model

We conducted this project using TRP1 as a model antigen in mice to demonstrate proof of principle for the biological impact of tumour targeted CTLA-4 inhibition. Interpretation of the results and extrapolation to the human setting should acknowledge the fundamental differences that exist between species.

The TRP1 TCR was generated from white-based brown B^{w} mutant mice which lack TRP1 protein in melanocytes and other tissues. For this reason, the TCR is highly avid, not having been subject to central or peripheral deletion. This makes adoptive transfer of these cells a highly artificial system, and liable to over-represent the true efficacy of immune modulatory

interventions tested in it. Naturally occurring TCRs of this avidity are unusual, but it is conceivable that genetically modified TCR or CAR transgenic T cells can be designed to these specifications.

7.6   Future directions

Through this project we have shown that tumour reactive T cells can be genetically modified to secrete a functional antibody, can continue to perform normal effector functions, and can be successfully transferred in vivo. The biological mAb effect is more prominent in the tumour and relates to concentration of the mAb in the tumour by virtue of the mode of delivery through tumour-homing, tumour-reactive T cells. This tumour-targeted approach could be an attractive approach for patients who have not responded to other systemically administered immunomodulatory treatments. However, what has become increasingly apparent through this project is that selection of the immunotherapeutic target for investigation/manipulation is key. Unfortunately, CTLA-4 appears to be a suboptimal target for the reasons discussed earlier.

The programmed cell death-1 receptor (PD-1) is an immunologic checkpoint that prevents autoimmunity. It is expressed on activated T cells and ligation of its ligands PD-L1 or PD-L2 on APCs effectively switches off T cell effector functions. Nivolumab is a humanised IgG4 αPD-1 receptor blocking mAb which has been shown to enhance T cell effector responses and cytokine secretion in pre-clinical studies (141). Clinical trials have confirmed significant anti-tumour activity in combination with Ipilimumab (overall response rates 61%), but grade 3 or 4 autoimmune toxicity was reported in 54% of all treated patients, and most were treated with immunosuppressive medication for this (142). Nivolumab is an efficacious, non-depleting αPD-1 antibody for which the therapeutic impact resides in its target blocking rather than depleting properties. It bestows significant immune toxicity upon over half of all recipients as part of a combinatorial therapy. For these reasons it would make an excellent candidate for the local intratumural secretion strategy discussed in this project, particularly as there is no requirement for depletion to induce the anti-tumour effect. Clearly a depleting mAb in this setting would be detrimental as it would mediate depletion of effector T cells. It is possible that PD-1 also represents a better target for cell intrinsic ablation. To my knowledge, PD-1 is not susceptible to an effector extrinsic effect, unlike CTLA-4.

Taking this forward, there is still much work to be done to understand, explain and standardise these strategies. Unlike the controlled administration of a pharmacokinetically and −

dynamically predictable exogenous mAb, transfer of a cell population that secretes mAb generates an array of variables such as expansion potential, survival and tissue infiltration that are susceptible to a range of biological factors, and a concern arising from our data is that extensive migration of transferred cells into the tumour can lead to activation, upregulated transcription of the transgene, and an enormous payload secretion of therapeutic mAb that may contribute to non-specific immune toxicity in addition to targeted toxicity. To circumvent concerns regarding the possible toxicity of these gene modified cells, we have access to a compact sort-suicide gene which could be incorporated into any vector for future clinical applications (143).

The rapid development of CAR T cell therapeutics and the limitations thereof (low engraftment and poor persistence of gene-modified cell product), underlines the potential value of concurrent manipulation of immune regulation pathways. Brentjens et al have published a patent (US2014/1341665A1) to promote the simultaneous expression of chimeric antigen receptor (CAR) and secreted scFv targeting immunomodulatory molecules to augment CAR T cell expansion.

We believe that secretion of full length mAb from T cells offers an additional biological tool with the potential for clinical application. Selection of the right antigenic target will be critical to the success of the approach.

BIBLIOGRAPHY

1.   Thomas S, Stauss HJ, Morris EC. Molecular immunology lessons from therapeutic T-cell receptor gene transfer. Immunology. 2010;129(2):170-7.
2.   Park JH, Brentjens RJ. Adoptive immunotherapy for B-cell malignancies with autologous chimeric antigen receptor modified tumor targeted T cells. Discovery medicine. 2010;9(47):277-88.
3.   Pule MA, Savoldo B, Myers GD, Rossig C, Russell HV, Dotti G, et al. Virus-specific T cells engineered to coexpress tumor-specific receptors: persistence and antitumor activity in individuals with neuroblastoma. Nature medicine. 2008;14(11):1264-70.
4.   Yu P, Lee Y, Liu W, Krausz T, Chong A, Schreiber H, et al. Intratumor depletion of CD4+ cells unmasks tumor immunogenicity leading to the rejection of late-stage tumors. The Journal of experimental medicine. 2005;201(5):779-91.
5.   Bendle GM, Holler A, Pang LK, Hsu S, Krampera M, Simpson E, et al. Induction of unresponsiveness limits tumor protection by adoptively transferred MDM2-specific cytotoxic T lymphocytes. Cancer research. 2004;64(21):8052-6.
6.   Colella TA, Bullock TN, Russell LB, Mullins DW, Overwijk WW, Luckey CJ, et al. Self-tolerance to the murine homologue of a tyrosinase-derived melanoma antigen: implications for tumor immunotherapy. The Journal of experimental medicine. 2000;191(7):1221-32.
7.   Specenier P. Ipilimumab in melanoma. Expert review of anticancer therapy. 2012;12(12):1511-21.
8.   Walunas TL, Bakker CY, Bluestone JA. CTLA-4 ligation blocks CD28-dependent T cell activation. The Journal of experimental medicine. 1996;183(6):2541-50.
9.   Walker LS, Sansom DM. The emerging role of CTLA4 as a cell-extrinsic regulator of T cell responses. Nature reviews Immunology. 2011;11(12):852-63.
10.   Walunas TL, Lenschow DJ, Bakker CY, Linsley PS, Freeman GJ, Green JM, et al. CTLA-4 can function as a negative regulator of T cell activation. Immunity. 1994;1(5):405-13.
11.   Gribben JG, Freeman GJ, Boussiotis VA, Rennert P, Jellis CL, Greenfield E, et al. CTLA4 mediates antigen-specific apoptosis of human T cells. Proceedings of the National Academy of Sciences of the United States of America. 1995;92(3):811-5.
12.   Linsley PS, Bradshaw J, Greene J, Peach R, Bennett KL, Mittler RS. Intracellular trafficking of CTLA-4 and focal localization towards sites of TCR engagement. Immunity. 1996;4(6):535-43.
13.   Alegre ML, Noel PJ, Eisfelder BJ, Chuang E, Clark MR, Reiner SL, et al. Regulation of surface and intracellular expression of CTLA4 on mouse T cells. Journal of immunology (Baltimore, Md : 1950). 1996;157(11):4762-70.
14.   Perkins D, Wang Z, Donovan C, He H, Mark D, Guan G, et al. Regulation of CTLA-4 expression during T cell activation. Journal of immunology (Baltimore, Md : 1950). 1996;156(11):4154-9.
15.   Qureshi OS, Zheng Y, Nakamura K, Attridge K, Manzotti C, Schmidt EM, et al. Trans-endocytosis of CD80 and CD86: a molecular basis for the cell-extrinsic function of CTLA-4. Science (New York, NY). 2011;332(6029):600-3.
16.   Shiratori T, Miyatake S, Ohno H, Nakaseko C, Isono K, Bonifacino JS, et al. Tyrosine phosphorylation controls internalization of CTLA-4 by regulating its interaction with clathrin-associated adaptor complex AP-2. Immunity. 1997;6(5):583-9.
17.   Iida T, Ohno H, Nakaseko C, Sakuma M, Takeda-Ezaki M, Arase H, et al. Regulation of cell surface expression of CTLA-4 by secretion of CTLA-4-containing lysosomes upon activation of CD4+ T cells. Journal of immunology (Baltimore, Md : 1950). 2000;165(9):5062-8.
18.   Ling V, Wu PW, Finnerty HF, Sharpe AH, Gray GS, Collins M. Complete sequence determination of the mouse and human CTLA4 gene loci: cross-species DNA sequence similarity beyond exon borders. Genomics. 1999;60(3):341-55.

19.   Calvo CR, Amsen D, Kruisbeek AM. Cytotoxic T lymphocyte antigen 4 (CTLA-4) interferes with extracellular signal-regulated kinase (ERK) and Jun NH2-terminal kinase (JNK) activation, but does not affect phosphorylation of T cell receptor zeta and ZAP70. The Journal of experimental medicine. 1997;186(10):1645-53.

20.   Ostrov DA, Shi W, Schwartz JC, Almo SC, Nathenson SG. Structure of murine CTLA-4 and its role in modulating T cell responsiveness. Science (New York, NY). 2000;290(5492):816-9.

21.   Yokosuka T, Kobayashi W, Takamatsu M, Sakata-Sogawa K, Zeng H, Hashimoto-Tane A, et al. Spatiotemporal basis of CTLA-4 costimulatory molecule-mediated negative regulation of T cell activation. Immunity. 2010;33(3):326-39.

22.   Masteller EL, Chuang E, Mullen AC, Reiner SL, Thompson CB. Structural analysis of CTLA-4 function in vivo. Journal of immunology (Baltimore, Md : 1950). 2000;164(10):5319-27.

23.   Homann D, Dummer W, Wolfe T, Rodrigo E, Theofilopoulos AN, Oldstone MB, et al. Lack of intrinsic CTLA-4 expression has minimal effect on regulation of antiviral T-cell immunity. Journal of virology. 2006;80(1):270-80.

24.   Bachmann MF, Waterhouse P, Speiser DE, McKall-Faienza K, Mak TW, Ohashi PS. Normal responsiveness of CTLA-4-deficient anti-viral cytotoxic T cells. Journal of immunology (Baltimore, Md : 1950). 1998;160(1):95-100.

25.   Rosenberg SA, Restifo NP, Yang JC, Morgan RA, Dudley ME. Adoptive cell transfer: a clinical path to effective cancer immunotherapy. Nature reviews Cancer. 2008;8(4):299-308.

26.   Corse E, Allison JP. Cutting edge: CTLA-4 on effector T cells inhibits in trans. Journal of immunology (Baltimore, Md : 1950). 2012;189(3):1123-7.

27.   Sakaguchi S, Wing K. Immunology. Damping by depletion. Science (New York, NY). 2011;332(6029):542-3.

28.   Pandiyan P, Lenardo MJ. The control of CD4+CD25+Foxp3+ regulatory T cell survival. Biology direct. 2008;3:6.

29.   Sakaguchi S, Sakaguchi N, Asano M, Itoh M, Toda M. Immunologic self-tolerance maintained by activated T cells expressing IL-2 receptor alpha-chains (CD25). Breakdown of a single mechanism of self-tolerance causes various autoimmune diseases. Journal of immunology (Baltimore, Md : 1950). 1995;155(3):1151-64.

30.   Jonuleit H, Schmitt E. The regulatory T cell family: distinct subsets and their interrelations. Journal of immunology (Baltimore, Md : 1950). 2003;171(12):6323-7.

31.   Zou W. Regulatory T cells, tumour immunity and immunotherapy. Nature reviews Immunology. 2006;6(4):295-307.

32.   Terabe M, Berzofsky JA. Immunoregulatory T cells in tumor immunity. Current opinion in immunology. 2004;16(2):157-62.

33.   Beyer M, Schultze JL. Regulatory T cells: major players in the tumor microenvironment. Current pharmaceutical design. 2009;15(16):1879-92.

34.   Fontenot JD, Rasmussen JP, Gavin MA, Rudensky AY. A function for interleukin 2 in Foxp3-expressing regulatory T cells. Nature immunology. 2005;6(11):1142-51.

35.   Shevach EM. Mechanisms of foxp3+ T regulatory cell-mediated suppression. Immunity. 2009;30(5):636-45.

36.   Serra P, Amrani A, Yamanouchi J, Han B, Thiessen S, Utsugi T, et al. CD40 ligation releases immature dendritic cells from the control of regulatory CD4+CD25+ T cells. Immunity. 2003;19(6):877-89.

37.   Misra N, Bayry J, Lacroix-Desmazes S, Kazatchkine MD, Kaveri SV. Cutting edge: human CD4+CD25+ T cells restrain the maturation and antigen-presenting function of dendritic cells. Journal of immunology (Baltimore, Md : 1950). 2004;172(8):4676-80.

38.   Joly E, Hudrisier D. What is trogocytosis and what is its purpose? Nature immunology. 2003;4(9):815.

39.   Thornton AM, Piccirillo CA, Shevach EM. Activation requirements for the induction of CD4+CD25+ T cell suppressor function. European journal of immunology. 2004;34(2):366-76.

40.   Marson A, Kretschmer K, Frampton GM, Jacobsen ES, Polansky JK, MacIsaac KD, et al. Foxp3 occupancy and regulation of key target genes during T-cell stimulation. Nature. 2007;445(7130):931-5.

41.   Tivol EA, Borriello F, Schweitzer AN, Lynch WP, Bluestone JA, Sharpe AH. Loss of CTLA-4 leads to massive lymphoproliferation and fatal multiorgan tissue destruction, revealing a critical negative regulatory role of CTLA-4. Immunity. 1995;3(5):541-7.

42.   Chambers CA, Sullivan TJ, Allison JP. Lymphoproliferation in CTLA-4-deficient mice is mediated by costimulation-dependent activation of CD4+ T cells. Immunity. 1997;7(6):885-95.

43.   Wing K, Onishi Y, Prieto-Martin P, Yamaguchi T, Miyara M, Fehervari Z, et al. CTLA-4 control over Foxp3+ regulatory T cell function. Science (New York, NY). 2008;322(5899):271-5.

44.   Jain N, Nguyen H, Chambers C, Kang J. Dual function of CTLA-4 in regulatory T cells and conventional T cells to prevent multiorgan autoimmunity. Proceedings of the National Academy of Sciences of the United States of America. 2010;107(4):1524-8.

45.   Shimizu J, Yamazaki S, Sakaguchi S. Induction of tumor immunity by removing CD25+CD4+ T cells: a common basis between tumor immunity and autoimmunity. Journal of immunology (Baltimore, Md : 1950). 1999;163(10):5211-8.

46.   Quezada SA, Simpson TR, Peggs KS, Merghoub T, Vider J, Fan X, et al. Tumor-reactive CD4(+) T cells develop cytotoxic activity and eradicate large established melanoma after transfer into lymphopenic hosts. The Journal of experimental medicine. 2010;207(3):637-50.

47.   Persson J, Beyer I, Yumul R, Li Z, Kiem HP, Roffler S, et al. Immuno-therapy with anti-CTLA4 antibodies in tolerized and non-tolerized mouse tumor models. PloS one. 2011;6(7):e22303.

48.   Peggs KS, Quezada SA, Chambers CA, Korman AJ, Allison JP. Blockade of CTLA-4 on both effector and regulatory T cell compartments contributes to the antitumor activity of anti-CTLA-4 antibodies. The Journal of experimental medicine. 2009;206(8):1717-25.

49.   Hodi FS, O'Day SJ, McDermott DF, Weber RW, Sosman JA, Haanen JB, et al. Improved survival with ipilimumab in patients with metastatic melanoma. The New England journal of medicine. 2010;363(8):711-23.

50.   Weber JS, Kahler KC, Hauschild A. Management of immune-related adverse events and kinetics of response with ipilimumab. Journal of clinical oncology : official journal of the American Society of Clinical Oncology. 2012;30(21):2691-7.

51.   Yousaf N, Davidson M, Goode E, Thomas C, Hung R, Gore M, et al. The cost of ipilimumab toxicity: a single-centre analysis. Melanoma research. 2015.

52.   Schadendorf D, Hodi FS, Robert C, Weber JS, Margolin K, Hamid O, et al. Pooled Analysis of Long-Term Survival Data From Phase II and Phase III Trials of Ipilimumab in Unresectable or Metastatic Melanoma. Journal of clinical oncology : official journal of the American Society of Clinical Oncology. 2015.

53.   Ise W, Kohyama M, Nutsch KM, Lee HM, Suri A, Unanue ER, et al. CTLA-4 suppresses the pathogenicity of self antigen-specific T cells by cell-intrinsic and cell-extrinsic mechanisms. Nature immunology. 2010;11(2):129-35.

54.   Gozalo-Sanmillan S, McNally JM, Lin MY, Chambers CA, Berg LJ. Cutting edge: two distinct mechanisms lead to impaired T cell homeostasis in Janus kinase 3- and CTLA-4-deficient mice. Journal of immunology (Baltimore, Md : 1950). 2001;166(2):727-30.

55.   Tivol EA, Gorski J. Re-establishing peripheral tolerance in the absence of CTLA-4: complementation by wild-type T cells points to an indirect role for CTLA-4. Journal of immunology (Baltimore, Md : 1950). 2002;169(4):1852-8.

56.   Snyder A, Makarov V, Merghoub T, Yuan J, Zaretsky JM, Desrichard A, et al. Genetic basis for clinical response to CTLA-4 blockade in melanoma. The New England journal of medicine. 2014;371(23):2189-99.

57.   Breunis WB, Tarazona-Santos E, Chen R, Kiley M, Rosenberg SA, Chanock SJ. Influence of cytotoxic T lymphocyte-associated antigen 4 (CTLA4) common polymorphisms on outcome in treatment of melanoma patients with CTLA-4 blockade. Journal of immunotherapy (Hagerstown, Md : 1997). 2008;31(6):586-90.

58.   Kristiansen OP, Larsen ZM, Pociot F. CTLA-4 in autoimmune diseases--a general susceptibility gene to autoimmunity? Genes and immunity. 2000;1(3):170-84.

59.   Simmons AD, Moskalenko M, Creson J, Fang J, Yi S, VanRoey MJ, et al. Local secretion of anti-CTLA-4 enhances the therapeutic efficacy of a cancer immunotherapy with reduced evidence of systemic autoimmunity. Cancer immunology, immunotherapy : CII. 2008;57(8):1263-70.

60.   Dillman RO. Cancer Vaccines: Can They Improve Survival? Cancer biotherapy & radiopharmaceuticals. 2015.

61.   Quezada SA, Peggs KS, Curran MA, Allison JP. CTLA4 blockade and GM-CSF combination immunotherapy alters the intratumor balance of effector and regulatory T cells. The Journal of clinical investigation. 2006;116(7):1935-45.

62.   Schmidt EM, Wang CJ, Ryan GA, Clough LE, Qureshi OS, Goodall M, et al. Ctla-4 controls regulatory T cell peripheral homeostasis and is required for suppression of pancreatic islet autoimmunity. Journal of immunology (Baltimore, Md : 1950). 2009;182(1):274-82.

63.   Kavanagh B, O'Brien S, Lee D, Hou Y, Weinberg V, Rini B, et al. CTLA4 blockade expands FoxP3+ regulatory and activated effector CD4+ T cells in a dose-dependent fashion. Blood. 2008;112(4):1175-83.

64.   Liakou CI, Kamat A, Tang DN, Chen H, Sun J, Troncoso P, et al. CTLA-4 blockade increases IFNgamma-producing CD4+ICOShi cells to shift the ratio of effector to regulatory T cells in cancer patients. Proceedings of the National Academy of Sciences of the United States of America. 2008;105(39):14987-92.

65.   Waitz R, Solomon SB, Petre EN, Trumble AE, Fasso M, Norton L, et al. Potent induction of tumor immunity by combining tumor cryoablation with anti-CTLA-4 therapy. Cancer research. 2012;72(2):430-9.

66.   Dunn GP, Koebel CM, Schreiber RD. Interferons, immunity and cancer immunoediting. Nature reviews Immunology. 2006;6(11):836-48.

67.   Simpson TR, Li F, Montalvo-Ortiz W, Sepulveda MA, Bergerhoff K, Arce F, et al. Fc-dependent depletion of tumor-infiltrating regulatory T cells co-defines the efficacy of anti-CTLA-4 therapy against melanoma. The Journal of experimental medicine. 2013;210(9):1695-710.

68.   Bulliard Y, Jolicoeur R, Windman M, Rue SM, Ettenberg S, Knee DA, et al. Activating Fc gamma receptors contribute to the antitumor activities of immunoregulatory receptor-targeting antibodies. The Journal of experimental medicine. 2013;210(9):1685-93.

69.   Selby MJ, Engelhardt JJ, Quigley M, Henning KA, Chen T, Srinivasan M, et al. Anti-CTLA-4 antibodies of IgG2a isotype enhance antitumor activity through reduction of intratumoral regulatory T cells. Cancer immunology research. 2013;1(1):32-42.

70.   Furness AJ, Vargas FA, Peggs KS, Quezada SA. Impact of tumour microenvironment and Fc receptors on the activity of immunomodulatory antibodies. Trends in immunology. 2014;35(7):290-8.

71.   Overwijk WW, Lee DS, Surman DR, Irvine KR, Touloukian CE, Chan CC, et al. Vaccination with a recombinant vaccinia virus encoding a "self" antigen induces autoimmune vitiligo and tumor cell destruction in mice: requirement for CD4(+) T lymphocytes. Proceedings of the National Academy of Sciences of the United States of America. 1999;96(6):2982-7.

72.   Muranski P, Boni A, Antony PA, Cassard L, Irvine KR, Kaiser A, et al. Tumor-specific Th17-polarized cells eradicate large established melanoma. Blood. 2008;112(2):362-73.

73.   Pear WS, Nolan GP, Scott ML, Baltimore D. Production of high-titer helper-free retroviruses by transient transfection. Proceedings of the National Academy of Sciences of the United States of America. 1993;90(18):8392-6.

74.   Smith SD, Shatsky M, Cohen PS, Warnke R, Link MP, Glader BE. Monoclonal antibody and enzymatic profiles of human malignant T-lymphoid cells and derived cell lines. Cancer research. 1984;44(12 Pt 1):5657-60.

75.   van Elsas A, Hurwitz AA, Allison JP. Combination immunotherapy of B16 melanoma using anti-cytotoxic T lymphocyte-associated antigen 4 (CTLA-4) and granulocyte/macrophage

colony-stimulating factor (GM-CSF)-producing vaccines induces rejection of subcutaneous and metastatic tumors accompanied by autoimmune depigmentation. The Journal of experimental medicine. 1999;190(3):355-66.

76. Vile RG, Tuszynski A, Castleden S. Retroviral vectors. From laboratory tools to molecular medicine. Molecular biotechnology. 1996;5(2):139-58.

77. Riviere I, Brose K, Mulligan RC. Effects of retroviral vector design on expression of human adenosine deaminase in murine bone marrow transplant recipients engrafted with genetically modified cells. Proceedings of the National Academy of Sciences of the United States of America. 1995;92(15):6733-7.

78. Rasko JE, Battini JL, Gottschalk RJ, Mazo I, Miller AD. The RD114/simian type D retrovirus receptor is a neutral amino acid transporter. Proceedings of the National Academy of Sciences of the United States of America. 1999;96(5):2129-34.

79. Frebourg T, Sadelain M, Ng YS, Kassel J, Friend SH. Equal transcription of wild-type and mutant p53 using bicistronic vectors results in the wild-type phenotype. Cancer research. 1994;54(4):878-81.

80. Keler T, Halk E, Vitale L, O'Neill T, Blanset D, Lee S, et al. Activity and safety of CTLA-4 blockade combined with vaccines in cynomolgus macaques. Journal of immunology (Baltimore, Md : 1950). 2003;171(11):6251-9.

81. Griffin MD, Hong DK, Holman PO, Lee KM, Whitters MJ, O'Herrin SM, et al. Blockade of T cell activation using a surface-linked single-chain antibody to CTLA-4 (CD152). Journal of immunology (Baltimore, Md : 1950). 2000;164(9):4433-42.

82. Brummelkamp TR, Bernards R, Agami R. A system for stable expression of short interfering RNAs in mammalian cells. Science (New York, NY). 2002;296(5567):550-3.

83. Murray L, Luens K, Tushinski R, Jin L, Burton M, Chen J, et al. Optimization of retroviral gene transduction of mobilized primitive hematopoietic progenitors by using thrombopoietin, Flt3, and Kit ligands and RetroNectin culture. Human gene therapy. 1999;10(11):1743-52.

84. Davis HE, Rosinski M, Morgan JR, Yarmush ML. Charged polymers modulate retrovirus transduction via membrane charge neutralization and virus aggregation. Biophysical journal. 2004;86(2):1234-42.

85. Brandmaier AG, Leitner WW, Ha SP, Sidney J, Restifo NP, Touloukian CE. High-avidity autoreactive CD4+ T cells induce host CTL, overcome T(regs) and mediate tumor destruction. Journal of immunotherapy (Hagerstown, Md : 1997). 2009;32(7):677-88.

86. Zhang X, Goncalves R, Mosser DM. The isolation and characterization of murine macrophages. Current protocols in immunology / edited by John E Coligan [et al]. 2008;Chapter 14:Unit 14.1.

87. Tomida M, Yamamoto-Yamaguchi Y, Hozumi M. Purification of a factor inducing differentiation of mouse myeloid leukemic M1 cells from conditioned medium of mouse fibroblast L929 cells. The Journal of biological chemistry. 1984;259(17):10978-82.

88. Palacios R. Concanavalin A triggers T lymphocytes by directly interacting with their receptors for activation. Journal of immunology (Baltimore, Md : 1950). 1982;128(1):337-42.

89. van Meerten T, van Rijn RS, Hol S, Hagenbeek A, Ebeling SB. Complement-induced cell death by rituximab depends on CD20 expression level and acts complementary to antibody-dependent cellular cytotoxicity. Clinical cancer research : an official journal of the American Association for Cancer Research. 2006;12(13):4027-35.

90. Wing K, Yamaguchi T, Sakaguchi S. Cell-autonomous and -non-autonomous roles of CTLA-4 in immune regulation. Trends in immunology. 2011;32(9):428-33.

91. Papworth M, Kolasinska P, Minczuk M. Designer zinc-finger proteins and their applications. Gene. 2006;366(1):27-38.

92. Urnov FD, Miller JC, Lee YL, Beausejour CM, Rock JM, Augustus S, et al. Highly efficient endogenous human gene correction using designed zinc-finger nucleases. Nature. 2005;435(7042):646-51.

93. Miller JC, Tan S, Qiao G, Barlow KA, Wang J, Xia DF, et al. A TALE nuclease architecture for efficient genome editing. Nature biotechnology. 2011;29(2):143-8.

94.   Cong L, Ran FA, Cox D, Lin S, Barretto R, Habib N, et al. Multiplex genome engineering using CRISPR/Cas systems. Science (New York, NY). 2013;339(6121):819-23.

95.   Whitehead KA, Langer R, Anderson DG. Knocking down barriers: advances in siRNA delivery. Nature reviews Drug discovery. 2009;8(2):129-38.

96.   Boudreau RL, Martins I, Davidson BL. Artificial microRNAs as siRNA shuttles: improved safety as compared to shRNAs in vitro and in vivo. Molecular therapy : the journal of the American Society of Gene Therapy. 2009;17(1):169-75.

97.   Meister G, Landthaler M, Dorsett Y, Tuschl T. Sequence-specific inhibition of microRNA- and siRNA-induced RNA silencing. RNA (New York, NY). 2004;10(3):544-50.

98.   Pelham HR. The retention signal for soluble proteins of the endoplasmic reticulum. Trends in biochemical sciences. 1990;15(12):483-6.

99.   Munro S, Pelham HR. A C-terminal signal prevents secretion of luminal ER proteins. Cell. 1987;48(5):899-907.

100.   Rutkowski DT, Kaufman RJ. A trip to the ER: coping with stress. Trends in cell biology. 2004;14(1):20-8.

101.   Fire A, Xu S, Montgomery MK, Kostas SA, Driver SE, Mello CC. Potent and specific genetic interference by double-stranded RNA in Caenorhabditis elegans. Nature. 1998;391(6669):806-11.

102.   Elbashir SM, Harborth J, Lendeckel W, Yalcin A, Weber K, Tuschl T. Duplexes of 21-nucleotide RNAs mediate RNA interference in cultured mammalian cells. Nature. 2001;411(6836):494-8.

103.   Hunter T, Hunt T, Jackson RJ, Robertson HD. The characteristics of inhibition of protein synthesis by double-stranded ribonucleic acid in reticulocyte lysates. The Journal of biological chemistry. 1975;250(2):409-17.

104.   Yu Y, Wu H, Tang Z, Zang G. CTLA4 silencing with siRNA promotes deviation of Th1/Th2 in chronic hepatitis B patients. Cellular & molecular immunology. 2009;6(2):123-7.

105.   Iwamura K, Kato T, Miyahara Y, Naota H, Mineno J, Ikeda H, et al. siRNA-mediated silencing of PD-1 ligands enhances tumor-specific human T-cell effector functions. Gene therapy. 2012;19(10):959-66.

106.   Bollard CM, Cooper LJ, Heslop HE. Immunotherapy targeting EBV-expressing lymphoproliferative diseases. Best practice & research Clinical haematology. 2008;21(3):405-20.

107.   Wrzesinski C, Paulos CM, Kaiser A, Muranski P, Palmer DC, Gattinoni L, et al. Increased intensity lymphodepletion enhances tumor treatment efficacy of adoptively transferred tumor-specific T cells. Journal of immunotherapy (Hagerstown, Md : 1997). 2010;33(1):1-7.

108.   Muranski P, Restifo NP. Adoptive immunotherapy of cancer using CD4(+) T cells. Current opinion in immunology. 2009;21(2):200-8.

109.   Xie Y, Akpinarli A, Maris C, Hipkiss EL, Lane M, Kwon EK, et al. Naive tumor-specific CD4(+) T cells differentiated in vivo eradicate established melanoma. The Journal of experimental medicine. 2010;207(3):651-67.

110.   Katsuhara A, Fujiki F, Aoyama N, Tanii S, Morimoto S, Oka Y, et al. Transduction of a Novel HLA-DRB1*04:05-restricted, WT1-specific TCR Gene into Human CD4+ T Cells Confers Killing Activity Against Human Leukemia Cells. Anticancer research. 2015;35(3):1251-61.

111.   Martin-Orozco N, Muranski P, Chung Y, Yang XO, Yamazaki T, Lu S, et al. T helper 17 cells promote cytotoxic T cell activation in tumor immunity. Immunity. 2009;31(5):787-98.

112.   Barthlott T, Moncrieffe H, Veldhoen M, Atkins CJ, Christensen J, O'Garra A, et al. CD25+ CD4+ T cells compete with naive CD4+ T cells for IL-2 and exploit it for the induction of IL-10 production. International immunology. 2005;17(3):279-88.

113.   Laurent S, Queirolo P, Boero S, Salvi S, Piccioli P, Boccardo S, et al. The engagement of CTLA-4 on primary melanoma cell lines induces antibody-dependent cellular cytotoxicity and TNF-alpha production. Journal of translational medicine. 2013;11:108.

114.   Peggs KS, Mackinnon S. Immune reconstitution following haematopoietic stem cell transplantation. British journal of haematology. 2004;124(4):407-20.

115.   Eshima K, Chiba S, Suzuki H, Kokubo K, Kobayashi H, Iizuka M, et al. Ectopic expression of a T-box transcription factor, eomesodermin, renders CD4(+) Th cells cytotoxic by activating both perforin- and FasL-pathways. Immunology letters. 2012;144(1-2):7-15.

116.   Krummel MF, Allison JP. CD28 and CTLA-4 have opposing effects on the response of T cells to stimulation. The Journal of experimental medicine. 1995;182(2):459-65.

117.   Lane P, Gerhard W, Hubele S, Lanzavecchia A, McConnell F. Expression and functional properties of mouse B7/BB1 using a fusion protein between mouse CTLA4 and human gamma 1. Immunology. 1993;80(1):56-61.

118.   Gough SC, Walker LS, Sansom DM. CTLA4 gene polymorphism and autoimmunity. Immunological reviews. 2005;204:102-15.

119.   Fishwild DM, O'Donnell SL, Bengoechea T, Hudson DV, Harding F, Bernhard SL, et al. High-avidity human IgG kappa monoclonal antibodies from a novel strain of minilocus transgenic mice. Nature biotechnology. 1996;14(7):845-51.

120.   Kershaw MH, Teng MW, Smyth MJ, Darcy PK. Supernatural T cells: genetic modification of T cells for cancer therapy. Nature reviews Immunology. 2005;5(12):928-40.

121.   Park TS, Rosenberg SA, Morgan RA. Treating cancer with genetically engineered T cells. Trends in biotechnology. 2011;29(11):550-7.

122.   Anderson DE, Bieganowska KD, Bar-Or A, Oliveira EM, Carreno B, Collins M, et al. Paradoxical inhibition of T-cell function in response to CTLA-4 blockade; heterogeneity within the human T-cell population. Nature medicine. 2000;6(2):211-4.

123.   Griffin MD, Holman PO, Tang Q, Ashourian N, Korthauer U, Kranz DM, et al. Development and applications of surface-linked single chain antibodies against T-cell antigens. Journal of immunological methods. 2001;248(1-2):77-90.

124.   Clynes RA, Towers TL, Presta LG, Ravetch JV. Inhibitory Fc receptors modulate in vivo cytotoxicity against tumor targets. Nature medicine. 2000;6(4):443-6.

125.   de Haij S, Jansen JH, Boross P, Beurskens FJ, Bakema JE, Bos DL, et al. In vivo cytotoxicity of type I CD20 antibodies critically depends on Fc receptor ITAM signaling. Cancer research. 2010;70(8):3209-17.

126.   Johnson P, Glennie M. The mechanisms of action of rituximab in the elimination of tumor cells. Seminars in oncology. 2003;30(1 Suppl 2):3-8.

127.   Nimmerjahn F, Ravetch JV. Antibodies, Fc receptors and cancer. Current opinion in immunology. 2007;19(2):239-45.

128.   Ravetch JV, Lanier LL. Immune inhibitory receptors. Science (New York, NY). 2000;290(5489):84-9.

129.   Kalergis AM, Ravetch JV. Inducing tumor immunity through the selective engagement of activating Fcgamma receptors on dendritic cells. The Journal of experimental medicine. 2002;195(12):1653-9.

130.   Nimmerjahn F, Ravetch JV. Divergent immunoglobulin g subclass activity through selective Fc receptor binding. Science (New York, NY). 2005;310(5753):1510-2.

131.   Nimmerjahn F, Bruhns P, Horiuchi K, Ravetch JV. FcgammaRIV: a novel FcR with distinct IgG subclass specificity. Immunity. 2005;23(1):41-51.

132.   Hamaguchi Y, Xiu Y, Komura K, Nimmerjahn F, Tedder TF. Antibody isotype-specific engagement of Fcgamma receptors regulates B lymphocyte depletion during CD20 immunotherapy. The Journal of experimental medicine. 2006;203(3):743-53.

133.   Weiskopf K, Weissman IL. Macrophages are critical effectors of antibody therapies for cancer. mAbs. 2015;7(2):303-10.

134.   Kerkar SP, Sanchez-Perez L, Yang S, Borman ZA, Muranski P, Ji Y, et al. Genetic engineering of murine CD8+ and CD4+ T cells for preclinical adoptive immunotherapy studies. Journal of immunotherapy (Hagerstown, Md : 1997). 2011;34(4):343-52.

135.   Robert C, Thomas L, Bondarenko I, O'Day S, Weber J, Garbe C, et al. Ipilimumab plus dacarbazine for previously untreated metastatic melanoma. The New England journal of medicine. 2011;364(26):2517-26.

136.   Bangs SC, Baban D, Cattan HJ, Li CK, McMichael AJ, Xu XN. Human CD4+ memory T cells are preferential targets for bystander activation and apoptosis. Journal of immunology (Baltimore, Md : 1950). 2009;182(4):1962-71.

137.   Stevenson GT. Three major uncertainties in the antibody therapy of cancer. Haematologica. 2014;99(10):1538-46.

138.   Wang W, Wang EQ, Balthasar JP. Monoclonal antibody pharmacokinetics and pharmacodynamics. Clinical pharmacology and therapeutics. 2008;84(5):548-58.

139.   Brennan FR, Morton LD, Spindeldreher S, Kiessling A, Allenspach R, Hey A, et al. Safety and immunotoxicity assessment of immunomodulatory monoclonal antibodies. mAbs. 2010;2(3):233-55.

140.   Walker LS, Sansom DM. Confusing signals: Recent progress in CTLA-4 biology. Trends in immunology. 2015.

141.   Wang C, Thudium KB, Han M, Wang XT, Huang H, Feingersh D, et al. In vitro characterization of the anti-PD-1 antibody nivolumab, BMS-936558, and in vivo toxicology in non-human primates. Cancer immunology research. 2014;2(9):846-56.

142.   Postow MA, Chesney J, Pavlick AC, Robert C, Grossmann K, McDermott D, et al. Nivolumab and Ipilimumab versus Ipilimumab in Untreated Melanoma. The New England journal of medicine. 2015.

143.   Philip B, Kokalaki E, Mekkaoui L, Thomas S, Straathof K, Flutter B, et al. A highly compact epitope-based marker/suicide gene for easier and safer T-cell therapy. Blood. 2014;124(8):1277-87.

145.   Pelham HR. Multiple Targets for Brefeldin A. Cell. Vol. 67, 449-451, November 1, 1991.

146.   Gattinoni L1, Lugli E, Ji Y, Pos Z, Paulos CM, Quigley MF et al. A human memory T cell subset with stem cell-like properties. Nat Med. 2011 Sep 18;17(10):1290-7.

147.   Wherry EJ1, Kurachi M1. Molecular and cellular insights into T cell exhaustion. Nat Rev Immunol. 2015 Aug;15(8):486-99.

148.   Bochkov YA, Palmenberg AC.Translational efficiency of EMCV IRES in bicistronic vectors is dependent upon IRES sequence and gene location. Biotechniques. 2006 Sep;41(3):283-4, 286, 288 passim.

149.   Wu Y1, Borde M, Heissmeyer V, Feuerer M, Lapan AD, Stroud JC et al. FOXP3 controls regulatory T cell function through cooperation with NFAT. Cell. 2006 Jul 28;126(2):375-87.

150.   Gibson HM, Hedgcock CJ, Aufiero BM, Wilson AJ, Hafner MS, Tsokos GC,et al. Induction of the CTLA-4 gene in human lymphocytes is dependent on NFAT binding the proximal promoter. J Immunol. 2007 Sep 15;179(6):3831-40.